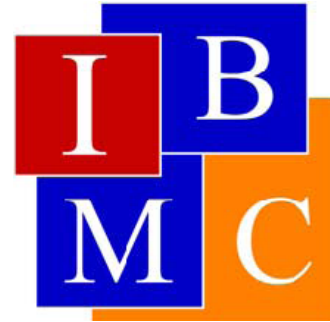


TESIS DOCTORAL

BÚSQUEDA Y CARACTERIZACIÓN
BIOFÍSICA DE LAS REGIONES
MEMBRANOTRÓPICAS DE LAS
PROTEÍNAS ESTRUCTURALES DEL VIRUS
DE LA HEPATITIS C.
BÚSQUEDA DE INHIBIDORES DE LA
ENTRADA DEL VIRUS

Ana Joaquina Pérez Berná
2008

UNIVERSIDAD MIGUEL HERNÁNDEZ DE ELCHE

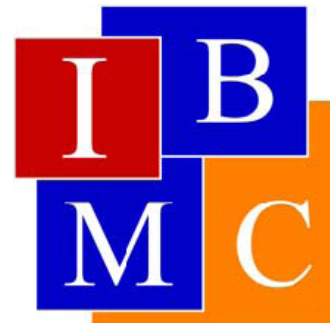


UNIVERSIDAD MIGUEL HERNÁNDEZ DE ELCHE
INSTITUTO DE BIOLOGÍA MOLECULAR Y CELULAR

“Búsqueda y caracterización biofísica de regiones
membranotrópicas de las proteínas estructurales de
HCV. Búsqueda de inhibidores de la entrada del
virus”

“Search and biophysical characterization of the
membranotropic regions in the structural Hepatitis
C virus proteins. Searching for Hepatitis C virus
entry inhibitors”

Ana Joaquina Pérez Berná
TESIS DOCTORAL 2008
PH.D. THESIS 2008



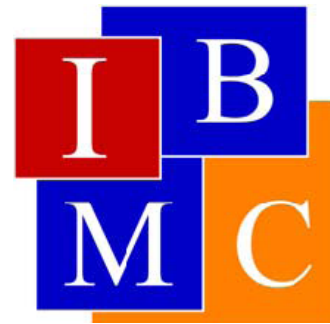
D. José Manuel González Ros, Profesor y Director del Instituto de Biología Molecular y Celular de la Universidad Miguel Hernández de Elche,

Da su conformidad a la lectura de la tesis doctoral titulada: “Búsqueda y caracterización biofísica de regiones membranotrópicas de las proteínas estructurales de HCV. Búsqueda de inhibidores de la entrada del virus” presentada por Doña. Ana Joaquina Pérez Berná,

Para que conste y surta los efectos oportunos, firma el presente certificado en

Elche, 25 de Junio de 2008

Fdo. Prof. José Manuel González Ros



D. José Villalaín Boullón, Doctor en Ciencias y Catedrático de Bioquímica y Biología Molecular de la Universidad Miguel Hernández de Elche,

CERTIFICA:

Que el trabajo de investigación que conduce a la obtención del grado de doctor titulado: “Búsqueda y caracterización biofísica de regiones membranotrópicas de las proteínas estructurales de HCV. Búsqueda de inhibidores de la entrada del virus” del que es autor D. Ana Joaquina Pérez Berná, ha sido realizado bajo su dirección en el Instituto de Biología Molecular y Celular de la Universidad Miguel Hernández de Elche.

Para que conste y surta los efectos oportunos, firma el presente certificado en

Elche, 25 de Junio de 2008

Fdo. Prof. José Villalaín Boullón

AGRADECIMIENTOS

Muy pocas veces en la vida se presenta la oportunidad de dejar plasmado en un documento escrito la gratitud y el aprecio hacia las personas que te han ayudado. La Tesis doctoral no es sólo un trabajo de investigación sino que es el punto final de una formación académica que encierra parte de mi vida, por tanto la deuda que tengo con las personas que enumero a continuación es tanto laboral como personal.

Deseo expresar mi agradecimiento a mi director de tesis, Dr. José Villalain, por permitirme realizar la tesis en su laboratorio. Por el apoyo, seguimiento, control y valoración de mis resultados experimentales, por la confianza depositada en mí al permitirme comenzar una línea experimental independiente basada en HCV, gracias por tus consejos personales y experimentales, por tus aportaciones a los artículos, con cualquier otro director de tesis el número de mis publicaciones sería sin duda diferente.

Al Dr. José Manuel González Ros por haber creado tan cerca de mi casa este magnífico instituto de Investigación. Aquí en esta creación tuya, he pasado en los últimos 4 años más horas que en mi casa y me he formado como científico junto a esta gran familia que es el IBMC.

Me gustaría también agradecer como colaboradores de una parte de este trabajo, quizá la parte más difícil de mi tesis, a Jesús Sanz y en especial a Beatriz Maestro quien mostró mucha diligencia, habilidad y paciencia para conseguir expresar un péptido prácticamente inexpressable.

A Reyes Mateo y a José Antonio Poveda, por sus consejos sobre fluorescencia.

También agradezco a todos los profesores y compañeros del IBMC que no nombro, (porque estos agradecimientos son excesivamente largos) la ayuda que siempre he encontrado cuando la he necesitado, de todo corazón muchas gracias.

A los megasecretarios que reciben y atienden con una gran eficacia unida siempre a una gran simpatía y alegría. Sin vosotros la burocracia sería muchísimo más dura. Muchas gracias May, Javier y Carmen.

A toda mi familia Villalainita, empezando por mis papis en el laboratorio, el tito Rober y Angelita quienes desde el principio me enseñaron gran parte de toda la biofísica que sé. Me resolvieron pacientemente todas las dudas que se me ocurrían y me enseñaron como funciona la ciencia. A Miguel por los largos debates científicos, las nuevas ideas experimentales, las ranitas, las palmas y por ser el fundador del leakageTeam. A Jaimuchi, soy incapaz de imaginar como hubieran sido estos años sin ti, no sólo porque eres uno de mis mejores amigos, sino porque has sido mi hermanito en el laboratorio, hemos compartido liposomas, experimentos, artículos, cerdadas (tu con tu pulmón, yo con mis higadillos), los inolvidables momentos en el RMN, las fiestas de bioquímicas, hogueras, los dos hemos estado de estancia al mismo tiempo y hemos escrito la tesis al mismo tiempo. Tenerte como compañero es una de las mejores cosas que me ha podido pasar, muchas gracias Jaime. A mi Ani, mi técnico, mi profesora y amiga no sé que hubiera hecho sin ti. Muchas gracias por ayudarme siempre que has podido, el laboratorio se llenó de alegría cuando entraste en él. A mis padawan Diego y Alejandro por alegrar el laboratorio y en especial a mi portuguesa Doctora Salomé, por tu ayuda durante los meses que duró tu estancia.

Ich verdanke die ganze Leute in Institute of Biophysics and Nanosystems Research nach Graz weil Ihr in ganze Experimenten mir helftet und die Röntgenspektroskopie mir lehrtet. Ich möchte die danke ganz besonders vor Peter Laggner, Georg, Yasemin, Beate, Johann Krebs, Manfred, Gudrun geben.

A Estefanía, Javi, Clemente, Rocío y Aarón, por ser tan buenos compañeros conmigo desde las clases de bioquímica con mis dinosaurios hasta hoy, en especial a mi Roci por ser siempre tan

encantadora y comprensiva conmigo, porque todos los días me has escuchado y apoyado con mi tesis, sin ti mi vida en el IBMC no hubiera sido tan alegre como has conseguido que sea, muchas gracias.

Gracias al señor de Orthnak, el gran Clemente el blanco, gracias por compartir conmigo tu sabiduría y tus consejos. Independientemente de donde nuestros senderos nos guíen, los palantir entre Isengard y Lorien siempre estarán activos.

A Víctor, mi otro vecino, gracias porque has conseguido que la hora del café se haya convertido en uno de los mejores momentos del día, gracias por escucharme, por el apoyo que día a día me has demostrado, por confiar en mí, gracias por convertirte en otro de mis mejores amigos

A mi compi de inglés Lourdes, por compartir tus resúmenes, los cafés, la hora de comer y convertirte en una nueva amiga dentro del IBMC.

A mi madrileña nacionalizada catalana favorita, a mi exvecina Isabel, por todos tus consejos de fluorescencia y de la vida.

A Mayte, por ayudarme siempre que te he necesitado, sobre todo al principio de la tesis junto con Jaime con los horribles botecitos de las peptidotecas que no había forma de abrirlos y con el lento calorímetro.

A Olga, por acompañarnos durante los momentos experimentales más emocionantes de la tesis, las semanas de RMN, gracias por tu ayuda durante esos días.

Al resto de amigos en el IBMC, María José, Estefanía, María, Ángeles, Marí Carmen, David, Lorena, Nuria, Alfonso, Olga, Laura, Mónica, Nuria, Luis, Isabel, Alberto.....

También me gustaría agradecer la ayuda, a otras personas que me han ayudado durante mi formación:

A mis amigas de toda la vida, las que me han acompañado desde que era una medietra a Verónica, Mayte y M^a Milagros por estar siempre cuando os he necesitado.

A mis compañeros del Instituto Helena, Colón, Pedrero y Laura por los viejos ratos en Santo Domingo.

A mis compañeros de mi etapa como Bióloga por esos momentos felices que pasamos en Alicante a Javi, Carlos, Ani, Cristina, Miriam, Esther, Víctor, Santi, Charo...

A mi tío el reverendo Juan, por sus oraciones, sus cartas y su alegría, también me gustaría agradecer a mis tías Loli, Carmen Pérez, Carmen Serna y Basilisa y a mis tíos David y Antonio, a mis primas Trini, Fina, Clementina y a mis primos Clementino y Jesús, por la ayuda y el apoyo que desde siempre me habéis prestado. Habéis estado en los momentos más importantes, los más felices y los más tristes de mi vida. Cuando más lejos me encontraba de casa más cerca hacíais que me sintiera, muchas gracias.

He tenido la suerte tener un núcleo familiar muy fuerte, desde siempre hemos estado todos muy unidos y las alegrías y penas de cualquiera de nosotros también lo eran para el resto. Vosotros sois todo lo que soy y si empezara a escribir todo lo que debo agradecer esta parte de mi tesis superaría sin duda la tesis de Matías Navarro del Doctor Juan, así que tendré que abreviar:

En primer lugar están mi MamaTrini y PapaJuan, gracias por que a pesar de mi corta edad tuvisteis mucha confianza en mí.

A mis abuelitos Joaquín y Ángeles os quiero dar las gracias por haber centrado vuestras vidas en mí, gracias porque “vuestras vidas fueran para nosotros”, sólo os pido que el día de mi tesis estéis como siempre imaginé que estuvierais en primera fila escuchando y ayudando a vuestra nieta.

A mis hermanos Juan y Pedro quiero agradecerles el que siempre fuerais el modelo a seguir, excepto claro en el punto en que mis pentagramas son las membranas y las notas los péptidos, siempre habéis estado cuando os he necesitado y ni la distancia en el espacio o en la edad han supuesto una barrera para nosotros, vosotros me habéis inculcado el ansia por saber y aprender y habéis ayudado a completar la formación en humanidades que a los científicos nos falta.

A Pamela, por que poco a poco te has ido convirtiendo en la hermana que siempre quise tener.

A mis queridas Clarita y Aurorita, las niñas más guapas del mundo, muchas gracias por regalarme vuestra felicidad y alegría.

A D. Pedro de la Tejera, mi padre, quiero agradecerle todo su esfuerzo para procurarme la mejor formación y los mejores medios para convertirme en lo que soy, gracias también por enseñarme el valor y la importancia del trabajo y el esfuerzo. Por último quiero agradecerle a mi madre todo, el ser mi amiga, compañera, con la que he compartido los momentos más felices y duros de mi vida. Gracias papás por apoyarme en todas las decisiones de mi vida y tener fe en mí, esta tesis no es mía, sino vuestra.

Carlos, no me he olvidado de ti. Esta tesis se la he dedicado a las personas más importantes de mi vida y por supuesto tú también eres una de ellas. Estas palabras que te escribo no son sólo para agradecerte todo el ánimo, la confianza, las correcciones de inglés y alemán, o los artículos bajados, que me han ayudando a elaborar esta tesis, sino sobretudo por este viaje tan maravilloso que emprendimos hace 4 años en Santander. Muchas gracias por aguantarme con mis defectos y esos momentos tan horribles que me ha tocado vivir, creo que no hubiera podido superarlos sin ti. A lo largo de estos años hemos ido cambiando y evolucionando progresivamente, hemos superado la distancia Alicante-Madrid y los 7 meses de Austria, ahora sólo nos quedan 2 retos más, los doctorados y las despedidas, y me he propuesto acabar lo antes posible con ambos.

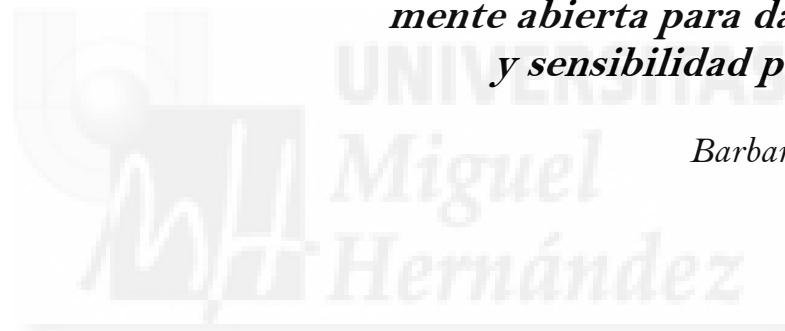
Juan Hernández



A mis abuelitos

*“Para investigar hace falta tiempo para mirar,
paciencia para oír lo que el material te dice,
mente abierta para darle cabida
y sensibilidad por lo vivo”*

Barbara McClintock



ABREVIATURAS

ACE2	Enzima convertora de angiotensina 2
CD	Dicroísmo Circular
Chol	Colesterol
CLDN1	Claudinina 1
Di-8-ANEPPS	1-(3-sulfonatopropyl)-4- $\left[\text{b} \left[2-(\text{di-}n\text{-octylamino})-6\text{-naphthyl} \right] \text{vinyl} \right]$ pyridinium betaina
DMPA	1,2-Dimiristil- <i>sn</i> -glicero-3-ácido fosfatídico
DMPC	1,2-Dimiristil- <i>sn</i> -glicero-3-fosfocolina
DMPG	1,2-Dimiristil- <i>sn</i> -glicero-3-[fosfo-rac-(1-glicerol)]
DMPS	1,2-Dimiristil- <i>sn</i> -glicero-3-fosfoserina
DNA	Ácido desoxirribonucleico
DO	Densidad óptica
DOPC	1,2-Dioleoil- <i>sn</i> -glicero-3-fosfocolina
DPH	1,6-Difenil-1,3,5-hexatrieno
DSC	Calorimetría diferencial de barrido
EL	<i>Extracellular loop</i>
EPA	Ácido fosfatídico de yema de huevo
FP	Péptido de fusión
GUV	Vesículas unilamelares gigantes
H _I	Fase hexagonal-H _I
H _{II}	Fase hexagonal invertida-H _{II}
HIV	Virus de la inmunodeficiencia humana
HCV	Virus de la Hepatitis C
HCVpp	Pseudopartículas de HCV
HDL	Lipoproteínas de alta densidad
IFP	Péptido de fusión interno
INF	Interferón
ILA	Asociación interlamelar

IRES	<i>Internal Ribosome Entry Site</i>
ISDR	<i>Interferon sensitivity determining region</i>
K_p	Coeficiente de partición
K_{SV}	Constante de Stern Volmer
L_α	Fase lamelar líquido-cristalina
L_β	Fase lamelar gel
$L_{\beta'}$	Fase lamelar gel inclinada
$L_{\beta I}$	Fase lamelar gel interdigitada
L_c	Fase cristalina
L_o	Fase líquido-ordenada
LDL	Lipoproteínas de baja densidad
LEL	Large extracellular loop
LPC	Lisofosfatidilcolina
LUV	Vesículas unilamelares grandes
MAS	<i>Magic angle spinning</i>
MHV	Virus de la hepatitis murina
MLV	Vesículas multilamelares
MLV	<i>Murine Leucemia Virus</i>
MVV	Vesículas multivesiculares
NBD-PE	N-(7-Nitrobenz-2-oxa-1,3-diazol-4-il)-1,2-dihexadecanil-snglicero-3-fosfoetanolamina Lissamine rhodamina B 1,2-dihexadecanil-sn-glicero-3-fosfoetanolamina
NS	Proteínas no estructurales
ORF	<i>Open reading frame</i>
PA	Ácido fosfatídico
PA-DPH	Ácido propiónico 1,6-difenil-1,3,5-hexatrieno
$P_{\beta'}$	Fase lamelar gel ondulada
PC	Fosfatidilcolina
PE	Fosfatidiletanolamina
PG	Fosfatidilglicerol

PI	Fosfatidilinositol
POPC	1-Palmitoil-2-oleil- <i>sn</i> -glycero-3-fosfocolina
PS	Fosfatidilserina
PreTM	Región pretransmembrana
RBD	<i>Receptor binding domain</i>
RBV	Ribavirina
RT-PCR	Transcripción inversa y reacción en cadena de la polimerasa.
RE	Retículo endoplasmático
RNA	Ácido ribonucleico
RMN	Resonancia magnética nuclear
SEL	<i>Small extracellular loop</i>
SARS	Síndrome respiratorio agudo severo
SIDA	Síndrome de la inmunodeficiencia adquirida
SM	Esfingomielina
SUV	Vesículas unilamelares pequeñas
T _c	Temperatura de inicio de la transición de fase gel a líquido cristalina
T _H	Temperatura de transición de fase lamelar a fase hexagonal-H _{II}
T _m	Temperatura de transición principal
TBEV	Virus de la encefalitis terminal de garrapata
TM	Región transmembrana
TMA-DPH	1-(4-Trimetilamoniofenil)-6-fenil-1,3,5-hexatrieno
TMC	Contacto trans-monocapa
VLDL	Lipoproteínas de muy baja densidad
VSV	Virus de la estomatitis vesicular
5NS	Ácido 5-doxil-esteárico
16NS	Ácido 16-doxil-esteárico

ÍNDICE

Abreviaturas.....	15
Índice.....	18
Resumen/Abstract.....	21
CAPÍTULO I: Introducción general.....	29
1.- Membranas Biológicas.	31
1.1.- Composición de la membranas cas.....	32
1.2.- Composición lipídica y clasificación de los lípidos.....	33
1.3.- El polimorfismo lipídico.....	37
1.4.- Estructura de la bicapa lipídica.....	40
1.5.- Procesos de fusión de membranas.....	42
1.6.- Lípidos implicados en la fusión de membranas virales.....	45
2.- Proteínas de fusión víricas.....	47
3.- Hepatitis C.....	50
3.1.- La enfermedad.....	50
3.2.- Genotipos de HCV.....	51
3.3.- El tratamiento.....	53
3.4.- Tratamiento futuro.....	54
3.5.- HCVpp.....	55
3.6.- Replicación en cultivo del HCV.....	55
3.7.- Receptores del HCV.....	57
3.8.- Ciclo viral del HCV.....	59
3.9.- Organización genómica.....	61
3.10.- Proteína Core.....	62
3.11.- Glicoproteínas E1 y E2.....	64
3.12.- Proteína P7.....	67
CAPÍTULO II: Metodología General.....	69
2.1.- Sistemas modelo de membrana.....	71
2.2.- Espectroscopia Infrarroja.....	73
2.3.- Dicroísmo circular.....	77
2.4.- Calorimetría diferencial de barrido.....	79
2.5.- Fluorescencia.....	81
2.5.1.- Cálculo del coeficiente de partición.....	82
2.5.2.- Ensayos de atenuación de fluorescencia.....	83
2.5.3.- Ensayos de transferencia de energía (FRET).....	84

2.5.4.- Ensayos de mezclas de lípidos (Hemifusión y Fusión).....	85
2.5.5.- Ensayos con dominios de dehidroergosterol.....	85
2.5.6.- Anisotropía con sondas extrínsecas.....	86
2.5.7.- Estudios del potencial electrostático.....	87
2.5.8.- Estudio del potencial bipolar.....	89
2.6.-Resonancia magnética nuclear.....	90
2.6.1- Resonancia magnética nuclear de rotación en MAS.....	91
2.7.- Difracción de Rayos X.....	92
CAPÍTULO III: Objetivos y presentación del trabajo.....	97
CAPÍTULO IV: Anexo de publicaciones aceptadas.....	103
1.- Hepatitis C virus core protein binding to lipid membranes: the role of domains 1 and 2.....	105
2.- Identification of the membrane-active regions of HCV p7 protein. Biophysical characterization of the loop region.....	119
3.- The membrane-active regions of the Hepatitis C virus E1 and E2 envelope Glycoproteins.....	135
4.- Interaction of the most membranotropic region of the HCV E2 envelope glycoprotein with membranes.....	151
5 - The pre-transmembrane region of the HCV E1 envelope glycoprotein. Interaction with model membranes.....	167
CAPÍTULO V: Anexo de publicaciones en proceso de aceptación	181
6.- Biophysical characterization of the fusogenic region of E1 envelope glycoproteins from HCV.....	183
7.- Effect of the pre-transmembrane region of the HCV E1 envelope glycoprotein. On DEPE polymorphism.....	199
8.- Searching of HCV inhibition viral-cell fusion.....	215
CAPÍTULO VI: Resultados.....	231
CAPÍTULO VII: Discusión.....	243
CAPÍTULO VIII: Conclusiones.....	248
CAPÍTULO IX: Bibliografía.....	255

RESUMEN

El virus de la hepatitis C (HCV) es el agente causal de enfermedades hepáticas humanas tanto crónicas y como agudas, incluyendo entre éstas, hepatitis crónicas, cirrosis y hepatocarcinomas (Penin et al., 2004; Tan et al., 2002). En todo el mundo hay entre 170 y 300 millones de infectados por este virus. A pesar de su gran incidencia, no existe vacuna alguna que pueda evitar la infección viral y los agentes terapéuticos no son suficientemente eficientes para contrarrestar la enfermedad (Qureshi, 2007). El genoma viral del HCV es muy heterogéneo, por ello las regiones envueltas en los procesos de fusión de membrana o la morfogénesis de los viriones previo a la entrada y salida del virus, ambos procesos requieren interacción de las proteínas virales con las membranas, cobran en este virus más importancia, ya que las regiones implicadas en estos procesos están más conservadas en todas las estirpes. Nos propusimos como primer objetivo encontrar las regiones membranotrópicas de las proteínas estructurales del HCV para utilizarlas como dianas contra las que buscar inhibidores de interacción entre la proteína y las membranas. Esta nueva estrategia puede permitirnos encontrar nuevos agentes terapéuticos contra el HCV. Las proteínas estructurales del HCV son: la proteína *core*, la cual forma la nucleocápsida viral y las glicoproteínas de la envuelta *E1* y *E2* y la proteína *p7*.

La proteína *core* está altamente conservada entre las diferentes estirpes de HCV (Cha et al., 1992). Esta proteína tiene varias funciones, sin embargo su misión más importante es el ensamblaje de los viriones y la salida viral. Nosotros hemos analizado e identificado las regiones 29-46, 57-74, 85-123 y 155-172 como las regiones membranotrópicas de la proteína *core*. Futuros estudios tomando como dianas estas regiones podrían permitir el desarrollo de nuevas estrategias antivirales basadas en inhibidores del ensamblaje viral.

La proteína *p7* es esencial para el ensamblaje y la salida eficiente de los viriones, indicando que *p7* está involucrada en la fase tardía del ciclo de replicación viral (Steinmann et al., 2007). Nosotros hemos identificado el dominio del bucle entre las hélices como la región más membranotrópica de la proteína. Un péptido de 18 aminoácidos de longitud

derivado de este dominio mimetiza la formación de poros cuyo tamaño está comprendido entre 6 y 23 Å, el mismo diámetro de poro que debería formar la proteína nativa. Por ello esta región puede ser esencial para la actividad del canal. De acuerdo con los resultados obtenidos, el bucle de *p7* podría ser un buen candidato para desarrollar nuevas estrategias antivirales dirigidas a la fase tardía del ciclo viral.

Las glicoproteínas de la envuelta viral *E1* y *E2* son proteínas de fusión truncadas de clase II. (Garry and Dash, 2003). Para estudiar las bases estructurales de la fusión de membranas del HCV e identificar nuevas dianas para buscar inhibidores de fusión hemos realizado un análisis de las diferentes regiones de las glicoproteínas de la envuelta *E1* y *E2*, las cuales interactúan con las membranas fosfolípicas (Lavillette et al., 2006). Tras la localización de las regiones fusogénicas, hemos realizado una exhaustiva caracterización de la interacción de ellas con sistemas modelo de membrana. Hemos encontrado la región 603-634, como una de las regiones más fusogénicas de la proteína *E2*, la cual puede estar implicada en el proceso de fusión afectando la estructura de la membrana y ayudando en el proceso de fusión al péptido de fusión para perturbar la topología y desestabilizar la membrana del endosoma. Esto podría implicar que ambas proteínas *E1* y *E2* estarían directamente implicadas en el mecanismo que hace posible la entrada del virus a la célula huésped. Hemos propuesto el segmento 309-340 de la glicoproteína *E1*, localizado inmediatamente adyacente al dominio TM, como dominio implicado en la fusión de manera similar a los dominios PreTM de las proteínas de fusión de clase I. Un péptido derivado de esta región es capaz de unirse a la superficie de la membrana con alta afinidad y modular las propiedades biofísicas de los fosfolípidos. Su localización en la superficie le permitiría perturbar la arquitectura y desestabilizar la membrana de la envuelta viral. Para los sistemas modelo de membranas basadas en DEPE en presencia del péptido la temperatura a la cual la transición entre fase líquido cristalina y hexagonal ocurre disminuye, debido a que el péptido estabilizaría estructuras de membrana no lamelares. Estos datos sugieren que la región de *E1* donde se localiza el péptido preTM puede ser fundamental para el proceso de fusión. Hemos localizado el péptido de fusión de HCV, tanto por homología con otros péptidos de fusión de otras proteínas de clase II, como experimentalmente por actividad fusogénica, en la región 274-298. Hemos observado que un péptido derivado de esta región perturba la membrana y se inserta en la interfase de la

bicapa lipídica. El péptido muestra, al igual que las HCVpp, un incremento en su efecto fusogénico con la presencia de colesterol. Péptidos derivados de esta región estabilizan estructuras no lamelares de membrana, como la fase hexagonal que aparece a una temperatura inferior a la esperada en presencia de péptido. Esta región también podría ser esencial durante el proceso de fusión.

Hemos estudiado diferentes regiones membranotrópicas que están directamente implicadas en el proceso de fusión. La hipótesis de partida es que si estas regiones no interaccionan con la membrana, el proceso de fusión podría no suceder y por ello el virus no entraría en la célula. Hemos intentado evitar la interacción de estas regiones membranotrópicas con otros péptidos derivados de las glicoproteínas de la envuelta. Después de varias búsquedas hemos encontrado dos péptidos inhibidores contra el péptido de fusión que reducen un 93% y 98% *in vitro* el efecto fusogénico de su diana. Tras esto, hemos ensayado *in vivo* la neutralización de la infección de estos péptidos por medio de HCVpp que expresan en la superficie las glicoproteínas de la envuelta *E1* y *E2*, mimetizando la entrada del HCV a la célula. Los péptidos inhibidores E15 y F28 neutralizaron un 51% y 36% respectivamente la infección de HCVpp de la estirpe 1BCG a una concentración de 0.1mM. Actualmente nos encontramos intentando aumentar la afinidad del inhibidor por la región diana, sin embargo lo más importante es que un estudio exhaustivo de la interacción lipido-péptido posibilitaría el desarrollo de compuestos anti-HCV dirigidos a evitar la infección viral. Además las regiones membranotrópicas determinadas en este trabajo podrían ser utilizadas como dianas terapéuticas permitiendo el desarrollo de nuevas vacunas.



ABSTRACT

Hepatitis C virus (HCV) is the leading cause of acute and chronic liver disease in humans, including chronic hepatitis, cirrhosis, and hepatocellular carcinoma (Penin et al., 2004; Tan et al., 2002). There is no vaccine to prevent the HCV infection and current therapeutic agents have had a limited success against HCV infection (Qureshi, 2007). The HCV genome is widely heterogeneous; therefore, the regions implicated in fusion and/or budding have important significance because they are the most conservative region along the virus sequence. Finding protein-membrane and protein-protein interaction inhibitors should be a good strategy against HCV infection as they might become in potential therapeutic agents. The structural proteins of HCV consist of the *core* protein, which forms the viral nucleocapsid, the envelope glycoproteins *E1* and *E2*, both of them transmembrane proteins and the *p7* protein.

The HCV *core* protein is well conserved among the different HCV strains (Cha et al., 1992). This protein has many functions, although one of the most important is its implication in the budding process. We have analysed and identified regions 29-46, 57-74, 85-123 and 155-172 as the most membrane-active regions of the HCV *core* protein. Future studies of these regions could be important for understanding the molecular mechanism of viral budding as well as making possible the future development of HCV assembly inhibitors which may lead to new vaccine strategies.

Protein *p7* is essential for the efficient assembly and release of infectious virions indicating that *p7* is primarily involved in the late phase of the virus replication cycle (Steinmann et al., 2007). We have reported the identification of a membranotropic region in *p7* coincidental with the loop domain of this protein. One peptide from this domain forms pores whose size is comprised between 6 and 23 Å, which is a similar pore diameter that the pore formed by the native protein. Therefore this protein domain may be essential for the formation of the active ion channel. Accordingly, the *p7* loop appears to be an attractive candidate for antiviral drug development leading to new vaccine strategies.

The HCV envelope glycoproteins *E1* and *E2* are truncated class II fusion proteins (Garry and Dash, 2003). To investigate the structural basis of HCV membrane fusion and identify new targets for searching new fusion inhibitors, we have carried out the analysis of the different regions of HCV *E1* and *E2* envelope glycoproteins which might interact with phospholipid membranes. After the location of the fusion domain we have made an in-depth biophysical characterization of their interaction with the membrane. We propose the region 603-634, one of the most *E2* fusogenic region, to be implicated in the fusion process, affecting the structure of the membrane and helping in the fusion process to the fusion peptide in the disruption the membrane topology and destabilization the target membrane. We have proposed the segment encompassing residues 309-340 of the HCV *E1* glycoprotein, another region implicated in the fusion process, in a similar way than the PreTM domain of class I fusion proteins (Guillen et al., 2007; Sainz et al., 2005; Suarez et al., 2000). The peptide binds to the membrane surface and modulates the phospholipid biophysical properties, is located in the membrane surface and perturbs significantly the bilayer architecture. We suggest that the *E1* region where the *E1*_{PTM} peptide is located might be a fusion determinant and probably has an essential role in the membrane fusion process. If that were true, it would imply that both HCV *E1* and *E2* glycoproteins are directly implicated in the mechanism that makes possible the entry of the HCV virus into its cellular host. We have located the fusion peptide of HCV in the region 274-298 in the *E1* glycoprotein. We have observed that the peptide disturbs the membrane and it is inserted into the lipid bilayer interphase. The peptide showed, similarly to HCVpp, an increased fusogenic effect in the presence of cholesterol as well as it stabilised non-lamellar structures in the membrane. This region might be essential for the assistance and enhancement of the viral and cell fusion process.

As a working hypothesis, if these membranotropic regions of the proteins would not interact with the membrane, the fusion process could not happen, and therefore the virus could not enter into the host cell. We have tried to prevent the interaction of these membranotropic regions with the membrane by using other peptides from the envelope glycoproteins which might interact between them. After several screenings, we have found two peptides directed against the fusion peptide region that reduced about 93% and 98% the leakage and hemifusion effect of the target. We have assayed *in vivo* the entry

neutralization of these two peptides using HCVpp that express *E1-E2* envelope glycoproteins. We have found that the peptide inhibitors E15 and F28 neutralized about 51% and 36 % respectively, the infection of 1BCJ HCVpp at a concentration of 0.1 mM. The affinity of the inhibitor for the target could be improved, but the most important fact is that we have found with an exhaustive study of lipid-peptide interactions, the possibility of the future development of anti-HCV drugs targeted to viral entry. The membranotropic regions we have found could be used as new targets, as inhibition of their interaction with the membrane could lead to new vaccine strategies.







CAPÍTULO I

INTRODUCCION GENERAL



1. Membranas biológicas

El cuerpo humano está compuesto por millones de células subdivididas en más de doscientos tipos celulares, todas ellas compuestas de membranas lipídicas. Las membranas biológicas constituyen un elemento esencial en la vida de los organismos puesto que no sólo le confieren a las células sus características de individualidad al separarlas de su entorno, sino que al mismo tiempo cumplen una serie de funciones biológicas fundamentales para la misma. Mientras que en las células procarióticas existe un único compartimento generado por la membrana plasmática, en las células eucarióticas además de la membrana plasmática existen una gran variedad de membranas intracelulares que componen compartimentos cerrados u orgánulos, cada uno de los cuales presentan una especialización funcional. Las membranas biológicas establecen estructuras dinámicas en las que se desempeñan una gran cantidad de procesos y reacciones. Actúan como barreras de permeabilidad selectiva, regulando la composición iónica y molecular del medio intracelular permitiendo el mantenimiento de gradientes iónicos a ambos lados de la membrana (y por lo tanto el potencial de membrana) gracias a proteínas transportadoras; sirven como soporte de numerosas proteínas generando un ambiente óptimo para el desarrollo de una multitud de procesos funcionales e intervienen en procesos de señalización celular entre otras funciones. El mantenimiento de la integridad de las membranas resulta vital puesto que pequeñas modificaciones podrían tener fatales consecuencias para la vida de la célula. Procesos tan importantes como la regulación de la conversión de energía también tiene lugar en las membranas, donde la fotosíntesis, el transporte electrónico y la fosforilación oxidativa no podrían realizarse sin una organizada batería de enzimas que se disponen ordenadamente en ellas. Además de estos procesos, las membranas también juegan un papel central en las comunicaciones entre las células y su medio ambiente ya que son capaces de generar señales químicas o eléctricas y/o presentar receptores específicos para señales externas controlando de este modo el flujo de información entre las células.

1.1. Composición de la membrana biológica

Las membranas biológicas están compuestas por proteínas y lípidos unidos por interacciones no covalentes, y carbohidratos, aunque éstos están presentes en forma de glicolípidos o glicoproteínas. La composición, presencia y proporción de cada uno de estos elementos varía según el tipo de membrana, manifestando la gran variedad de funciones y procesos en los que pueden encontrarse implicadas y, por lo tanto, los requerimientos del ambiente en el que se encuentran. Sin embargo, presentan una unidad estructural básica que es la bicapa lipídica (Bangham and Horne, 1964). El modelo de bicapa lipídica propone que los lípidos se hallan ordenados en bicapas generando la matriz donde se distribuyen las proteínas que pueden ser extrínsecas (interaccionan superficialmente con la bicapa) o integrales (interaccionan con la bicapa en profundidad) (Figura 1.1). La distribución de los lípidos y las proteínas es asimétrica generando diferencias en ambas hemicapas. En la bicapa lipídica, las moléculas lipídicas presentan movilidad pudiendo difundir rápidamente en el plano de la membrana (difusión lateral), encontrarse en constante movimiento rotacional, o en menor medida en difusión transversal o flip-flop, dotando de este modo a la bicapa de fluidez y flexibilidad. El grado de fluidez de la membrana viene, definido por la longitud de las cadenas hidrocarburadas y por el grado de insaturación de los ácidos grasos constituyentes. En este modelo de membrana también se postula que las proteínas que penetran la membrana (integrales) presentan aminoácidos con cadenas laterales hidrofóbicas, mientras que las proteínas periféricas o extrínsecas presentan aminoácidos con cadenas laterales esencialmente hidrofílicas en sus superficies interaccionando mediante interacciones electrostáticas con la superficie de la bicapa. Las proteínas, siempre que no presenten interacciones especiales, pueden

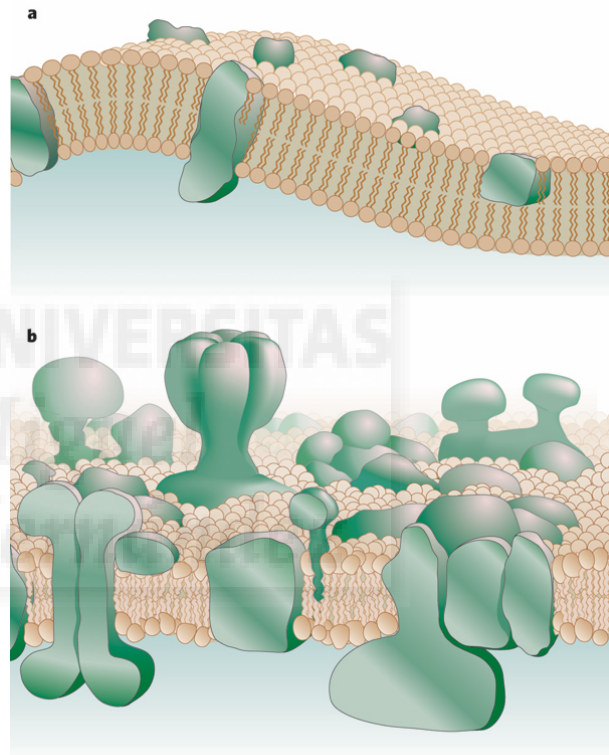


Figura 1.1. (A) El modelo de mosaico fluido propuesto por Singer y Nicholson en 1972. (B) Nuevo modelo super-red.

difundir lateralmente, pero no son capaces de pasar de un lado a otro de la membrana. Sin embargo, el modelo clásico de mosaico fluido de Singer y Nicholson (1972) (Figura 1.1) postulaba que tanto los lípidos de la bicapa como las proteínas eran libres de difundir, hoy en día sabemos que la estructura lateral de una membrana es mucho más compleja y refinada, y que los lípidos no tienen libertad total de difundir lateralmente ya que la distribución lateral de lípidos y proteínas es heterogénea y muy compleja (Ohvo-Rekila et al., 2002). Los datos disponibles en la actualidad proponen un nuevo modelo, denominado modelo de super-red o supertrama (o de distribución irregular). Este modelo propone que la distribución lateral de los lípidos en la membrana sigue un patrón regular en el que las fuerzas responsables de la distribución lateral serían tanto atractivas (interacciones de Van der Waals positivas) como de repulsión (impedimentos estéricos, repulsión electrostática, etc.) (Sommerharju et al., 1999).

1.2. Composición lipídica y clasificación de lípidos

Dentro de la célula, los diferentes compartimentos membranales presentan diferentes composiciones lipídicas, las cuales vienen reguladas por el metabolismo lipídico local y el sistema de transporte lipídico (Cho & Stahelin, 2005). Los lípidos forman un grupo muy heterogéneo de sustancias que tienen en común su baja solubilidad en agua.

Los principales tipos de lípidos que se pueden encontrar en las membranas biológicas son: glicerosfolípidos, glicoglicerolípidos, esfingolípidos y esteroides.

-*Glicerosfolípidos*, también denominados fosfoglicéridos o fosfolípidos, son los lípidos más abundantes de las membranas. En estos lípidos uno de los grupos hidroxilo de la

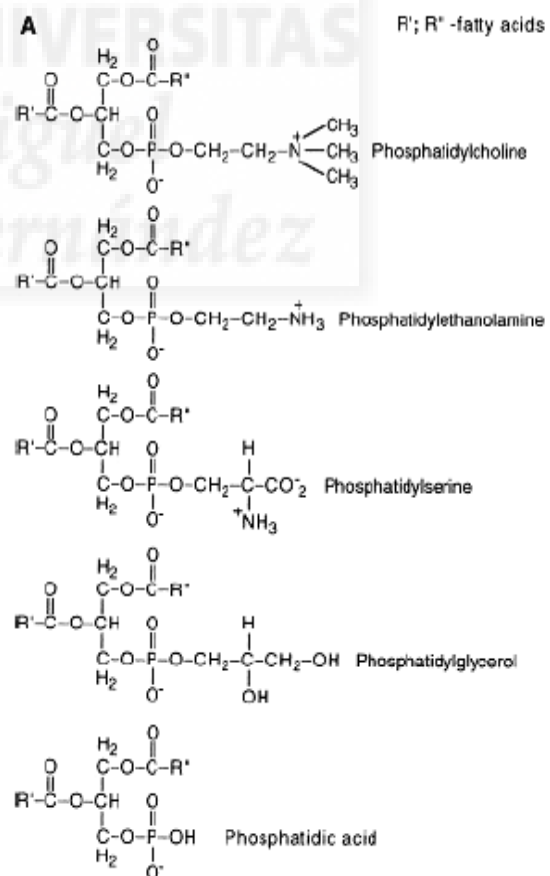


Figura 1.2. Ejemplo de algunas estructuras químicas de las cabezas polares de las moléculas de fosfolípido. (Bach & Wachtel, 2003))

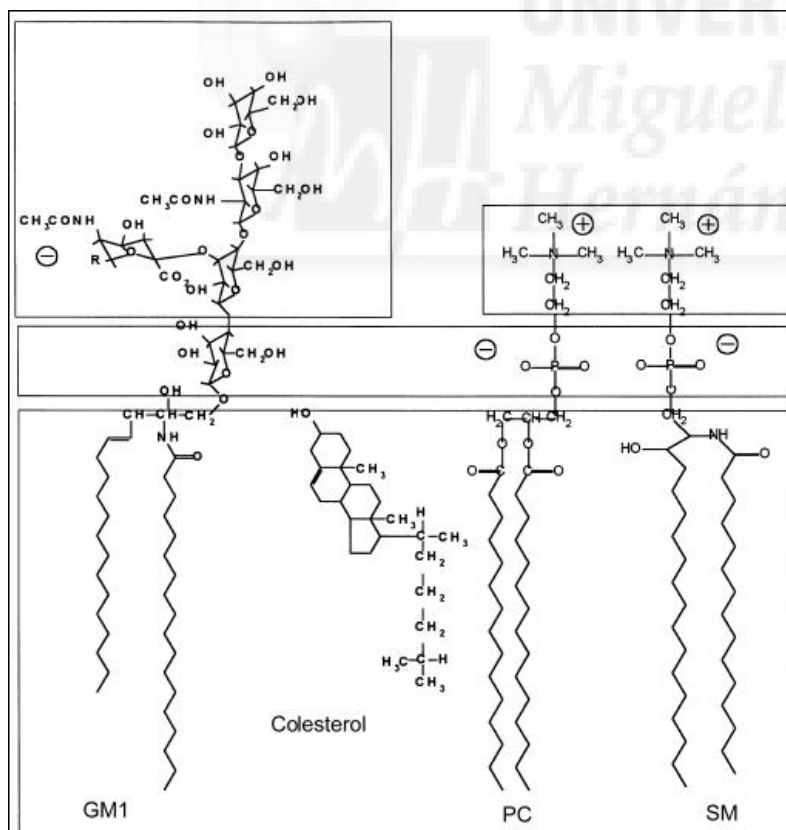
molécula de glicerol se une a un grupo polar que contiene fosfato y los otros dos grupos hidroxilo se unen a sendos grupos carboxilos de dos cadenas de ácidos grasos de cadena larga. Los fosfoglicéridos naturales, y en general todos los lípidos que se basan en un esqueleto de glicerol, se nombran sistemáticamente según la numeración estereoquímica *sn*. La mayoría de los fosfoglicéridos tienen el fosfato en la posición *sn-3* del glicerol. Cuando los otros dos grupos hidroxilo del glicerol se unen a ácidos grasos mediante un enlace éster se denominan 1,2-diacilfosfoglicéridos. Los 1,2-diacilfosfoglicéridos forman un grupo de moléculas muy amplio (Dowhan, 1997), que se diferencian según la longitud y la saturación de sus cadenas acílicas, y según el sustituyente unido al fosfato en posición *sn-3* del glicerol. En la Figura 1.2 se muestran las estructuras de varias cabezas polares de fosfolípidos a las que se puede unir el grupo fosfato.

La fosfatidilcolina (PC) es el fosfolípido más común en las membranas biológicas. La cabeza polar es zwitteriónica, y debido a la ausencia de donadores de enlaces de hidrógeno no es capaz de formar enlaces de hidrógeno entre sí. La fosfatidiletanolamina (PE), posee una cabeza polar zwitteriónica y al contrario que las PCs, éstas forman enlaces de hidrógeno entre ellas. Las moléculas de PE se pueden ensamblar de tres formas diferentes: fase lamelar gel, fase lamelar líquido-cristalina y fase hexagonal, la cual se forma a temperaturas altas. La fosfatidilserina (PS) se encuentra en la mayoría de membranas de mamíferos, siendo el fosfolípido negativo más abundante. A pH neutro, la PS tiene una carga negativa de -1: una carga negativa en el grupo carboxilo, una segunda en el grupo fosfato y una carga positiva en el grupo amino. Las cabezas polares tienen tanto donadores como aceptores de enlaces de hidrógeno, pudiendo así formar enlaces de hidrógeno entre ellas, lo que permite al fosfolípido tener temperaturas de transición altas. El ácido fosfatídico (PA) tiene una carga de -1 a pH neutro. Como en el caso de la PS, la PA se estabiliza por la formación de enlaces de hidrógeno intermoleculares, lo que hace incrementar su temperatura de transición en comparación con la PC. El fosfatidilglicerol (PG) también tiene una carga negativa de -1 a pH neutro, debido a la ionización del grupo fosfato. Sin embargo, el PG no se estabiliza por la formación de enlaces de hidrógeno: su temperatura de transición es similar a la correspondiente con las PCs. Los fosfolípidos que contienen colina, la PC, se encuentran preferentemente en la monocapa externa, mientras que los lípidos que contienen aminas, como la PE y la PS se encuentran preferentemente localizados en la monocapa interna. La PC y la PS proporcionan superficies de membrana hidratadas o cargadas, permitiendo al agua e iones unirse a sus cabezas polares. En contraste, las superficies ricas en PE son hidrofóbicas, poco hidratadas y promueven interacciones entre superficies de membrana

diferentes sin la unión directa de proteínas. Puesto que la PE no se hidrata fácilmente, promueve la formación de estructuras de tipo no lamelar para compensar el efecto hidrofóbico, como se comentaba anteriormente. La inestabilidad inherente de este fosfolípido es necesaria en funciones celulares como la fusión de membranas.

-*Glicoglicerolípidos*, se diferencian de los glicerofosfolípidos en el sustituyente unido al hidroxilo del carbono *sn*-3 del esqueleto de glicerol. En los glicoglicerolípidos se forma un enlace glicósido con un carbohidrato, en vez de unirse a un fosfato como ocurre en los fosfoglicéridos. Los glicoglicerolípidos predominan en la membrana de los cloroplastos y también abundan en bacterias.

-*Esfingolípidos*, lípidos cuya unidad estructural es la ceramida. La ceramida está compuesta generalmente por esfingosina (4-esfingenina, un aminodiol transmonoinsaturado de 18 átomos de carbono) unida mediante un enlace amida a un ácido graso. Los diferentes tipos de



esfingolípidos se clasifican en función del grupo polar que se une al hidroxilo libre del carbono en posición 1 de la ceramida. Cuando el grupo polar es fosforilcolina, el esfingolípido se denomina esfingomiélinea (SM) (Figura 1.3), cuando se incorpora un azúcar simple son cerebrósidos, mientras que cuando es un oligosacárido más complejo, en el que además se incluye uno o más residuos de ácido siálico, se denominan gangliósidos (Figura 1.3).

Figura 1.3. Ejemplos de dos estructuras de esfingolípidos, Gangliósido (GM1) y esfingomiélinea (SM). Colesterol (Chol) y fosfatidilcolina (PC). (Langner & Kubica, 1999)

La SM es un componente fundamental de la membrana plasmática de las células eucariotas (Ramstedt and Slotte, 2002). En muchas células de mamíferos los contenidos de SM varían en un rango entre el 2 y el 15% de los fosfolípidos totales del organismo, dependiendo del tejido estudiado. La SM actúa como componente estructural de las membranas biológicas junto a otros fosfolípidos, glicolípidos, colesterol y algunas proteínas integrales de membrana. Adicionalmente a su función estructural también participa en procesos de señalización celular. La región interfacial de la SM tiene regiones donadoras yceptoras de enlaces de hidrógeno, comparado con la región correspondiente de la PC, la cual sólo contiene grupos aceptores de enlaces de hidrógeno (Ohvo-Rekila et al., 2002). Los esfingolípidos difieren de la mayoría de los fosfolípidos biológicos en que contienen cadenas acílicas largas y muy saturadas, esto les permite empaquetar fácilmente, esta propiedad da a los esfingolípidos temperaturas de fusión mucho mayores que las del resto de (glico)fosfolípidos de la membrana, que son ricos en cadenas acílicas insaturadas (Brown, 1998). Las diferentes capacidades de empaquetamiento de esfingolípidos y fosfolípidos son uno de los factores que contribuyen a la formación de dominios en la membrana.

-Esteroles, se encuentran en las membranas de las plantas, animales y microorganismos eucarióticos. En contraste con la gran diversidad de fosfolípidos, las células de mamíferos contienen un esteroles mayoritario, el colesterol, que es necesario para la viabilidad y la proliferación celular. El anillo plano de esteroles y la cola hidrofóbica orientan al colesterol dentro del núcleo de la membrana (Figura 1.3), mientras que el grupo 3- β -hidroxilo contribuye a las propiedades de la superficie de la bicapa (Villalain, 1996). El colesterol es soluble en todos los fosfolípidos, pero la carga negativa de las cabezas polares de los fosfolípidos negativos (PS, PA, PG y PI) reduce su solubilidad en ellas en comparación con los lípidos zwitteriónicos. La estructura del colesterol (Figura 1.3) le permite reducir la libertad de movimiento de las cadenas acílicas de los fosfolípidos, rigidificando así la membrana, lo que puede tener un impacto significativo en las funciones de membrana. La adición de colesterol en membranas aumenta la rigidez de la fase fluida y la adición de éste en membranas en fase gel aumenta la fluidez de la membrana, incluso puede conducir a la formación de fases líquido ordenadas (l_o). La importancia de la contribución del colesterol a las propiedades de la membrana se refleja en su distribución ubicua y su necesidad para el correcto crecimiento y función celular.

1.3. Polimorfismo lipídico

La importancia biológica del polimorfismo lipídico se pone de manifiesto en procesos tan diversos como la fusión de membranas, el tráfico de proteínas mediado por vesículas, el movimiento transversal de moléculas a través de la membrana, o la estabilización de complejos de proteínas de membrana (Cullis et al., 1978). Como polimorfismo lipídico se entiende la capacidad que poseen los lípidos para adoptar diferentes formas o “áreas de Van der Waals” dependiendo del área proporcional que represente la cabeza polar y la parte hidrofóbica dentro de la molécula, aunque la morfología que adoptan los lípidos al dispersarse en medios acuosos depende, entre otros, de la temperatura, de la presión, de la fuerza iónica y del pH (Cullis and de Kruijff, 1979). Las fases lipídicas pueden clasificarse según el tipo de red u organización de largo alcance, según el orden de las cadenas acílicas (fluidas o extendidas) y según la curvatura de la fase (normal o inversa). La nomenclatura más ampliamente utilizada es la propuesta por Luzzati (Luzzati and Husson, 1962), que se compone de una letra y un subíndice. En primer lugar, el tipo de orden de largo alcance se indica con una letra mayúscula: *L* unidimensional (lamelar), *H* bidimensional (hexagonal), *P* bidimensional oblicua, *Q* tridimensional cúbica y *C* tridimensional cristalina. La conformación de las cadenas hidrocarbúridas se indica mediante un subíndice

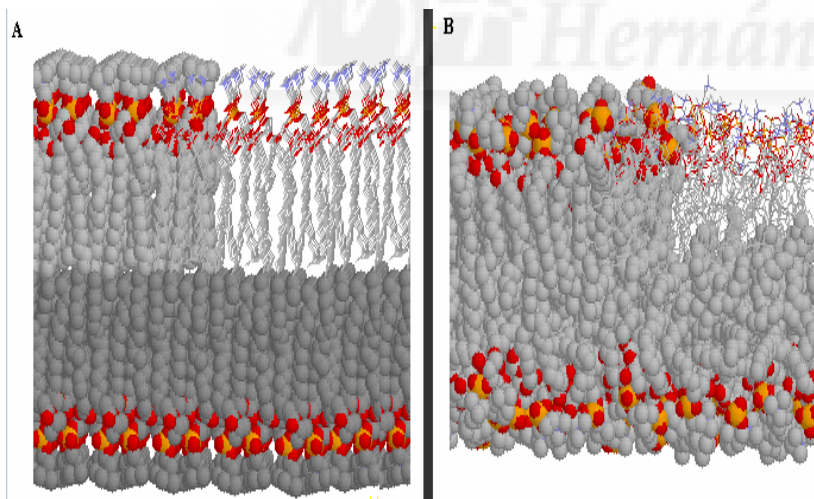


Figura 1.4. Disposición molecular propuesta para diferentes fases lamelares. (A), fase gel normal (L_{β}) y (B) fase líquido-cristalina, L_{α} (Marsh, 1980).

formado por una letra griega: α se refiere a cadenas acílicas desordenadas (fluido), β ordenadas (gel) y β' ordenadas inclinadas. Además, la organización lipídica puede ser de tipo I, cuando los elementos estructurales (lamelar, hexagonal, etc.) están rellenos con las cadenas

acílicas del lípido (interior hidrofóbico), o de tipo II (invertidas) cuando el disolvente acuoso está rodeado por una matriz hidrofóbica (interior hidrofílico). Las estructuras lipídicas de mayor relevancia biológica son las estructuras lamelares, hexagonales y cúbicas.

Las fases lamelares (L) o bicapas son estructuras periódicas en una dimensión que se pueden dividir, a su vez, en varios tipos de fases. Las más importantes son la fase gel y la fase fluida (Figura 1.4).

En la fase gel, las cadenas acílicas de los lípidos están rígidas y se empaquetan en redes bidimensionales cuasi-hexagonales, que se pueden disponer de tres formas diferentes: paralelas a la normal de la bicapa (L_{β}) (Figure 1.4A), inclinadas (L_{β}) (Figure 1.5), o interdigitadas (L_{β}) (Marsh, 1980). En la fase lamelar fluida (L_{α}) (Figura 1.4B), también denominada líquido-cristalina o líquido desordenada, se caracteriza por el desorden de las cadenas acílicas. En la fase L_{α} las moléculas difunden con mayor rapidez en el plano de la bicapa que en la fase gel y aumenta el área superficial por molécula de lípido y disminuye la anchura de la bicapa.

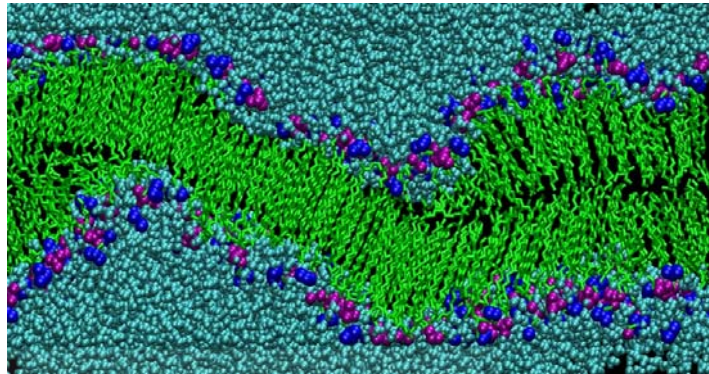


Figura 1.5. Disposición molecular propuesta para la fase gel inclinada (L_{β})

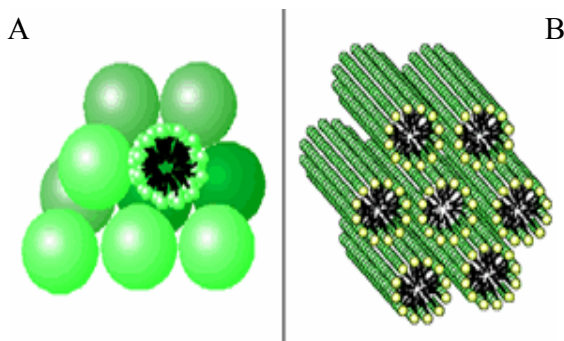


Figura 1.6. Representación de las estructuras propuestas para las (A) fase hexagonal normal (H_I) y (B) fase hexagonal invertida (H_{II}).

La fase hexagonal (H) es una estructura fluida periódica en dos dimensiones que consiste en cilindros paralelos empaquetados hexagonalmente y con una longitud mucho mayor que las dimensiones del lípido (tiende a una longitud infinita) (Figura 1.6). Las fases hexagonales más simples y mejor definidas son la normal e invertida H_I y H_{II} . En la fase H_I los lípidos se agregan en micelas circulares cilíndricas que se empaquetan en una red hexagonal (Figura 1.6A), con una región continua de agua que ocupa el volumen entre los cilindros. En la fase invertida (H_{II}) por otro lado, los cilindros contienen núcleos de agua rodeados por las cabezas polares del fosfolípido, con el restante volumen ocupado completamente por las cadenas hidrocarbonadas (Figure 1.6B). A pesar de que la fase

H_I es muy común en sistemas surfactantes simples, no suele formarse en diacil-fosfolípidos. La fase H_{II}, sin embargo, es muy común en lípidos como la fosfatidiletanolamina, con cabezas polares pequeñas y débilmente hidratadas con interacciones atractivas entre ellas (de Kruijff, 1997; Epend, 1998).

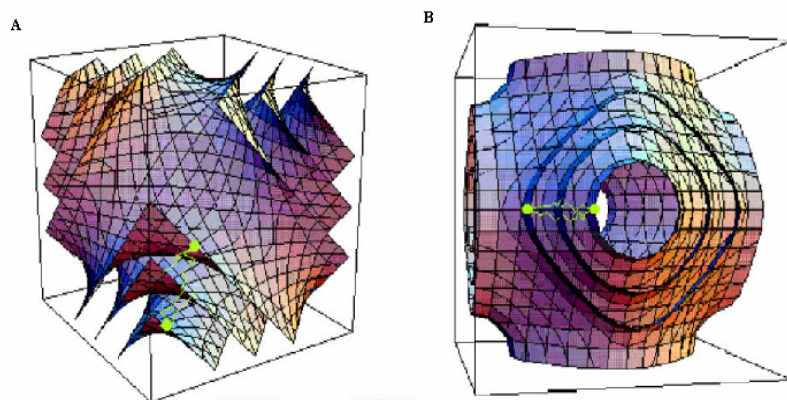


Figura 1.7. Representación de las estructuras propuestas para la fase cúbica bicontinua Q224 (A) y (B) fase cúbica bicontinua Q228. (Epend, 1998)

Las fases cúbicas (Q) son estructuras periódicas en tres dimensiones (Figura 1.7) Las fases cúbicas pueden ser bicontinuas, cuando la red tridimensional, es continua en lípido, o discontinuas, cuando la continuidad es de la fase acuosa (Luzzati, 1997).

La metodología idónea para identificar y caracterizar estructuras de membrana es la difracción de rayos X. Gracias al desarrollo de la radiación sincrotón ha sido posible usar la difracción de rayos X para estudiar el mecanismo de la transición de fase. Otra metodología complementaria es la calorimetría diferencial de barrido que permite obtener información termodinámica como la temperatura de transición y el cambio entálpico del proceso.

La geometría molecular de los lípidos también puede utilizarse como argumento para racionalizar su comportamiento de fase (Hafez and Cullis, 2001) (Figura 1.8). Aquellos fosfolípidos que presenten un área de cabeza polar proporcionalmente mayor al área de sus cadenas hidrocarbonadas tendrán una geometría tipo

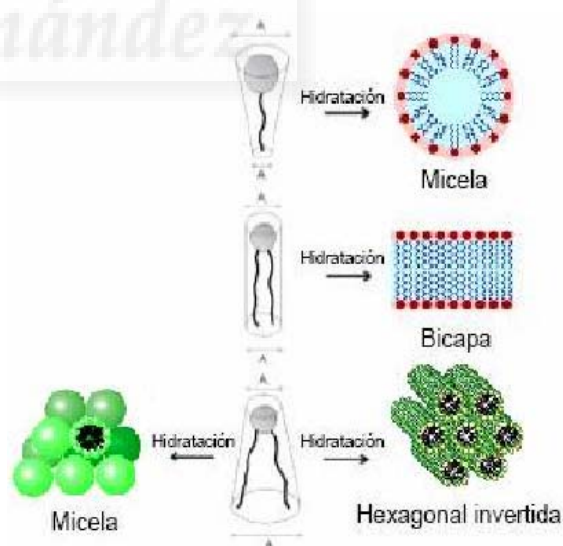


Figura 1.8 Posibles geometrías moleculares de los lípidos y su asociación preferencial en estructuras morfológicamente distintas (Hafez&Cullis, 2001).

cono (como es el caso de los lisofosfolípidos) y su tendencia natural será a formar micelas y estructuras con curvatura positiva. Los lípidos que presentan un área de cabeza polar similar a la de su región hidrocarbonada tendrán geometría cilíndrica, y se acoplarán formando bicapas. Los lípidos con cabezas polares que ocupen un área menor que la de sus cadenas acílicas (como las fosfatidiletanolaminas) tenderán a formar fases invertidas (como la fase hexagonal invertida, H_{II}) o fases cúbicas, que presentan curvatura negativa. Del mismo modo, mezclas complementarias de lípidos con diferente tendencia a formar estructuras con curvatura negativa y estructuras con curvatura positiva pueden adoptar estructuras de tipo bicapa (Hafez and Cullis, 2001).

La temperatura es un factor determinante de la fase en la que se encuentra el lípido. Esto es debido a que cada fosfolípido tiene una temperatura de fusión (T_m) característica, que es la temperatura a la que el lípido cambia su estado de fase, pasando de un estado ordenado tipo gel a un estado menos ordenado tipo líquido-cristalino que es el que usualmente está presente en las membranas biológicas. Los lípidos que se empaquetan de manera más compacta tienen mayores T_m , mientras que los lípidos que favorecen una fase fluida tienen menores T_m . La T_m de un lípido es altamente dependiente de la estructura de sus cadenas acílicas. La T_m aumenta cuanto mayor es la longitud de las cadenas y su grado de saturación, mientras que disminuye conforme aumenta el grado de insaturación, ya que los dobles enlaces en posición *cis* interfieren con el empaquetamiento lateral. Otro factor que afecta a la T_m es la cabeza polar, por ejemplo, los glicoesfingolípidos tienden a tener mayores T_m que los esfingolípidos (Koynova and Caffrey, 1995), debido a los enlaces de hidrógeno que se forman entre las cabezas polares de los glicoesfingolípidos.

1.4. Estructura de la bicapa lipídica

La estructura lamelar de las bicapas lipídicas es la conformación lipídica más habitual presente en las membranas biológicas. Las bicapas fluidas se dividen en una región interfacial y en una región central hidrocarbonada. En base a la estructura del 1,2- dioleil-sn-glicero-3-fosfatidilcolina (DOPC) en fase L_α , determinada por cristalografía de rayos X (Wiener and White, 1992), se ha determinado la distribución promediada de los grupos cuasi-moleculares que componen el fosfolípido a lo largo del eje transmembranal (Figura 1.9).

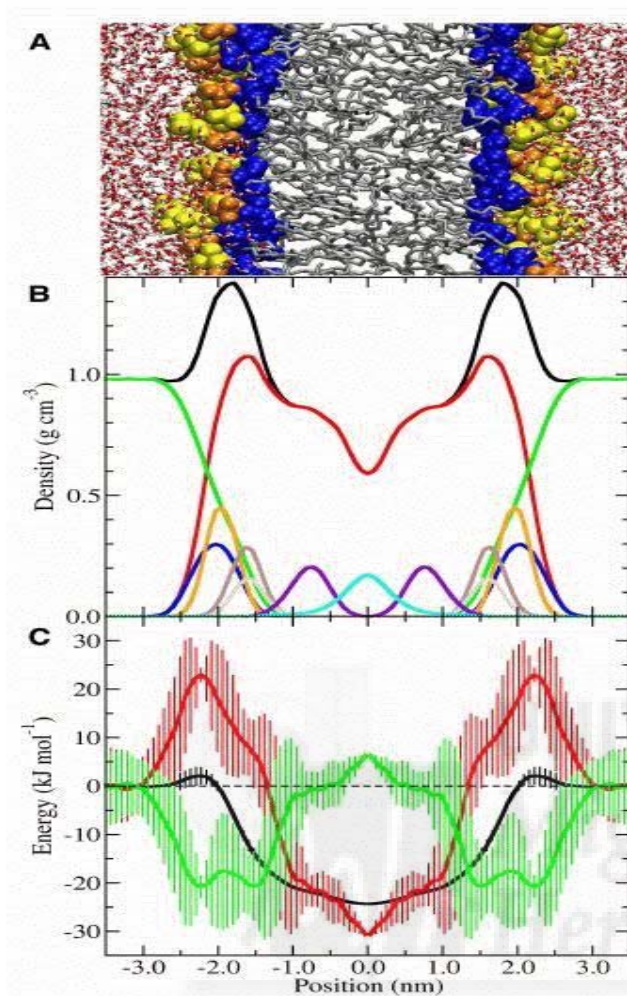


Figure 1.9 (A) Bicapa de DOPC. (B) Medida parcial del perfil de electrodensidad para varios grupos funcionales. Negro: densidad total, rojo: densidad lipídica, verde: densidad del agua, azul: densidad de la colina, naranja: densidad del grupo fosfato, marrón: densidad del glicerol, gris: densidad del grupo carbonilo, púrpura: densidad de los dobles enlaces, ciano: densidad de los metilos. (C) Energía libre de partición a hexano desde disolución acuosa, negro es la energía libre, rojo es el componente entrópico de energía libre $-T\Delta S$; verde es el componente entálpico de energía libre, ΔH . Las líneas verticales indican el error obtenido en las medidas

En la Figura 1.9 se puede observar como el espacio que abarca la interfase es aproximadamente el mismo que ocupa la región hidrofóbica (alrededor de 30\AA). La región de la interfase está compuesta por una mezcla compleja de agua, fosforilcolina, glicerol, carbonilos y grupos metileno, que ofrecen muchas posibilidades para formar interacciones no covalentes con péptidos y proteínas. La distribución del agua comienza a partir de la región del glicerol más cercana al centro de la bicapa y se hace máxima a medida que se aleja de la bicapa. El grosor de la interfase de cada una de las dos hemicapas de la bicapa (también denominadas monocapas) es de aproximadamente 15\AA , que tiene un tamaño suficiente como para acomodar una hélice α (diámetro $\sim 10\text{\AA}$) dispuesta de forma paralela

a la bicapa. Las interfases presentan una gran heterogeneidad química y tienen un gradiente de polaridad, que se reduce hacia el centro de la bicapa. Por lo tanto, la heterogeneidad química y los gradientes de polaridad que caracterizan a las interfases de las bicapas las convierten en un lugar ideal para que se produzcan interacciones con proteínas de membrana no constitutivas (Wiener and White, 1992).

1.5. Procesos de fusión de membranas

La fusión de membranas es un fenómeno universal que se ha incorporado a muchos procesos biológicos durante la evolución. Las reacciones de fusión de membranas están implicadas en multitud de procesos biológicos fundamentales, a pesar de las fuertes barreras energéticas implicadas, debidas a fuerzas de repulsión electrostáticas, de hidratación y de tipo estérico que están presentes en estos procesos (Chernomordik and Kozlov, 2003). En los sistemas biológicos, estas barreras energéticas se superan mediante el uso de proteínas de fusión, cuya función es disminuir la energía de activación del proceso. Se pueden distinguir al menos tres tipos de fusión:

-*Fusión extra- e intracelular de organismos patógenos con las células huésped*, como es el caso de los virus con envuelta, cuya membrana fusiona con la membrana celular mediante proteínas de fusión presentes en la membrana viral.

-*Fusión extracelular de células eucariotas*, como la fusión de los espermatozoides con los ovocitos o la formación de sincitios en las células musculares.

-*Fusión intracelular de organelas*. Estos procesos están mediados por complejos de proteínas pertenecientes a familias altamente conservadas, como por ejemplo, las proteínas del complejo *SNARE*, que participan en el proceso de la sinapsis.

A pesar de esta diversidad, todas las reacciones de fusión incluyen un proceso elemental que consiste en el contacto entre ambas membranas, la fusión de las membranas y la apertura de un poro de fusión (Jahn and Grubmuller, 2002). Las membranas deben aproximarse entre sí, superando las fuerzas electrostáticas que tienden a mantenerlas separadas para que los lípidos de las hemicapas externas puedan interaccionar. La interfase entre las regiones hidrofílica e hidrofóbica debe ser desestabilizada. Y por último, se generan estados de transición no-lamelares que culminan en la apertura del poro de fusión. Todos los estados de transición están gobernados por fuerzas que minimizan la exposición de las superficies no polares al agua y necesitan ser superadas para alcanzar los estados de transición metaestables que conducen a la fusión. Las membranas biológicas utilizan proteínas de fusión específicas para alcanzar este objetivo. Cómo estas proteínas consiguen fusionar membranas es uno de los principales enigmas

de la biología celular. Se han propuesto dos vías de acción opuestas que sugieren que el poro inicial puede ser principalmente proteico o lipídico. En el primer caso, el poro estaría formado por una proteína que atraviesa ambas membranas y formaría un anillo proteico que comunicaría el interior de ambas. Las proteínas actuarían sobre los lípidos en los puntos de contacto mediante la formación de estructuras diferentes a la bicapa que no podrían formarse en ausencia de estas proteínas. En el segundo caso, la fusión estaría mediada principalmente por los fosfolípidos. Los lípidos pueden jugar un papel importante en este proceso modulando la curvatura de la membrana o formando microdominios, como los *Rafts*. Las proteínas de fusión estarían implicadas en la disminución de la energía de activación del proceso. Este modelo asume que el poro está formado por fosfolípidos y que su formación debe estar en concordancia con las leyes físicas determinantes de las fases lipídicas (Jahn and Sudhof, 1999). De acuerdo al segundo caso de fusión, se han descrito varias versiones de un modelo de fusión conocido con el nombre de modelo de tallo (*stalk*) (Kozlov et al., 1989; Siegel, 1993; Siegel, 1999), el cual relaciona la fusión de membranas con el polimorfismo lipídico. Según el modelo original de tallo (Kozlov et al., 1989) la propensión que tienen las bicapas lipídicas para fusionar se basa en la capacidad que tienen las monocapas que la constituyen de doblarse o flexionarse, siendo las membranas más fusogénicas las que poseen curvatura negativa y positiva espontánea en las monocapas *cis* y *trans*, respectivamente (Basanez, 2002; Basanez et al., 2002).

El proceso de fusión consiste en una sucesión de pasos controlados. Comienza con la aproximación de las dos bicapas, la viral y la celular con una deshidratación local en el punto de contacto. Se piensa que la energía liberada durante los cambios proteicos estructurales hasta alcanzar la conformación más estable es usada para conducir la aposición de las membranas y la subsiguiente fusión de las bicapas. Esto podría aplicarse tanto a los procesos de fusión virales como a los intracelulares (Blumenthal et al., 2003). A la aposición inicial de membranas le sigue la fusión de las hemicapas externas (paso de la hemifusión). Tras esto se forma un intermediario de fusión llamado tallo (*stalk*) (Chernomordik and Kozlov, 2005), prosiguiendo la fusión de las hemicapas internas y la formación del poro. Esto permite la fusión de los compartimentos internos, por lo que el genoma viral es transferido al citoplasma de la célula huésped y la replicación viral puede comenzar (Figura 1.10).

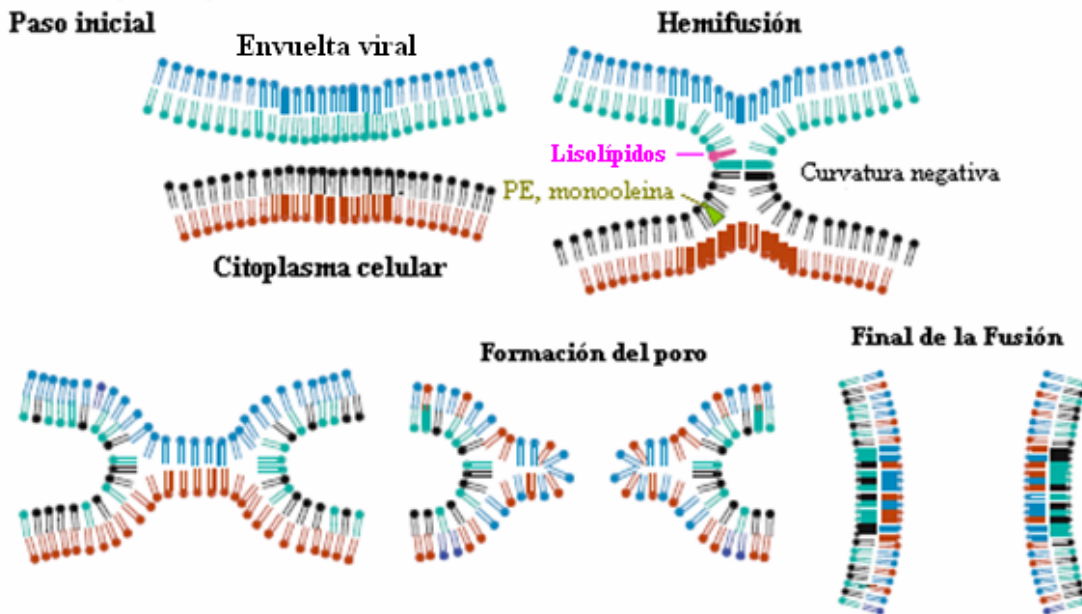


Figure 1.10. Esquema de la deformación de la membrana durante la fusión de membranas (las proteínas de fusión no están representadas). Las membranas virales y celulares primero se aproximan lo que permite el primer paso de la fusión de membranas, la hemifusión de las hemicapas externas. Este paso puede ser bloqueado por la presencia de lisofosfolípidos y promovido por la presencia de PE, colesterol o monooleínas. La mezcla de las hemicapas internas de las membranas termina con la formación de un poro de fusión temprano. Es en este punto donde el material genético viral es liberado al citoplasma celular.

Trabajos posteriores (Siegel, 1993, Siegel 1999) sugieren que el modelo de tallo original se contradice, ya que la estructura propuesta tendría regiones de baja densidad de lípido resultantes del espacio que queda libre entre las monocapas *cis* y *trans*. Estos espacios son energéticamente muy desfavorables de mantener, ya que requieren alta energía para crear una cavidad hidrofóbica dentro de las membranas fusogénicas, muy similar a la energía que promueve la transición de la fase lamelar a la fase H_{II} . Se piensa que dichas cavidades hidrofóbicas no favorecen la expansión de la región hemifusionada, por lo que el tallo se estancaría en una estructura local altamente hemifusionada, donde sólo existirían contactos de las monocapas *trans* (TMC, *trans monolayer contact*). Para favorecer la formación del poro, el intermediario TMC debería reconfigurarse para dar lugar a un acoplamiento interlamelar (ILA, *Interlamellar attachment site*), el cual vendría gobernado por la ruptura de tensión de la bicapa, la cual depende de la composición lipídica. De acuerdo con los cálculos realizados por Siegel, el poro de fusión (formación de ILA) se favorecería cuando las monocapas *trans* poseyeran curvatura espontánea negativa (Siegel, 1993; Siegel, 1999), no curvatura espontánea positiva

como se propone en el modelo original de tallo (Kozlov et al., 1989). Además, Siegel plantea que los ILAs son los precursores de las fases bicontinuas Q_{II} , y que el mecanismo de formación de los intermediarios de fusión es similar al mecanismo de formación de los precursores de las fases bicontinuas Q_{II} (Siegel, 1999). Estas consideraciones son consistentes con la alta fusogenidad de sistemas de membrana con curvaturas espontáneas negativas en ambas monocapas, y con la tendencia de tales dispersiones lipídicas para formar fases bicontinuas Q_{II} .

La hipótesis del tallo está apoyada por un gran número de evidencias que muestran que tanto la fusión viral como la de los liposomas se ve favorecida por la presencia en la cara *cis* de lípidos con tendencia natural a adoptar curvatura negativa (ejemplo, por PEs). La inclusión de fosfolípidos que disminuyesen los niveles de energía de los vacíos creados en los intermediarios de fusión (ejemplo, por largas cadenas acílicas), estabilizaría el estado de transición y favorecería la formación de un diafragma. Del mismo modo, compuestos que favorecen la formación de curvatura positiva (ejemplo, LPCs) son capaces de inhibir la fusión de membranas (Basanez et al., 2002). Recientemente se ha podido tener la primera evidencia de estructura del tallo o de TMC por análisis de tomografía electrónica de una delgadísima sección cónica de muestras de zonas activas de sinapsis corticales de rata (Zampighi et al., 2006). En resumen, el papel de los catalizadores de la fusión es acelerar este proceso, es decir, disminuir la energía de activación de la fusión. La desestabilización de la bicapa como resultado de la interacción de segmentos de proteínas de fusión con membranas provee un medio de disminuir las barreras energéticas. Un gran número de estudios muestran que péptidos sintéticos capaces de inducir la fusión de liposomas provocan también la desestabilización de la bicapa. Por lo tanto la maquinaria de fusión como los lípidos son necesarios para que la fusión ocurra.

1.6. Lípidos implicados en la fusión de membranas virales

La composición lipídica de las membranas animales es compleja, pero de los cuatro tipos de lípidos comentados anteriormente destacaremos algunos que pueden estar implicados en los procesos de fusión.

Dentro de los glicerofosfolípidos, la fosfatidiletanolamina está presente en un 20% en muchas membranas biológicas. Tiene una estructura molecular en forma de cono, lo que le permite promover transiciones de bicapa a fase hexagonal lo que podría facilitar la fusión por el

incremento en curvatura negativa de la membrana (Chernomordik and Kozlov, 2005; Siegel and Epan, 1997). La fosfatidilserina está mayoritariamente localizada en la hemicapa interna de la membrana plasmática y aparece en el membrana externa como señalización de apoptosis y coagulación sanguínea. Los lisofosfolípidos aparecen en la membrana por la metabolización de fosfolípidos por parte de la fosfolipasa A. Los lisofosfolípidos tienen forma de cono invertido que puede inhibir la formación del tallo de hemifusión cuando se encuentran presentes en la hemicapa externa al incrementar la curvatura positiva de la membrana (Chernomordik and Kozlov, 2005).

Dentro de los glicoesfingolípidos y esteroides, las membranas con esfingomiélin y colesterol forman microdominios líquido ordenados de la membrana plasmática llamadas balsas lipídicas o *Raft*. Estos dominios se pueden considerar plataformas organizadas implicadas en una gran variedad de funciones celulares incluyendo la organización y agrupamiento de proteínas de membrana y los procesos de señalización celular (Brown and London, 2000). Aunque hay evidencias para pensar que ciertos virus usan las balsas lipídicas o microdominios similares a estos durante el ensamblaje viral (Suomalainen, 2002), la cuestión es si estas estructuras se requieren en el lugar de fusión entre la membrana celular y la viral, ya que todavía no se tiene muy clara su función. Por lo tanto, es importante considerar si el colesterol y/o los esfingolípidos se requieren para la fusión, ya que estos están presentes en las balsas lipídicas, o si estos sirven de forma independiente para otro propósito. Por ejemplo, el colesterol podría interactuar directamente con la proteína de fusión, como lo hace con la región pretransmembrana de gp41 del HIV-1 (Vincent et al., 2002), facilitando la inserción de la proteína en la membrana celular. Otra posible alternativa podría ser que las balsas lipídicas tuvieran la capacidad para concentrar receptores virales. Incluso una tercera posibilidad sería que el colesterol confiriese fluidez en la membrana, promoviendo la curvatura negativa en la misma (Chen and Rand, 1997), u otra propiedad biofísica necesaria para disminuir la barrera energética de la fusión.

Varios estudios sugieren la necesidad de microdominios como las balsas lipídicas para la entrada del virus como el Ébola y el virus Marburg (*Filoviruses*), el virus de la viruela (*Orthopoxvirus*), el virus de la hepatitis murina (MHV, *Coronavirus*), el virus de la coriomeningitis linfocítica (LCMV, *Arenavirus*) y el herpes simple (HSV, *Herpesvirus*) (Aman et al., 2003; Bavari et al., 2002; Bender et al., 2003; Chung et al., 2005; Shah et al., 2006; Thorp and

Gallagher, 2004; Yonezawa et al., 2005), ya que reduciendo el colesterol de la membrana plasmática de las células diana se reduce la infección vírica o la fusión célula-célula. Por otro lado para algunos virus los receptores celulares de la entrada viral residen en los microdominios enriquecidos en colesterol, por lo que el aumento en densidad de los receptores facilitaría el reconocimiento viral. Para algunos virus la presencia de balsas lipídicas *per se* no son necesarias para la fusión, sino que podrían concentrar los receptores virales para favorecer el acoplamiento del virus a la célula.

En el caso del HCV se ha demostrado que la entrada del virus a la célula es colesterol-dependiente. Experimentos de HCV_{pp} en sistemas modelo de membrana muestran que los esteroides facilitan la fusión

2. Proteínas de fusión víricas

Diferentes virus con diferente rango de hospedador muestran similares mecanismos de entrada. Actualmente hay tres tipos diferentes de proteínas de fusión y entre ellas muestran características comunes (Basanez, 2002):

- 1- Las proteínas sufren un proceso de maduración resultando en estructuras metaestables, preparadas para un cambio conformacional a estados más estables tras recibir la señal apropiada (bajada de pH o unión al receptor).
- 2- En el estado fusogénico, las proteínas víricas fusogénicas están formando trímeros, y la agregación de múltiples trímeros ayuda en la formación del poro fusogénico.
- 3- Típicamente cada monómero dentro del oligómero se puede, convencionalmente dividir, en tres segmentos: una parte extraviral, conocida como ectodominio, un dominio transmembrana, y un segmento o tallo citoplasmático.
- 4- En el desencadenamiento de la fusión, regiones del ectodominio se unen a la membrana e incluso algunas de ellas se insertan. De especial relevancia es el péptido de fusión, un péptido relativamente corto, hidrofóbico y bien conservado, indispensable para la fusión.

5- El péptido de fusión, escondido dentro del ectodominio, es el primer responsable de la etapa inicial del proceso de fusión, mientras que el dominio pre-transmembrana parece ser fundamental para los últimos pasos de la fusión.

Estructuralmente, los ectodominios de las proteínas virales de fusión se pueden clasificar en tres grupos principales (Kielian, 2006; Weissenhorn et al., 2007) (Figura 1.11):

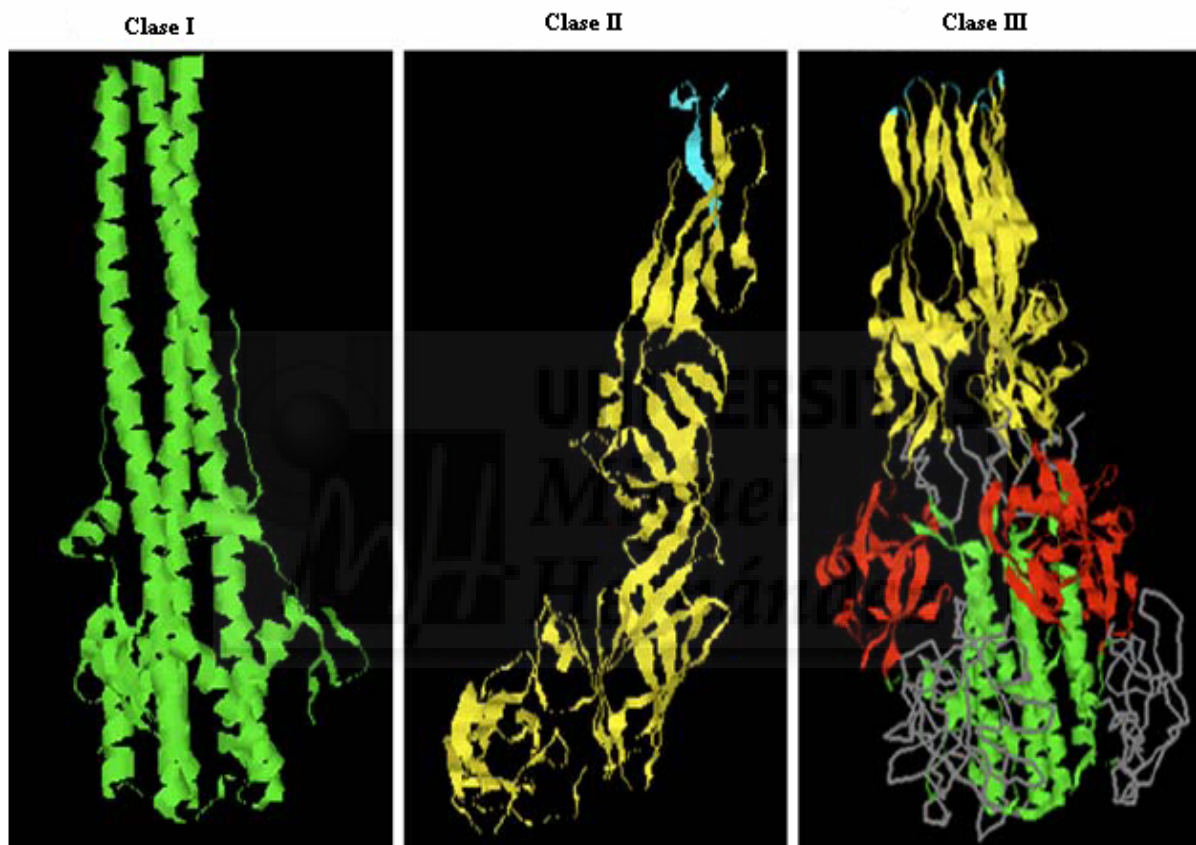


Figura 1.11. Estructura 3D de un prototipo de cada clase de proteínas de fusión: Para la clase I, se muestra el trímero formado por la hemaglutinina de influenza a pH bajo. (Bullough et al ,1994) (estructura de tres coiled-coils de alfa-hélices (el péptido de fusión no aparece por ausencia de estructura)). Para las proteínas de la clase II se muestra el monómero de la proteína E del TBEV a pH neutro, compuesto mayoritariamente de láminas-beta (El péptido de fusión aparece arriba en azul (Rey et al, 2006)). Para la Clase III mostramos el trímero de VSV-G a bajo pH (Roche et al 2006): se reseña en verde las tres coiled-coils centrales, las regiones en amarillo, corresponden a láminas-beta donde se resalta el péptido de fusión en lo alto en azul y en rojo la región que no tiene homología con ninguna de las clases anteriores.

-Proteínas de fusión de clase I. Su orientación es perpendicular a la membrana del virión. Presentan mayoritariamente hélice α en su estructura secundaria. El estado oligomérico de la forma metaestable y fusogénica está en forma de trímero. Una característica de la estructura del núcleo del ectodominio en su estado post-fusogénico consiste en un ovillo de seis hélices α el cual está formado por un *coiled-coil* interno de tres hélices α al cual se acoplan las tres hélices α

CHR de forma antiparalela ocupando las cavidades del *coiled coil*. Estas proteínas fusogénicas de clase I se sintetizan como homotrómeros en forma de un precursor inmaduro que se escinden para dar lugar a una subunidad de unión al receptor y una subunidad fusogénica, que posee el péptido de fusión cerca del N-terminal. Algunas proteínas de fusión de clase I serían las pertenecientes a las familias de orthomixovirus (ej., virus de la gripe), retrovirus (ej., HIV), filovirus (ej., virus del Ébola), paramixovirus (ej., virus Sendai) y coronavirus (ej., SARS).

- *Proteínas de fusión de clase II*. A diferencia de las anteriores, su orientación es paralela a la membrana del virión. Presentan cadenas polipeptídicas casi exclusivamente plegadas en hojas β antiparalelas. El estado oligomérico de la forma metaestable está en forma de dímero, mientras que el estado fusogénico está en forma de trímero. Otra diferencia estaría en el paso de maduración de las dos proteínas fusogénicas, que consiste en un corte proteolítico de una proteína inmadura para dar lugar a las dos proteínas fusogénicas, las cuales heterodimerizan por interacciones no covalentes. Y, por otra parte, el péptido de fusión se localiza en un bucle del interior de la secuencia primaria, a diferencia de las de clase I. Algunos ejemplos de proteínas de fusión de clase II serían las pertenecientes a las familias flavivirus (ej., HCV) o alfavirus (ej., *Semliki forest virus*).

- *Proteínas de fusión de clase III*. Son proteínas descritas recientemente (Roche et al., 2006; Roche et al., 2007) que presentan ciertas similitudes con las proteínas de fusión pertenecientes a los otros dos grupos, como por ejemplo, estas proteínas están glicosiladas, forman homotrómeros en la superficie del virión y sufrir cambios conformacionales a pH ácido que facilita el proceso de fusión. Sin embargo, y a diferencia del resto de proteínas de fusión, los cambios conformacionales inducidos por el pH son reversibles, no es necesaria la proteólisis para que la proteína sea activa en la fusión, no contiene un péptido de fusión altamente hidrofóbico en la región N-terminal (proteínas de fusión clase I), ni interno (proteínas de fusión clase II). Al igual que las proteínas de fusión de clase I forma una estructura en horquilla de seis hélices α en su conformación post-fusogénica. Por otra parte, al igual que las proteínas de fusión de clase II presentan bucles y conformaciones en hoja β . Un ejemplo de proteína de fusión de clase III sería la perteneciente a la familia *rabdovirus* (ej., Virus de la estomatitis vesicular G).

3. Hepatitis C

El Virus de la Hepatitis C fue descubierto en 1989 por los investigadores de Chiron Inc. Una porción del genoma de HCV se aisló a partir de la búsqueda en librerías de expresión de cDNA de RNA y DNA de chimpancés infectados con el suero de pacientes infectados mediante post-transfusiones de hepatitis no-A y no-B. Ellos llamaron a este nuevo tipo de Hepatitis, hepatitis C. Más tarde varios grupos clonaron el genoma entero de HCV.

HCV es un virus RNA de cadena sencilla y positiva clasificado dentro de la familia de los *Flaviviridae*. El genoma de aproximadamente 10,000 nucleotidos codifica una poliproteína de unos 3000 aminoácidos. Esta poliproteína se procesa tanto por proteasas de la célula huésped como por proteasas virales en cuatro proteínas estructurales y varias proteínas no estructurales necesarias para la replicación viral.

3.1 La enfermedad

La hepatitis C es una enfermedad infectocontagiosa que afecta al hígado. La infección con HCV consiste en varias fases:

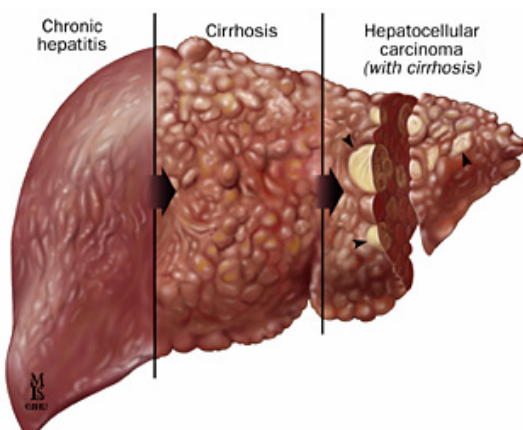


Figure 1.12. Evolución del hígado durante la enfermedad

La fase aguda: La fase aguda de la enfermedad dura entre 3 y 6 meses, pero se puede alargar hasta 1 año. En esta fase se pueden incluir curaciones espontáneas que se han producido en los 6 segundos meses. Los síntomas físicos como ictericia son raros, y el cansancio asociado a las hepatitis puede pasar desapercibido. Como mínimo, un 20% de las infecciones se curan solas, en el 80% restante la enfermedad se cronifica.

Fase crónica: Esta fase puede alargarse 20 y 30 años sin más síntomas que algunas alteraciones de los marcadores hepáticos. Después puede empezar una fase de fibrosis del hígado algo más rápida que desemboca en cirrosis en unos años y posteriormente en cáncer de hígado (Figura 1.12). El diagnóstico de cáncer de hígado en pacientes de hepatitis C no es superior al 5%, y muchos pacientes podrían superar los 30 años de cronicidad sin desarrollar grandes lesiones hepáticas. Otro sector importante de los afectados de hepatitis C, un 30% de los infectados no presenta síntomas clínicos de ningún tipo, (marcadores hepáticos normales) y estos pacientes tienen mejor pronóstico que los demás. Parece también comprobado que el pronóstico es mejor cuanto más tempranamente se haya contraído la enfermedad, y esto independientemente de la viremia (cantidad de virus por unidad de sangre). La viremia no parece afectar a la evolución de la enfermedad y, quizá, sólo modifique lo potencialmente contagioso que es cada paciente.

La hepatitis C se transmite por vía parenteral a partir del contacto con sangre infectada. Las vías más frecuentes de contagio son: prácticas médicas con mala esterilización (odontólogo, podólogo, etc.), pincharse con una aguja contaminada con sangre infectada, compartir agujas para inyectarse drogas, inhalar drogas por aspiración compartiendo el instrumento con que se aspira, ser nacido de una madre que tiene la hepatitis C y mediante relaciones sexuales, aunque se calcula que este tipo de contagio representa un 2,7 % de los casos, y se da especialmente cuando en la relación sexual existe sangrado.

Antes de 1992 el método más común de contagio fueron las transfusiones de sangre y los trasplantes de órganos ya que los médicos no podían detectar el virus de la hepatitis C en la sangre, por lo que multitud de personas recibieron sangre infectada.

3.2 Genotipos de HCV

Un hecho que diferencia la actividad de las maquinarias replicativas de los virus RNA respecto a las maquinarias celulares, tanto de procariotas como de eucariotas, es la fidelidad de copia de cada una de ellas. Así, las DNA polimerasas celulares son consideradas maquinarias muy fieles, mientras que las RNA polimerasas virales presentan tasas de error mucho mayores. La polimerasa del HCV (NS5B) no presenta actividad correctora de errores y se ha podido

calcular que se equivoca en la copia de aproximadamente 1 a 10 nucleótidos de cada genoma en cada generación (Pawlotsky, 2003). Esta tasa de error es la responsable de la generación de estructuras poblacionales denominadas *cuasiespecies*, en las que los genomas de los virus que infectan un mismo organismo, e incluso la misma célula, son diferentes entre sí aunque están íntimamente relacionados. Esta variabilidad, junto a la explosiva tasa de replicación de los virus RNA+ (se producen aproximadamente 1000 partículas nuevas de HCV cada día) confiere a la población una elevada capacidad de adaptación a cambios ambientales, incluyendo la respuesta inmune o el tratamiento antiviral (Neumann et al., 2000). Además, la alta variabilidad, unida a la alta prevalencia en todo el mundo, ha provocado en el caso del HCV, al igual que con otros virus RNA+, al establecimiento de diferentes genotipos. Para el HCV, los genotipos descritos hasta la fecha se han denominado con los números del 1 al 6 (Simmonds et al., 2005) Estos genotipos se diferencian entre sí, no solo en su prevalencia geográfica, sino también en la progresión de la enfermedad y la respuesta al tratamiento.

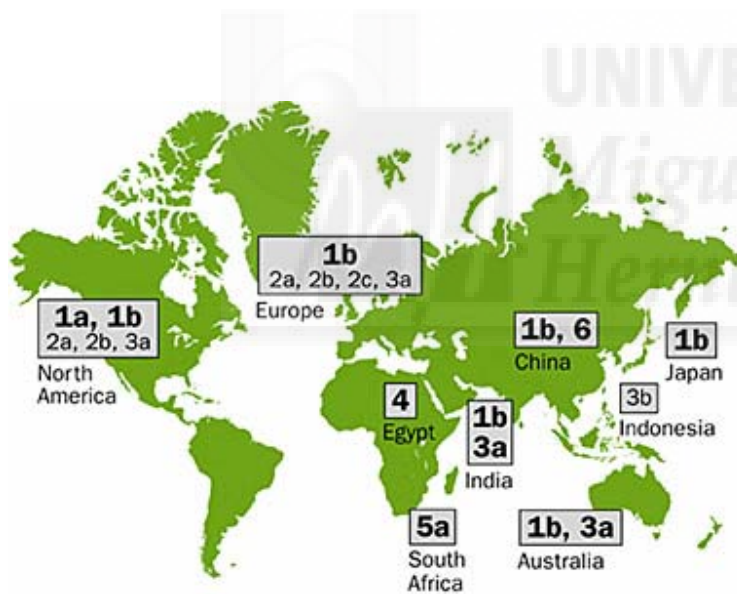


Figura 1.13. Distribución geográfica de los genotipos de HCV

encontrarse en diferentes poblaciones de todo el mundo (Figura 1.13):

- Genotipo 1: el subtipo 1a suele encontrarse en Estados Unidos y Europa. El subtipo 1b se encuentra principalmente en Japón y Europa.
- Genotipo 2: los subtipos 2a, 2b, 2c y 2d se encuentran principalmente en Japón y China.
- Genotipo 3: los subtipos 3a, 3b, 3c, 3d, 3e y 3f se encuentran principalmente en Escocia y algunas regiones del Reino Unido.

La historia de la epidemiología del HCV está basada en la tasa de cambios de sus secuencias nucleotídicas. Modelos matemáticos apuntan a que el primer ancestro común del virus de la hepatitis C se remontaría a más de 2000 años, la divergencia de genotipos a 500 años, y las diferencias entre 1a y 1b a 300 años. Existen 6 genotipos de la hepatitis C, que pueden

- Genotipo 4: los subtipos 4a, 4b, 4c, 4d, 4e, 4f, 4g, 4h, 4i y 4j suelen encontrarse en Medio Oriente y África.
- Genotipo 5: el subtipo 5a se encuentra principalmente en Canadá y Sudáfrica.
- Genotipo 6: el subtipo 6a se encuentra principalmente en Hong Kong y Macao.

3.3 Tratamiento

El tratamiento farmacológico más eficaz se basa en la asociación de interferón pegilado administrado por vía subcutánea, con ribavirina administrada por vía oral.

Los interferones empleados actualmente en la clínica son de tipo 1 y, como el resto de los miembros de esta familia, presentan actividades antivirales, antiproliferativas e inmunomoduladoras (Feld et al, 2005). La respuesta al tratamiento con IFN depende de un gran número de factores, siendo los más importantes, el genotipo del virus y la carga viral. Así, las respuestas mantenidas se obtienen en mayor medida en aquellos pacientes infectados con genotipos 2 y 3, y que presentan cargas virales bajas. La resistencia al tratamiento con IFN se ha podido asociar a la secuencia de la región ISDR, que forma parte de la secuencia codificante para la proteína NS5A. Los efectos secundarios del interferón son numerosos: incluyendo síntomas similares a la gripe, dolor de cabeza, fiebre, fatiga, pérdida del apetito, náuseas, vómitos y depresión. El tratamiento con interferón también puede interferir en la producción de glóbulos blancos y plaquetas, y al cabo de los meses puede provocar pérdida de masa muscular. Todos estos síntomas revierten al finalizar el tratamiento.

La ribavirina (RBV), que fue sintetizada en el año 1970, es un nucleósido análogo de la guanósina con actividad frente al virus de la hepatitis C, aunque su mecanismo de acción no se conoce. En un principio se pensó que la RBV tenía un efecto «cosmético», disminuyendo sólo las transaminasas. Ensayos en monoterapia con este compuesto no resultaron en bajadas en la carga viral del HCV ni en la clarificación del virus (Di Bisceglie et al., 1995). Sin embargo, cuando se empleó en combinación con IFN se obtuvieron buenos resultados en el número de respuestas sostenidas y, por tanto, la RBV fue aprobada para su uso en el tratamiento de la infección por HCV, aunque únicamente en combinación con IFN (McHutchison and Poynard, 1999). Los efectos secundarios de la ribavirina son la anemia severa (conteo bajo de glóbulos rojos) y las

modificaciones que afectan a la reproducción; los hijos de un paciente recientemente tratado con ribavirina pueden nacer disminuidos psíquicos o con deformidades físicas (efecto teratológico).

El porcentaje de éxito (eliminación del virus en sangre mantenida hasta un año después de terminado el tratamiento) es algo superior al 50% dependiendo del tipo de virus. Aproximadamente el 40% de los pacientes con infección genotipo 1 responderán al tratamiento, en cambio el genotipo 1b es el más difícil de curar y requiere tratamiento de un año. La hepatitis C puede evolucionar en cirrosis o incluso en un tipo específico de cáncer de hígado. En este caso, la alternativa del trasplante de hígado es poco eficaz y alarga la supervivencia pocos años, pero no cura la hepatitis C. La comunidad médica no reconoce por el momento casos de curación espontánea (negativización del virus en sangre mantenida durante un año) más allá del periodo inicial de un año que corresponde a la fase aguda.

3.4 Tratamiento futuro

A pesar de los buenos resultados obtenidos con la terapia de combinación IFN+RBV en pacientes infectados con genotipo no 1, no hay que olvidar que estos tratamientos tienen considerables efectos secundarios y una larga lista de contraindicaciones. Por todo ello existe una batería de nuevos compuestos en desarrollo (De Francesco and Migliaccio, 2005). Las compañías farmacéuticas están centrando sus estudios en la proteína NS5B, ya que presenta unas características especiales que hacen de ella una diana perfecta para el desarrollo de nuevos fármacos antivirales:

- ◆ Tiene una actividad RNA-polimerasa dependiente de RNA (RdRp). Hasta la fecha, no se han identificado proteínas con este tipo de actividad en células de mamífero.
- ◆ Localización subcelular. Se localiza en la cara citosólica del retículo endoplásmico, una zona de más fácil acceso que el interior del núcleo o de la mitocondria que es donde actúan las polimerasas celulares.

- ◆ Comparte motivos estructurales con otras polimerasas virales, como la transcriptasa inversa (RT) de HIV, para la que existe un gran número de estudios que podrían ser extrapolables y de gran utilidad.

En esta tesis hemos estado intentando encontrar inhibidores de la entrada viral buscando compuestos que la inhiban, uniéndose a regiones de las glicoproteínas de la envuelta viral que median la fusión de membranas, para así impedir la entrada del virus a la célula.

3. 5 HCVpp

Hasta el 2005 no aparecieron sistemas de cultivo eficientes que permitieran la amplificación del HCV in vitro. Por ello se desarrollaron pseudopartículas virales de HCV, HCVpp. Los retrovirus se han elegido como plataformas sobre las que ensamblar has pseudopartículas porque sobre el núcleo de proteínas que ostentan la replicación viral se pueden sustituir las proteínas de la envuelta propias del virus, por otras, y así incorporar una gran variedad de diferentes proteínas celulares o virales. Las HCVpp, utilizadas en esta tesis se generan por ensamblaje de las glicoproteínas *E1* y *E2* de HCV en un núcleo replicativo de proteínas derivadas del MLV (Figura 1.14). Las

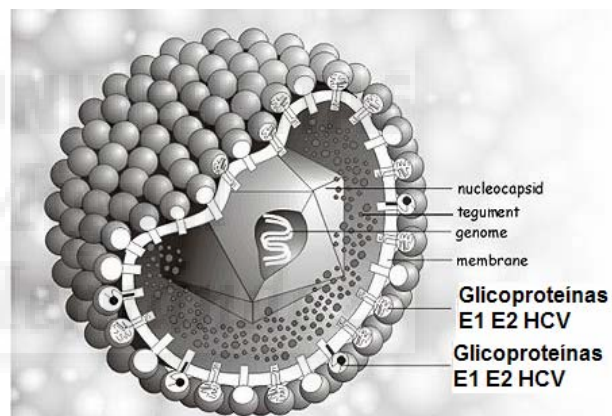


Figure 1.14: Esquema de las HCVpp

HCVpp ensamblan las glicoprotínas de la envuelta del HCV sin modificaciones y funcionales. Estos sistemas virales se han utilizados en los estudios de caracterización de la entrada del HCV a la célula así como de los receptores de HCV y en la búsqueda de nuevo compuestos antivirales ya que mimetizan los pasos primarios de la infección viral.

3.6 Replicación en cultivo del Virus de la Hepatitis C

Se han realizado múltiples ensayos para infectar células en cultivo con virus provenientes de suero de pacientes infectados. Los mejores resultados se han obtenido utilizando cultivos primarios de hepatocitos humanos o de chimpancé, única especie que, además de la humana,

puede ser infectada. Sin embargo, los rendimientos son extremadamente bajos y no son útiles para estudios de laboratorio. Para solucionar este problema y para obtener un genoma viral autorreplicativo, un grupo de investigación alemán propuso un sistema, el replicón, que permite obtener niveles de replicación 100,000 veces mayores a los que se obtienen en los cultivos primarios. Para tal efecto, el genoma del HCV, originalmente de RNA, es convertido mediante transcripción inversa y la reacción en cadena de la polimerasa (RT-PCR) en una cadena doble de DNA que, posteriormente, se inserta en un plásmido que posee un promotor para la polimerasa del fago T7. A partir de la secuencia clonada se puede obtener ARN de cadena sencilla en sentido positivo (como el genoma viral) mediante transcripción *in vitro*, el cual se introduce a las células en cultivo donde podrá replicarse de manera autónoma ya que contiene las secuencias que codifican para las proteínas necesarias, entre ellas una RNA polimerasa dependiente de RNA, y las proteasas que permiten la maduración de sus proteínas (Bartenschlager and Pietschmann, 2005). El sistema se estableció originalmente con un genoma incompleto que carecía de las proteínas estructurales, por lo que no es posible que se formaran partículas virales, lo cual no es necesario para que el replicón funcione. Este sistema ha sido utilizado principalmente en estudios de replicación, con los que se han podido determinar algunos componentes y condiciones mínimas para que este proceso se lleve a cabo. Un objetivo muy importante ha sido también su uso en el desarrollo de probables fármacos con actividad antiviral dirigidos específicamente contra la replicación. No obstante, el sistema del replicón tiene poca utilidad en otro tipo de estudios que requieren necesariamente la formación de partículas virales infecciosas, tales como aspectos inmunológicos sistémicos en animales de laboratorio, o para determinar aspectos importantes del ciclo viral. Recientemente, la colaboración de los grupos de investigación de Takaji Wakita (Tokio, Japón) y de Ralf Bartenschlager (Heidelberg, Alemania), usando como base las técnicas de construcción del replicón, lograron obtener partículas virales infectantes en los sobrenadantes de cultivos celulares (Wakita et al., 2005). Para este trabajo, se realizó la copia completa del genoma viral que se introdujo en un plásmido para después ser sometido a transcripción *in vitro* y obtener copias del genoma completo del HCV. Datos relevantes de este trabajo son que las partículas virales obtenidas son capaces de infectar nuevamente las células Huh-7, así como los chimpancés mediante inoculaciones experimentales. Antes de que este hallazgo fuera publicado formalmente en la revista Nature Medicine, otro grupo de investigación, dirigido por Francis Chisari (La Jolla, E.U.A.), solicitó la colaboración de Takaji Wakita para producir partículas virales en cultivo. En este caso se usó la línea celular Huh-7.5.1, derivada de las células Huh-7, obteniéndose mejores resultados en la producción de

los viriones (Zhong et al., 2005) ya que los genomas y proteínas virales son capaces de producirse más rápido y en mayor cantidad que en las células Huh-7 originalmente utilizadas. Sin duda esta serie de trabajos contribuirá en gran medida al estudio detallado del ciclo de replicación viral así como a la obtención de nuevos fármacos para el tratamiento de la infección por el HCV.

3.7 Receptores del HCV

La densidad del HCV en el suero de pacientes es heterogéneo y sorprendentemente bajo. Esto ha sido atribuido a la asociación del HCV con partículas de baja densidad y muy baja densidad (LDL y VLDL), incluso cuando los detalles de esta interacción no se han aclarado (Thomssen et al., 1992;). Como resultado de la hipotética relación entre el HCV y las LDL, el receptor de LDL, LDL-R se ha propuesto como un receptor potencial del HCV (figura 1.15).

La proteína de superficie CD81 se ha identificado como un factor potencial de entrada por medio de la proteína *E2* (Song et al., 2004). CD81 pertenece a la familia de las tetraspaninas, cuyos miembros presentan varias funciones celulares tales como adhesión, morfología, o diferenciación celular. Como todos los miembros de la familia de las tetraspaninas CD81 está compuesto por cuatro segmentos transmembrana, un pequeño bucle extracelular (SEL) y un gran bucle extracelular (LEL) (Seigneuret, 2006) (Figura 1.15). Los anticuerpos monoclonales anti CD81 LEL (Song et al., 2004) inhibe la entrada de pseudopartículas de HCV. Los residuos de CD81 implicadas en la interacción con *E2* han sido localizados dentro del LEL. En la glicoproteína *E2* los residuos 420, 437, 438, 441, 442, 527, 529, 530 y 535 participan en la interacción con CD81 (Drummer and Pountourios, 2004). Por otro lado se ha visto que el heterodímero *E1E2* tiene una interacción más fuerte con CD81 que *E2*, lo que sugiere que *E1* puede modular la unión de *E2* con CD81 (Cocquerel et al., 2000). El acceso de unión a CD81 de *E2* está reducido por la presencia de glicanos en la posición 417, 532 y 645 (Helle et al., 2007) sugiriendo que esos glicanos rodean el sitio de unión. Aunque el papel exacto de CD81 en la entrada no se ha elucidado, se cree que actúa en el paso de post-unión, determinándose para pseudopartículas el tiempo de entrada en 17 min (Evans et al., 2007). El tropismo de HCV está restringido a células hepáticas humanas que expresan CD81, pero la expresión ectópica de CD81 en células no hepáticas no permite la infección (Bartosch et al., 2003), lo que indica que otras moléculas son esenciales para la entrada de HCV. Los miembros de la familia de las

tretraspaninas pueden interactuar con otras proteínas de la misma familia o con otras proteínas formando complejos multimoleculares llamados “tetraspaninas web“ (Boucheix and Rubinstein, 2001).

El receptor humano *scavenger* clase B, tipo I (SR-BI) es una proteína de superficie celular que ha sido identificado como otro factor potencial de entrada para HCV (Eickmann et al., 2003). SR-BI es una proteína de 509 aminoácidos que contiene dos dominios cortos citoplasmáticos, dos segmentos transmembrana y un bucle extracelular largo (Figura 1.15) (Rhains and Brissette, 2004). Aunque la interacción *E2*-CD81 parece específica (Eickmann et al., 2003) la interacción con el heterodímero *E1* y *E2* no se ha observado. Pero sí se ha confirmado su papel en la entrada con pseudopartículas de HCV (Bartosch et al., 2003). SR-BI se expresa en la mayoría de las células humanas pero su expresión es especialmente alta en el hígado (Bartosch et al., 2003). SR-BI es el receptor para LDL acetiladas y oxidadas, y también para lipoproteínas de alta densidad (HDL) (Acton et al., 1994). Varios estudios sugieren que la presencia de la región hipervariable 1 de *E2* es importante para su interacción con SR-BI (Eickmann et al., 2003). El papel exacto de SR-BI en la entrada del HCV no está explicada, aunque recientes estudios sugieren una interacción directa entre la partícula viral y SR-BI (Evans et al., 2007), pero también se ha propuesto que HCV pueda interactuar con SR-BI a través de su asociación con las lipoproteínas (Maillard et al., 2006), y que el primer contacto con SR-BI puede necesitar una interacción previa con CD81 (Evans et al., 2007). Finalmente, SR-BI puede modificar la composición lipídica de la membrana plasmática (Peng et al., 2004) , y es posible que el aumento en la actividad de entrada del HCV sea consecuencia de esta

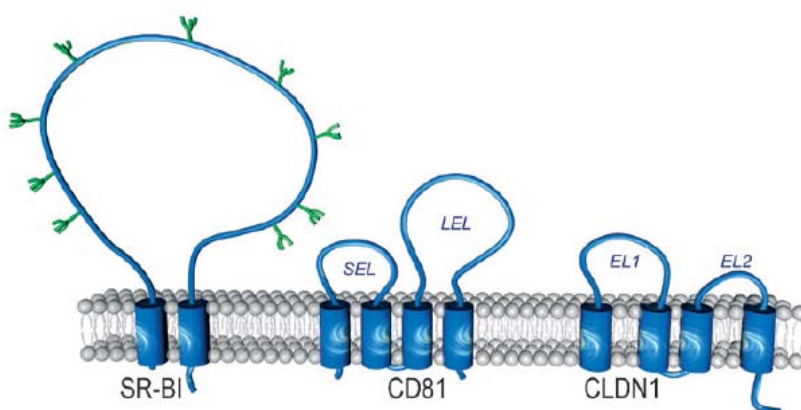


Figure 1.15: Esquema representativo de los receptores de HCV

modificación, facilitando algunos pasos en el ciclo de vida del HCV. En línea con esta hipótesis, se ha visto que las HDL aceleran la endocitosis de las HCVpp (Dreux et al., 2006).

Se ha identificado recientemente una nueva proteína implicada en la

entrada del HCV a la célula, la Claudin-1 (CLDN1) (Evans et al., 2007). CLDN1, la cual se expresa predominantemente en hígado (Furuse et al., 1998; Van Itallie and Anderson, 2006). Pertenece a una familia compuesta de 24 miembros responsables de la formación de “conexiones rígidas” (*tight junction*). Estas pequeñas proteínas (20 y 27 KDa) contienen dos bucles extracelulares, tres dominios intracelulares y cuatro regiones transmembrana (Figura 1.15). Se caracterizan por presentar el dominio W-GLWC-C en el EL1 (Van Itallie and Anderson, 2006). La expresión de CLDN1 en células hepáticas 293T que permiten la infección de las HCVpp. CLDN1 es la primera proteína descrita que confiere a las células susceptibilidad a la infección del HCV a células no hepáticas. La región de CLDN1 involucrada con la entrada del virus corresponde al primer bucle extracelular, particularmente al residuo I32 y E48. Los dominios C-terminal intracelular y las regiones de palmitoilación, los cuales permiten la interacción con otras proteínas relacionadas con las “*tight junction*” no están implicadas en la entrada del virus. Anticuerpos dirigidos contra un epítipo insertado en el primer bucle extracelular inhibe la infectividad de HCV. Además, la mitad del tiempo máximo de inhibición de la entrada de HCVpp en la célula se ha determinado en aproximadamente 73 min (Evans et al., 2007), sugiriendo que CLDN1 juega un papel en el último paso del proceso de entrada, probablemente después de que el virus se una e interaccione con CD81. No se ha reportado una interacción directa entre CLDN1 y partículas del HCV, pero no se puede excluir la idea de que la interacción requiera un cambio conformacional en las glicoproteínas de la envuelta desencadenado por una primera interacción entre E2 y otro factor como CD81 o SR-BI. El preciso papel de CLDN1 en la entrada del HCV sigue siendo materia de estudio. Sin embargo, como CLDN1 está estrictamente localizada en las “*tight junction*” en hepatocitos polarizados, por lo que se especula que CLDN1 actúe tras la migración lateral del complejo virus-receptor a las *tight junction*.

3.8 Ciclo viral del HCV

Tras la unión al receptor específico, la entrada del virus a la célula huésped implica la fusión de las envueltas lipídicas del virus y de la membrana celular. El uso de inhibidores de la acidificación del endosoma, tales como bafilomicina A1, concanamicina, clorhidro amónico o cloroquina inhiben la entrada del virus (Meertens et al., 2006). Además el uso de pequeños RNA de transferencia contra clatrina impiden también la entrada del virus a la célula, lo que indica que la entrada del HCV a la célula es endocitosis mediada por clatrina (Figura 1.16) (Meertens

et al., 2006). El HCV entra a la célula huésped por medio de endocitosis, el pH ácido provoca un cambio conformacional en las proteínas. En estudios *in vitro* con liposomas y HCVpp se ha visto que el pH ácido umbral para que las HCVpp fusionen liposomas es 6.3, teniendo su óptimo para la fusión en 5.5. El proceso de fusión a bajo pH de las HCVpp depende de la temperatura y está facilitado por la presencia de colesterol (Lavillette et al., 2006). Las HCVpp no requieren la presencia de ninguna proteína para fusionar liposomas. Tras la fusión de la membrana viral y la membrana del endosoma temprano el genoma viral es liberado en el citosol (Meertens et al., 2006).

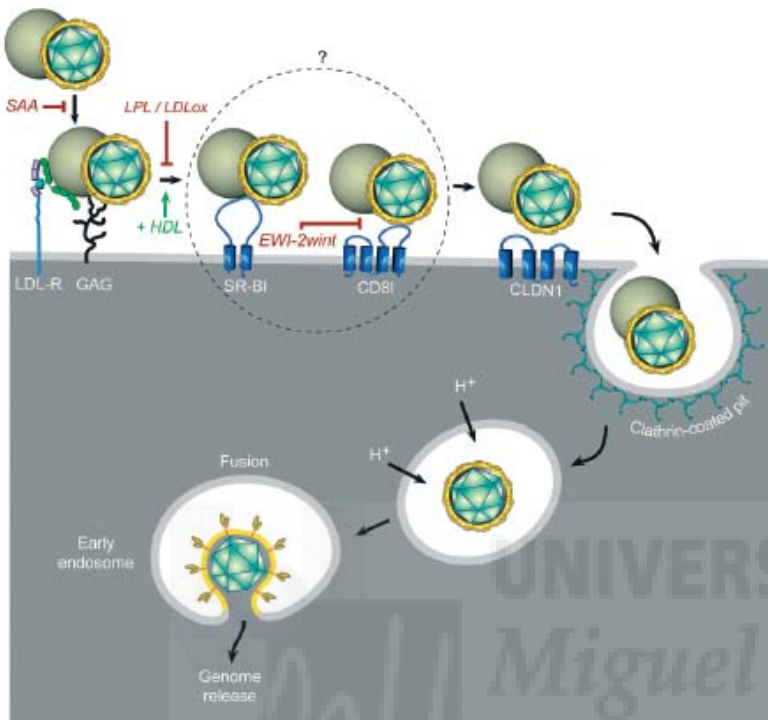


Figure 1.16. :Modelo de entrada del HCV a la célula

la fusión en 5.5. El proceso de fusión a bajo pH de las HCVpp depende de la temperatura y está facilitado por la presencia de colesterol (Lavillette et al., 2006). Las HCVpp no requieren la presencia de ninguna proteína para fusionar liposomas. Tras la fusión de la membrana viral y la membrana del endosoma temprano el genoma viral es liberado en el citosol (Meertens et al., 2006).

El HCV sigue una estrategia replicativa similar a la de otros virus RNA+. Una vez que el virus ha entrado en la célula y se ha desencapsidado, la región IRES (internal ribosome entry site) promueve la traducción de la región codificante para dar lugar a la poliproteína, que es procesada para generar las proteínas maduras. De ellas, la proteína NS5B, al presentar actividad RNA-polimerasa dependiente de RNA, es la pieza central de la maquinaria replicativa que usa el genoma viral

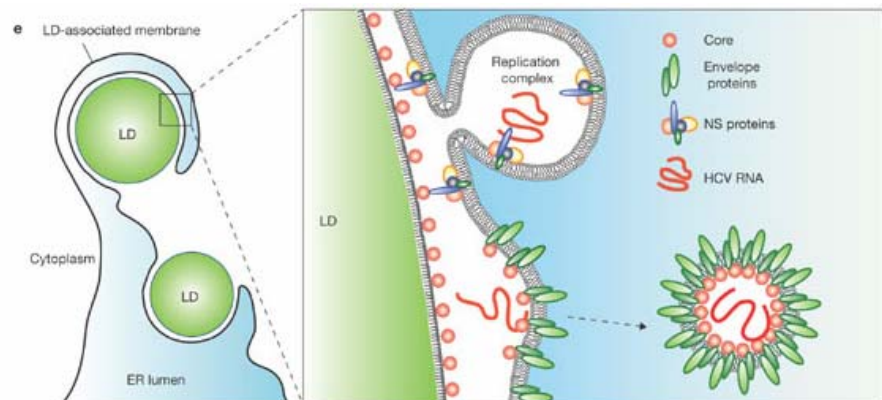


Figura 1.17. Modelo para la producción del HCV.

como molde para la transcripción de una molécula de RNA complementaria de cadena negativa. La cadena negativa sirve, por su parte, como molde para la síntesis de nuevas moléculas de RNA de polaridad positiva, que pueden ser empleadas para traducirse, replicarse o bien empaquetarse en los virus progenie. A diferencia de las polimerasas del hospedador que catalizan la transcripción y replicación del DNA en el interior del núcleo de la célula, la polimerasa del HCV se localiza asociada a la cara citoplásmica de la membrana lipídica del retículo endoplásmico (ER) y a gotas de grasa intracelulares. (Schmidt-Mende et al., 2001). Las proteínas *core* estarían localizadas mayoritariamente en las monocapas de la membrana que rodean las gotas de grasa (Figura 1.16). El HCV induciría la aposición de las gotas de grasa a las membranas derivadas del retículo endoplasmático. La proteína *core* reclutaría a las proteínas NS y por tanto al complejo replicativo a las gotas de grasa asociadas a membranas. Las proteínas NS alrededor de las gotas de grasa participarían en la producción de virus infecciosos (Figura 1.17). La proteína *E2* estaría también localizada alrededor de las gotas de grasa. A través de estas asociaciones, los viriones se ensamblarían en este ambiente localizado (Miyanari et al., 2007). Finalmente, la progenie viral encapsidada en asociación con membranas intracelulares por medio del aparato secretor celular alcanzaría el medio extracelular (Seeger, 2005).

La lesión hepatocelular está producida por linfocitos T citotóxicos (CD8+) (Koziel et al., 1992), probablemente el mecanismo patogénico se deba a una compleja interacción entre la infección vírica y la inmunorrespuesta del huésped. El virus no utiliza en su replicación ningún intermediario de ADN ni se integra en el genoma del huésped. Se propone que el virus replica a través de un intermediario de ARN de sentido negativo (Chambers et al., 1990) que se ha detectado en hígado y células mononucleares de sangre periférica. Este hecho nos indica que el HCV es hepatotropo y linfotropo (Zignego et al., 1992).

3.8 Organización genómica

Este virus contiene una sola región translacional o región de lectura abierta (ORF), que abarca casi su totalidad y codifica una poliproteína precursora de 3.010 aminoácidos (Choo et al., 1991). Precediendo al ORF, en su extremo 5' existe una región de 324-341 nucleótidos, que se denomina 5' no codificante (5'UTR) (Figura 1.17), cuya secuencia está altamente conservada entre los distintos aislados del HCV, con una homología superior al 98 %, por lo que esta región juega un papel importante en la regulación de la replicación vírica, controlando la síntesis de la

poliproteína de la que derivan las distintas proteínas víricas (Takamizawa et al., 1991). En el

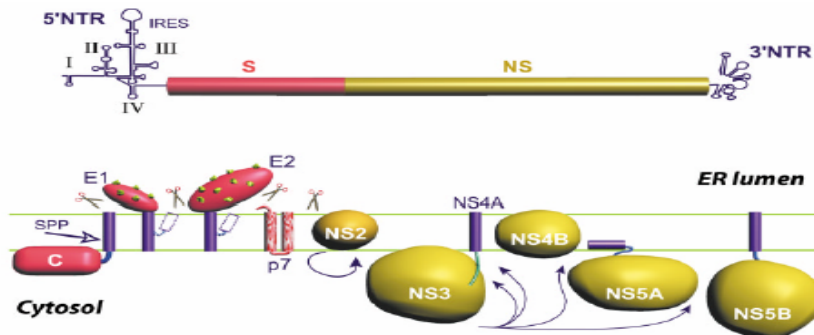


Figura 1.18. Esquema de la organización genómica y las proteínas estructurales y no estructurales del virus.

extremo 3' del genoma existe una cola de poliadenina lo que implica que el ARN vírico puede funcionar como ARN mensajero (Kato et al., 1990) (Figura 1.18).

La poliproteína codificada origina las diferentes proteínas individuales por la acción combinada de proteasas virales y celulares (Hijikata et al., 1991) originando las proteínas que forman parte de la estructura del virión, y las proteínas no estructurales (NS) que están implicadas en la replicación del HCV.

La partícula viral está formada por las proteínas *core*, la cual forma la nucleocápsida, las glicoproteínas de la envuelta *E1* y *E2* y una pequeña proteína que se desconoce si forma o no parte de las proteínas estructurales llamada *p7* (Figura 1.19).

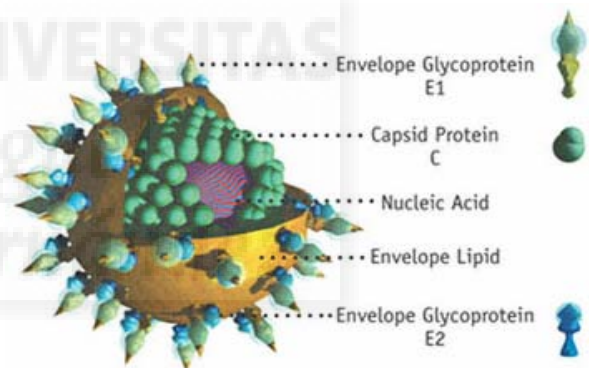


Figure 1.19. Esquema de la partícula viral de HCV

3.9 Proteína *Core*

La proteína *core* es uno de los componentes estructurales mayoritarios de la nucleocápsida. Su función principal es empaquetar el genoma viral, aunque presenta funciones muy diferentes. Está implicada en la patogénesis de la Hepatitis C. Interacciona con más de una docena de proteínas celulares, actuando en la presentación inmune, apoptosis, transformación celular hasta hepatocarcinoma, metabolismo lipídico y transcripción del RNA. La expresión en células eucariotas de esta proteína resulta en la producción de dos especies con distinto peso molecular, una de 19kDa (p19) y otra de 21 kDa (p21) (Acosta-Rivero et al., 2002), siendo p19

de 179 aminoácidos de longitud la forma madura de la proteína. La proteína *core* está estructurada en tres dominios (Figura 1.20),

- ◆ *Dominio I*, del aminoácido 1 al 122. Contiene una alta proporción de residuos básicos. Es responsable de la unión al RNA.
- ◆ *Dominio II*, del aminoácido 123-174. Este dominio es más hidrofóbico que el dominio I. Este dominio es esencial para el plegamiento y la oligomerización de la proteína.

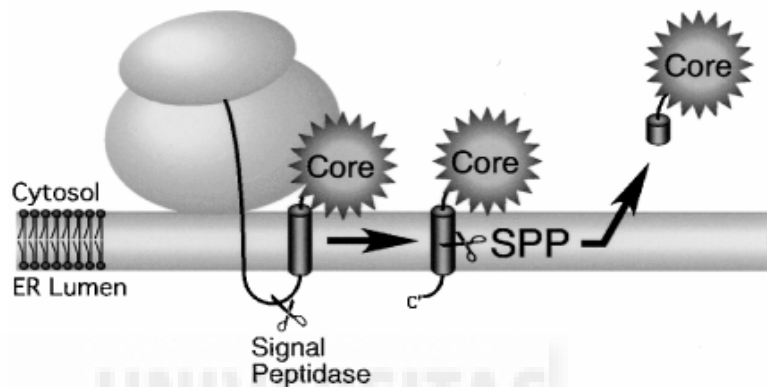


Figura 1.20 Procesado de la proteína core

- ◆ *Dominio III*, del aminoácido 174-191. Este dominio es también muy hidrofóbico. Esta región corresponde con el péptido señal de translocación de *E1* al retículo endoplasmático. Este dominio no está presente en la proteína madura.

Ensayos de inmunolocalización han encontrado a la proteína *core* en pequeñas proporciones en el núcleo (Yasui et al., 1998), unida al retículo endoplasmático, en la superficie de gotas de lípidos intracelulares (Argenziano et al., 2006) y también se ha encontrada la proteína *core* asociada a lípidos *Raft* (Matto et al., 2004). Se piensa que el dominio II de la proteína está implicado en esta interacción con los lípidos (Hope and McLauchlan, 2000). La proteína *core* oligomeriza en multímeros, y la acumulación de la proteína *core* en el sitio de ensamblaje permitiría la formación de la partícula viral. La forma soluble de la proteína produce partículas de un tamaño, forma y densidad idénticas a la nucleocápsida de HCV (Majeau et al., 2005).

También se ha propuesto que la proteína *core* interacciona con la glicoproteína *E1*, siendo este paso importante para el ensamblaje viral (Nakai et al., 2006).

La proteína *core* es una importante diana de diagnóstico de la infección por el HCV, ya que se ha identificado la región del N-terminal de HCV como un dominio altamente inmunodominante (Jolivet-Reynaud et al., 1998).

3.10 Glicoproteínas *E1* y *E2*

Las glicoproteínas de la envuelta viral son *E1* y *E2*, ambas esenciales para la entrada del virus a la célula. Estas proteínas tienen regiones hidrofóbicas altamente conservadas necesarias para mantener la estructura tridimensional y la estabilidad de las proteínas; otras regiones formadas mayoritariamente por aminoácidos hidrofílicos y básicos localizados en la superficie de las proteínas tienen un alto porcentaje de mutación. Estas regiones de mutación se concentran en las regiones hipervariables 1 (residuos 384-410), 2 (residuos 474-482) y 3 (residuos 431-466) de la proteína *E2*. El resultado final es que la proteína cambia, permitiendo al virus evadir el sistema inmune, pero manteniendo la estructura tridimensional. *E1* y *E2* son proteínas de fusión de Clase II. Como se comentó anteriormente, tienen predominantemente estructura en hebra-beta, y su péptido de fusión se encuentra en un bucle de fusión hidrofóbico interno de la proteína. Presentan una arquitectura en 3 dominios, Dominio I N-terminal, Dominio II que contiene el péptido de fusión interno y un Dominio III C-terminal. En el caso del HCV, estos tres dominios se encontrarían repartidos en las 2 proteínas de fusión *E1* y *E2*, en lugar de estar los 3 en una proteína única como es el caso de la proteína E de fusión del TBEV. (Jardetzky and Lamb, 2004).

E1 y *E2* tienen un ectodominio N-terminal de 160 y 334 aminoácidos respectivamente con cortos dominios C-terminal transmembrana de 30 aminoácidos aproximadamente. *E1* y *E2* forman un heterodímero unido por medio de interacciones no covalentes. Para la adecuada estructura de ambas proteínas deben de expresarse juntas y glicosilarse adecuadamente. En la heterodimerización el dominio transmembrana tiene un papel crucial, si se sustituye este dominio transmembrana por otro de otras proteínas los heterodímeros no se forman (Cocquerel et al., 2000). Además el dominio transmembrana tiene un papel fundamental en la localización subcelular de direccionamiento al RE.

El dominio transmembrana de *E1* es una secuencia que retiene la proteína en el RE, es el péptido señal que direcciona *E2* al RE y además tiene una señal de corte para una peptidasa

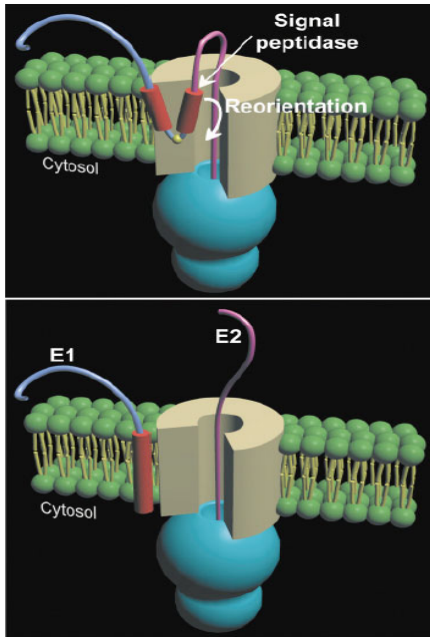


Figure 1.21 Esquema de Los segmentos transmembrana de HCV.

celular cuya acción separa *E1* de *E2*, unido a que este dominio es importante en la heterodimerización.

El dominio transmembrana está formado por 2 regiones hidrofóbicas separadas por segmentos que contienen al menos un residuo cargado (*E1* Lys370 y *E2* Asp728 y Arg 730). Si se reemplaza esos residuos por Ala se altera la función del TM, modificándose la localización, el ensamblaje y la formación del complejo *E1-E2*. El contacto temprano entre las 2 proteínas se inicia en el TM, y es necesario para atraer los ectodominios para que contacten, y esto es necesario para tener estructura nativa. Péptidos sintéticos de estas

regiones adoptan alfa-hélices. Los residuos cargados en el centro de la hélice TM sirven para retener las proteínas en el RE. Además antes de cortar las proteínas *E1* y *E2* el TM de estas glicoproteínas forma una estructura de horquilla. Tras el corte la segunda región de residuos hidrofóbicos se reorienta. Esta estructura es posible por la presencia de los residuos cargados, si éstos se cambian por Ala la estructura de horquilla no se puede adoptar (Figura 1.21) (Op De Beeck et al., 2004). Las proteínas *E1* y *E2* muestran a pesar de su gran variabilidad, sitios de glicosilación altamente conservados, sugiriendo que la asociación con glicanos juega un papel esencial en el ciclo de vida del virus de la hepatitis C. Durante la síntesis el ectodominio de las proteínas *E1* y *E2* del HCV se direcciona hacia el lumen

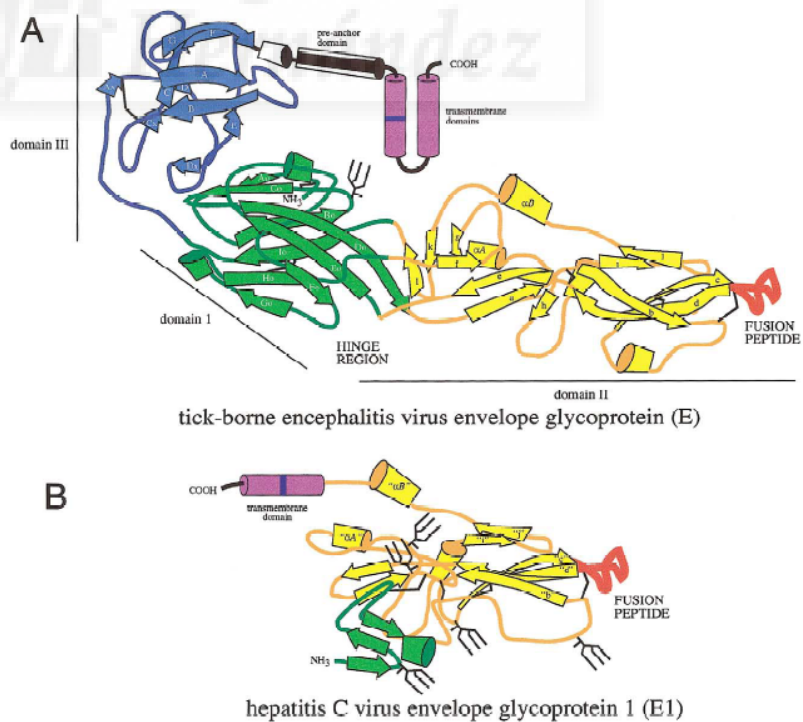


Figura 1.22. Esquema en dominios de la proteína E del TBEV y de E1 del HCV.

del RE donde es N-glicosilado. *E1* tiene 5 sitios potenciales de glicosilación y confirmado experimentalmente se glicosilan 196, 209, 234 y 305. En la estirpe 1b también se glicosila 250 (Goffard et al., 2006). *E2* tiene 11 lugares de glicosilación y se ha demostrado que se glicosilan 417, 423, 430, 448, 476 (75%), 532, 540, 556, 576, 623, 645. Cuando estas proteínas se expresan solas no se glicosilan igual, indicando qué factores implicados en el plegamiento de la proteína podrían modular la eficiencia de la glicosilación. Si la proteína no está glicosilada *E1* y *E2* aparecen mal plegadas. Además las glicosilaciones podrían estar implicadas en aumentar la afinidad de las glicoproteínas por las chaperonas calnexina y calreticulina. La ausencia de tipos complejos de glicosilación excluye el tránsito de estas proteínas por el Golgi. Las observaciones sugieren que el *budding* de las partículas del HCV ocurre en el RE, y se liberan por la célula vía de exocitosis (Robert F Garry). También se ha demostrado que las glicosilaciones en las posiciones 417,532 y 645 (*E2*N1, *E2*N6 y *E2*N11) reducen la sensibilidad de las HCVpp a los anticuerpos de neutralización y reducen el acceso de CD81 a su sitio de unión con *E2*, sugiriendo que las glicosilaciones pueden contribuir a la evasión del HCV a la respuesta inmune humoral por enmascaramiento del sitio de unión con CD81.

El ectodominio de la proteína *E1* es una versión truncada de las proteínas clase II. El péptido de fusión estaría en *E1* en los aminoácidos 272-281, según su alineación con el péptido de fusión del TBEV (Figura 1.22), estando flanqueado por láminas β . Otros alineamientos sugieren que la región del péptido de fusión se encuentra en la región 253-294.

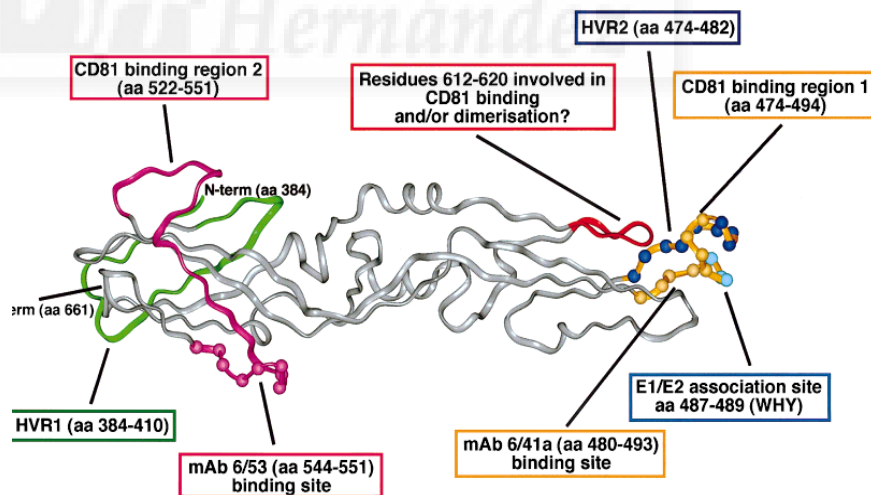


Figura 1.23. Modelo de la glicoproteína E2 de HCV

La proteína *E2* se alinea con el dominio III de las proteínas de fusión de clase II, (549-743). La proteína *E2* tiene un alto contenido en hebras β . Tiene diferentes dominios: Un

dominio en forma de barril beta, un dominio II de dimerización y un dominio III. Las regiones caracterizadas de estas proteínas predicen que la unión a su receptor CD81 se da en los aa 480-493, 544-551, las dos regiones hipervariables del HVR: 474-494, 522-551; una posible región para oligomerizar con *E1* sería 612-620 y 484-494 y una última región con motivo de unión a heparina: 559-614, típica del dominio III de las proteínas de fusión clase II (Figura 1.23).

3.11 Proteína p7

La proteína *p7* se encuentra codificada en el genoma entre las proteínas estructurales y las no estructurales, específicamente entre la proteína *E2* y NS2. Tras la traducción de la poliproteína, *p7* se procesa en el retículo endoplasmático por peptidasas celulares. *p7* está incluida dentro de la familia de las vioporinas. Las vioporinas son proteínas pequeñas altamente hidrofóbicas y que se encuentran en virus que interaccionan con membranas modificando la permeabilidad celular a iones y pequeñas moléculas. Típicamente comprenden entre 60-120 aminoácidos, contienen un dominio hidrofóbico formado por una hélice anfipática. La inserción de estas proteínas en la membrana va seguida de una oligomerización, creando el típico poro hidrofílico con los residuos hidrofóbicos interaccionando con la bicapa lipídica y los residuos hidrofílicos formando el poro.

La principal función de las vioporinas es modificar la permeabilidad de las membranas, por lo que estas proteínas están implicadas en los procesos de entrada o salida viral (Gonzalez and Carrasco,

2003). En los últimos años las vioporinas se han convertido en nuevas dianas para la quimioterapia antiviral, ya que la inhibición de la actividad de las vioporinas podría disminuir la

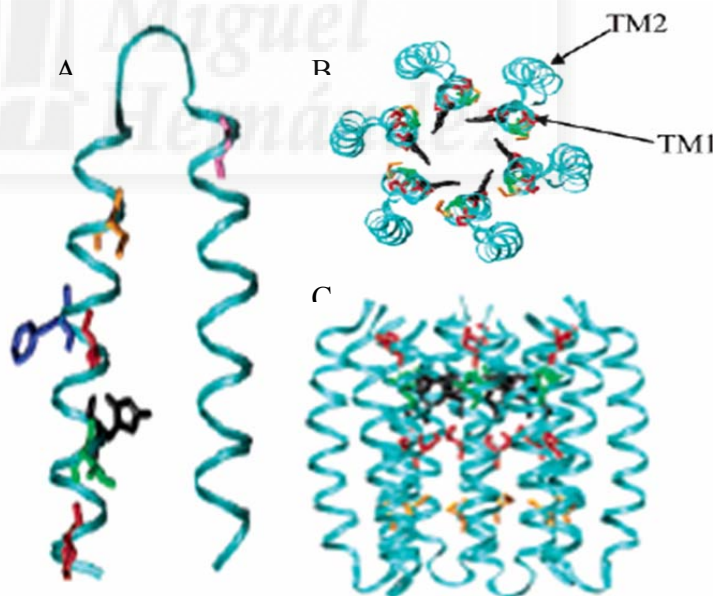


Figure 1.24. Modelo de p7 (A) Monómero de p7, (B) y (C) estructura resultante de la hexamerización de p7.

producción de un amplio espectro viral, por la alta homología que hay entre todas las proteínas de esta familia (Gonzalez and Carrasco, 2003).

No se tiene información estructural de *p7*, ni su estado oligomérico, lo único que disponemos es de experimentos de microscopía electrónica, datos bioquímicos y su alto grado de homología con las viroporinas. Con toda esta información se ha propuesto por modelado molecular un modelo de esta proteína (Figura 1.24) (Patargias et al., 2006).

p7 está formada por 63 aminoácidos que forman dos regiones transmembrana conectadas por un corto bucle cargado positivamente y altamente conservado en todas las estirpes de HCV (Carrere-Kremer et al., 2002). El modelo propone que *p7* oligomeriza en hexámeros formando un canal con poro interno de 1.5 nm y un diámetro de la estructura completa de 4.5 nm (figura 1.23). La estructura oligomérica de *p7* forma un canal que permite el flujo de cationes a través de la membrana (Griffin et al, 2003). El alto grado de conservación en este bucle básico sugiere que esta región es importante para la funcionalidad del canal. Mutaciones en el bucle de la proteína eliminan la funcionalidad del canal y la salida del virus de la célula (Griffin et al., 2004).

La amantadina es una molécula que inhibe la actividad de la viroporina M2 de Influenza (Okada et al., 2001), y esta molécula también inhibe la actividad de *p7*. El modo de acción de la amantadina no está claro, aunque se está usando en clínica con poco éxito para el HCV (Weegink et al., 2003).

CAPÍTULO II

UNIVERSITAS

Miguel

METODOLOGIA GENERAL



2.1 Sistemas modelo de membrana

Las membranas en forma de bicapas cerradas o liposomas, preparadas a partir de moléculas anfifílicas dispersas en medio acuoso están ampliamente reconocidas como modelos simples de las membranas celulares y como vehículos potenciales para el transporte y liberación de compuestos. El estudio de componentes lipídicos aislados de las membranas biológicas en sistemas modelo simple ha permitido la caracterización tanto de dichos lípidos y de su comportamiento dentro de la bicapa como la caracterización de su interacción con diferentes componentes de la membrana, como por ejemplo interacciones lípido-lípido, lípido-proteína, etc. Los liposomas se clasifican según su tamaño y morfología (Jones, 1995). Los cuatro principales tipos de liposomas son:

- Vesículas unilamelares pequeñas (Small Unilamellar Vesicles o SUVs): Son vesículas consistentes en una única bicapa de lípidos, con un diámetro de entre 15-30 nm, y se preparan generalmente mediante sonicación, bien en baño o mediante una sonda.

- Vesículas unilamelares grandes (Large Unilamellar Vesicles o LUVs): vesículas de una sola bicapa, cuyo tamaño oscila en el rango de 50 y 500 nm. Pueden prepararse mediante extrusión en prensa francesa o a través de filtros de

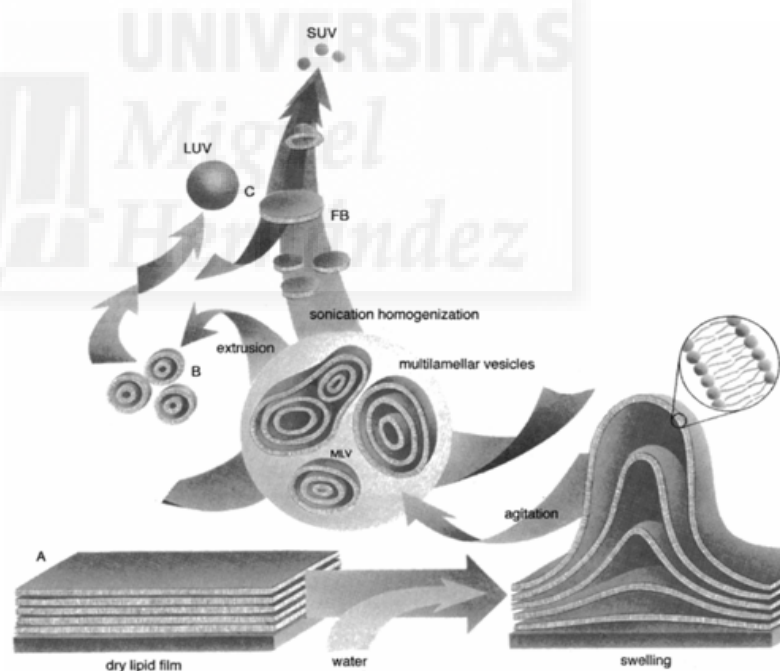


Figura 2.1: Preparación de liposomas

policarbonato, diálisis en detergentes, por fusión de SUVs, por fusión de SUVs inducida por Ca^{+2} , por evaporación de un disolvente orgánico en fase reversa, etc.

- Vesículas multilamelares (Large Multilamellar Vesicles o MLVs): Son estructuras que consisten en bicapas concéntricas que se forman espontáneamente cuando se hidratan los lípidos

anfífilicos. El diámetro promedio de los MLVs es de unos 700 nm, aunque su tamaño puede variar entre 100 y 5000 nm de diámetro y el número medio de lamelas (bicapas concéntricas) está comprendido entre 7 y 10. Este tipo de liposoma posee la desventaja de que tan solo el 10-15% de los fosfolípidos se encuentra en la bicapa más externa, es decir, que sólo una pequeña fracción de lípidos puede interactuar con agentes externos.

- Vesículas multivesiculares (Multivesicular Vesicles o MVVs): Están formadas por vesículas individuales englobadas dentro de una vesícula de tamaño mayor.

- Vesículas unilamelares gigantes (Giant Unilamellar Vesicles o GUVs): vesículas de una sola bicapa, cuyo tamaño oscila en el rango de 5 a 200 micras de diámetro.

Los liposomas mejor caracterizados y de mayor utilidad son los que están compuestos por una sola bicapa de lípido, principalmente los SUVs y LUVs. La mayor diferencia entre estos dos, a parte de su tamaño, reside en la proporción de lípido que hay en las hemicapas interna y externa. En el LUV de ~95 nm (que es el que mayoritariamente se ha utilizado en los ensayos de esta Tesis) la distribución es casi simétrica, 50% en cada hemicapa según Mayer et al. (Mayer et al., 1986), o 54% en la hemicapa externa y 46% en la hemicapa interna según Butko et al. (Butko et al., 1996). Sin embargo, el pequeño radio de curvatura de los SUVs fuerza a que una proporción más alta de lípidos se sitúe en la hemicapa externa, entre un 60 y un 70% (Szoka and Papahadjopoulos, 1980). La proporción diferente de lípidos a cada lado de la bicapa tiene una serie de consecuencias: (1) el empaquetamiento de los lípidos de la hemicapa externa es diferente al empaquetamiento de los situados en la hemicapa interna; (2) por calorimetría diferencial de barrido se observa una disminución de la temperatura de transición gel-líquido cristalina de 4° C de promedio, un ensanchamiento de la banda y una reducción de la entalpía; (3) por debajo de la temperatura de transición las cadenas lipídicas de los SUVs se encuentran más desordenadas que en la fase de los LUVs o MLVs; (4) se reduce la movilidad lateral de los lípidos y disminuye la miscibilidad de los lípidos lo que favorece la coexistencia de dominios lipídicos de distinta composición dentro de la bicapa, incluso por encima de la temperatura de transición (New, 1990). Por lo tanto, los LUVs son los liposomas más apropiados para la realización de estudios biofísicos de interacción lípido-proteína.

Los liposomas comenzaron a utilizarse como sistemas modelos de membranas a partir de los trabajos de Bangham et al. (Bangham et al., 1965a; Bangham et al., 1965b), donde se comprobó mediante microscopía electrónica que los liposomas eran sistemas de membranas cerradas. Desde entonces se han utilizado ampliamente tanto en ciencia básica como en ciencia aplicada. Las primeras experiencias de estos modelos de membranas estuvieron dirigidas hacia el estudio de la permeabilidad y comportamiento osmótico de las vesículas a algunas sustancias encapsuladas en ellas, utilizándose una gran variedad de composiciones lipídicas así como varios tipos de iones y electrolitos. El uso de los liposomas también ha permitido caracterizar las propiedades químico-físicas de los lípidos en sí y, además, las interacciones del lípido con otras moléculas, ya sean proteicas o no-proteicas, donde hay una infinidad de trabajos al respecto, empleando una gran diversidad de metodologías biofísicas: resonancia de spin electrónico, resonancia magnética nuclear, calorimetría diferencial de barrido, espectroscopía de infrarrojo, fluorescencia, etc.

Históricamente, la determinación de la estructura de las proteínas de membrana se ha visto obstaculizada por las dificultades experimentales derivadas de la presencia de sus dominios insertados en la membrana. La dificultad para cristalizar proteínas de membrana en su estado nativo y determinar su estructura tridimensional por cristalografía de rayos X, hace que en muchos casos se recurra a técnicas de baja resolución para el estudio de la estructura de las proteínas de membrana. Si bien estas técnicas no nos ofrecen información sobre las estructuras terciaria y cuaternaria de las proteínas, sí nos van a permitir determinar los porcentajes de los distintos elementos de estructura secundaria de éstas, y no solo ello, sino que en muchas ocasiones los cambios en estructura secundaria son parámetros fiables para determinar la agregación de proteínas, así como su estabilidad. También son sensibles a la introducción de perturbaciones en el sistema (cambios de temperatura, de pH, etc.) o a la interacción de dichas proteínas con otras proteínas, ligandos, etc. (Arrondo and Goni, 1999).

2.2 Espectroscopía Infrarroja

La espectroscopía infrarroja (IR) mide las transiciones de baja energía entre niveles vibracionales dentro de un mismo nivel electrónico, resultantes de la absorción de radiación en la región infrarroja del espectro electromagnético. Estos niveles vibracionales están generados

por movimientos característicos (tensión, flexión, aleteo, etc.) que se dan en los diferentes enlaces químicos presentes en los grupos funcionales de una molécula. La escala de tiempos de dichas vibraciones moleculares es muy corta (cerca de 10^{13} s^{-1}). La espectroscopía infrarroja de proteínas ha avanzado enormemente en las dos últimas décadas, principalmente debido a los avances no sólo en la instrumentación, sino también en los métodos de tratamiento y análisis de datos. Una de las grandes ventajas de esta técnica es la facilidad que presenta para adquirir espectros de gran calidad a partir de cantidades muy pequeñas de proteínas ($\sim 100 \mu\text{g}$) (Barth, 2007; Mantsch and McElhaney, 1991). Es más, la espectroscopía infrarroja también permite el estudio de proteínas en medios de elevada turbidez sin que esto afecte a la resolución de los espectros obtenidos. En este último caso, esta técnica es además especialmente útil para el estudio de las membranas lipídicas (transiciones polimórficas de los fosfolípidos, conformación y dinámica de los fosfolípidos en sus diferentes estados, etc.)

El tipo de interferómetro utilizado es el interferómetro de Michaelson. Su desarrollo, junto con la aplicación del algoritmo de la transformada de Fourier, introdujo importantes mejoras en la relación señal/ruido. Todo ello, unido a las ventajas de esta técnica, incrementó el interés por ésta en el estudio y cuantificación de la estructura secundaria de proteínas, llevándose a cabo grandes avances tecnológicos y matemáticos en este campo. Los espectrómetros de infrarrojo con transformada de Fourier producen un patrón interferométrico que, tras pasar a través de la muestra, alcanzan un detector.

Una vez que se ha recogido un interferograma, es necesario convertirlo en un espectro. Esto se consigue a través del algoritmo de la transformada de Fourier rápida (Fast Fourier Transform o FFT) desarrollado por Cooley y Tukey en 1965. El interferograma es una representación de la intensidad respecto al movimiento del espejo. Tras la aplicación de la transformada de Fourier y la apodización y corrección de fase de los datos, se obtiene un único espectro de la muestra, que dividido por el fondo (un espectro tomado en ausencia de muestra), da lugar a una representación de intensidad vs. frecuencia (expresada en cm^{-1}). Como se ha explicado anteriormente, el espectro de infrarrojo procede de las diferentes transiciones vibracionales de los diferentes grupos funcionales de las moléculas (Figura 2.2). Si bien al aplicar los diferentes modos vibracionales a una molécula biológica obtendríamos un complicado espectro vibracional, dicho espectro se ve simplificado por el hecho experimental de que ciertos

grupos de átomos dan lugar a bandas vibracionales a frecuencias muy similares, independientemente de la molécula de la que estén formando parte, siendo característica esa frecuencia de dicho grupo químico (independientemente de si forma parte de un fosfolípido, una proteína, etc.). Sin embargo, el número de onda al que un determinado grupo vibra, puede verse afectado por factores inter- o intramoleculares, como es el

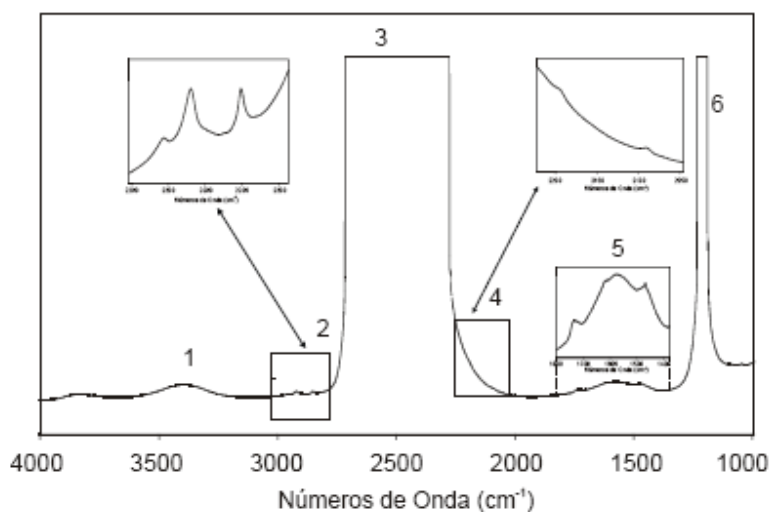


Figure 2.2. Espectro de infrarrojo de un péptido incorporado en vesículas de DMPC_{d54}/DMPA en tampón D₂O. Se muestran las bandas de absorción del agua para H₂O residual (1 y 5), y para D₂O (3 y 6) y las vibraciones de tensión de los metilo y los metilenos del DMPA (2) y del DMPC_{d54} (4). La zona 5 también muestra la región del C=O, la banda Amida I' y la vibración de flexión del CH.

caso de la formación de puentes de hidrógeno, acoplamiento mecánico, electronegatividad, etc. En el caso del enlace peptídico, en el espectro de IR se originan nueve bandas, correspondientes a los modos vibracionales de los diferentes grupos funcionales que lo componen, y que se denominan Amida A, B, I, II, etc. (ver Tabla I) las cuales están descritas en términos del desplazamiento de las ocho coordenadas, cinco en el plano y tres fuera de él (Arrondo and Goni, 1999; Surewicz et al., 1993). De todas ellas, la más utilizada comúnmente es la Amida I, cuyos

modos vibracionales se originan de la vibración de tensión del grupo C=O de la amida (acoplado a la vibración de flexión del N-H y flexión del enlace C-N) y que da lugar a una banda en la región 1600-1700 cm⁻¹. La capacidad de formación de puentes

Tabla I.
Bandas características asociadas con el enlace peptídico (Arrondo y col., 1993).

Simetría	Descripción		Frecuencia aproximada (cm ⁻¹)	Descripción.
En el plano	Amida	A	3300	NH _s (100%)
		B	3100	
		I	1650	CO _s (80%), CN _s , CCN _d
Fuera del plano	Amida	II	1550	NH _{ib} (60%), CN _s (40%), CO _{ob} , CC _s , NC _s
		III	1300	CN _s (40%), NH _{ib} (30%), CC _s ' (20%), CO _{ib}
		IV	625	CO _d (40%), CC _s (30%), CNC _d
		V	725	Nh _{ob} , CN _r
		VI	600	CO _{ob} , CN _r
		VII	200	NH _{ob} , CN _t , CO _{ob}

s, tensión; d, deformación; t, torsión; ib, flexión en el plano; ob, flexión fuera del plano; s', tensión metilo-C.

de hidrógeno de estos grupos y la formación de dipolos transitorios, hacen que la banda Amida I sea sensible a la conformación de las proteínas. El acoplamiento de los dipolos transitorios provoca la división de la banda Amida I, y dicho acoplamiento depende de la orientación y la distancia de los dipolos implicados, por lo que permite obtener información acerca de la disposición espacial de los grupos peptídicos de un polipéptido. Cada componente de estructura secundaria contribuye por separado al espectro de infrarrojo, por lo que la banda Amida I va a ser una suma de todas las bandas que la componen (Surewicz et al., 1993). La dificultad principal en el análisis estructural de las bandas componentes radica en que usualmente la anchura de cada banda es mayor que la distancia que separa su máximo de frecuencia. La Tabla II resume la correlación entre la estructura secundaria de las proteínas con las frecuencias de la banda Amida. La mayoría de las frecuencias de dicha banda disminuyen aproximadamente 10 cm^{-1} durante el intercambio H/D. Los modos Amida en D_2O son referidos como Amida I', II', etc., y en principio las bandas Amida I y Amida I' poseen la misma información estructural. En el caso de los fosfolípidos, cabe diferenciar entre los modos vibracionales de las cadenas acílicas, los de la región interfacial y los modos vibracionales de las cabezas polares (Arrondo et al., 1993; Casal and Mantsch, 1984; Mantsch and McElhaney, 1991). Los principales modos vibracionales de las cadenas acílicas se deben a las vibraciones del enlace carbono-hidrógeno (CH_3 , CH_2 y $=\text{C-H}$). La vibración de tensión de los grupos metileno da lugar a una banda compuesta por dos bandas, uno centrado a $\sim 2929\text{ cm}^{-1}$ que corresponde a la vibración de tensión antisimétrica del CH_2 , y otro centrado a $\sim 2850\text{ cm}^{-1}$ correspondiente a la vibración de tensión simétrica del CH_2 . La frecuencia de estas bandas es sensible a la proporción de isómeros trans/gauche de las cadenas hidrocarburadas de los fosfolípidos, y puesto que dicha relación aumenta con la transición de fase gel a líquido cristalino, la frecuencia de esta banda será sensible a la fase del fosfolípido, pudiendo utilizarse para monitorizar la transición. El intercambio H/D en las cadenas hidrocarburadas desplaza esta banda a una frecuencia entre $2000\text{-}2300\text{ cm}^{-1}$, lo que nos permite estudiar simultáneamente el comportamiento de dos fosfolípidos distintos utilizando uno de ellos deuterado. Las bandas de tensión de los grupos CH_3 aparecen como pequeños hombros en la banda de tensión de los grupos CH_2 centrados a $\sim 2956\text{ cm}^{-1}$ (antisimétrico) y $\sim 2870\text{ cm}^{-1}$ (simétrico). El resto de modos vibracionales son menos utilizados, como es el caso de la banda de flexión de los metilenos, que aparece centrada entre $1462\text{-}1474\text{ cm}^{-1}$. La región más utilizada para el estudio de la interfase glicerol-cadena hidrocarburada es la banda de tensión del grupo

carbonilo. Dicha banda aparece entre 1700 y 1750 cm^{-1} . Esta banda es sensible a la polaridad y a la formación de puentes de hidrógeno. La banda de vibración de tensión del grupo CO esta formada por dos componentes centrados a 1742 cm^{-1} y 1728 cm^{-1} . El primero corresponde a aquellos grupos carbonilo que no se encuentran formando puentes de hidrogeno. La frecuencia de estos componentes no suele variar al alterar el microambiente de esta región, pero sí varía su intensidad, lo que va a provocar variaciones de la frecuencia de la banda global. La banda vibracional más característica de las cabezas polares de los fosfolípidos es la banda de vibración de tensión del grupo fosfato, que da bandas intensas entre 1220 (en condiciones de hidratación) y 1240 cm^{-1} (en condiciones de deshidratación) correspondiente a la vibración de tensión antisimétrica y una banda a 1085 cm^{-1} originada por la vibración de tensión simétrica del grupo PO_2^- , siendo esta ultima banda menos sensible a las condiciones de hidratación que la banda de tensión antisimétrica.

Tabla II.

Asignación de frecuencias (cm^{-1}) de componentes de la banda Amida I a diferentes motivos de estructura secundaria de proteínas.

Estructura Secundaria	Frecuencia de la Amida I (cm^{-1})
Hélice α	1648-1660
Hélice 3_{10}	1660-1668
No ordenadas	1640-1648
Giros β	1660-1685
Hoja $\beta_{intermolecular}$	1680-1690 1630-1640
Hoja $\beta_{intramolecular}$	1670-1695 1610-1625

2.3 Dicroísmo circular

La teoría de dicroísmo circular (CD) fue desarrollada por Biot y Fresnel (Neumann N, 1990). Un haz de luz polarizado en un plano puede considerarse formado por dos componentes polarizados circularmente, uno a la derecha y el otro a la izquierda. Estos componentes están en fase y son de la misma amplitud. Al pasar por un medio ópticamente activo, cada componente interactúa de manera diferente con los centros quirales de las moléculas presentes. La interacción de la radiación con la muestra induce un desfaseamiento y un cambio de magnitud diferenciales en ambos componentes circularmente polarizados de la luz, y estos fenómenos provocan una rotación del plano de polarización en un ángulo y la distorsión de este plano genera una elipse .

Los cromóforos de interés en las cadenas polipeptídicas son sus enlaces peptídicos. Estos absorben por debajo de los 240 nm debido a transiciones electrónicas de carácter $n\pi^*$ a 220 nm y $\pi\pi^*$ a 190 nm, las cadenas laterales de los aminoácidos aromáticos, con transiciones $\pi\pi^*$, absorbiendo principalmente en el rango de 260 a 320 nm y los puentes disulfuro que presentan

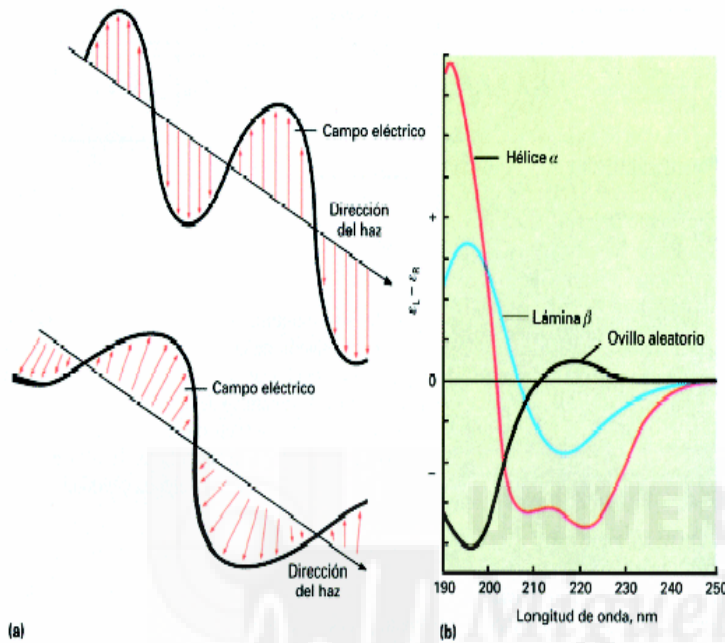


Figura 2.3. (A) Haces de luz polarizada horizontal y vertical. (B) Espectros de CD en ultravioleta lejano asociado con varios tipos de estructura secundaria.

una banda débil y ancha en torno a 260 nm por transiciones $n\pi^*$. A partir de los datos que se extraen de estos cromóforos por CD se puede obtener información sobre la estructura secundaria y terciaria de las proteínas (Kelly et al., 2005). Mediante CD en el ultravioleta lejano (180-260 nm), se pueden observar espectros definidos para cada estructura secundaria (Figura 2.3). El espectro típico de hélice α presenta dos bandas

negativas a 222 nm y 208 nm y una positiva en torno a 190 nm. El espectro para una lámina β es menos intenso, presentando dos bandas negativas, una sobre 217 nm y otra a 180 nm, y una banda positiva en torno a 195 nm. Se ha visto que hay más variedad en estos espectros para modelos de estructuras en láminas β que para modelos en hélice α , lo que se atribuye a que las láminas β pueden ser paralelas, antiparalelas o mixtas, intra o intermoleculares, y con diferentes extensiones. Los giros pueden adquirir conformaciones distintas (giros de tipo I, II y III) por lo que no hay un espectro típico de CD característico para este tipo de estructura. En estructuras desordenadas el espectro típico presenta sólo una banda negativa cerca de 200 nm, sin embargo, se ha visto que para péptidos como poli(Lys), poli(Glu) y poli(ProL), presentan una banda positiva alrededor de 220 nm; si esta banda es negativa indica que el péptido presenta algún tipo de conformación local, que puede ser tanto hélice α como lámina β .

2.4 Calorimetría Diferencial de Barrido

La calorimetría diferencial de barrido (DSC) es la técnica más directa para el estudio de los cambios que tienen lugar al calentar o enfriar una muestra, registrándose el exceso o defecto de capacidad calorífica aparente (C_p) de la muestra como función continua de la temperatura. De este modo, esta técnica es ideal para el estudio de la energía de las transiciones conformacionales de macromoléculas biológicas. Los calorímetros actuales se denominan diferenciales puesto que miden la diferencia de la capacidad calorífica de dos celdas idénticas. Una de ellas contiene la muestra problema, y en la otra se sitúa el mismo tampón en el que se encuentra preparada la muestra, de forma que actúa como celda de referencia. Ambas celdas se encuentran situadas dentro de una cámara adiabática y están conectadas a una termopila de gran sensibilidad que mide la diferencia de temperatura entre las dos celdas. Así mismo, cada celda está conectada a una resistencia. Puesto que las capacidades caloríficas de la muestra y la referencia van a ser diferentes, se necesitará comunicar una potencia térmica a través de la resistencia a la celda más fría para mantener ambas celdas a la misma temperatura. Dicha potencia comunicada a la celda de medida, siempre que el barrido de temperatura se realice a una velocidad constante, será

proporcional a la diferencia de capacidad calorífica entre ambas celdas, y esa será la magnitud fundamental de medida del instrumento (Jelesarov and Bosshard, 1999). A partir de la capacidad calorífica, la calorimetría diferencial de barrido nos permite obtener, siempre que el sistema esté bien definido, el resto de parámetros termodinámicos asociados a la transición inducida por temperatura (Figura 2.4): cambios de entalpía (ΔH), de entropía (ΔS), de

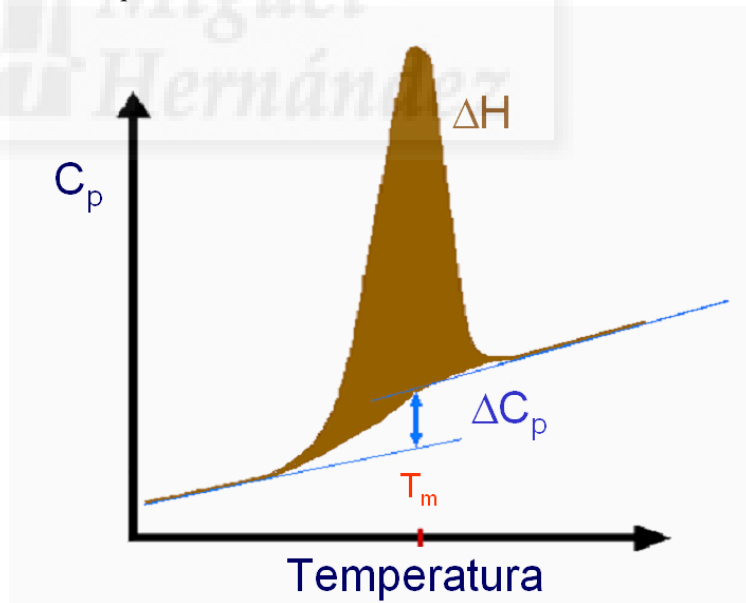


Figura 2.4. Curva de capacidad calorífica (trazo continuo) en función de la temperatura. C_p representa la capacidad calorífica del estado basal y C_{dp} la del estado a mayor temperatura. El área encerrada entre las dos curvas equivale a la entalpía de desnaturalización, ΔH . T_m es la temperatura del máximo de la transición y ΔC_p es el incremento de capacidad calorífica entre el estado basal y a mayor temperatura.

energía libre de Gibbs (ΔG) y de la capacidad calorífica (ΔC_p).

El estado físico de los fosfolípidos está íntimamente relacionado con la temperatura, de manera que pueden experimentar diversos cambios de fase a través del calentamiento. Los fosfolípidos en fase L_c , tras ser calentados, sufren un aumento del desorden de sus cadenas polares, dando lugar en su espectro de DSC a una pretransición. Así, en la fase gel, como ya se explicó anteriormente, podremos encontrar las moléculas de fosfolípido con su cabeza polar ocupando un área seccional mayor que la que ocupan las dos cadenas hidrocarburadas, que en este estado se encontrarían en conformación todo-trans e inclinadas con respecto al plano de la bicapa o bien con las cadenas hidrocarburadas perpendiculares al plano de la bicapa ($L_{\beta'}$) quedando en cualquier caso altamente empaquetadas y favoreciendo las interacciones de Van der Waals debido al estrecho contacto entre ellas. Al aumentar la temperatura, aún en estado gel, las cadenas hidrocarburadas pueden formar superficies onduladas ($P_{\beta'}$), siendo este un estado más desordenado que la fase $L_{\beta'}$. Este empaquetamiento se pierde abruptamente cuando la temperatura alcanza la T_m , debido a la isomerización trans-gauche de los enlaces carbono-carbono, que hace que el volumen molar del fosfolípido sea mucho mayor a temperaturas superiores a la T_m que a temperaturas inferiores a esta. La transición de fase gel a fase líquido cristalino es la que va a venir acompañada por la mayor entropía y por tanto nos va a dar el pico más intenso en el termograma (Huang and Li, 1999).

La Figura 2.5 muestra un termograma del fosfolípido DPPC. Comparando los termogramas de fosfolípidos puros y de fosfolípidos en presencia de péptidos, proteínas, moléculas orgánicas, etc., podremos analizar el efecto de estos últimos sobre el comportamiento termotrópico de los lípidos, muchas veces clave en el mecanismo de acción de dichas moléculas.

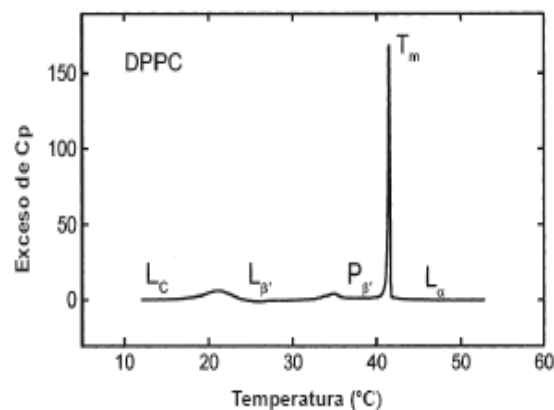


Figura 2.5.- Calorimetría diferencial de barrido de una muestra de DPPC preincubada a 0°C durante 24 h. El termograma muestra tres transiciones endotérmicas, correspondientes a las transiciones de fase $L_c \rightarrow L_{\beta'}$, $L_{\beta'} \rightarrow P_{\beta'}$ y $P_{\beta'} \rightarrow L_\alpha$.

2.5 Fluorescencia

La luminiscencia es la emisión de la luz de alguna molécula y ocurre desde estados electrónicamente excitados. La luminiscencia se divide formalmente en dos categorías, fluorescencia y fosforescencia, dependiendo de la naturaleza del estado excitado. En este apartado nos referiremos al fenómeno de fluorescencia. Su estudio proporciona una valiosa información sobre aspectos estructurales de la molécula responsable, o de su relación con el ambiente que la rodea. Algunas moléculas como consecuencia de la absorción de un fotón, un electrón pasa desde el estado fundamental al estado excitado. Dicha transición debe cumplir una serie de reglas de selección deducidas de la mecánica cuántica ondulatoria. Una vez en el estado excitado el electrón tiende a pasar al estado fundamental. Este retorno se puede llevar a cabo de múltiples formas, las cuales compiten entre sí. Puede ocurrir de una forma no radiativa (sin emitir radiación electromagnética) o radiativa (emitiendo un fotón); a estas últimas se les conoce con el nombre de luminiscentes. Los procesos de emisión fluorescente son procesos de relajación radiativos en los que el electrón “cae” desde el modo vibracional de menor energía del estado excitado a uno de los modos vibracionales del estado fundamental mediante la emisión de un fotón de luz. El retorno del modo vibracional excitado puede dar lugar a distintos modos vibracionales del estado fundamental. Como consecuencia, aunque todas las moléculas se exciten a la misma longitud de onda, los fotones emitidos pueden tener distintas longitudes de onda de emisión, originando el espectro de emisión fluorescente. La emisión de fluorescencia a una única longitud de onda, excitando a diferentes valores de longitud de onda permite obtener el espectro de excitación. En muchos casos el espectro de emisión es la imagen especular del de absorción, pero desplazado hacia el rojo, además, si una molécula posee un único fluoróforo el espectro de excitación debería coincidir con el espectro de absorción. Para que una molécula pueda emitir fluorescencia es necesario que sea capaz de absorber luz y, por tanto, poseer cromóforos, es decir, enlaces o conjuntos de enlaces responsables de dicha absorción de la luz. Los fluoróforos se pueden dividir en intrínsecos y extrínsecos según formen parte natural de la muestra o se añadan artificialmente para conferirle las propiedades fluorescentes deseadas. Los fluoróforos presentes en las proteínas son los aminoácidos aromáticos (triptófano, tirosina y fenilalanina). En el caso de las membranas lipídicas, éstas no presentan fluorescencia natural, por lo que para el estudio de las propiedades de la bicapa es necesario utilizar sondas fluorescentes que se

inserten en ella. A continuación se mostrarán una serie de técnicas fluorescentes utilizadas (Lakowicz, 2006).

2.5.1 Cálculo del coeficiente de partición de péptidos en membrana mediante espectroscopia de fluorescencia

La información que podemos obtener de la emisión de fluorescencia de una molécula es muy variada. Según la Ley de Stokes, el fotón emitido por fluorescencia tiene siempre menor energía que el fotón absorbido, dando lugar a que la frecuencia de la luz emitida por los fluoróforos sea siempre menor que la de la radiación incidente, es decir, que esté desplazada hacia el rojo con respecto a ella. En el caso de los fluoróforos polares este desplazamiento de Stokes va a ser mucho mayor en presencia de un disolvente polar, debido a interacciones entre el fluoróforo excitado y su entorno. Este es el caso, por ejemplo del triptófano. Esta propiedad de los fluoróforos polares nos va a dar información sobre el microambiente en el que se encuentren situados, ya que, por ejemplo, en el caso del triptófano, el desplazamiento hacia el rojo de la radiación emitida será mucho mayor en un disolvente polar que en uno apolar, por lo que se podrá utilizar la longitud de onda de la luz emitida como parámetro para la monitorización de la desnaturalización de una proteína (en el caso de que el Trp se encuentre aislado del medio en el interior de la proteína). Por otra parte, también se puede monitorizar el cambio del máximo de la longitud de onda hacia el azul de la radiación emitida, conjuntamente con el aumento de la intensidad de la fluorescencia del triptófano, cuando el triptófano de la proteína pasa de un medio acuoso a un medio más apolar, como puede ser una membrana lipídica. En el caso de la tirosina o de la fenilalanina el cambio de medio polar-apolar no se detecta por cambios en la longitud de onda del espectro de emisión, sino por un aumento en la intensidad del mismo. El coeficiente de partición (K_p) de un péptido en una membrana se puede definir como la relación entre la cantidad de péptido que hay unido a la membrana con respecto a la cantidad de péptido que hay libre en el tampón. Se pueden utilizar diversas metodologías de espectroscopía para el cálculo del K_p de una molécula fluorescente entre la fase lipídica y la acuosa (Santos et al., 2003). Para obtener los valores de K_p mostrados en esta Tesis se ha utilizado la intensidad de fluorescencia de los residuos fluorescentes de los péptido en un medio polar (tampón acuoso) y en presencia de distintas concentraciones de vesículas..

2.5.2 Ensayos de atenuación de fluorescencia

La atenuación (*quenching*) de la fluorescencia es otro parámetro de utilidad a la hora de caracterizar un sistema estudiado. Según el mecanismo de acción del atenuador (*quencher*) se distinguen dos tipos de atenuación. La atenuación colisional o dinámica, es aquella en la que el atenuador devuelve al fluoróforo a su estado fundamental mediante un proceso de difusión. Si el fluoróforo se encuentra en el estado excitado, pasa al estado fundamental sin emitir radiación, al disiparse la energía en forma de energía cinética de la molécula de atenuador. La eficacia de este proceso depende de la probabilidad estadística de que se produzca un encuentro entre un par fluoróforo-atenuador. Durante el proceso ninguna de las dos moléculas sufre cambios en su estructura. El otro tipo de atenuación se denomina estática, donde el atenuador puede asociarse al fluoróforo, incluso aunque éste se encuentre en el estado fundamental, formando un complejo permanente en equilibrio químico con las especies separadas, de tal manera que el fluoróforo se puede encontrar libre o asociado. Si se excita un fluoróforo en su estado libre, la emisión de fluorescencia tendrá lugar según su rendimiento cuántico. Pero, si la que se excita es una molécula de fluoróforo asociada a su atenuador, dicha molécula pasará al estado fundamental sin emitir radiación. Tanto en el caso de la atenuación colisional o dinámica como en el de la estática, la pérdida de intensidad de emisión fluorescente dependerá de la concentración de atenuador que haya en el medio. Existen multitud de atenuadores que van a mostrar diferentes preferencias por entornos distintos. Esta característica de los atenuadores puede ser utilizada para determinar la accesibilidad al solvente de un fluoróforo, así como su localización dentro de una proteína, bicapa, etc. En esta Tesis, para estudiar la localización de aminoácidos fluorescentes de péptidos en la membrana, se realizaron experimentos de atenuación de la fluorescencia de los aminoácidos fluorescentes mediante atenuadores lipofílicos asociadas a membrana, sondas 5NS y 16NS. Estas moléculas de ácido esteárico están derivatizadas con grupos doxiles (atenuadores) en la cadena hidrocarbonada, específicamente en los carbonos 5 (5NS) y 16 (16NS). Estas moléculas se utilizan para determinar la profundidad del fluoróforo, por ejemplo, el triptófano, la fenilalanina o la tirosina de un péptido tras insertarse en la membrana. El 5NS es un atenuador más eficaz para moléculas que se sitúan en la interfaz de la membrana o cerca de ella, mientras que el 16NS atenúa mejor las moléculas que se sitúan en la profundidad de la membrana (Fernandes et al., 2002). Para estudiar la exposición de los residuos fluorescentes de los péptidos al solvente cuando éstos están interaccionando con la membrana, se realizaron experimentos de atenuación con acrilamida. La acrilamida es una molécula soluble

que tiene la capacidad de atenuar la fluorescencia de los residuos fluorescentes de las proteínas. Se utiliza normalmente en estudios de proteínas, para determinar cuanto de expuesto(s) está(n) el o los triptófanos, tirosinas o fenilalanina de una proteína en distintas condiciones (Eftink and Ghiron, 1976). En nuestro caso la finalidad de la acrilamida es la misma, pero en los sistemas lípido-péptido.

2.5.3. Ensayos de transferencia de energía (FRET)

Además de los fenómenos de desexcitación de un fluoróforo en su estado excitado, existe otro muy común. Ocurre como consecuencia de la transferencia de energía de excitación desde el fluoróforo a una molécula vecina, provocando en ella otra excitación. Es decir, se produce una transferencia de la excitación desde el fluoróforo (donador, D) a otra molécula que actúa como aceptor (A). Esta transición se produce, en primera instancia, como consecuencia de una interacción dipolo-dipolo entre el donador y aceptor, disminuyendo el tiempo de vida natural del estado excitado y compitiendo con otras formas de desexcitación. Esta transferencia de energía se produce sin que medie emisión de un fotón por el donador. Influyen diversos factores para la eficacia del proceso:

- ◆ Es necesario que el espectro de la emisión del donador tenga un elevado grado de solapamiento con el espectro de absorción del aceptor. Cuanto mayor sea este solapamiento, mayor será la probabilidad de transferencia de la excitación.
- ◆ Dependerá de las intensidades de los espectros de emisión del donador y de absorción del aceptor, que estarán a su vez relacionados con el rendimiento cuántico de fluorescencia del donador y con el coeficiente de extinción molar del aceptor en la zona del solapamiento de los espectros.
- ◆ Dependerá de la distancia entre el aceptor y el donador, lo que hace que esta técnica sea extremadamente sensible a cambios en la distancia entre el donador y el aceptor. La probabilidad de transferencia decrece con la sexta potencia de la distancia entre ambos.
- ◆ Depende también de la orientación relativa de los dipolos transitorios de las moléculas de aceptor y donador. En principio, salvo que ambos dipolos sean perpendiculares, la probabilidad de la transferencia siempre es distinta de cero.

2.5.4 Ensayos de mezcla de lípidos (hemifusión y fusión)

La mezcla de lípidos es un proceso generalmente mediado por un agente externo por el que los lípidos de diferentes vesículas se mezclan debido a la ruptura de la capa de hidratación de los liposomas. Para estudiar el fenómeno se ha utilizado la metodología de Struck et al. (Struck et al., 1981), que está basada en la

transferencia de energía entre un par donador-aceptor. Se utilizaron dos derivados fluorescentes de la fosfatidiletanolamina (PE): la N-[7-nitrobenzeno-2-oxa-1,3-diazol-4-1]

fosfatidiletanolamina (NBD-PE) y la N-(lisamina-rodamina B-sulfonil) fosfatidiletanolamina (RhB-PE), donador

y aceptor, respectivamente. Las dos sondas fluorescentes están unidas al grupo amino libre del grupo polar de la PE, de tal forma que se puede incorporar con facilidad a los liposomas. Este par donador-aceptor se incorpora en la membrana de una misma población de liposomas, los cuales se mezclan con liposomas libres de ambas sondas, en una relación 1:4. Si hay hemifusión o fusión se producirá una dilución del par donador-aceptor, lo cual producirá un alejamiento entre ambas sondas, que a su vez producirá una disminución en la transferencia de energía entre ambas sondas. En el ensayo de hemifusión no se puede discriminar la mezcla de lípidos de la hemicapa externa (hemifusión) de la mezcla de lípidos de la hemicapa interna (fusión). Sin embargo, en el ensayo de fusión se añade exógenamente ditionito para eliminar la fluorescencia de las sondas de la hemicapa externa. Por lo tanto, si se observara transferencia de energía se debería a la mezcla de lípidos de la hemicapa interna de liposomas diferentes, por lo que podríamos decir que está ocurriendo un proceso de fusión (Figura 2.6).

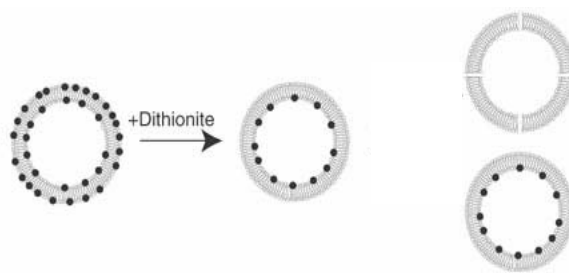


Figura 2.6.- Esquema de la reducción producida por el ditionito

2.5.5. Ensayos con dominios de dehidroergosterol (DHE)

Los procesos de fusión de la envuelta de muchos virus con la membrana celular huésped son dependientes de la composición lipídica de la membrana celular. Un ejemplo es el HIV-1, donde el colesterol es un componente fundamental para una óptima actividad de fusión con su

célula huésped (Viard et al., 2002). El estudio de la interacción de un péptido o proteína con regiones ricas en colesterol de una vesícula o la segregación de estas regiones inducidas por el péptido o proteína pueden llevarse a cabo mediante estudios de FRET. Realizamos un estudio de transferencia de energía entre un análogo fluorescente del colesterol, conocido como dehidroergosterol (DHE, ergosta-5,7,9(11),22-tetraen-3 β -ol) actuando como aceptor y los triptófanos del péptido estudiado actuando como donadores de energía. Se considera que el comportamiento biofísico del DHE en la membrana y su interacción con moléculas de Chol para la formación de dominios es similar al comportamiento que presenta una molécula de Chol, debido a la gran similitud entre sus estructuras (Loura & Prieto, 1997).

2.5.6. Anisotropía con sondas extrínsecas

Otra característica de los fluoróforos es que pueden ser excitados fotoselectivamente, dado que las moléculas fluorescentes absorben preferentemente los fotones cuyo vector eléctrico es paralelo al momento de transición de su dipolo. Si se excita una población de fluoróforos con luz polarizada, se excitará selectivamente a aquellos fluoróforos que estén orientados con su momento de transición paralelo al vector eléctrico de la excitación. Del mismo modo, la emisión tendrá lugar en forma de luz polarizada a lo largo de un eje fijo en el fluoróforo. La velocidad con la que un fluoróforo es capaz de rotar durante su tiempo de vida en el estado excitado

determinará su polarización o anisotropía.

Esta característica de los fluoróforos se ha utilizado ampliamente para determinar el volumen de las proteínas (puesto que está relacionado directamente con el tiempo de correlación rotacional), y la viscosidad o fluidez del interior de las bicapas lipídicas. Para estudiar los cambios en el orden de la membrana a distintas profundidades, se realizaron experimentos de polarización de fluorescencia en estado estacionario con las siguientes sondas: 1,6-difenil-1,3,5-hexatrieno (DPH), y dos derivadas de ella:

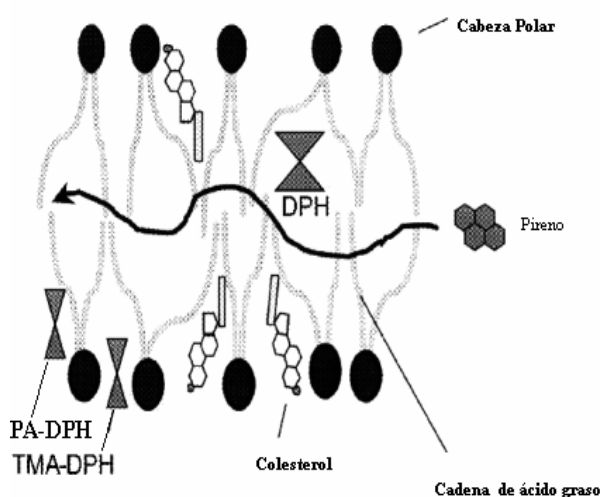


Figura 2.7. Localización de las sondas extrínsecas TMA-DPH, PA-DPH y DPH en la membrana

1-(4-trimetilamoniofenil)-6-fenil-1,3,5-hexatrieno (TMA-DPH) y ácido propiónico 1,6-difenil-1,3,5-hexatrieno (PA-DPH). El DPH presenta ciertas propiedades que permiten su localización en la profundidad de la membrana lipídica (Figura 2.7):

- ◆ Se trata de una molécula altamente hidrofóbica, por lo que se espera que se sitúe en la profundidad de la membrana;
- ◆ Es una molécula con una longitud aproximada de 14 Å;
- ◆ Su estructura en forma de varilla permite que el DPH se empaquete bien entre las cadenas acílicas de los fosfolípidos (Florine-Casteel, 1990).

El uso de derivados del DPH también ayuda a localizar la molécula de DPH a distintas profundidades dentro de la membrana. En esta Tesis se han utilizado dos derivados del DPH: TMA-DPH y PA-DPH (Figura 2.7). Las profundidades a las que quedan los grupos unidos a la molécula de DPH desde el centro de la membrana son las siguientes: TMA-DPH a 19 Å y DPH a 8-11 Å (Kaiser and London, 1998, Kaiser and London 1999).

2.5.7 Estudios del potencial electrostático en la superficie de la membrana

Existen tres tipos principales de potenciales electrostáticos asociados a las membranas: el potencial electrostático de superficie (ψ_s), el potencial dipolar (Φ_d) y el potencial transmembrana ($\Delta\psi$) (Figura 2.8).

El potencial electrostático de superficie (ψ_s) existe como una interfase lípido-agua donde las membranas biológicas están cargadas, predominantemente como resultado de grupos ionizados y polares de la membrana. Estos grupos son parte de los propios lípidos, glicolípidos y proteínas de membrana, como por ejemplo, la presencia de cabezas polares de fosfolípidos cargados negativamente (PG, PS, PI, etc), los cuales están neutralizados por los correspondientes contra-iones. La carga de la interfase membrana-agua también puede ser debida a la adsorción no equitativa de los iones de la fase acuosa sobre la superficie de la membrana, esto es en el caso de los fosfolípidos zwitteriónicos, tal como la PC. Esta capa de carga desde la superficie de la membrana hasta la fase acuosa es de aproximadamente 20 nm de espesor, lo cual es comparable al espesor de la región del glicocáliz de la membrana (Cevc,

1990). Se asume que la diferencia de potencial entre la superficie de la membrana y la fase acuosa es electroneutra en un punto infinitamente distante de la superficie de membrana. Las distribuciones de iones en la fase acuosa están afectadas por el Ψ_s resultando en la atracción

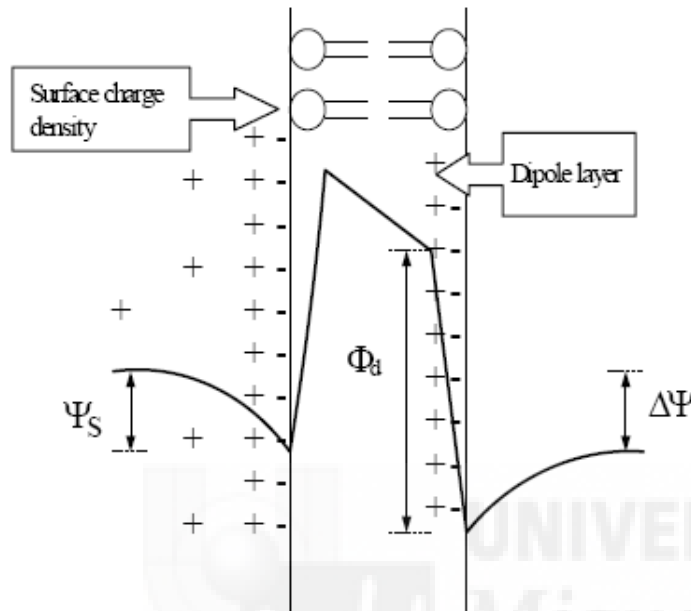


Figura 2.8. - Potenciales electrostáticos de la membrana. Perfil energético de la interacción de una carga positiva de prueba con los campos electrostáticos que podría encontrarse en una bicapa lipídica. La densidad de carga superficial, σ , debida a la presencia de proteínas o lípidos con carga, produce un potencial electrostático en la superficie de la membrana (Ψ_s). La capa de dipolo de la membrana da lugar a un gran potencial dipolar interno (Φ_d), que alcanza un valor de aproximadamente 250 mV en bicapas de PC. El potencial dipolar es el responsable de que el núcleo hidrocarbonado de la bicapa sea positivo respecto a la fase acuosa. Cuando se producen separaciones de carga entre ambos lados de la bicapa se forma un potencial electrostático transmembranal ($\Delta\Psi$). Por claridad, las cargas y dipolos sólo se muestran en un lado de la bicapa. (Clarke, 1997, Gross et al., 1994).

electrostática de los contra-iones y la repulsión de los co-iones desde la fase acuosa hacia la superficie de la membrana. El modelo de Gouy-Chapman ha resultado ser especialmente válido para predecir el potencial electrostático de superficie de las membranas (Cafiso et al., 1989; Cevc, 1990). Las cuatro condiciones que asume este modelo son las siguientes:

- ◆ Se considera que las cargas están distribuidas uniformemente en la superficie de la membrana, lo que permite definir una densidad de carga superficial, σ (las cargas de la membrana no se consideran como puntuales).
- ◆ Los iones en disolución se tratan como cargas puntuales sin considerar su tamaño.
- ◆ Se ignora la repulsión entre los iones móviles del mismo signo eléctrico.
- ◆ La constante dieléctrica de la fase acuosa es válida hasta la misma superficie de la membrana.

La combinación de la ecuación de Boltzmann en su forma logarítmica con la ecuación de Henderson-Hasselbach resulta en la ecuación: $pK_s = pK_B + \psi_s$, la cual relaciona la respuesta del ψ_s con los grupos ácidos localizados en la superficie de la membrana. Esta última ecuación demuestra que el pK de un grupo ácido en una superficie electronegativa (la cual posee un potencial de superficie) sería distinto si se comparara con el mismo grupo en una fase acuosa. Esto indica que la concentración relativa de protones, en la superficie de una membrana, difiere de la de la fase acuosa. De esta manera, para un indicador fluorescente de pH, como por ejemplo el grupo de fluoresceína de la molécula fluoresceína-fosfatidiletanolamina (FPE), localizado en la superficie de la membrana, cambios del ψ_s en un medio con un pH constante afectarán el estado de protonación de la sonda FPE, produciendo cambios en su fluorescencia. Por lo tanto, cambios en ψ_s producirán cambios en el pK aparente de la sonda FPE. En otras palabras, el rendimiento de la fluorescencia ofrece una medida directa del potencial electrostático, alrededor del grupo de fluoresceína. De ahí que la sonda FPE pueda detectar moléculas cargadas que estén interaccionando con la superficie de la membrana (Wall et al., 1995).

2.5.8 Estudios del potencial bipolar

El potencial dipolar de membrana (ϕ) tiene su origen en la polarizaciones moleculares, asociadas con el grupo carbonilo ($C^{\delta+}=O^{\delta-}$) y los componentes del fosfato unidos al oxígeno ($O^{\delta-}-P^{\delta+}$) de los fosfolípidos en la membrana. Estas polarizaciones ocurren entre la superficie de membrana y la interfase hidrofóbica de la membrana. Además, moléculas individuales de agua adoptan una estructura organizada a lo largo de la superficie de la membrana, contribuyendo de esta manera como dipolos moleculares permanentes (Brockman, 1994). Se piensa que los grupos dipolares se organizan de tal forma que el interior de la membrana es positivo con respecto a la fase acuosa externa, teniendo una magnitud de varios cientos de milivoltios. Dependiendo de la estructura del lípido, esta magnitud puede variar de 100 a más de 400 mV, positivo en el interior de la membrana (Schamberger and Clarke, 2002). El potencial del dipolo ocupa las regiones cercanas a la superficie de membrana. En 1979, Loew et al. introdujeron la sonda fluorescente potenciométrica 1-(3- sulfonatopropyl)-4-[[b[2-(di-n-octylamino)-6-naphthyl]vinyl] pyridinium betaina, conocida como Di-8-ANEPPS (Loew et al., 1979). Las propiedades fluorescentes de la molécula di- 8-ANEPPS dependen en gran parte de su ambiente, siendo no fluorescente cuando se encuentra en solución acuosa (Fluhler et al., 1985). Esta sonda se utiliza para medidas del

potencial del dipolo de la membrana usando un método fluorescente que relaciona dos longitudes de onda (Cladera et al., 1999; Cladera and O'Shea, 1998; Cladera et al., 1997; Clarke and Kane, 1997). Di-8-ANEPPS permite medir la variación en la magnitud del potencial dipolo y monitorizar las interacciones moléculas-membrana (Cladera and O'Shea, 1998). También puede usarse como indicador de la inserción de macromoléculas dentro de la membrana, ya que la macromolécula podría aumentar o disminuir el potencial del dipolo de la membrana, dependiendo de su carga y orientación en su inserción.

2.6 Resonancia magnética Nuclear

La espectroscopía de Resonancia Magnética Nuclear (RMN) en disolución es una de las técnicas más poderosas para la elucidación estructural de compuestos moleculares mediante la caracterización de los desplazamientos químicos, los acoplamientos y las intensidades relativas de los picos de resonancia. La RMN en disolución es complementaria de la cristalografía de rayos-X ya que la primera permite estudiar la estructura tridimensional de las moléculas en fase líquido o disuelta en un cristal líquido, mientras que la cristalografía de rayos-X, como su nombre indica, estudia las moléculas en fase sólido. La RMN puede utilizarse también para el estudio de muestras en estado sólido. Si bien en su estado actual queda lejos de poder proporcionar con buen detalle la estructura tridimensional de una biomolécula. En el estado sólido las moléculas están estáticas y no existe, como ocurre con las moléculas en disolución, un promediado de la señal de RMN por el efecto de la rotación térmica de la molécula respecto a la dirección del campo magnético. Las moléculas de un sólido están prácticamente inmóviles, y cada una de ellas experimenta un entorno electrónico ligeramente diferente, dando lugar a una señal diferente. Esta variación del entorno electrónico disminuye la resolución de las señales y dificulta su interpretación. A diferencia de los espectros en disolución, los espectros en estado sólido son mucho más anchos en los que se pierde la “alta resolución” que se obtiene en los RMN de líquidos. Al aplicar esta técnica a los sólidos se trata de recuperar la resolución que tienen los espectros en líquidos. La sensibilidad de las señales también depende de la presencia de núcleos magnéticamente-susceptibles a la RMN y, por tanto, de la abundancia natural de tales núcleos. Para el caso de biomoléculas los núcleos más abundantes y magnéticamente susceptibles son los isótopos de hidrógeno ^1H y fósforo ^{31}P . Otros átomos como el ^{12}C , ^{28}Si , ^{56}Fe

en su isótopo más común tienen $I=0$ y por tanto no dan espectros de RMN. Mientras que hay núcleos con número cuántico de espín $=3/2, 5/2$ e incluso $7/2$.

2.6.1 Resonancia magnética nuclear de rotación en ángulo mágico.



Figura 2.9. Sonda Bruker 4mm CP-MAS

Raymond Andrew fue uno de los pioneros en el desarrollo de métodos de alta resolución para resonancia magnética nuclear en estado sólido. Él fue quien introdujo la técnica de la rotación en el ángulo mágico *Magic Angle Spinning* (MAS) que permitió aumentar la resolución de los espectros de sólidos varios órdenes de magnitud. El MAS consiste en el uso de las sondas de sólidos donde la muestra se rota a 55° y $44'$ respecto del campo magnético externo aplicado (Figura 2.9). En estas condiciones el término $(1-3\cos^2\theta)$, se hace cero por lo que el ensanchamiento por interacciones dipolares se anula. A este ángulo de rotación se le denomina ángulo mágico (MAS NMR). Además, si se rota lo suficientemente rápido, 9 kHz para el fósforo, las interacciones de desplazamiento

químico se reducen al mínimo por lo que no contribuyen al ensanchamiento de las resonancias. Alex Pines en colaboración con John Waugh revolucionaron también la RMN de sólidos introduciendo la técnica de la polarización cruzada que consigue incrementar la sensibilidad de núcleos poco abundantes. Esta técnica consiste en una secuencia de pulsos acoplando el protón del núcleo que se quiere estudiar.

Las membranas biológicas están mayoritariamente compuestas por fosfolípidos, éstos en disolución acuosa pueden formar diferentes fases con variadas superestructuras. La naturaleza de estas conformaciones, así como el porcentaje de conversión entre ellas puede ser estudiado por medio de resonancia magnética nuclear de ^{31}P . El estudio de RMN de ^{31}P permite conocer la conformación de la cabeza polar de los fosfolípidos en las membranas y la naturaleza de las fases formadas por los lípidos. El desplazamiento químico del enlace fosfodiéster tal y como lo encontramos en los lípidos presentes en la membrana depende de la orientación del grupo con respecto al campo magnético del espectrómetro. El espectro de ^{31}P es la suma de los espectros

para todas las orientaciones posibles. En el caso del fósforo unido a los fosfolípidos se observa un rápido movimiento anisotrópico que puede promediar algunos de los componentes del tensor de desplazamiento químico, por lo que las diferencias en la amplitud del desplazamiento químico es una medida del grado de orden del grupo fosfato. La forma y anchura del patrón depende de la orientación del eje de la media de movimiento con el espectro al componente principal del tensor de desplazamiento químico (Thayer and Kohler, 1981). Dos procesos de difusión contribuyen a promediar el espectro: uno es el movimiento browniano rápido de la vesícula entera, y el otro es la difusión lateral de los lípidos dentro de la vesícula. La efectividad del proceso de promediado por el movimiento, aumentará con la disminución de la forma de la vesícula, ya que vesículas muy pequeñas tienen un movimiento muy rápido, por lo que la media de la anisotropía es completa y el espectro resultante es una estrecha resonancia como si se tratara de un desplazamiento químico isotópico. Este resultado es el que se obtiene en liposomas muy pequeños, estructuras micelares, detergentes o fosfolípidos sonicados.

Ciertos lípidos pueden formar diferentes tipos de estructura en las cuales las moléculas se proyectan radialmente del centro hacia el exterior formando cilindros (Luzzati and Husson, 1962). La difusión lateral rápida dentro de la fase solo afecta a la forma de la resonancia del P^{31} cuando las hemicapas cercanas tienen un radio muy pequeño. Los cilindros en fase hexagonal tienen un radio muy pequeño y por ello la difusión lateral sobre el eje del cilindro puede afectar además a la media del componente del tensor. La red resultante del patrón de fósforo en fase hexagonal tiene una diferencia en el desplazamiento químico que es aproximadamente la mitad de lo que le corresponde a la fase bicapa. La forma, cuya intensidad está aumentada, aparece como un componente axial al otro lado del desplazamiento químico. Por todas estas razones, se pueden usar los patrones de anchura y posición de la resonancia de P^{31} como diagnóstico de la presencia de fases.

2.7. Difracción de rayos X

La caracterización estructural de los sistemas modelo de membrana fue iniciada por los trabajos de Luzzati y colaboradores (Luzzati and Husson, 1962) por medio de la difracción de rayos X. La técnica de difracción supuso un avance por el hecho de que los lípidos se agregan en MLV, apilamientos de membranas lamelares repetidas de 50 a 150 capas, además de formar vesículas unilamelares. La así llamada estructura periódica unidimensional permite la aparición del pico de refracción de Bragg, el cual se puede analizar por el método de Fourier (Figura 2.10).

Sin embargo, por las fluctuaciones del sistema, la información es limitada y por tanto técnicas especiales y teorías se han desarrollado para compensar la pérdida de información. La difracción de rayos X se produce por la interferencia de ondas dispersadas por un objeto cuando es excitado con una radiación energética incidente. En el caso de una muestra de rayos X, hasta la energía de un fotón de rayos X es muy grande comparada con la energía de unión de un átomo, por lo que todos los electrones de un átomo individual se convertirán en una fuente de dispersión de la onda. Esta dispersión de ondas interfieren de una manera coherente, que

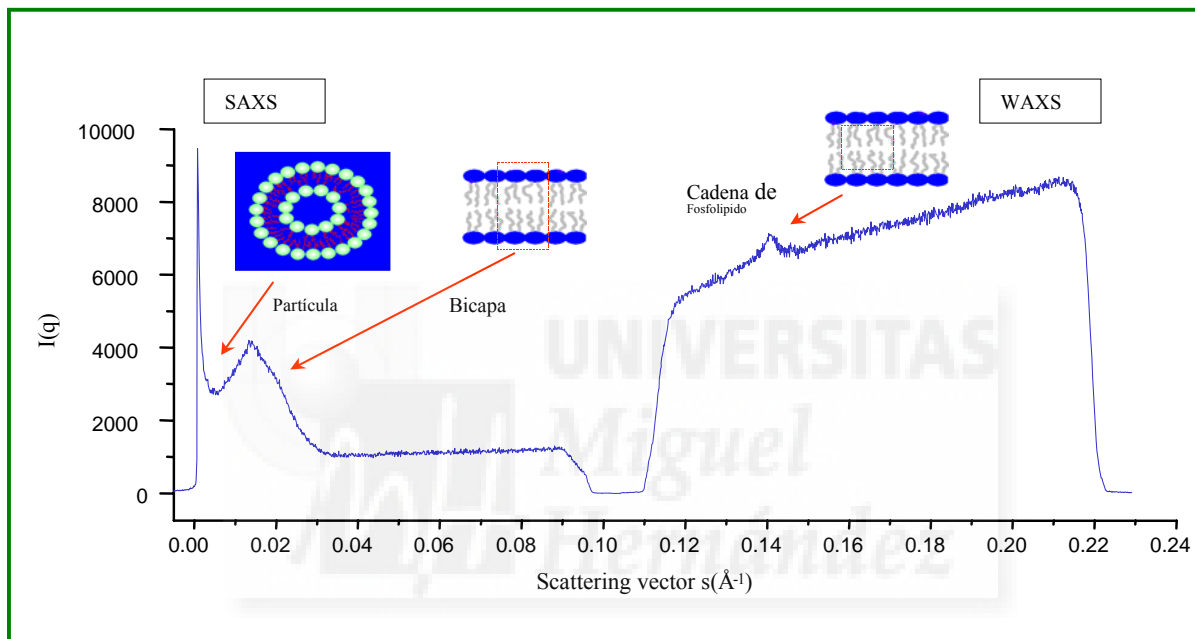


Figura 2.10. Ejemplo de difractograma de intensidad (I) de X-ray frente al vector de difracción (q), indicando el tipo de información de cada parte del difractograma.

significa que la amplitud de la onda que son de igual magnitud, se suman y difieren solo en su fase. La teoría de la difracción de rayos X es muy extensa y no será abarcada en esta Tesis; sin embargo destacaremos algunos parámetros físicos que se pueden medir y permiten una visión de la muestra estudiada. La intensidad del patrón de las medidas de rayos X pueden ser diversas, dependiendo de la estructura mas o menos ordenada de la muestra, variando también la forma del pico (Figura 2.10). La forma del pico de difracción, llamada pico de Bragg requiere la diferente ruta entre el haz reflejado del entramado de planos adyacentes por ser un numero entero de la longitud de onda . Esto es descrito como la Ley de Bragg (Laggner, 1988). Si el

difractograma muestra el pico de Bragg típico de vesículas multilamelares, la distancia lamelar repetida o d-spacing (d) que comprende el grosor de la membrana más una capa de agua entre dos membranas consecutivas para los MLV, puede ser obtenida por la posición del pico de Bragg (Figura 2.11).

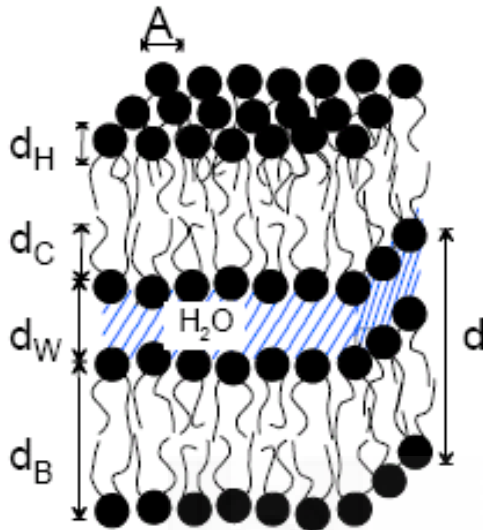


Figura 2.11: Supervisión de los parámetros estructurales que se pueden obtener de sistemas multilamelares de bicapas lipídicas es la unidad repetida de membranas. d_w la extensión de la capa de agua intersticial, d_B el grosor de la membrana que puede ser subdividido en el grosor de la cabeza polar d_H y d_C longitud de la cadena hidrocarbonada

Las propiedades de membrana caracterizadas por estudios experimentales en vesículas o bicapas en soporte sólido pueden ser divididas en características locales o globales. Las propiedades locales pueden ser por ejemplo diferentes modos de movimientos y vibraciones moleculares, difusión, orientación de las cadenas y también el desorden en la vecindad. En cambio, las propiedades globales de membrana es una media de la estructura en bicapa, curvatura, rigidez, interacciones de la bicapa, empaquetamiento de las cadenas. En particular la difracción de Rayos-X es una técnica no destructiva ampliamente aplicada, para obtener una vista de la estructura de la membrana o sus interacciones. Aunque las propiedades globales y locales se pueden derivar por separado utilizando varias técnicas experimentales estas están íntimamente acopladas. Por ejemplo, el empaquetamiento de la cadena hidrocarbonada o la cabeza polar y sus cambios pueden ser inducidos por interacciones por compuestos membrano-activos que pueden originar un amplio grado de efectos, lo que permite ajustar una estructura media global estructural. Las propiedades globales de membrana se pueden obtener por medio de experimentos con vesículas de difracción de rayos X de ángulo pequeño, pudiendo obtenerse la estructura y características mecánicas de la bicapa usando modelos descritos de membrana. Aunque no se pueda ver cambios en las propiedades locales de la membrana, se pueden determinar su interacción por los cambios que ellos causan globalmente.

Los modelos aplicados al factor estructural $S(q)$ de acuerdo con la teoría de Caillé y la forma del factor $F(q)$ dada por la transformación de Fourier unida a la aplicación de simples picos de gaussianas, describen el perfil de electrodensidad de la membrana. (Figura 2.12). Para

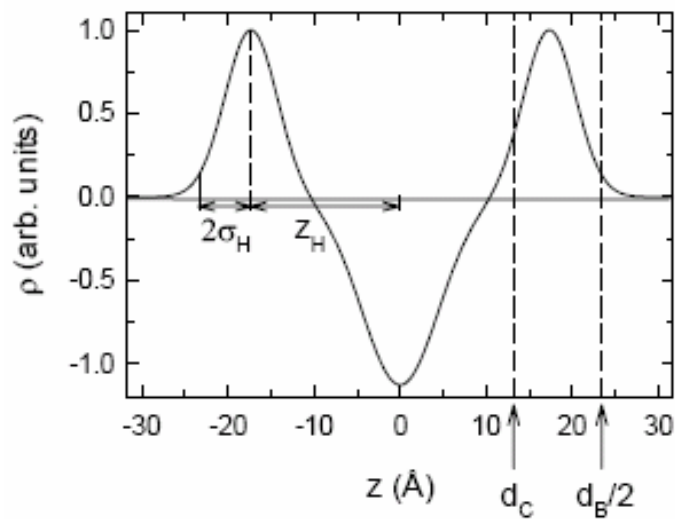


Figura 2.12. Modelo del perfil de electro densidad representado por el sumatorio de 3 gaussianas. La gaussiana centrada en $\pm z_H$ caracteriza el grupo de la cabeza polar, y $2\sigma_H$ ancho hacia las capa de aguas definiendo el limite de la bicapa, $d_B/2$. El limite de la region hidrocarbonada, d_C , se calcula considerando la forma de la cabeza polar.

ello a los modelos de membrana debemos aplicar una teoría con un factor dependiente de la estructura de los patrones de difracción de MLVs. La teoría Caillé debe ser usada para el análisis de los patrones de difracción de la fase L_α . En cambio la teoría Paracrystalina no cumple las fluctuaciones por curvatura, y considera solo el desorden colocacional. Esta teoría puede ser aplicable a la fase lamelar gel L_β (o $L_{\beta 1}$), las cuales tienen una rigidez que es un orden de magnitud mayor que en la fase fluida.





CAPÍTULO III

OBJETIVOS Y PRESENTACIÓN

DEL TRABAJO



OBJETIVOS Y PRESENTACIÓN DE TRABAJOS

I

Búsqueda de las regiones membranotrópicas de las proteínas estructurales del HCV:

- a) Proteína *core*, implicada en la salida del virus
- b) Canal de membrana *p7*, implicado en la salida del virus.
- c) Glicoproteínas de la envuelta viral *E1* y *E2*, implicadas en el proceso de fusión de membranas.

Estos objetivos se plasmaron en las siguientes publicaciones científicas seleccionadas para formar parte de la presente Tesis Doctoral:

1. *Hepatitis C virus core protein binding to lipid membranes: the role of domains 1 and 2.*
Pérez-Berná AJ, Veiga AS, Castanho MA, Villalaín J.
Journal of Viral Hepatitis, 15, 346-56, 2007.
2. *Identification of the membrane-active regions of HCV p7 protein. Biophysical characterization of the loop region*
Pérez-Berná AJ, Guillén J, Moreno MR, Bernabeu A, Pabst G, Laggner P, Villalaín J.
Journal of Biological Chemistry, 283, 8089-101, 2008.
3. *The membrane-active regions of the Hepatitis C virus E1 and E2 envelope Glycoproteins.*
Pérez-Berná A J, M R. Moreno, J Guillén, ABernabeu, and J Villalaín.
Biochemistry, 45, 3755-3768, 2006

II

Caracterización biofísica de las regiones membranotrópicas de las glicoproteínas *E1* y *E2* de la envuelta viral involucradas en el proceso de entrada viral. La finalidad de estos estudios fue proponer un modelo de interacción lipido-péptido potencialmente extrapolable a la proteína nativa. Para ello se estudió:

- a) La interacción y unión de los péptidos seleccionados con membranas modelo mediante espectroscopia de fluorescencia, por medio de la fluorescencia intrínseca de los péptidos y con sondas fluorescentes.
- b) El efecto de los péptidos en la desestabilización de sistemas modelo de membrana por medio de sondas fluorescentes, calorimetría diferencial de barrido y espectroscopia de infrarrojo por transformada de Fourier.
- c) La caracterización de la capacidad de los péptidos de promover rotura y fusión de liposomas.
- d) El estudio de la conformación de los péptidos en disolución y en presencia de membranas por medio de dicroísmo circular y espectroscopia infrarroja.
- e) El estudio de la estructura de los sistemas modelo de membrana como consecuencia de la interacción de los péptidos mediante resonancia magnética nuclear y difracción de rayos X.

Los ensayos se realizaron con diversas composiciones lipídicas para evaluar el papel que juegan los diferentes lípidos en el proceso de fusión y la dependencia por determinados lípidos que pudieran tener los péptidos caracterizados.

Este objetivo se plasmó en las siguientes publicaciones científicas seleccionadas para formar parte de la presente Tesis Doctoral:

4. *Interaction of the most membranotropic region of the HCV E2 envelope glycoprotein with membranes.*
Pérez-Berná AJ, Moreno MR, Guillén J, Gomez-Sanchez AI, Pabst G, Laggner P, Villalaín J.
Biophysical Journal, 94, 4737-50, 2008
5. *The pre-transmembrane region of the HCV E1 envelope glycoprotein. Interaction with model membranes.*
Pérez-Berná AJ, Guillén J, Moreno MR, Bernabeu A, Villalaín J.
Biochimica et Biophysica Acta. Doi: 18424260, Aceptado en abril, 2008.

Los siguientes artículos también se encuentran dentro de los objetivos de la tesis, aunque se añaden en el anexo de publicaciones en proceso de aceptación, ya que estos artículos se encuentran todavía en proceso de revisión:

6. *Biophysical characterization of the fusogenic region of HCV E1 envelope glycoprotein.*
Pérez-Berná AJ, Pabst G, Laggner P, Villalaín J.
7. *Effect of the pre-transmembrane region of the HCV E1 envelope glycoprotein on DEPE polymorphism*
Ana J. Pérez-Berná, Alejandro González-Álvarez, Georg Pabst, Peter Laggner and José Villalaín

III

Búsqueda de inhibidores peptídicos dirigidos contra las regiones membranotrópicas de las glicoproteínas *E1* y *E2*, con el objetivo de inhibir la entrada del virus en la célula. Para esta búsqueda se usó una técnica de barrido de alto rendimiento haciendo uso de diferentes librerías peptídicas. Para comprobar *in vivo* el potencial neutralizador de la infección de los péptidos inhibidores encontrados tras el barrido se realizaron estudios de entrada de pseudopartículas de HCV en células hepáticas.

La consecución de este objetivo se llevó a cabo en el siguiente artículo, el cual se encuentra todavía en proceso de revisión

8. *Searching of HCV inhibition viral-cell fusion*
Ana Joaquina Pérez-Berná, Dimitri Lavillette, and José Villalaín



The background of the page is a dense field of flowers, primarily purple and yellow, with some pink and white blossoms interspersed. The flowers are in various stages of bloom, creating a vibrant and textured appearance. The lighting is soft, highlighting the delicate petals and the bright centers of the flowers.

CAPÍTULO IV

ANEXO DE PUBLICACIONES

ACEPTADAS

Publicación 1

Hepatitis C virus core protein binding to lipid membranes: the role of domains

1 and 2

A. J. Pérez-Berná¹, A. S. Veiga², M. A. R. B. Castanho²
and J. Villalaín¹

¹Instituto de Biología Molecular y Celular, Universidad “Miguel
Hernández”, Elche-Alicante, Spain

²Centro de Química e Bioquímica, Faculdade de Ciências da
Universidade de Lisboa, Campo Grande, Lisboa, Portuga

Journal of Viral Hepatitis, 2008, 15, 346–356



Hepatitis C virus core protein binding to lipid membranes: the role of domains 1 and 2

A. J. Pérez-Berná,¹ A. S. Veiga,² M. A. R. B. Castanho² and J. Villalain¹ ¹Instituto de Biología Molecular y Celular, Universidad “Miguel Hernández”, Elche-Alicante, Spain; and ²Centro de Química e Bioquímica, Faculdade de Ciências da Universidade de Lisboa, Campo Grande, Lisboa, Portugal

Received July 2007; accepted for publication October 2007

SUMMARY. We have analysed and identified different membrane-active regions of the Hepatitis C virus (HCV) core protein by observing the effect of 18-mer core-derived peptide libraries from two HCV strains on the integrity of different membrane model systems. In addition, we have studied the secondary structure of specific membrane-interacting peptides from the HCV core protein, both in aqueous solution and in the presence of model membrane systems. Our results show that the HCV core protein region comprising the C-terminus of domain 1 and the N-terminus of domain 2 seems to be the most active in membrane interaction, although a role in protein–protein interaction cannot

be excluded. Significantly, the secondary structure of nearly all the assayed peptides changes in the presence of model membranes. These sequences most probably play a relevant part in the biological action of HCV in lipid interaction. Furthermore, these membranotropic regions could be envisaged as new possible targets, as inhibition of its interaction with the membrane could potentially lead to new vaccine strategies.

Keywords: assembly, capsid, core protein, HCV, hepatitis, lipid.

INTRODUCTION

Hepatitis C virus (HCV) is an enveloped positive single-stranded RNA virus that belongs to the genus *Hepacivirus* in the family *Flaviviridae*, and is the leading cause of acute and chronic liver disease in humans, including chronic hepatitis, cirrhosis, and hepatocellular carcinoma [1–3]. There exists no vaccine to prevent HCV infection and current therapeutic agents have limited success against HCV [4]. The HCV genome consists of one translational open reading frame encoding a polyprotein precursor, including structural and non-structural proteins, that is cleaved by host and viral proteases (Fig. 1a). The structural proteins consist of the core protein, which forms the viral nucleocapsid, and the envelope glycoproteins E1 and E2, both of them transmem-

brane proteins. The HCV cell entry is achieved by the fusion of viral and cellular membranes, and the morphogenesis and virion budding has been suggested to take place in the endoplasmic reticulum [5]. HCV proteins are very sensitive to folding, assembly, mutations or deletions. Besides, the HCV genome is widely heterogeneous; the errors during its replication cause a high rate of mutations. Therefore, the region implicated in fusion and/or budding must interact with the membranes and should be a conservative sequence. Finding protein–membrane and protein–protein interaction inhibitors could be a good strategy against HCV infection as they might prove to be potential therapeutic agents.

The HCV core protein is highly basic and shows homology with the nucleocapsid protein of other flaviviruses. This protein is well conserved among the different HCV strains [6] and is important for HCV infection diagnosis by the detection of either specific anti-HCV core protein antibodies or circulatory viral antigens. The core protein has regulatory roles on cell functions like immune presentation, apoptosis, lipid metabolism and transcription [7–9]. Additionally, this protein has oncogenic potential playing an important role in the regulation of HCV-infected cell growth, transformation to a tumorigenic phenotype and development of hepatocellular carcinoma [10]. Recombinant cDNA expression studies of this protein have identified two major protein core species, p23 and p21 [8]. The later is the predominant species and is

Abbreviations: CF, 5-Carboxyfluorescein; Chol, cholesterol; EPC, egg 1-phosphatidylcholine; HCV, hepatitis C virus; LUV, large unilamellar vesicles; MLV, multilamellar vesicles; NBD-PE, N-(7-nitrobenz-2-oxa-1,3-diazol-4-yl)-1,2-dihexadecanoyl-sn-glycero-3-phosphoethanolamine; N-RhB-PE, lissamineTM rhodamine B 1,2-dihexadecanoyl-sn-glycero-3-phosphoethanolamine; SM, egg sphingomyelin; T_m, temperature of the gel–liquid crystalline phase transition.

Correspondence: Dr. José Villalain, Instituto de Biología Molecular y Celular, Campus de Elche, Universidad “Miguel Hernández”, E-03202 Elche-Alicante (España-Spain). E-mail: jvillalain@umh.es

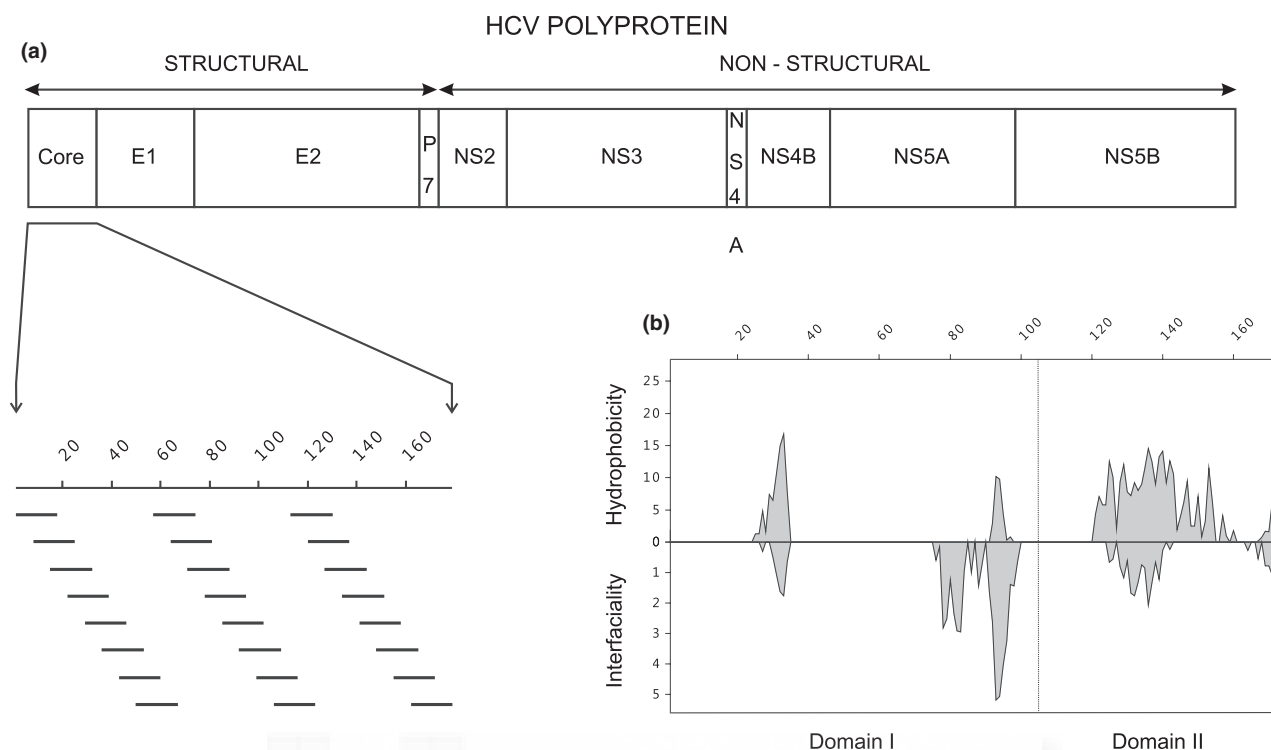


Fig. 1 (a) Scheme of the hepatitis C virus (HCV) structural and non-structural proteins according to literature consensus. The sequence and relative location of the twenty-seven 18-mer peptides derived from the HCV core protein are shown with respect to the sequence of the protein. Maximum overlap between adjacent peptides is 11 amino acids. (b) Analysis of the hydrophobicity and interfaciality distribution according to the scales of Wimley and White [22,23] using a window of 11 amino acids along the HCV core sequence without any assumption about secondary structure.

found in viral particles from infected sera, probably being the mature form of the protein. Although the three dimensional structure of this protein is unknown three distinct domains can be considered in the full-length immature protein [11,12], i.e. domain 1, comprising amino acids 1–117 and having several positive charges involved in RNA binding and including the immunodominant antigenic site, domain 2, comprising amino acids 117–171 and putatively responsible of its association with lipid droplets, and domain 3, comprising amino acids 171–191, a signal peptide upstream of the E1 glycoprotein. Significantly, the mature core protein is a dimeric helical protein exhibiting membrane protein features [11].

Recently, we have identified the membrane-active regions of the human immunodeficiency virus (HIV) gp41, severe acute respiratory syndrome coronavirus (SARS-CoV) spike and HCV E1 and E2 glycoproteins by observing the effect of glycoprotein-derived peptide libraries on model membrane integrity [13–15]. These results have permitted us to suggest the possible location of different segments in these proteins which might be implicated in protein–lipid and protein–protein interactions, helping us to understand the processes which give rise to the interaction between the protein and the membrane. Additionally, HCV membrane assembly and budding is an attractive target for anti-HCV therapy, as it

has been proposed that the core protein has an important role in viral assembly. To investigate the structural basis of the protein core interaction with the membrane and identify new targets for searching viral assembly inhibitors, we have analysed and identified different membrane-active regions of the HCV core protein by observing the effect of 18-mer core-derived peptide libraries from two HCV strains, namely, HCV 1AH77 and HCV 1B4J, on the integrity of different membrane model systems. Furthermore, we have studied the secondary structure of specific membrane-interacting peptides, both in aqueous solution and in the presence of model membrane systems, to understand the molecular mechanism of viral budding as well as making possible the future development of HCV assembly inhibitors which may lead to new vaccine strategies.

MATERIALS AND METHODS

Materials and reagents

Egg L-phosphatidylcholine (EPC), egg sphingomyelin (SM), liver lipid extract (a 2:1 chloroform:methanol extract of liver tissue) and cholesterol (Chol) were obtained from Avanti Polar Lipids (Alabaster, AL, USA). 5-Carboxyfluorescein (CF) (>95% by high performance liquid chromatography), and

sodium dithionite were from Sigma-Aldrich (Madrid, Spain). Lissamine rhodamine B 1,2-dihexadecanoyl-snglycero-3-phosphoethanolamine (N-RhB-PE) and N-(7-nitrobenz-2-oxa-1,3-diazol-4-yl)-1,2-dihexadecanoyl-sn-glycero-3-phosphoethanolamine (NBD-PE) were obtained from Molecular Probes Inc. (Eugene, OR, USA). Three sets of 18-mer peptides derived from the core protein (Fig. 1a) of hepatitis C virus strains 1B4J and 1AH77 having 11-amino acid overlap between sequential peptides were obtained through the NIH AIDS Research and Reference Reagent Program (Division of AIDS, NIAID, NIH, Bethesda, MD, USA). All other reagents used were of analytical grade from Sigma-Aldrich. Water was deionized, twice-distilled and passed through a Milli-Q equipment (Millipore Ibérica, Madrid, Spain) to a resistivity better than 18 MΩ cm.

Sample preparation

For infrared spectroscopy, aliquots containing the appropriate amount of lipid in chloroform/methanol (2:1, v/v) were placed in a test tube containing 100 μg of dried lyophilized peptide to obtain a final lipid/peptide mole ratio of 50:1. After vortexing, the solvents were removed by evaporation under a stream of O₂-free nitrogen, and finally, traces of solvents were eliminated under vacuum in the dark for more than 3 h. The samples were hydrated in 100 μL of D₂O buffer containing 20 HEPES, 50 NaCl, 0.1 mM EDTA, pH 7.4 and incubated at 10 °C above the gel to liquid-crystalline phase transition temperature (T_m) of the phospholipid mixture with intermittent vortexing for 45 min to hydrate the samples and obtain multilamellar vesicles (MLV). The samples were frozen and thawed five times to ensure complete homogenization and maximization of peptide/lipid contacts with occasional vortexing. Finally the suspensions were centrifuged at 15 000 rpm at 25 °C for 15 min to remove the peptide possibly unbound to the membranes. The pellet was resuspended in 30 μL of D₂O buffer. The phospholipid and peptide concentrations were measured by methods described previously [16,17].

Membrane-leakage measurement

Aliquots containing the appropriate amount of lipid in chloroform/methanol (2:1 v/v) were placed in a test tube, the solvents were removed by evaporation under a stream of O₂-free nitrogen, and finally traces of solvents were eliminated under vacuum in the dark for more than 3 h. For assays of vesicle leakage at pH 7.4, buffer containing 10 Tris-HCl, 20 NaCl, 40 CF, and 0.1 mM EDTA, pH 7.4, was used [13]. To obtain MLV, 1 mL of buffer was added to the dry phospholipid mixture and vortexed at room temperature until a clear suspension was obtained. Large unilamellar vesicles (LUV) with a mean diameter of 90 nm were prepared from MLV by the extrusion method [14] using polycarbonate filters with a pore size of 0.1 μm (Nuclepore Corp.,

Cambridge, CA, USA). Breakdown of the vesicle membrane leads to content leakage. Non-encapsulated CF was separated from the vesicle suspension through a Sephadex G-75 filtration column (Pharmacia, Uppsala, Sweden) eluted with buffer containing either 10 Tris-HCl, 100 NaCl and 0.1 mM EDTA, pH 7.4. Membrane rupture (leakage) of intraliposomal CF was assayed by treating the probe-loaded liposomes (final lipid concentration, 0.125 mM) with the appropriate amounts of peptide on microtitre plates using a microplate reader (FLUOstar; BMG Labtech, Offenburg, Germany), stabilized at 25 °C with the appropriate amounts of peptide, each well containing a final volume of 170 μL. The medium in the microtitre plates was continuously stirred to allow the rapid mixing of peptide and vesicles. Leakage was assayed until no more change in fluorescence was obtained. Changes in fluorescence intensity were recorded with excitation and emission wavelengths set at 492 and 517 nm, respectively. Excitation and emission slits were set at 5 nm. One hundred per cent release was achieved by adding Triton X-100 to the microtiter plate to a final concentration of 0.5% (wt/wt). Fluorescence measurements were made initially with probe-loaded liposomes, afterwards by adding peptide solution and finally by adding Triton X-100 to obtain 100% leakage. Leakage was quantified on a percentage basis according to the equation,

$$\%L = \frac{(F_f - F_0) \times 100}{F_{100} - F_0}$$

where F_f is the equilibrium value of fluorescence after peptide addition, F_0 is the initial fluorescence of the vesicle suspension, and F_{100} is the fluorescence value after the addition of Triton X-100.

Phospholipid-mixing measurement

Peptide-induced vesicle lipid mixing (hemifusion) was measured by resonance energy transfer [18]. This assay is based on the decrease in resonance energy transfer between two probes (NBD-PE and RhB-PE) when the lipids of the probe-containing vesicles are allowed to mix with lipids from vesicles lacking the probes. The concentration of each of the fluorescent probes within the liposome membrane was 0.6 mol%. For assays of lipid mixing, 1 mL of buffer (10 HEPES, 100 mM NaCl, pH 7.4) was added to the dry phospholipid mixture (containing either 0.6 mol % NBD-PE and N-RhBPE or 0.12 mol% NBD-PE and N-RhB-PE, or no probes), and MLV were obtained by vortexing at room temperature. LUV were prepared from MLV by the extrusion method as above, using polycarbonate filters with a pore size of 0.2 μm (Nuclepore Corp). The use of 0.2 μm pore-size filters gives place to larger liposomes and henceforth greater fluorescence intensity per surface unit. Labelled and unlabelled vesicles in a proportion 1:4 were placed in a 5 mm × 5mm fluorescence cuvette at a final lipid

concentration of 100 μM in a final volume of 400 μL , stabilized at 25 °C under constant stirring. The fluorescence was measured using a Varian Cary Eclipse fluorescence spectrometer using 467 nm and 530 nm for excitation and emission, respectively. Excitation and emission slits were set at 10 nm. As labelled and unlabelled vesicles were mixed in a proportion of 1 to 4 respectively, 100% phospholipid mixing was estimated with a liposome preparation in which the membrane concentration of each probe was 0.12%. Phospholipid mixing was quantified on a percentage basis according to the equation,

$$\% \text{ PM} = \frac{(F_f - F_0) \times 100}{F_{100} - F_0},$$

F_f being the equilibrium value of fluorescence after peptide addition to a liposome mixture containing liposomes having 0.6% of each probe plus liposomes without any fluorescent probe, F_0 the initial fluorescence of the vesicles and F_{100} is the fluorescence value of the liposomes containing 0.12% of each probe.

Inner-monolayer phospholipid-mixing measurement

Peptide-induced phospholipid-mixing (fusion) of the inner monolayer was measured by a modification of the phospholipid-mixing measurement stated above [19]. LUVs were treated with sodium dithionite to completely reduce the NBD-labelled phospholipid located at the outer monolayer of the membrane. Final concentration of sodium dithionite was 100 mM (from a stock solution of 1 M dithionite in 1 M TRIS, pH 10.0) and incubated for approximately 1 h on ice in the dark. Sodium dithionite was then removed by size exclusion chromatography through a Sephadex G-75 filtration column (Pharmacia, Uppsala, Sweden) eluted with buffer containing 10 TRIS, 100 NaCl, 1 mM EDTA, pH 7.4. The proportion of labelled and unlabelled vesicles, lipid concentration and other experimental and measurement conditions were the same as indicated above for the phospholipid mixing assay.

Infrared spectroscopy

Approximately 30 μL of a pelleted sample in D_2O were placed between two CaF_2 windows separated by 56- μm thick Teflon spacers in a liquid demountable cell (Harrick, Ossining, NY, USA). The spectra were obtained in a Bruker IFS55 spectrometer (Bruker, Ettlingen, Germany) using a deuterated triglycine sulphate detector. Each spectrum was obtained by collecting 200 interferograms with a nominal resolution of 2 / cm, transformed using triangular apodization and, to average background spectra between sample spectra over the same time, a sample shuttle accessory was used to obtain sample and background spectra. The spectrometer was continuously purged with dry air at a dew point of -40 °C to remove atmospheric water vapour from the bands of interest.

All samples were equilibrated at the lowest temperature for 20 min before acquisition. An external bath circulator connected to the infrared spectrometer controlled the sample temperature. For temperature studies, samples were scanned using 20 °C intervals and a 15-min delay between each consecutive scan. Subtraction of buffer spectra taken at the same temperature as the samples was performed interactively using either GRAMS/32 or Spectra-Calc (Galactic Industries, Salem, MA, USA) as described previously [20,21]. Frequencies at the centre of gravity, when necessary were measured by taking the top 10 points of each specific band and fitted to a Gaussian band. The criterion used for buffer subtraction in the C=O and amide regions was the removal of the band near 1210 / cm, and a flat baseline between 1800 and 2100 / cm.

RESULTS

The peptide libraries used in this study and their correlation with the HCV core protein sequence are depicted in Fig. 1a, where it can be observed that the 18-mer peptide libraries include the whole HCV core protein sequence. Two and three consecutive peptides in the library have an overlap of 11 and 4 amino acids, respectively. The analysis of the hydrophobicity and interfaciality distribution along the core sequence of HCV 1B4J strain (the data obtained for the HCV 1AH77 strain is nearly identical) without any assumption about secondary structure is shown in Fig. 1b [13,22,23]. Although the three dimensional structure of the core protein is not known, these data give us a depiction of the potential surface zones that could be possibly implicated in either the modulation of membrane binding or protein-protein interaction or both. As it is observed in Fig. 1b, it is evident about the existence of different regions with large hydrophobic and interfacial values along the core sequence; these surfaces should be biologically functional in their roles as these patches of positive hydrophobicity and interfaciality along the surface of the core protein could favour the interaction with other similar patches along other core proteins, different proteins or with the surface of the membrane.

Membrane rupture, hemifusion and fusion

We have studied the effect of the 18-mer peptide libraries derived from the HCV core protein 1AH77 and 1B4J strains on membrane rupture, i.e. leakage, for different liposome compositions (Fig. 2); the lipidic composition of the model membranes have been EPC/Chol at a phospholipid molar ratio of 5:1, EPC/SM at a phospholipid molar ratio of 5:1, EPC/SM/Chol at a phospholipid molar ratio of 5:1:1, and a lipid extract of liver membranes [containing 42% EPC, 22% PE, 7% Chol, 8% phosphatidylinositol (PI), 1% lysophosphatidylcholine (LPC), and 21% neutral lipids]. The presence of both SM and Chol has been related to the occurrence of laterally segregated membrane microdomains or 'lipid rafts', and it has been found that there is

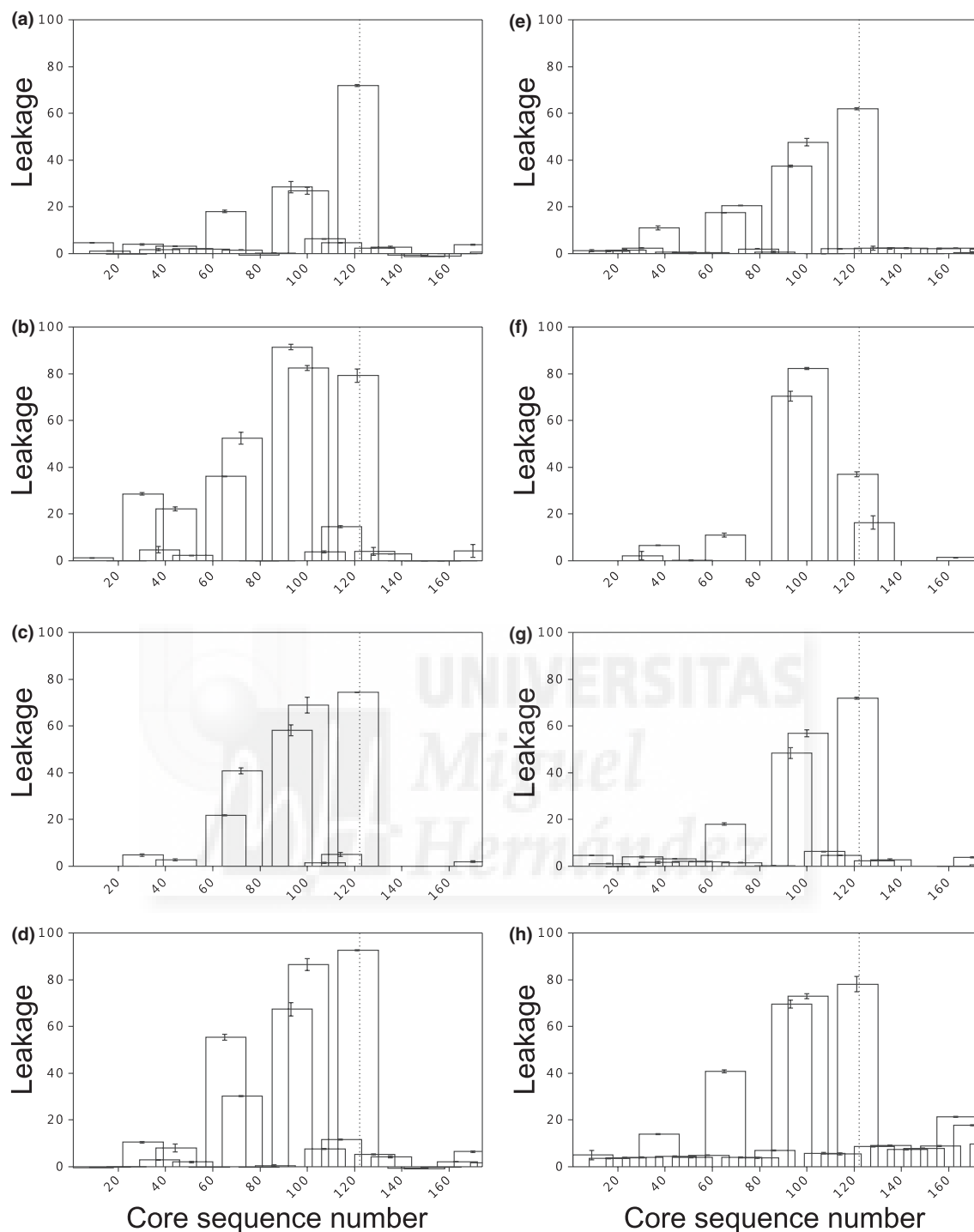


Fig. 2 Effect of the 18-mer peptides derived from the hepatitis C virus (HCV) core protein of HCV 1AH77 (a–d) and HCV 1B4J (e–h) strains on the release (membrane rupture) of large unilamellar vesicles (LUV) contents for different lipid compositions. Leakage data for LUVs composed of (a,e) egg L-phosphatidylcholine/cholesterol (EPC/Chol) at a phospholipid molar ratio of 5:1, (b,f) EPC/egg sphingomyelin (SM) at a phospholipid molar ratio of 5:1, (c,g) EPC/SM/Chol at a phospholipid molar ratio of 5:1:1, and (d,h) lipid extract of liver membranes. Vertical bars indicate SDs of the mean of triplicate samples. The dotted line divides regions corresponding to core domains I and II.

an important relationship between membrane interaction and Chol and SM membrane content for several viruses [24].

When the 18-mer peptides were assayed on EPC/Chol liposomes, some peptides exerted a significant leakage effect (Figs 2a,f). The most remarkable effects were induced

by peptide comprising residues 113–130. Other peptides which elicited important leakage values were peptides comprising residues 57–74, 85–102 and 92–109 for strain 1AH77 and 29–46, 57–74, 64–81, 85–102 and 92–109 for strain 1B4J. The leakage pattern was slightly different when liposomes composed of EPC/SM were tested (Figs 2b,f), as the most significant effect appeared now for peptides comprising residues 85–102 and 92–109. Peptide 113–130 also showed a significant leakage effect. Other significant leakage values were found for peptides 22–39, 36–53, 57–74 and 64–81 for strain 1AH77 and 64–81 and 120–137 for strain 1B4J. When liposomes composed of EPC/SM/Chol at a molar ratio of 5:1:1 were assayed (Figs 2c,g), a similar pattern to liposomes containing EPC/Chol was found. The most notable effect was induced by peptide comprising residues 113–130, whereas peptides 57–74, 64–81, 85–102 and 92–109 for strain 1AH77 and peptides 57–74, 85–102, and 92–109 for strain 1B4J elicited also significant leakage values. For liposomes composed of a lipid extract of liver membranes, the same peptide sequences displayed significant leakage values (Figs 2d,h). As it was found above, the most significant values were found for the peptide comprising residues 113–130, but peptides 85–102 and 92–109 showed also significant leakage. Peptides 57–74 and 64–81 for strain 1AH77 and peptide 57–74 for strain 1B4J displayed significant leakage values.

When the 18-mer core derived peptides from strain 1AH77 were assayed for hemifusion on both EPC/SM/Chol and liver extract liposomes, peptide comprising residues 29–46 displayed significant values (Figs 3a,b). Other peptides which elicited important hemifusion values (10%) defined a region comprising amino acids 85–130, with hemifusion values ranging from 10 to 25%. Slightly lower hemifusion values were found for core-derived peptides from strain 1B4J than for strain 1AH77 using both types of liposomes, EPC/SM/Chol and liver extract (Figs 3e,f). When the 18-mer core-derived peptides from strains 1AH77 and 1B4J were assayed for fusion on both EPC/SM/Chol and liver extract liposomes, peptide comprising residues 29–46 was the one which displayed significant fusion values (Figs 3c,d,g,h). The region comprising amino acids 85–130 (five peptides in total) was also found to have relatively high hemifusion and fusion values for both strains.

The summary of membrane leakage, membrane hemifusion and membrane fusion results obtained for both 1AH77 and 1B4J strains is presented in Fig. 4a, whereas the global average result is displayed in Fig. 4b. It is possible to detect various segments with large leakage values, which coincide with segments displaying significant hemifusion and fusion values. However, it is also possible to detect segments displaying high hemifusion and fusion values but low leakage ones. These results have permitted us to study specific peptides comprising different zones by infrared spectroscopy as shown below.

Fourier-transformed infrared spectroscopy structural assays

Peptides which displayed significant leakage, hemifusion and fusion effects (Fig. 4b), i.e. peptides corresponding to sequences 29–46, 57–74, 85–102, 106–123, and 155–172 were chosen for structural infrared assays both in aqueous solution [aqueous solutions of peptides 85–102 and 153–172 additionally contained 10% trifluoroethanol (TFE)] and in the presence of membrane model systems composed of either EPC/SM/Chol at a 5:1:1 molar ratio or a liver lipid extract (Fig. 5). Spectra were obtained at five different temperatures (5, 25, 45, 65 and 85 °C) and no any significant differences was found between them, indicating a high degree of conformational stability of the peptides. For simplicity, we will describe spectra obtained at 25 °C. The assignment of the Amide I' component bands to specific structural features has been described previously [25]. As observed in Fig. 5, there were significant changes in the Amide I' envelope band depending on the peptide and the specific lipid composition used.

The Amide I' band of the peptide derived from the core 29–46 region in aqueous solution (Fig. 5a) displays a narrow band at 1672 /cm and a shoulder with at least two broad bands at about 1645 and 1628 /cm. The band envelope of the Amide I' band of the peptide bound to raft model membranes was significantly different to that found for the peptide in aqueous solution, as maximum of the band appeared at about 1628 /cm with small bands at about 1672 and 1644 /cm (Fig. 5a). In the presence of liver lipid extract membranes, the Amide I' band was similar to the one found in the presence of raft-containing membranes, but a more intense band at about 1671 /cm. These differences in band intensities for the 29–46 peptide would imply that β -turn should be the most significant secondary structure in aqueous solution, whereas in the presence of both raft and liver extract model membranes the most significant one should be β -sheet.

The Amide I' band of the peptide derived from the core 57–74 sequence in aqueous solution displayed a broad band with a maximum at about 1672 /cm and a shoulder at about 1648 /cm (Fig. 5b). The band envelope of the Amide I' band of this peptide bound to raft model membranes was significantly different to that found for the peptide in aqueous solution, as the maximum of the band appeared at about 1637 /cm with a small shoulder at about 1648 /cm. In the presence of model membranes composed of liver lipid extract, the Amide I' band of the peptide displayed a maximum at about 1648 /cm. The intensity maxima for the core 57–74 sequence would imply that the most significant structure in aqueous solution and in the presence of liposomes composed of a liver extract should be random, but β -sheet in the presence of EPC/SM/Chol at a molar ratio of 2:1:1.

The peptides derived from the core 85–102 sequence of strains 1AH77 and 1B4J have similar sequences: the cysteine present in the 91 position of the strain 1AH77 is replaced by a

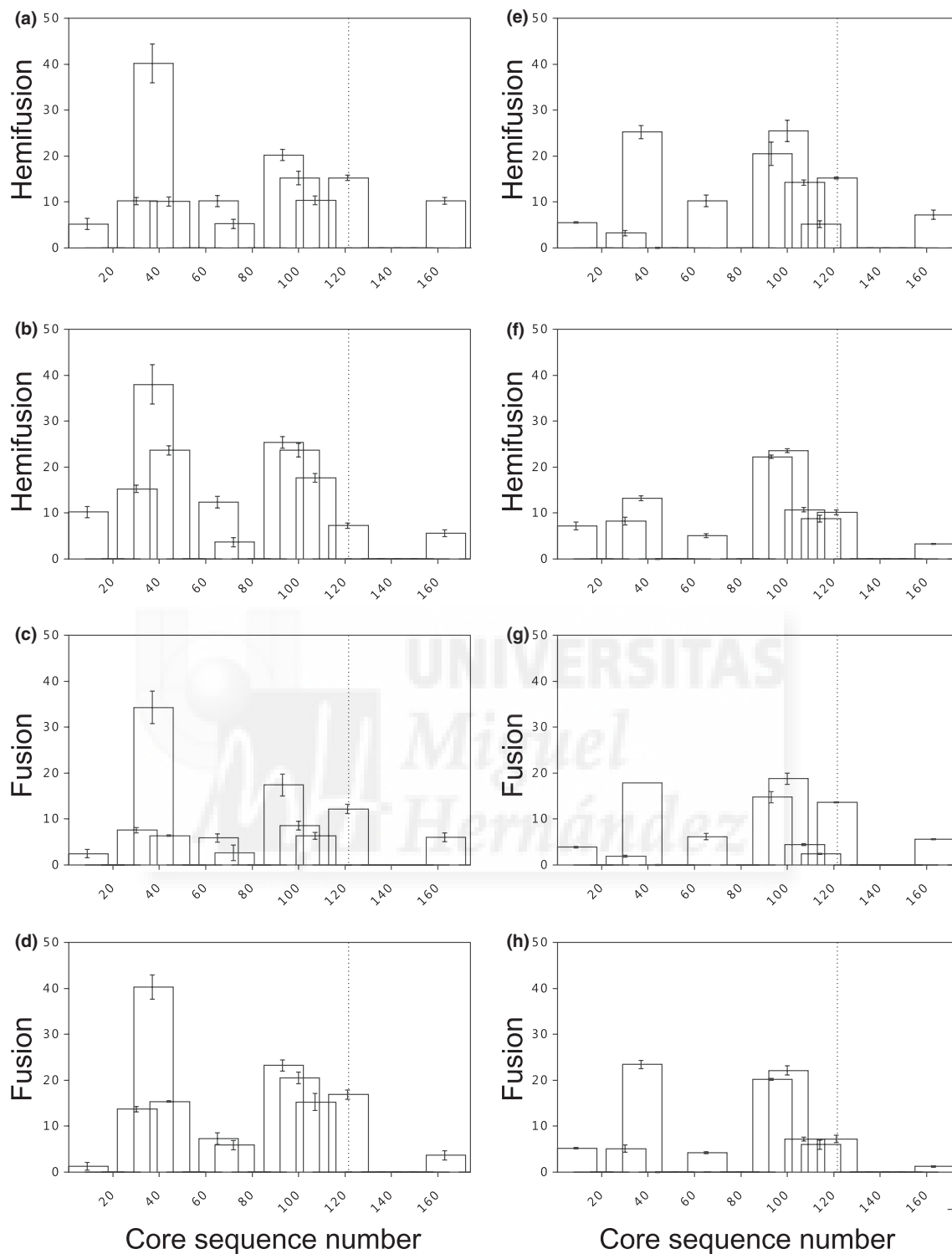


Fig. 3 Effect of the 18-mer peptides derived from the hepatitis C virus (HCV) core protein of HCV 1AH77 (a–d) and HCV 1B4J (e–h) strains on hemifusion (a,b,e,f) and fusion (c,d,g,h) for large unilamellar vesicles composed of (a,c,e,g) egg L-phosphatidylcholine/egg sphingomyelin/cholesterol at a phospholipid molar ratio of 5:1:1, and (b,d,f,h) lipid extract of liver membranes. Vertical bars indicate SDs of the mean of triplicate samples. The dotted line divides regions corresponding to core domains I and II.

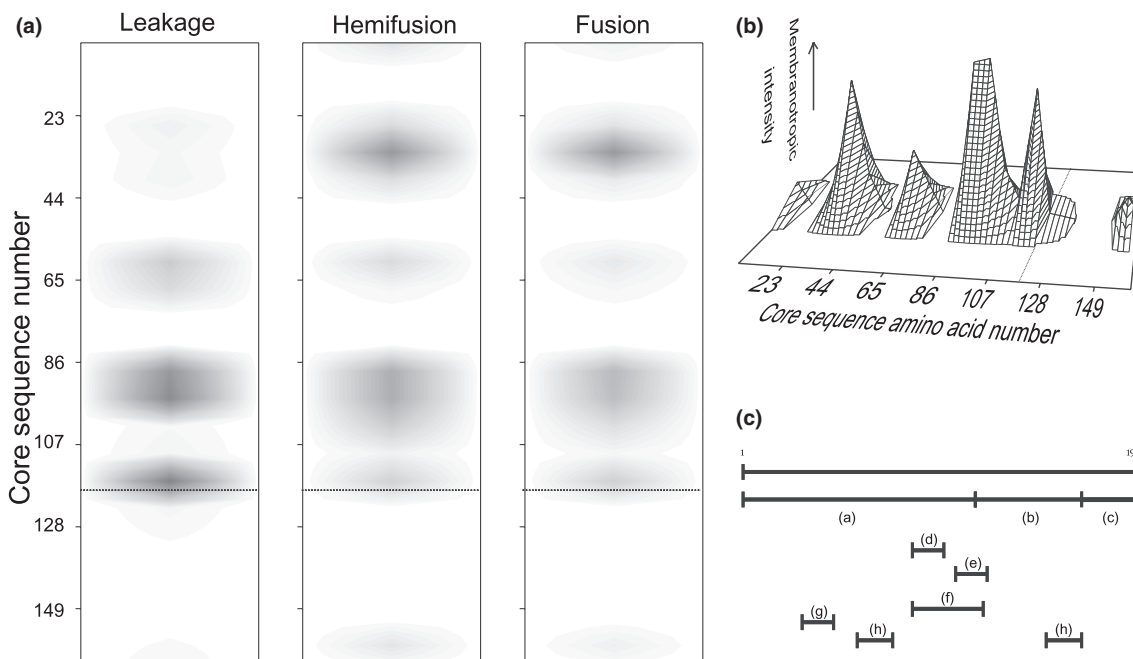


Fig. 4 (a) Summary of all experimental membrane leakage, hemifusion and fusion data presented in this work corresponding to the core-derived 18-mer peptides for both 1AH77 and 1B4J strains representing the full core sequence and for all liposome compositions studied (the darker, the greater membrane-active effect). (b) Summary of all the experimental data along the consensus scheme of the core protein highlighting the experimentally determined membrane-active regions. The dotted line divides regions corresponding to core domains I and II. (c) Pictorial survey of the most important membrane-active regions of hepatitis C virus (HCV) core protein. Membrane-active sequences found in this study (d,e,g,h) are depicted along sequences reported in the literature (a,b,c,f). (a) Domain 1: this sequence is regarded as the RNA-binding region with immunodominant antigenic properties [11,36]. (b) Domain 2: putatively responsible for the association with lipids [11,36]. (c) Domain 3: signal peptide [11,36]. (d) Membrane-leakage, hemifusion, and fusion activities with high interfacial values (see results section). (e) Membrane-leakage activity (see results section). (f) Homotypic interactions [27] and association to endoplasmic reticulum (ER) and mitochondrial membranes [35]. (g) Maximal hemifusion and fusion activities (see results section); part of the HCV major antigenic domain sequence; exposed region for protein-membrane interaction. (h) Both sequences have low but constant rupture, hemifusion and fusion properties (see results section).

leucine in the 1B4J strain. In aqueous solution, both peptides show a relatively broad Amide I' band with a maximum at approximately 1647 / cm and a shoulder at about 1672 / cm, much more intense for the peptide derived from the 1B4J strain than for the 1AH77 one (Figs 5c,d). In the presence of raft model membranes, the maximum of the Amide I' band in both cases is shifted to lower wavenumbers, displaying an Amide I' maxima at about 1638 / cm with a shoulder at about 1671 / cm. In the presence of liver lipid extract membranes, the Amide I' band of both peptides display a broad band with a maximum at about 1650 / cm. These differences in band intensities would imply that disordered structure should be the most significant secondary structure in aqueous solution for the 1AH77 derived peptide, but random and β -turn for the 1B4J peptide; however, in the presence of both raft and liver extract model membranes, the most significant one should be either disordered structure and/or β -sheet.

The Amide I' band of the peptide derived from the core 106–123 and 155–172 sequences in aqueous solution display a narrow band at about 1672 / cm and a shoulder at

about 1647 / cm (Figs 5e,f). The band envelope of the Amide I' band of both peptides bound to raft model membranes was significantly different to that found for the peptides in aqueous solution, as the maximum of the band appeared at about 1638 / cm with shoulders at about 1667 / cm. In the presence of model membranes composed of liver lipid extract, the Amide I' band of both peptides were rather similar to the ones found in the presence of raft membranes, but the band at 1665 / cm presented a higher intensity. These differences in band intensities for the core 106–123 and 155–172 sequences would imply that β -turn should be the most significant secondary structure in aqueous solution, together with random structure, whereas in the presence of both raft and liver extract model membranes, the most predominant secondary structure should be β -helix followed by β -turn.

DISCUSSION

Viral morphogenesis is one of the most important steps in the viral cycle involving lipid membranes and is not as well

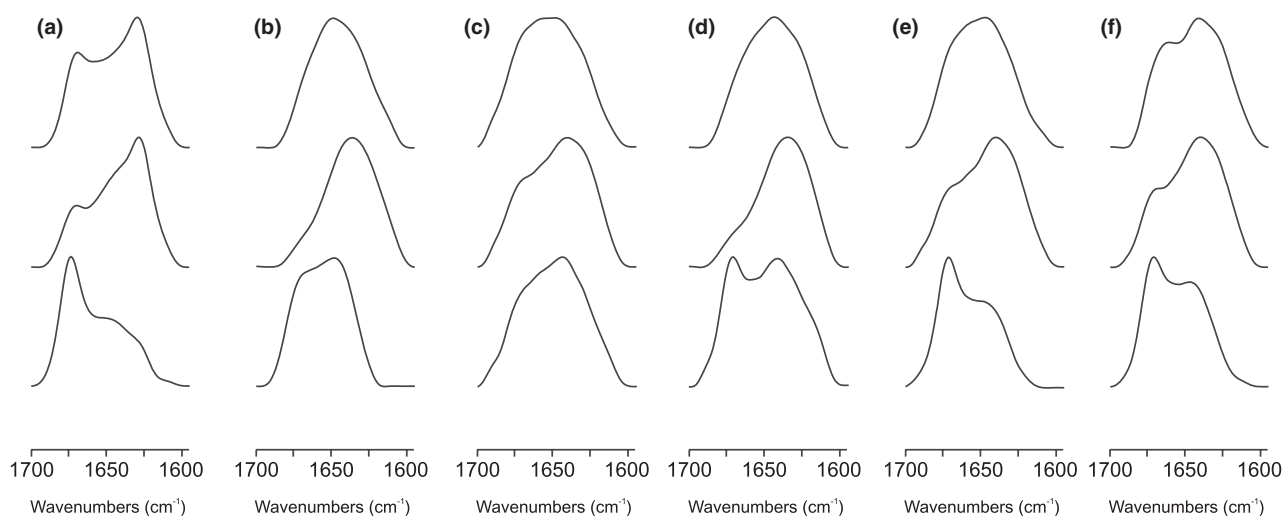


Fig. 5 Amide I' band spectra of peptides at 25 °C corresponding to core sequences (a) 29–46, (b) 57–74, (c) 85–102 (1AH77 strain), (d) 85–102 (1B4J strain), (e) 106–123 and (f) 155–172 in aqueous solution (lower spectra), in the presence of liposomes composed of egg L-phosphatidylcholine/egg sphingomyelin/ cholesterol at a 5:1:1 molar ratio (middle spectra) and in the presence of liposomes composed of a liver lipid extract (upper spectra).

characterized as the fusion event. For enveloped viruses, the assembly of the virions takes place in the host cell membrane and in the case of HCV it has been suggested that the virus particles assembly occurs in the endoplasmic reticulum membranes [26] where the core protein might play a central role in viral particle formation as well as it might drive the budding process [27]. Significantly, the HCV core protein is very well conserved among different HCV strains [6] and has important regulatory roles on different cell functions. Interestingly, the HCV core protein has been reported to be associated with raft sub-domains in the absence of other viral non-structural proteins [28]. Rafts, rigid membrane sub-domains located predominantly in the plasma membrane are described to be important in the HCV replication cycle, assembly of virions and budding from the host cell. For this reason, we have chosen membrane model systems composed not only of a liver lipid extract but also of EPC, SM and Chol [29,30], as mimetic of model membranes containing raft domains. As the biological roles of the HCV core protein can be modulated by membranes, we have identified the membrane-active regions of the HCV core protein by studying the effect of two core-derived peptide libraries from HCV on the integrity of membrane model systems. Furthermore, to obtain information on the structural basis of the interaction of the protein with model membranes, we have studied the secondary structure of specific membrane-interacting peptides both in aqueous solution and in the presence of model membrane systems. In this way, it would be possible to identify important regions which might be implicated in the budding molecular mechanism, and therefore could be used as new targets for searching viral assembly inhibitors as well as making possible the future development of HCV

assembly inhibitors which may lead to new vaccine strategies.

As it can be observed in Figs 4a,b, we have been able to discern different zones along the core sequence displaying different membranotropic properties. When leakage was assayed, and all the values were taken into account for all membrane compositions assayed, two zones displayed significant membrane rupture activity, i.e. regions defined by amino acids 85–102 and 106–123. The first region displayed a high interfacial value along its sequence; however, the second one did not show significant hydrophobic and interfacial values. In this context, it is interesting to note that the region comprising residues 85–123 has been described to be important in homotypic interactions which might be a prerequisite for assembly and budding of HCV-like viral particles [27,31]. Significantly, mutant core proteins without the 80–118 amino acid residues reduced, but did not abolish the association with lipid droplets [32,33]. Interestingly, the interaction of a region composed of amino acids 72–91 with the E1 glycoprotein [34] has been described; this region might be also important for association with the endoplasmic reticulum and the mitochondrial outer membranes [35]. Notably, region 85–102 coincides with a hydrophobic cluster located in domain 1 of the core protein and region 106–123 partially overlaps with another one located in domain 2 [36]. By infrared spectroscopy, it was possible to observe that the 85–102 region displayed different types of secondary structure, as random structure was the major one in aqueous solution but an increase in β -sheet in the presence of model membranes was observed. Although these regions present high levels of membrane rupture, hemifusion and fusion in the whole protein context, this region might be implicated in protein homodimerization but not in protein-membrane interactions.

Sequences 85–102 and 106–123, apart from being the ones which elicited the most leakage effect, displayed also significant hemifusion and fusion activities but region 29–46 displayed the highest hemifusion and fusion values together with low-leakage values (Fig. 4). As observed in Fig. 1b, this region displays high hydrophobicity and interfaciality values along its sequence. By infrared spectroscopy, it was determined that in aqueous solution, the predominant secondary structure was β -turn but β -sheet in the presence of model membranes composed of either raft or liver extract lipids. This region has two sequential glycines which might confer a high flexibility to the peptide and might act as a hinge around which the conformation could change. Moreover, this region is part of the HCV major antigenic domain sequence [37], being probably exposed and implicated in protein-membrane interactions. On the other hand, it has been demonstrated that uniformly packed virus particles are generated only by segment composed by amino acid residues 1–82, whereas region 29–46 is the only one in the N-terminal half of the core protein found to interact with lipids [38]. For this reason, this region might be an important one for the HCV assembly. Another interesting core sequences pertain to the 57–74 and 155–172 regions, as they displayed low but constant membrane rupture, hemifusion and fusion activities (Fig. 4a). It has been described that the ability of the core protein to associate with lipid droplets is lost when the 153–172 region containing the YATG motif is deleted [27]. These regions, having low but significant membrane-active activities, might be implicated in the interaction with membranes.

Additionally to its role in the viral morphogenesis and budding, the core protein is also important in the disassembly event during the viral uncoating that occurs at the target cell in a post-fusion stage. For this reason, this protein is very flexible [5]. The predicted structure of the whole protein using circular dichroism (CD) indicated that the protein has 16% of β -helix structure, 29% β -sheet structure and β -turns and 55% of random coil, whereas the C-terminal truncated protein was largely unordered [9]. As shown in this work, nearly all the peptides we have assayed display a major random coil or turn structure in solution; however, their structure changes in the presence of model membranes. This information could suggest that the membranotropic regions which we have detected along the core sequence might be involved in the interaction, not only with membranes, but also with proteins, even other core proteins and therefore responsible of their oligomerization.

Altogether, our results show that most of the HCV core protein membrane-active regions we have presented in this work are located in domain 1 (Fig. 4c), whatever interaction parameter is considered. However, the prevalent idea is that domain 1 might be the RNA-binding region whereas domain 2 of the HCV core protein would be responsible for membrane-binding (domain 3 is a signal peptide) [11,12].

Gathering related results in the literature, it is clear that a domain 1 vs domain 2 reasoning is not appropriate to unravel the foundations of HCV core-protein interaction with lipids. The region comprising the C-terminus of domain 1 and N-terminus of domain 2 seems to be the most active in membrane interaction, although a role in protein-protein interaction cannot be excluded. There is a sequence in domain 1 of maximal fusion and hemifusion (sequence f in Fig. 4c) that belongs to the major antigenic sequence of HCV. This sequence most probably plays a part in the biological action of HCV in lipid interaction whether during assembly, or fusion, or both. A more exhaustive study of these lipid-peptide interactions might help in the understanding of the HCV budding molecular mechanism as well as making possible the future development of anti-HCV drugs targeted to budding. These membranotropic regions could be envisaged as new possible targets, as inhibition of its interaction with the membrane could potentially lead to new vaccine strategies.

ACKNOWLEDGEMENTS

A. J. Pérez-Berná is a recipient of pre-doctoral fellowship from the Autonomous Government of the Valencian Community, Spain. A. S. Veiga acknowledges a grant (SFRH/BD/14336/2003) under the program POCTI to FCT-MCIES (Portugal). This study was funded in full by Ministerio de Ciencia y Tecnología, Spain, grant number BFU2005-00186-BMC (J. Villalaín). We are especially grateful to the National Institutes of Health AIDS Research and Reference Reagent Program, Division of AIDS, NIAID, NIH, for the peptides used in this work, as well as to Ana I. Gómez for expert technical assistance.

REFERENCES

- 1 Chen SL, Morgan TR. The natural history of hepatitis C virus (HCV) infection. *Int J Med Sci* 2006; 3(2): 47–52.
- 2 Penin F, Dubuisson J, Rey FA, Moradpour D, Pawlotsky JM. Structural biology of hepatitis C virus. *Hepatology* 2004; 39(1): 5–19.
- 3 Tan SL, Pause A, Shi Y, Sonenberg N. Hepatitis C therapeutics: current status and emerging strategies. *Nat Rev Drug Discov* 2002; 1(11): 867–881.
- 4 Qureshi SA. Hepatitis C virus-biology, host evasion strategies, and promising new therapies on the horizon. *Med Res Rev* 2007; 27(3): 353–373.
- 5 Vauloup-Fellous C, Pene V, Garaud-Aunis J *et al.* Signal peptide peptidase-catalyzed cleavage of hepatitis C virus core protein is dispensable for virus budding but destabilizes the viral capsid. *J Biol Chem* 2006; 281(38): 27679–27692.
- 6 Cha TA, Beall E, Irvine B *et al.* At least five related, but distinct, hepatitis C viral genotypes exist. *Proc Natl Acad Sci USA* 1992; 89(15): 7144–7148.
- 7 Lee SK, Park SO, Joe CO, Kim YS. Interaction of HCV core protein with 14-3-3epsilon protein releases Bax to activate

- apoptosis. *Biochem Biophys Res Commun* 2007; 352(3): 756–762.
- 8 Irshad M, Dhar I. Hepatitis C virus core protein: an update on its molecular biology, cellular functions and clinical implications. *Med Princ Pract* 2006; 15(6): 405–416.
 - 9 Kunkel M, Watowich SJ. Biophysical characterization of hepatitis C virus core protein: implications for interactions within the virus and host. *FEBS Lett* 2004; 3: 174–180.
 - 10 Kato N. Molecular virology of hepatitis C virus. *Acta Med Okayama* 2001; 55(3): 133–159.
 - 11 Boulant S, Vanbelle C, Ebel C, Penin F, Lavergne JP. Hepatitis C virus core protein is a dimeric alpha-helical protein exhibiting membrane protein features. *J Virol* 2005; 79(17): 11353–11365.
 - 12 McLauchlan J. Properties of the hepatitis C virus core protein: a structural protein that modulates cellular processes. *J Viral Hepat* 2000; 7(1): 2–14.
 - 13 Guillen J, Perez-Berna AJ, Moreno MR, Villalain J. Identification of the membrane-active regions of the severe acute respiratory syndrome coronavirus spike membrane glycoprotein using a 16/18-mer peptide scan: implications for the viral fusion mechanism. *J Virol* 2005; 79(3): 1743–1752.
 - 14 Perez-Berna AJ, Moreno MR, Guillen J, Bernabeu A, Villalain J. The membrane-active regions of the hepatitis C virus E1 and E2 envelope glycoproteins. *Biochemistry* 2006; 45(11): 3755–3768.
 - 15 Moreno MR, Giudici M, Villalain J. The membranotropic regions of the endo and ecto domains of HIV gp41 envelope glycoprotein. *Biochim Biophys Acta* 2006; 1758(1): 111–123.
 - 16 Böttcher CSF, Van Gent CM, Fries C. A rapid and sensitive sub-micro phosphorus determination. *Anal Chim Acta* 1961; 106(1): 203–204.
 - 17 Edelhoch H. Spectroscopic determination of tryptophan and tyrosine in proteins. *Biochemistry* 1967; 6(7): 1948–1954.
 - 18 Struck DK, Hoekstra D, Pagano RE. Use of resonance energy transfer to monitor membrane fusion. *Biochemistry* 1981; 20(14): 4093–4099.
 - 19 Meers P, Ali S, Erukulla R, Janoff AS. Novel inner monolayer fusion assays reveal differential monolayer mixing associated with cation-dependent membrane fusion. *Biochim Biophys Acta* 2000; 1467(1): 227–243.
 - 20 Contreras LM, Aranda FJ, Gavilanes F, Gonzalez-Ros JM, Villalain J. Structure and interaction with membrane model systems of a peptide derived from the major epitope region of HIV protein gp41: implications on viral fusion mechanism. *Biochemistry* 2001; 40(10): 3196–3207.
 - 21 Pascual R, Moreno MR, Villalain J. A peptide pertaining to the loop segment of human immunodeficiency virus gp41 binds and interacts with model biomembranes: implications for the fusion mechanism. *J Virol* 2005; 79(8): 5142–5152.
 - 22 Wimley WC, White SH. Experimentally determined hydrophobicity scale for proteins at membrane interfaces. *Nat Struct Biol* 1996; 3(10): 842–848.
 - 23 White SH, Wimley WC. Membrane protein folding and stability: physical principles. *Annu Rev Biophys Biomol Struct* 1999; 28: 319–365.
 - 24 Ahn A, Gibbons DL, Kielian M. The fusion peptide of Semliki Forest virus associates with sterol-rich membrane domains. *J Virol* 2002; 76(7): 3267–3275.
 - 25 Pascual R, Contreras M, Fedorov A, Prieto M, Villalain J. Interaction of a peptide derived from the N-heptad repeat region of gp41 Env ectodomain with model membranes. Modulation of phospholipid phase behavior. *Biochemistry* 2005; 44(43): 14275–14288.
 - 26 Ait-Goughoulte M, Hourieux C, Patient R, Trassard S, Brand D, Roingard P. Core protein cleavage by signal peptide peptidase is required for hepatitis C virus-like particle assembly. *J Gen Virol* 2006; 4: 855–860.
 - 27 Hourieux C, Ait-Goughoulte M, Patient R *et al.* Core protein domains involved in hepatitis C virus-like particle assembly and budding at the endoplasmic reticulum membrane. *Cell Microbiol* 2007; 9(4): 1014–1027.
 - 28 Matto M, Rice CM, Aroeti B, Glenn JS. Hepatitis C virus core protein associates with detergent-resistant membranes distinct from classical plasma membrane rafts. *J Virol* 2004; 78(21): 12047–12053.
 - 29 de Almeida RF, Fedorov A, Prieto M. Sphingomyelin/phosphatidylcholine/cholesterol phase diagram: boundaries and composition of lipid rafts. *Biophys J* 2003; 85(4): 2406–2416.
 - 30 de Almeida RF, Loura LM, Fedorov A, Prieto M. Lipid rafts have different sizes depending on membrane composition: a time-resolved fluorescence resonance energy transfer study. *J Mol Biol* 2005; 346(4): 1109–1120.
 - 31 Nolandt O, Kern V, Muller H *et al.* Analysis of hepatitis C virus core protein interaction domains. *J Gen Virol* 1997; 6: 1331–1340.
 - 32 Hope RG, McLauchlan J. Sequence motifs required for lipid droplet association and protein stability are unique to the hepatitis C virus core protein. *J Gen Virol* 2000; 8: 1913–1925.
 - 33 Hope RG, Murphy DJ, McLauchlan J. The domains required to direct core proteins of hepatitis C virus and GB virus-B to lipid droplets share common features with plant oleosin proteins. *J Biol Chem* 2002; 277(6): 4261–4270.
 - 34 Nakai K, Okamoto T, Kimura-Someya T *et al.* Oligomerization of hepatitis C virus core protein is crucial for interaction with the cytoplasmic domain of E1 envelope protein. *J Virol* 2006; 80(22): 11265–11273.
 - 35 Suzuki R, Sakamoto S, Tsutsumi T *et al.* Molecular determinants for subcellular localization of hepatitis C virus core protein. *J Virol* 2005; 79(2): 1271–1281.
 - 36 Boulant S, Montserret R, Hope RG *et al.* Structural determinants that target the hepatitis C virus core protein to lipid droplets. *J Biol Chem* 2006; 281(31): 22236–22247.
 - 37 Jolivet-Reynaud C, Dalbon P, Viola F *et al.* HCV core immunodominant region analysis using mouse monoclonal antibodies and human sera: characterization of major epitopes useful for antigen detection. *J Med Virol* 1998; 56(4): 300–309.
 - 38 Majeau N, Gagne V, Boivin A *et al.* The N-terminal half of the core protein of hepatitis C virus is sufficient for nucleocapsid formation. *J Gen Virol* 2004; 4: 971–81.

Publicación 2

**Identification of the Membrane-active
Regions of Hepatitis C Virus *p7* Protein**
***BIOPHYSICAL CHARACTERIZATION
OF THE LOOP REGION***

A. J. Pérez-Berná¹, J Guillén¹, M. R. Moreno¹,
A. Bernabeu¹, G. Pabst², P. Laggner² and J. Villalaín¹

¹Instituto de Biología Molecular y Celular, Universidad “Miguel
Hernández”, Elche-Alicante, Spain

²Biophysics and Nanosystems Research, Austrian Academy of Sciences,
Graz A-8042, Austria

**THE JOURNAL OF BIOLOGICAL CHEMISTRY VOL. 283, NO. 13,
pp. 8089–8101, March 28, 2008**



Identification of the Membrane-active Regions of Hepatitis C Virus p7 Protein

BIOPHYSICAL CHARACTERIZATION OF THE LOOP REGION*

Received for publication, November 16, 2007, and in revised form, January 14, 2008. Published, JBC Papers in Press, January 15, 2008, DOI 10.1074/jbc.M709413200

Ana J. Pérez-Berná^{‡1}, Jaime Guillén^{‡1}, Miguel R. Moreno[‡], Angela Bernabeu[‡], Georg Pabst[§], Peter Laggner², and José Villalain^{‡2}

From the [‡]Instituto de Biología Molecular y Celular, Universidad "Miguel Hernández," E-03202 Alicante, Spain and the [§]Institute of Biophysics and Nanosystems Research, Austrian Academy of Sciences, Graz A-8042, Austria

We have identified the membrane-active regions of the hepatitis C virus p7 protein by performing an exhaustive study of membrane rupture, hemifusion, and fusion induced by a p7-derived peptide library on model membranes having different phospholipid compositions. We report the identification in p7 of a highly membranotropic region located at the loop domain of the protein. Here, we have investigated the interaction of a peptide patterned after the p7 loop (peptide p7_L), studying its binding and interaction with the lipid bilayer, and evaluated the binding-induced structural changes of the peptide and the phospholipids. We show that positively rich p7_L strongly binds to negatively charged phospholipids and it is localized in a shallow position in the bilayer. Furthermore, peptide p7_L exhibits a high tendency to oligomerize in the presence of phospholipids, which could be the driving force for the formation of the active ion channel. Therefore, our findings suggest that the p7 loop could be an attractive candidate for antiviral drug development, because it could be a target for antiviral compounds that may lead to new vaccine strategies.

Hepatitis C virus (HCV)³ is an enveloped positive single-stranded RNA virus included in the genus *Hepacivirus* that

belongs to the *Flaviviridae* family. HCV is an important public health problem because it is the leading cause of acute and chronic liver disease in humans, including chronic hepatitis, cirrhosis, and hepatocellular carcinoma (1–3). Currently, there are no vaccines to prevent HCV infection and the available therapeutic agents have very limited efficacy against the virus (4). The HCV genome consists of one translational open reading frame encoding a polyprotein precursor of ~3010 amino acids in length, including structural and non-structural proteins, which is cleaved by host and viral proteases (Fig. 1A). The HCV genome is widely heterogeneous; replication errors cause a high rate of mutations (5). HCV entry into the host cell is achieved by fusion of viral and cellular membranes, and the morphogenesis and virion budding has been suggested to take place in the endoplasmic reticulum (6). Therefore, the viral region implicated in fusion to and/or budding from the cells must interact with the membrane and should be a conserved sequence. The variability of the HCV proteins gives the virus the ability to escape the host immune surveillance system and notably hampers the development of an efficient vaccine. Thus, finding inhibitors of protein-membrane and protein-protein interactions involved in virus fusion and/or budding could be an alternative and valuable strategy against HCV infection because they could be potential therapeutic agents.

Protein p7 gene is located between the structural and the non-structural regions of the HCV polyprotein precursor, specifically between the E2 and NS2 genes. Cleavage of p7 is mediated by the endoplasmic reticulum (ER) signal peptidases of the host cell (7, 8). The protein p7 is classified neither as a structural protein nor as non-structural (9) and locates in the cell ER. The role of p7 in the virus life cycle has been elusive. It has been shown that p7 is not critical for RNA replication (10), although homologous proteins from other members of the *Flaviviridae* family are critical for cell culture infectivity (11). A recent report, however, demonstrated that p7 is essential for efficient assembly and release of infectious virions indicating that p7 is primarily involved in the late phase of the virus replication cycle (12).

At a molecular level, p7 is a small transmembrane protein of 63 amino acids with two transmembrane helical domains, TM1 and TM2, connected by a loop. Whereas the loop is oriented

phase transition; TM, transmembrane domain; TMA-DPH, 1-(4-trimethylammoniumphenyl)-6-phenyl-1,3,5-hexatriene; FPE, fluorescein phosphatidylethanolamine; ThT, thioflavin T; MAS, magic angle spinning; POPC, 1-palmitoyl-2-oleoyl-*sn*-glycero-3-phosphocholine.

* This work was supported in part by Grant BFU2005-00186-BMC from the Ministerio de Ciencia y Tecnología, Spain (to J. V.). The costs of publication of this article were defrayed in part by the payment of page charges. This article must therefore be hereby marked "advertisement" in accordance with 18 U.S.C. Section 1734 solely to indicate this fact.

¹ Recipients of pre-doctoral fellowships from the Autonomous Government of the Comunidad Valenciana, Spain.

² To whom correspondence should be addressed: IBMC, Universidad "Miguel Hernández," E-03202 Alicante, Spain. Tel.: 34-966-658-762; Fax: 34-966-658-758; E-mail: jvillalain@umh.es.

³ The abbreviations used are: HCV, hepatitis C virus; BPS, bovine brain L- α -phosphatidylserine; CF, 5-carboxyfluorescein; Chol, cholesterol; DHE, ergosta-5,7,9(11),22-tetraen-3 β -ol; di-8-ANEPPS, 4-(2-(6-(diethylamino)-2-naphthalenyl)-(ethenyl)-1-(3-sulfopropyl)-pyridinium inner salt; DMPA, 1,2-dimyristoyl-*sn*-glycero-3-phosphate; DMPC, 1,2-dimyristoyl-*sn*-glycero-3-phosphocholine; DMPG, 1,2-dimyristoyl-*sn*-glycero-3-[phospho-*rac*-(1-glycerol)]; DPH, 1,6-diphenyl-1,3,5-hexatriene; EPA, egg L- α -phosphatidic acid; EPC, egg L- α -phosphatidylcholine; ER, endoplasmic reticulum; FD10, fluorescein isothiocyanate dextran with an average molecular weight of 10,000; LUV, large unilamellar vesicles; MLV, multilamellar vesicles; NBD-PE, N-(7-nitrobenz-2-oxa-1,3-diazol-4-yl)-1,2-dihexadecanoyl-*sn*-glycero-3-phosphoethanolamine; N-RhB-PE, Lissamine rhodamine B 1,2-dihexadecanoyl-*sn*-glycero-3-phosphoethanolamine; NS, doxylstearic acid; PA-DPH, 3-(4-(6-phenyl)-1,3,5-hexatrienyl)-phenylpropionic acid; SAXD, small-angle X-ray diffraction; SM, sphingomyelin; T_m , temperature of the gel to liquid crystalline

toward the cytoplasm, the amino- and carboxyl-terminal tails are oriented toward the ER lumen (13, 14). Mutations in the loop region abrogate the channel activity of p7, which has been described to be a viroporin-like protein (12, 15, 16). These functional groups of proteins form ion channels that might be important for virus assembly and/or release; p7 is capable of forming cation-selective ion channels in artificial lipid membranes at physiological pH. Akin to other viral proteins such as M2, NB, and Vpu, secondary structure predictions suggest that p7 may form a hexameric bundle of helical dimers with a pore diameter of 3–5 nm (13, 16). One possible role for this protein could be the transport of ions from the ER to the cytoplasm of HCV-infected host cells. Amantadine, hexamethylene amiloride, and long alkyl-chain amino sugar derivatives are ion channel inhibitors that block ion transport mediated by p7 in lipid membranes (16–18), suggesting that p7 could be a attractive candidate for antiviral drug development.

We have recently identified the membrane-active regions of the HIV gp41, SARS-CoV spike, and HCV E1 and E2 glycoproteins by observing the effect of glycoprotein-derived peptide libraries on model membrane integrity (19–21). These results allowed us to propose the location of different segments in these proteins that are implicated in protein-lipid and protein-protein interactions. These studies have helped us to understand the mechanisms underlying the interaction between viral proteins and membranes. Using a similar approach, we have carried the analysis of the membrane-active regions of p7 by investigating the effect of a p7-derived peptide library from the HCV strain HCV_1B4J, on the integrity of different membrane model systems. Here, we report the identification of a membranotropic region in p7 coincidental with the loop domain of the protein, which exhibits membrane-interacting properties akin to those found for the loop domain of HIV gp41 (21–23). Furthermore, we have focused on the possible functional roles of the p7 loop domain by an in-depth study of a peptide patterned after this domain, peptide p7_L. We have studied the binding and interaction of p7_L with the lipid bilayer, as well as the structural changes induced in both the peptide and phospholipid molecules upon membrane binding. We show that p7_L strongly partitions into phospholipid membranes, interacts with negatively charged phospholipids, locates in a shallow position in the membrane, and oligomerizes in the membrane.

EXPERIMENTAL PROCEDURES

Materials and Reagents—Three sets of 11 peptides derived from HCV_1B4J protein p7 (strictly speaking, p7 spans from residue 746 to residue 809 of the HCV polyprotein precursor) were obtained through the National Institutes of Health AIDS Research and Reference Reagent Program (Division of AIDS, NIAID, NIH, Bethesda, MD). The peptide p7_L corresponding to the sequence ⁷⁷¹FFCAAWYIKGRLAPGAAY⁷⁸⁸ (with NH₂-terminal acetylation and COOH-terminal amidation) was obtained from Genemed Synthesis, San Francisco, CA. The peptide p7_L was purified by reverse-phase high pressure liquid chromatography (Vydac C-8 column, 250 × 4.6 mm, flow rate 1 ml/min, solvent A, 0.1% trifluoroacetic acid, solvent B, 99.9% acetonitrile and 0.1% trifluoroacetic acid) to better than 95% purity, and its composition and molecular mass were con-

firmed by amino acid analysis and mass spectroscopy. Because trifluoroacetate has a strong infrared absorbance at ~1673 cm⁻¹, which interferes with the characterization of the peptide Amide I band (24), residual trifluoroacetic acid, used both in peptide synthesis and in the high-performance liquid chromatography mobile phase, was removed by several lyophilization/solubilization cycles in 10 mM HCl (25). Egg L- α -phosphatidylcholine (EPC), egg L- α -phosphatidic acid (EPA), egg sphingomyelin (SM), bovine brain L- α -phosphatidylinositol; bovine brain L- α -phosphatidylserine (BPS), 1,2-dimyristoyl-*sn*-glycero-3-phosphocholine (DMPC), 1,2-dimyristoyl-*sn*-glycero-3-(phospho-*rac*-(1-glycerol)) (DMPG), 1,2-dimyristoyl-*sn*-glycero-3-(phospho-*L*-serine), 1,2-dimyristoyl-*sn*-glycero-3-phosphate (DMPA), cholesterol (Chol), liver lipid extract, Lissamine rhodamine B 1,2-dihexadecanoyl-*sn*-glycero-3-phosphoethanolamine (*N*-Rh-PE), and *N*-(7-nitrobenz-2-oxa-1,3-diazol-4-yl)-1,2-dihexadecanoyl-*sn*-glycero-3-phosphatidylethanolamine (NBD-PE) were obtained from Avanti Polar Lipids (Alabaster, AL). 5-Carboxyfluorescein (CF) (>95% by high pressure liquid chromatography), fluorescein isothiocyanate-labeled dextran FD10 (average molecular weight 10,000), 5-doxy-stearic acid (5-NS), 16-doxy-stearic acid (16-NS), dehydroergosterol (ergosta-5,7,9(11),22-tetraen-3 β -ol, DHE), sodium dithionite, deuterium oxide (99.9% by atom), Triton X-100, EDTA, and HEPES were purchased from Sigma. 1,6-Diphenyl-1,3,5-hexatriene (DPH), 3-(4-(6-phenyl)-1,3,5-hexatrienyl)-phenylpropionic acid (PA-DPH), 1-(4-trimethylammoniumphenyl)-6-phenyl-1,3,5-hexatriene (TMA-DPH), 4-(2-(6-(dioctylamino)-2-naphthalenyl)(ethenyl)-1-(3-sulfopropyl)-pyridinium inner salt (di-8-ANEPPS) were obtained from Molecular Probes (Eugene, OR). The lipid composition of the synthetic endoplasmic reticulum was EPC/BPS/bovine brain L- α -phosphatidylinositol/SM/Chol at a molar ratio of 51:2.4:5.3:7.48:33.42 (26). All other reagents used were of analytical grade from Sigma. Water was deionized, twice distilled, and passed through Milli-Q equipment (Millipore Ibérica, Madrid, Spain) to a resistivity better than 18 M Ω cm.

Vesicle Preparation—Aliquots containing the appropriate amount of lipid in chloroform/methanol (2:1, v/v) were placed in a test tube, the solvents were removed by evaporation under a stream of O₂-free nitrogen, and finally, traces of solvents were eliminated under vacuum in the dark for more than 3 h. The lipid films were resuspended in an appropriate buffer and incubated either at 25 or 10 °C above the phase transition temperature (*T_m*) with intermittent vortexing for 30 min to hydrate the samples and obtain multilamellar vesicles (MLV). The samples were frozen and thawed five times to ensure complete homogenization and maximization of peptide/lipid contacts with occasional vortexing. Large unilamellar vesicles (LUV) with a mean diameter of 0.1 and 0.2 μ m for either leakage or hemifusion and fusion experiments were prepared from multilamellar vesicles by the extrusion method (27) using polycarbonate filters with a pore size of 0.1 and 0.2 μ m (Nuclepore Corp., Cambridge, CA). The phospholipid and peptide concentration were measured by methods described previously (28, 29).

Membrane Leakage Measurement—LUVs with a mean diameter of 0.1 μ m were prepared as indicated above in buffer containing 10 mM Tris, 20 mM NaCl, pH 7.4, and either CF at a

concentration of 40 mM or FD10 at a concentration of 100 mg/ml. Non-encapsulated CF or FD10 were separated from the vesicle suspension through a filtration column containing Sephadex G-75 or Sephadex S500HR Sephacryl, respectively (GE Healthcare), eluted with buffer containing 10 mM Tris, 100 mM NaCl, 0.1 mM EDTA, pH 7.4. Membrane rupture (leakage) of intraliposomal CF was assayed by treating the probe-loaded liposomes (final lipid concentration, 0.125 mM) with the appropriate amounts of peptide on microtiter plates using a microplate reader (FLUOstar; BMG Labtech, Offenburg, Germany), stabilized at 25 °C, with the appropriate amounts of peptide, each well containing a final volume of 170 μ l. The medium in the microtiter plates was continuously stirred to allow the rapid mixing of peptide and vesicles. Membrane leakage of intraliposomal FD10 was carried out using 5 \times 5-mm quartz cuvettes stabilized at 25 °C in a final volume of 400 μ l (100 μ M lipid concentration). Leakage was assayed until no more change in fluorescence was obtained. The fluorescence was measured using a Varian Cary Eclipse spectrofluorimeter. Changes in fluorescence intensity were recorded with excitation and emission wavelengths set at 492 and 517 nm, respectively. Excitation and emission slits were set at 5 nm. One hundred percent release was achieved by adding Triton X-100 to either the microtiter plate or to the cuvette to a final concentration of 0.5% (w/w). For details see Refs. 30 and 31.

Phospholipid Mixing Measurement—Peptide-induced vesicle lipid mixing was measured by resonance energy transfer (32). This assay is based on the decrease in resonance energy transfer between two probes (NBD-PE and RhB-PE) when the lipids of the probe-containing vesicles are allowed to mix with lipids from vesicles lacking the probes. The concentration of each of the fluorescent probes within the liposome membrane was 0.6% mol. LUVs with a mean diameter of 0.2 μ m were prepared as described above. Labeled and unlabeled vesicles at a proportion of 1:4 were placed in a 5 \times 5-mm fluorescence cuvette at a final lipid concentration of 100 μ M in a final volume of 400 μ l, stabilized at 25 °C under constant stirring. The fluorescence was measured using a Varian Cary Eclipse fluorescence spectrometer using 467 and 530 nm for excitation and emission, respectively. Excitation and emission slits were set at 10 nm. The proportion of labeled and unlabeled vesicles, lipid concentration, and other experimental and measurement conditions were the same as indicated previously (31).

Inner Monolayer Phospholipid Mixing (Fusion) Measurement—Peptide-induced phospholipid mixing of the inner monolayer was measured by a modification of the phospholipid mixing measurement stated above (33). This assay is based on the decrease in resonance energy transfer between two probes (NBD-PE and RhB-PE) when the lipids of the probe-containing vesicles are allowed to mix with lipids from vesicles lacking the probes. The concentration of each of the fluorescent probes within the liposome membrane was 0.6% mol. LUVs with a mean diameter of 0.2 μ m were prepared as described above. LUVs were treated with sodium dithionite to completely reduce the NBD-labeled phospholipid located at the outer monolayer of the membrane. Final concentration of sodium dithionite was 100 mM (from a stock solution of 1 M dithionite in 1 M Tris, pH 10.0) and incubated for \sim 1 h on ice in the dark.

Sodium dithionite was then removed by size exclusion chromatography through a Sephadex G-75 filtration column (GE Healthcare) eluted with buffer containing 10 mM Tris, 100 mM NaCl, 1 mM EDTA, pH 7.4. The proportion of labeled and unlabeled vesicles, lipid concentration, and other experimental and measurement conditions were the same as indicated above for the phospholipid mixing assay.

Peptide Binding to Vesicles—The partitioning of the peptide into the phospholipid bilayer was monitored by the fluorescence enhancement of tryptophan. Fluorescence spectra were recorded in a SLM Aminco 8000C spectrofluorometer with excitation and emission wavelengths of 290 and 348 nm, respectively, and 4-nm spectral bandwidths. Measurements were carried out in 20 mM HEPES, 50 mM NaCl, 0.1 mM EDTA, pH 7.4. Intensity values were corrected for dilution, and the scatter contribution was derived from lipid titration of a vesicle blank. The data were analyzed as previously described (31).

Steady-state Fluorescence Anisotropy—DPH and its derivatives represent popular membrane fluorescent probes for monitoring the organization and dynamics of membranes; whereas DPH is known to partition mainly into the hydrophobic core of the membrane, PA-DPH and TMA-DPH probes are oriented at the membrane bilayer with their charge localized at the lipid-water interface, TMA-DPH nearer the membrane surface than PA-DPH (34). MLVs were formed in 100 mM NaCl, 0.05 mM EDTA, and 25 mM HEPES, pH 7.4. Aliquots of PA-DPH, TMA-DPH, or DPH in *N,N'*-dimethylformamide (2×10^{-4} M) were directly added into the lipid dispersion to obtain a probe/lipid molar ratio of 1:500. Samples were incubated for 15, 45, or 60 min when TMA-DPH, PA-DPH, or DPH were used, respectively, 10 °C above the gel to liquid-crystalline phase transition temperature T_m of the phospholipid mixture. Afterward, the peptides were added to obtain a peptide/lipid molar ratio of 1:15 and incubated 10 °C above the T_m of each lipid for 1 h, with occasional vortexing. All fluorescence studies were carried using 5 \times 5-mm quartz cuvettes in a final volume of 400 μ l (315 μ M lipid concentration). All the data were corrected for background intensities and progressive dilution. The steady-state fluorescence anisotropy, $\langle r \rangle$, was measured with an automated polarization accessory using a Varian Cary Eclipse fluorescence spectrometer, coupled to a Peltier device (Varian) for automatic temperature change. The data were analyzed as previously described (31).

Fluorescence Quenching of Trp Emission by Water-soluble and Lipophilic Probes—For acrylamide quenching assays, aliquots from a 4 M solution of the water-soluble quencher were added to the solution-containing peptide in the presence and absence of liposomes at a peptide/lipid molar ratio of 1:100. The results obtained were corrected for dilution and the scatter contribution was derived from acrylamide titration of a vesicle blank. The data were analyzed according to the Stern-Volmer equation (35), $I_0/I = 1 + K_{sv}(Q)$, where I_0 and I represent the fluorescence intensities in the absence and the presence of the quencher (Q), respectively, and K_{sv} is the Stern-Volmer quenching constant, which is a measure of the accessibility of Trp to acrylamide. Quenching studies with lipophilic probes were performed by successive addition of small amounts of 5-NS or 16-NS in ethanol to the samples of the peptide incubated with LUV. The final concentration of ethanol was kept

below 2.5% (v/v) to avoid any significant bilayer alterations. After each addition an incubation period of 15 min was kept before the measurement. The data were analyzed as previously described (31).

Fluorescence Measurements Using FPE-labeled Membranes—LUVs with a mean diameter of 0.1 μm were prepared in buffer containing 10 mM Tris-HCl, pH 7.4. The vesicles were labeled exclusively in the outer bilayer leaflet with FPE as described previously (36). Briefly, LUVs were incubated with 0.1 mol % FPE dissolved in ethanol (never more than 0.1% of the total aqueous volume) at 37 °C for 1 h in the dark. Any remaining unincorporated FPE was removed by gel filtration on a Sephadex G-25 column equilibrated with the appropriate buffer. FPE vesicles were stored at 4 °C until use in an oxygen-free atmosphere. Fluorescence time courses of FPE-labeled vesicles were measured after the desired amount of peptide was added into 400 μl of lipid suspensions (200 μM lipid) using a Varian Cary Eclipse fluorescence spectrometer. Excitation and emission wavelengths were set at 490 and 520 nm, respectively, using excitation and emission slits set at 5 nm. Temperature was controlled with a thermostatic bath at 25 °C. The contribution of light scattering to the fluorescence signals was measured in experiments without the dye and was subtracted from the fluorescence traces. Data were fitted either to a hyperbolic binding model (37) using the following equation, $F = (F_{\text{max}} [P]/K_d + [P])$, where F is the fluorescence variation, F_{max} the maximum fluorescence variation, $[P]$ the peptide concentration, and K_d the dissociation constant of the membrane binding process. The experimental points shown in the figures are the mean values of at least three measurements.

Thioflavin T Assay for Peptide Aggregation—Peptide aggregation was assayed by using thioflavin T (ThT). Thioflavin T associates rapidly with aggregated peptides giving rise to a new excitation maximum at 450 nm and an enhanced emission at 482 nm (38). Buffer contained 100 mM NaCl, 10 mM Tris-HCl, 25 μM ThT, pH 7.4, LUVs (final phospholipid concentration of 0.5 mM), and a peptide concentration of 5 μM . Fluorescence was measured before and after the desired amount of peptide was added into the cuvette using a Varian Cary Eclipse fluorescence spectrometer. Temperature was controlled with a thermostatic bath at 25 °C under constant stirring. Samples were excited at 450 nm (slit width, 5 nm) and fluorescence emission was recorded at 482 nm (slit width, 5 nm). Aggregation was quantified on a percentage basis according to equation: $\%A = [(F_f - F_0) \times 100] / (F_{\text{max}} - F_0)$, where F_f is the value of fluorescence after peptide addition, F_0 the initial fluorescence in the absence of peptide, and F_{max} is the fluorescence maximum obtained after peptide addition.

Measurement of the Membrane Dipole Potential Using Di-8-ANEPPS-labeled Membranes—Aliquots containing the appropriate amount of lipid in chloroform/methanol (2:1, v/v) and di-8-ANEPPS were placed in a test tube to obtain a probe/lipid molar ratio of 1:100 and LUVs, with a mean diameter of 90 nm, were prepared as described previously. Steady-state fluorescence measurements were recorded with a Varian Cary Eclipse spectrofluorimeter. Dual wavelength recordings with the dye di-8-ANEPPS were obtained by exciting the samples at two different wavelengths (450 and 520 nm) and measuring their

intensity ratio, $R(450:520)$, at an emission wavelength of 620 nm (39, 40). Changes in the total membrane dipole moment cause a shift in the excitation spectrum maximum of di-8-ANEPPS. By exciting the membrane suspensions at two different wavelengths corresponding to the maximum and the minimum of the difference spectrum, a fluorescence intensity ratio R can be calculated, which can be used as a measure of the relative changes in the magnitude of the dipole potential. The fluorescence ratio R is defined as the ratio of the fluorescence intensity at an excitation wavelength of 450 nm divided by that at 520 nm. The lipid concentration was 200 μM , and all experiments were performed at 25 °C.

Infrared Spectroscopy—For Fourier transfer infrared spectroscopy, the samples were prepared as above but in D_2O buffer. Approximately 25 μl of a pelleted sample in D_2O were placed between two CaF_2 windows separated by 50- μm thick Teflon spacers in a liquid demountable cell (Harrick, Ossining, NY). The spectra were obtained in a Bruker IFS55 spectrometer using a deuterated triglycine sulfate detector. Each spectrum was obtained by collecting 200 interferograms with a nominal resolution of 2 cm^{-1} , transformed using triangular apodization and, to average background spectra between sample spectra over the same time period, a sample shuttle accessory was used to obtain sample and background spectra. The spectrometer was continuously purged with dry air at a dew point of -40 °C to remove atmospheric water vapor from the bands of interest. All samples were equilibrated at the lowest temperature for 20 min before acquisition. An external bath circulator, connected to the infrared spectrometer, controlled the sample temperature. For temperature studies, samples were scanned using 2 °C intervals and a 2-min delay between each consecutive scan. The data were analyzed as previously described (30, 31).

Magic Angle Spinning (MAS) ^{31}P NMR—Samples were prepared as described above and concentrated by centrifugation (14,000 $\times g$ for 15 min). MAS ^{31}P NMR spectra were acquired on a Bruker 500 MHz Avance spectrometer (Bruker BioSpin, Rheinstetten, Germany) using a Bruker 4-mm broad band MAS probe under both static and MAS conditions. The samples were packed into 4-mm zirconia rotors and placed in the spinning module of the MAS probe; no cross-polarization was used. The spinning speed was 9 kHz, regulated to ± 3 Hz by a Bruker pneumatic unit and the temperature was 25 °C. A single ^{31}P 90° pulse (typically 5 μs) was used for excitation, a gated broadband decoupling of 10 W, 32k data points, 1600 transients, and 5-s delay time between acquisitions. Under static conditions, the samples showed a broad asymmetrical signal with a low-frequency peak and a high-frequency shoulder characteristic of bilayer structures (data not shown).

Small-angle X-ray Scattering Experiments—MLVs at a concentration of 5% (w/w) prepared without or with the peptide at a lipid/peptide molar ratio of 50:1 were prepared as stated above and submitted to 15 temperature cycles (heating at 45 °C and cooling at -20 °C). Small angle x-ray scattering (SAXD) measurements were carried out using a Hecus SWAX-camera (Hecus x-ray Systems, Graz, Austria) as described previously (41) using nickel-filtered Cu-K α radiation ($\lambda = 1,542$ Å) originating from a sealed tube x-ray generator (Seifert, Alvenburg, Germany) operating at a power of 2 kW (50 kV, 4 mA). Sample-

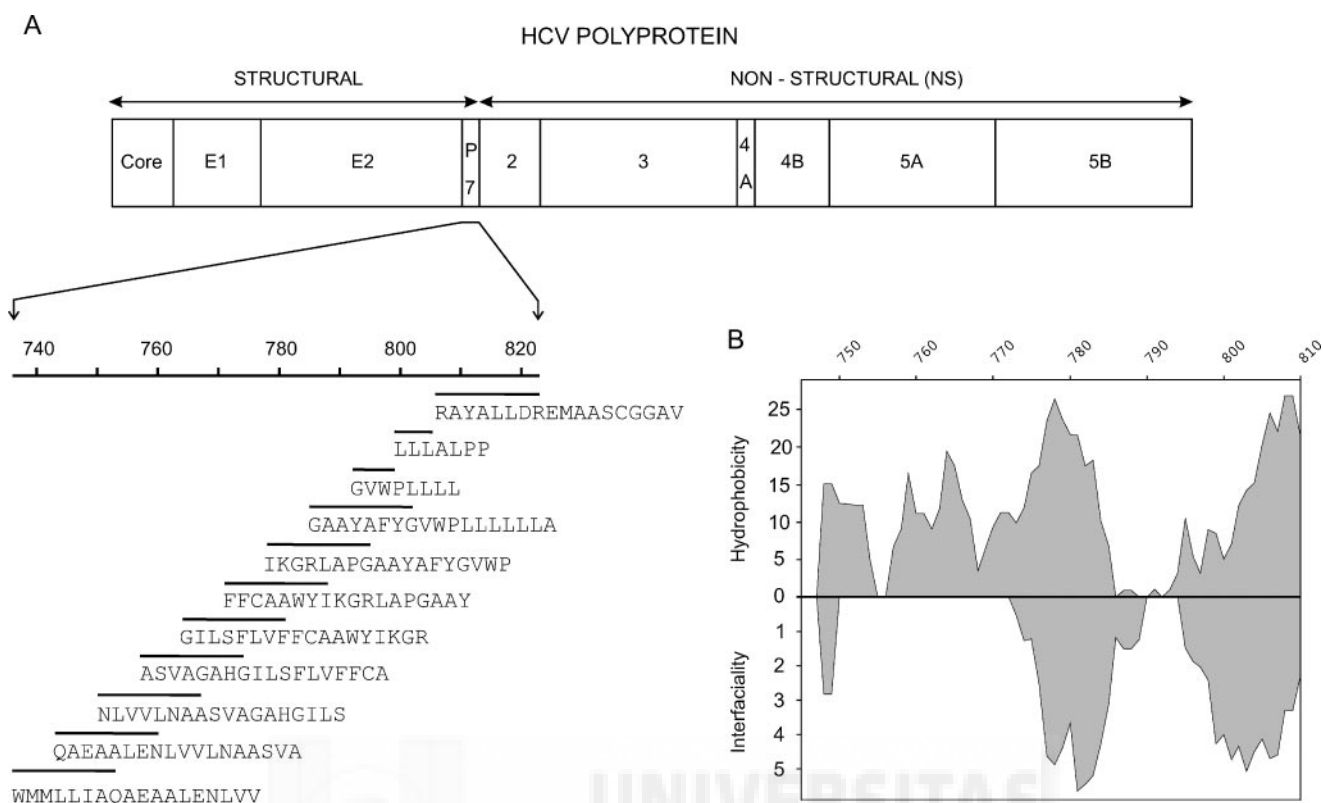


FIGURE 1. *A*, scheme of the HCV structural and non-structural proteins according to literature consensus. The sequence and relative location of the 11 peptides derived from the HCV p7 protein are shown with respect to the sequence of the protein. Maximum overlap between adjacent peptides is 11 amino acids. *B*, analysis of the hydrophobicity and interfaciality distribution according to the scales of Wimley and White (43, 44) using a window of 9 amino acids along the HCV p7 sequence without any assumption about secondary structure.

to-detector distance was 27.8 cm. A linear position-sensitive detector was used with 1024-channel resolution. SAXD angle calibration was done with silver stearate. The measurements were performed with the sample placed in a thin-walled 1-mm diameter quartz capillary held in a steel cuvette holder at different temperatures with an exposure time of 1 h. The SAXD curves were analyzed after background subtraction and normalization in terms of a full q -range model using the program GAP (42).

RESULTS

The peptide library used in this study and their correlation with the HCV p7 protein sequence is depicted in Fig. 1*A*. Note that the p7-derived peptides include the whole HCV p7 protein sequence (residues 746 to 809 of the HCV polyprotein precursor). Two and three consecutive peptides in the library have an overlap of 11 and 4 amino acids, respectively. Two peptides were 7 and 8 amino acid residues in length due to synthetic problems (Fig. 1*A*). The analysis of the hydrophobicity and interfaciality distribution along the p7 sequence of the HCV_1B4J strain, without any assumption on the secondary structure, is shown in Fig. 1*B* (19, 43, 44). The three-dimensional structure of the p7 protein is not known (13), but this analysis renders to us the potential surface zones potentially implicated in the modulation of membrane binding. As depicted in Fig. 1*B*, it is evident the existence of different regions with large hydrophobic and interfacial values in the p7 sequence. These regions could mediate the interaction with similar domains of other p7 proteins, other proteins, or with the surface of the membrane.

We have studied the effect of the p7-derived peptide library on membrane rupture by monitoring the CF leakage from six different liposome compositions (Fig. 2). The lipidic composition of the model membranes was EPC/Chol at a phospholipid molar ratio of 5:1, EPC/SM at a phospholipid molar ratio of 5:1, EPC/SM/Chol at a phospholipid molar ratio of 5:1:1, EPC/SM/Chol at a phospholipid molar ratio of 26:9:15, a complex lipid composition resembling the ER membrane (containing 51% EPC, 2.4% BPS, 5.3% bovine brain L - α -phosphatidylinositol, 7.48% SM, and 33.42% Chol (26)), and a lipid extract of liver membranes (containing 42% PC, 22% PE, 7% Chol, 8% PI, 1% lyso- α -phosphatidylcholine, and 21% neutral lipids as stated by the manufacturer). The presence of both SM and Chol has been related to the occurrence of laterally segregated membrane microdomains or "lipid rafts," and, for several viruses, a strong relationship between viral interaction with membranes and their content of Chol and SM was found (45). When the p7 peptides were assayed on liposomes, some exerted an important leakage effect (Fig. 2). The most remarkable effect was observed for peptide 771–788, which produced leakage values between 80 and 98%, depending on the specific lipid composition of the liposomes (Fig. 2). Other peptides that elicited significant leakage were those comprising residues 764–781 and 785–802, which displayed values between 15 and 65% depending on the lipid composition (Fig. 2). It is interesting to note that for liposomes composed of a natural lipid extract of liver membranes, the induced leakage was, in general, higher than for

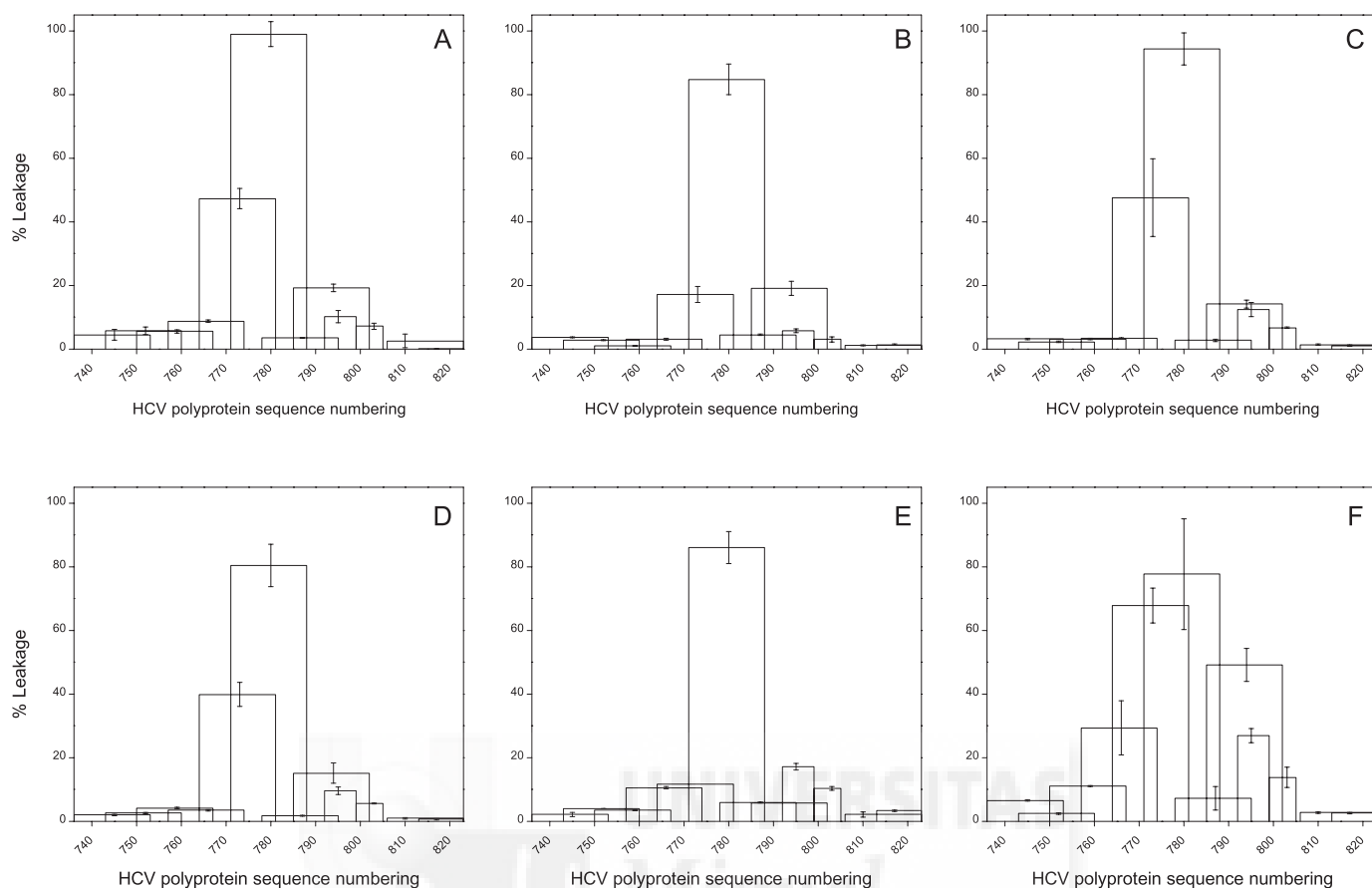


FIGURE 2. **Effect of the peptides derived from the HCV p7 protein of the HCV_1B4J strain on the release (membrane rupture) of LUV contents for different lipid compositions.** Leakage data for LUVs composed of EPC/Chol at a phospholipid molar ratio of 5:1 (A), EPC/SM/Chol at a phospholipid molar ratio of 5:1:1 (B), EPC/SM/Chol at a phospholipid molar ratio of 26:9:15 (C), synthetic ER membranes (E), and lipid extract of liver membranes (F). Vertical bars indicate S.D. of the mean of triplicate samples.

synthetic liposomes. Nevertheless, peptide 771–788 displayed the highest effect, followed by peptides 764–781 and 785–80.

The global average of membrane leakage obtained for the p7 peptides is illustrated in Fig. 3A. The segment corresponding to peptide 771–788 displays the largest leakage efficacy. Based on previous work (13), a model of p7 in the monomeric form is displayed in Fig. 3B. The model shows the specific residues that display the highest leakage effect. This sequence corresponds to the putative extracellular loop (the p7 loop domain) of the protein and it is the best candidate to interact with the phospholipid head groups. Taking into account these results, we performed an in-depth study of a peptide mimicking this domain, p7_L (Fig. 3B, inset). We investigated its binding and interaction with different membrane model systems, as well as characterized the structural changes taking place in both the peptide and phospholipid molecules.

The ability of the p7_L peptide to interact with lipid bilayers was determined from the increment in the intensity of the fluorescence emission maximum along with the shift toward shorter wavelengths (46) of the single p7_L Trp residue in the presence of phospholipid model membranes at different lipid/peptide ratios (Fig. 4A). The change in the Trp fluorescent spectral properties in the presence of phospholipids indicates that the p7_L peptide interacts with these model membranes. This approach has allowed us to obtain the peptide partition coefficient, K_p , which gave values in the 10^5 range for the different phospholipid compositions studied (Table 1). These K_p values are consistent with the tenet that the peptide was bound to the membrane surface with high affinity. Similar K_p values have been found for other peptides in the presence of model membranes (22, 23, 46, 47). Analysis of these data indicated that the peptide interacted stronger with negatively charged phospholipid-containing bilayers. These results were further corroborated by the larger displacement of the Trp emission frequency maximum of Trp in the presence of LUVs. In solution the peptide had an emission maximum centered at 344 nm, whereas in the presence of increasing concentrations of liposomes the emission maximum of the Trp presented a shift of about 9–11 nm to lower wavelengths depending on liposome composition. This finding implies that Trp sensed a low-polarity environment (entered in a hydrophobic environment) upon interaction with the membrane. We have also used the electrostatic surface potential probe FPE (48) to monitor the binding of the p7_L peptide to model membranes composed of different lipid compositions at different lipid/peptide ratios (Fig. 4B). As observed in the figure, p7_L had a higher affinity for model membranes containing negatively charged phospholipids than for the other compositions, including the liver lipid extract (Table 1).

Changes in the magnitude of the membrane dipole potential elicited by p7_L were monitored by means of the spectral shift of

the fluorescence probe di-8-ANEPPS (39, 49, 50). The variation of the fluorescence intensity ratio $R_{450/520}$ normalized as a function of the peptide concentration for different membrane compositions is shown in Fig. 4C. In the presence of the peptide, the greater decrease in the $R_{450/520}$ value was measured in bilayers with negatively charged lipids, demonstrating that the peptide was capable of inserting into the lipid bilayer and modifying the

dipole potential. Because the p7_L peptide has a positive net formal charge of +2, it is reasonable to assume that an electrostatic interaction underlies the high K_p values obtained with negatively charged phospholipids.

To investigate the accessibility of the Trp residues of the p7_L peptide to the aqueous phase in the presence of model membranes, we used acrylamide, a neutral, water-soluble, highly efficient quenching probe. Stern-Volmer plots for the quenching of Trp by acrylamide, recorded in the absence and presence of lipid vesicles, are shown in Fig. 5A. Linear Stern-Volmer plots indicate that the Trp residue is fairly accessible to acrylamide, and in all cases, the quenching of the peptide Trp residue showed an acrylamide-dependent concentration behavior. In aqueous solution the Trp residue was highly exposed to the solvent allowing for a more efficient quenching. However, in the presence of the phospholipid membranes, the extent of quenching was significantly reduced, indicating a poor accessibility of the Trp to the aqueous phase, consistent with its incorporation into the lipid bilayer. This notion is substantiated by the lower K_{sv} values obtained from the Stern-Volmer plots (Table 1). As expected, K_{sv} values were lower in the presence of negatively charged phospholipids than in the presence of zwitterionic ones, consistent with a deeper location in negative bilayers.

The transverse location of the p7_L peptide into the lipid bilayer was further investigated by monitoring the relative quenching of the Trp fluorescence by the lipophylic spin probes 5-NS and 16-NS when the peptide was incorporated in the fluid phase of the bilayers. These two derivatized fatty acids differ in the position of the quencher moiety along the hydrocarbon chain, thus allowing to determine the relative deepness of the peptide in the membrane. The 5-NS probe is a better quencher for molecules near or at the membrane interface, whereas the 16-NS probe is a better probe for molecules buried deeply in the bilayer. The variation of the fluorescence intensity as a function of the effective concentration of both 5-NS and 16-NS probes is shown in Fig. 5B, whereas the K_{sv} values for both probes are presented in Table 1. In general, 16-NS quenches the p7_L peptide fluorescence less efficiently than 5-NS, which is consistent with the location of the Trp residue in a shallow position in the membrane. The quenching

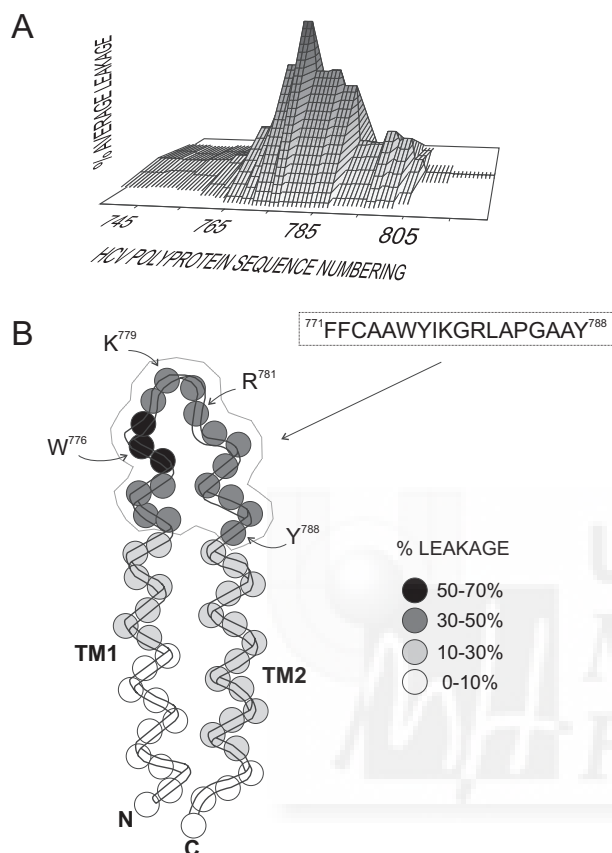


FIGURE 3. A, summary of the normalized global experimental membrane rupture data (leakage) corresponding to the peptide library derived from HCV_1B4J protein p7; and B, model of a monomer of the p7 protein showing the transmembrane α -helices TM1 and TM2 (13), the relative leakage effect for each p7 amino acid, key residues along the loop domain, as well as the sequence of the peptide p7_L studied in this work. See text for details.

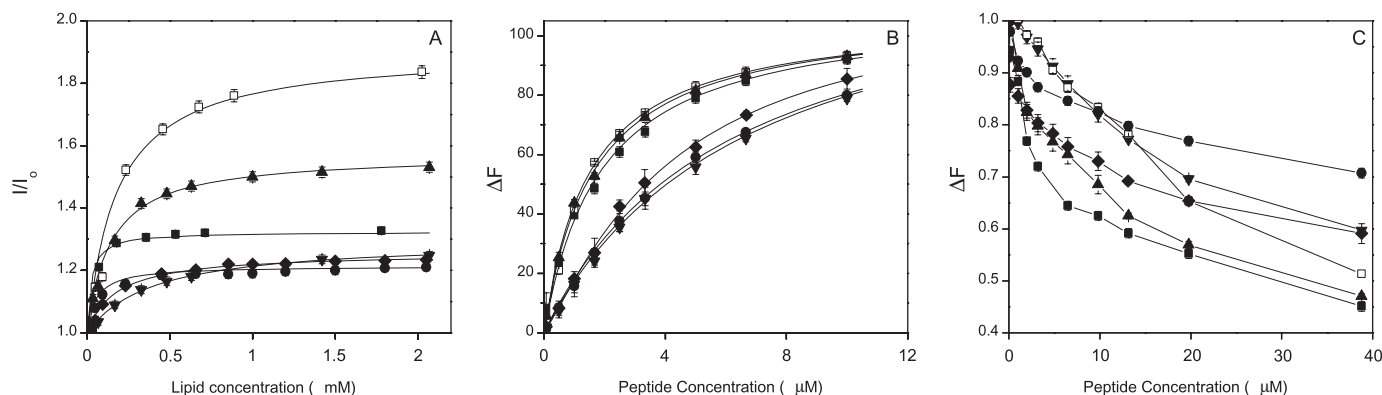


FIGURE 4. Determination of the partition constant (K_p) of p7_L through the change of the intrinsic tryptophan fluorescence in the presence of increasing lipid concentrations (A), determination of the dissociation constant (K_d) of p7_L through the change of the fluorescence signal amplitude of FPE (B), and effect of p7_L on the membrane dipole potential monitored through the fluorescence ratio (R) of di-8-ANEPPS in the presence of LUVs containing different lipid compositions at different lipid-to-peptide molar ratios. The lipid compositions were EPC/Chol at a molar ratio of 5:1 (●), BPS/Chol at a molar ratio of 5:1 (■), EPG/Chol at a molar ratio of 5:1 (□), EPA/Chol at a molar ratio of 5:1 (▲), EPC/SM/CHOL at a molar ratio of 5:1:1 (◆), and lipidic liver extract (▼). In B and C the lipid concentration was 200 μ M. Vertical bars indicate S.D. of the mean of triplicate samples.

TABLE 1

Partition coefficients, Stern-Volmer quenching constants, and maximal leakage, hemifusion, and fusion values at a phospholipid/peptide ratio of 5:1 for the p7_L peptide incorporated in LUVs of different compositions

LUV compositions	K_p , Trp	K_D , FPE	K_{sv}			Leakage	Hemifusion	Fusion
			Acrylamide	5-NS	16-NS			
EPG	$6.89 \pm 0.43 \times 10^5$	1.615	5.31	5.135	0.636	100.0	31.9	17.6
EPA	$3.95 \pm 0.67 \times 10^5$	1.609	2.91	5.918	0.575	100.0	32.7	14.1
BPS	$3.69 \pm 0.75 \times 10^5$	1.937	3.87	5.505	0.541	100.0	45.6	29.6
EPC	$1.78 \pm 0.67 \times 10^5$	6.459	5.67	4.135	0.818	79.9	28.1	15.2
Liver extract	$1.39 \pm 0.46 \times 10^5$	7.011	6.89	3.718	0.641	87.8	27.4	10.9
EPC/SM/Chol 5:1:1		7.101	11.9			87.5	28.6	16.1
p7 _L in buffer			13.28					

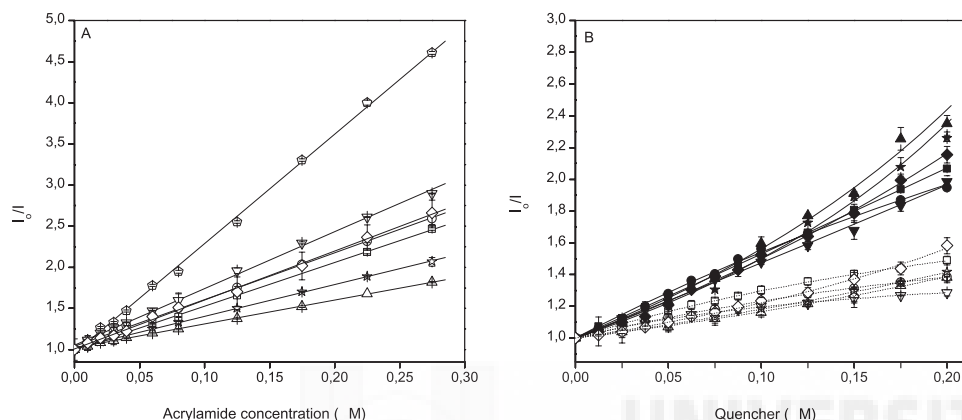


FIGURE 5. A, Stern-Volmer plots of the quenching of the Trp fluorescence emission of p7_L by acrylamide in aqueous buffer (\diamond), and in the presence of LUVs composed of EPC/Chol at a molar ratio of 5:1 (\square), EPA/Chol at a molar ratio of 5:1 (Δ), BPS/Chol at a molar ratio of 5:1 (\star), EPC/SM/Chol at a molar ratio of 5:1:1 (224) and lipidic liver extract (∇). B, depth-dependent quenching of the Trp fluorescence emission of p7_L by 5-NS (filled symbols) and 16-NS (empty symbols) in LUVs composed of EPC/Chol at a molar ratio of 5:1 (\bullet and \circ), EPG/Chol at a molar ratio of 5:1 (\blacksquare and \square), EPA/Chol at a molar ratio of 5:1 (\blacktriangle and \triangle), BPS/Chol at a molar ratio of 5:1 (\star and \ast), EPC/SM/Chol at a molar ratio of 5:1:1 (\blacklozenge and 224), and lipidic liver extract (\blacktriangledown and \triangledown). The lipid to peptide ratio was 50:1.

depends on phospholipid composition, because the peptide is quenched by 5-NS with higher efficacy in model membranes composed of negatively charged phospholipids.

To explore the effect of the p7_L peptide in the destabilization of membrane vesicles, we studied its effect on the release of the encapsulated fluorophores CF (Stokes radius around 6 Å) and FD10 (Stokes radius around 23 Å) in model membranes (51, 52). The extent of CF leakage observed at different peptide to lipid molar ratios and the effect on different phospholipid compositions is shown in Fig. 6A and Table 1. It is interesting to note that the p7_L peptide induced a high percentage of leakage (90–100%), even at lipid/peptide ratios as high as 30:1, for liposomes composed of BPS/Chol, EPG/Chol, and EPA/Chol (Fig. 6A). Lower, but significant, leakage values were obtained for liposomes composed of EPC/Chol, EPC/SM/Chol, and the liver extract (at the highest peptide to lipid ratio studied, *i.e.* 1:5, leakage values were about 80–90%). Next, we carried out a series of experiments using FD10 to characterize the size of the possible pores formed by p7_L. However, p7_L did not induce any leakage of FD10 entrapped in liposomes having different compositions (data not shown). Because p7_L promoted the leak of CF but not FD10, the pore size that would be formed by the peptide should be comprised between 6 and 23 Å.

The induction of outer and inner monolayer lipid mixing (hemifusion and true fusion, respectively) by the p7_L peptide

was tested with several types of vesicles utilizing a probe dilution assay (32, 33). As shown in Fig. 6, B and C, and Table 1, the higher hemifusion and fusion values were found for liposomes containing negatively charged phospholipids. Liposomes containing BPS/Chol, EPG/Chol, and EPA/Chol showed hemifusion and fusion values of about 30–45 and 12–27%, respectively. In all cases the highest values were found when liposomes containing BPS were used. It is worth noting that ER and the liver extract lipids contain negatively charged phospholipids but at lower relative quantities, consistent with their smaller hemifusion and fusion efficacies. The p7_L peptide exhibits a CRAC motif, characterized by the presence of the consensus sequence –L/V-(X)(1–5)-Y-(X)(1–5)-R/K-, where (X)(1–5) represents 1–5 residues of any amino acid (53). The CRAC motif has been suggested to induce formation of cholesterol-rich domains. Therefore, we studied the possibility that p7_L might interact specifically with cholesterol by a fluorescence resonance energy transfer strategy using DHE as an acceptor (54). We did not find any specificity of the peptide for cholesterol-rich domains (data not shown).

The p7_L peptide aggregation state in the presence of membranes was assayed using ThT (38). As observed in Fig. 6D, the peptide remained slightly aggregated in an aqueous medium, as the fluorescence increased after adding the peptide. However, the presence of liposomes composed of EPC/Chol, EPA/Chol, EPG/Chol, BPS/Chol, or a lipidic liver extract provoked a significant and fast peptide aggregation (Fig. 6D). These data suggest that the membrane insertion of the peptide concomitantly induces the peptide oligomerization.

The effect of the p7_L peptide on the structural and thermotropic properties of phospholipid membranes was also investigated by measuring the steady-state fluorescence anisotropy of the fluorescent probes DPH, PA-DPH, and TMA-DPH incorporated into DMPC, DMPA, and DMPG membranes as a function of the temperature (Fig. 7). DPH and its derivatives are very useful fluorescent probes for monitoring the organization and dynamics of membranes, because fluorescence polarization

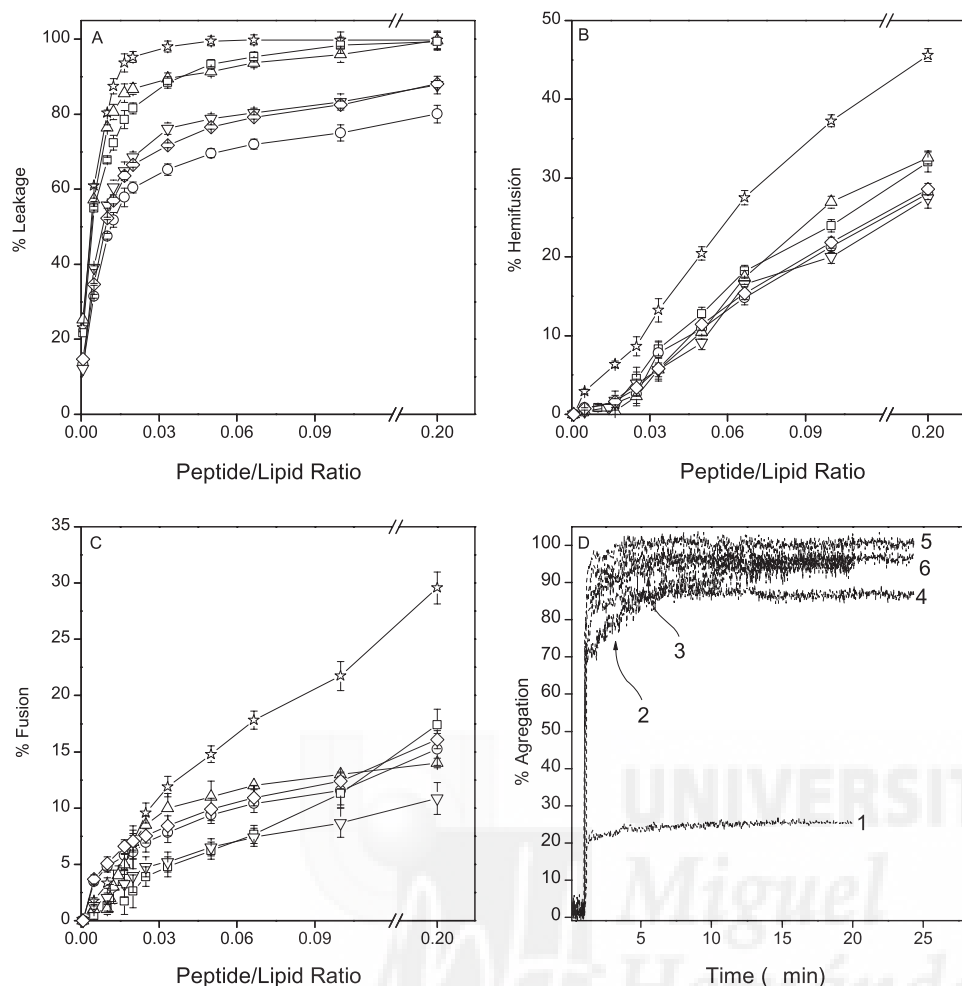


FIGURE 6. Effect of the p7_L peptide on (A) membrane rupture, i.e. leakage, (B) membrane phospholipid mixing of the outer monolayer, i.e. hemifusion, and (C) membrane phospholipid mixing of the inner monolayer, i.e. fusion, of fluorescent probes encapsulated in LUVs containing different lipid compositions at different lipid-to-peptide molar ratios. The lipid compositions used were EPC/Chol at a molar ratio of 5:1 (○), EPG/Chol at a molar ratio of 5:1 (□), EPA/Chol at a molar ratio of 5:1 (Δ), BPS/Chol at a molar ratio of 5:1 (☆), EPC/SM/Chol at a molar ratio of 5:1:1 (224), and lipidic liver extract (▽). The lines connecting the experimental data are merely guides to the eye. *D*, fluorescence variation of ThT after addition of the p7_L peptide to an aqueous solution (1) and in the presence of LUVs of EPC/Chol at a molar ratio of 5:1 (2), EPA/Chol at a molar ratio of 5:1 (3), EPG/Chol at a molar ratio of 5:1 (4), BPS/Chol at a molar ratio of 5:1 (5), and lipidic liver extract (6).

correlates with the rotational diffusion of membrane-embedded probes, which are highly sensitive to the packing of the fatty acyl chains (34). DPH is known to partition mainly into the hydrophobic core of the membrane, whereas TMA-DPH is oriented at the membrane bilayer with its charge localized at the lipid-water interface (34, 55, 56). Their different location and orientation in the membrane allows to analyze the effect of the p7_L peptide on the structural and thermotropic properties along the full-length of the membrane. For DMPC bilayers, the presence of the p7_L peptide decreased the cooperativity of the thermal transition as well as induced a decrease of the anisotropy of all types of probes. These data suggest that the peptide was able to increase the mobility of the phospholipid acyl chains when compared with the pure phospholipid (Fig. 7, A–C). In contrast, for DMPA we did not observe a significant decrease in cooperativity, although a slight shift of T_m to lower temperatures is evident, more apparent for TMA-DPH and PA-DPH than for DPH. Similarly, a small decrease in anisotropy for PA-

DPH and DPH was also seen (Fig. 7, D–F). For vesicles composed of DMPG, the p7_L peptide decreased the cooperativity of the thermal transition, as well as it decreased the anisotropy below the T_m of the phospholipid (Fig. 7, G–I). In this case, the presence of the peptide decreases the anisotropy values compared with the pure phospholipids, suggesting that the peptide was able to increase the mobility of the phospholipid acyl chains below but not above the T_m . These differences could suggest that the difference in charge between DMPC, DMPA, and DMPG could slightly affect the peptide incorporation into the lipid bilayer. Nevertheless, these data demonstrate that the p7_L peptide influences the fluidity of these phospholipids. Taking together all these results, it could be suggested that p7_L, although interacting with the membrane, should be primarily located at the lipid-water interface (23). It should be stressed that we did not observe quenching of the probes by the peptide in the concentration range used. Thus, this change of anisotropy cannot be ascribed to a shorter probe lifetime.

The infrared spectrum of the Amide I' region of the fully hydrated p7_L peptide in D₂O buffer at 25 °C and pH 7.4 is shown in Fig. 8A. The spectrum is formed by different underlying components that give place to a broad and asymmetric band with a maximum at about 1642 cm⁻¹. The maximum of the band did not change significantly upon increasing the temperature (data not shown), suggesting a high degree of conformational stability of the peptide in solution. The assignment of the Amide I' component bands to specific structural features has been described previously (46). The intensity maxima at about 1642 cm⁻¹ implies that the most significant structure in aqueous solution corresponds to a mixture of mainly unordered but also helical structures (57). The band envelope of the Amide I' region of the peptide bound to DMPC, DMPG, and DMPA model membranes at a phospholipid/peptide molar ratio of 15:1 was significantly different from that seen for the pure peptide in solution. The frequencies at the maximum of the band appeared at about 1624–1626 cm⁻¹ in all cases (Fig. 8B). As it was found for the peptide in solution, the maximum of the band did not change significantly upon increasing the temperature in the presence of the model membranes (data not shown), indicating also a high degree of conformational stabil-

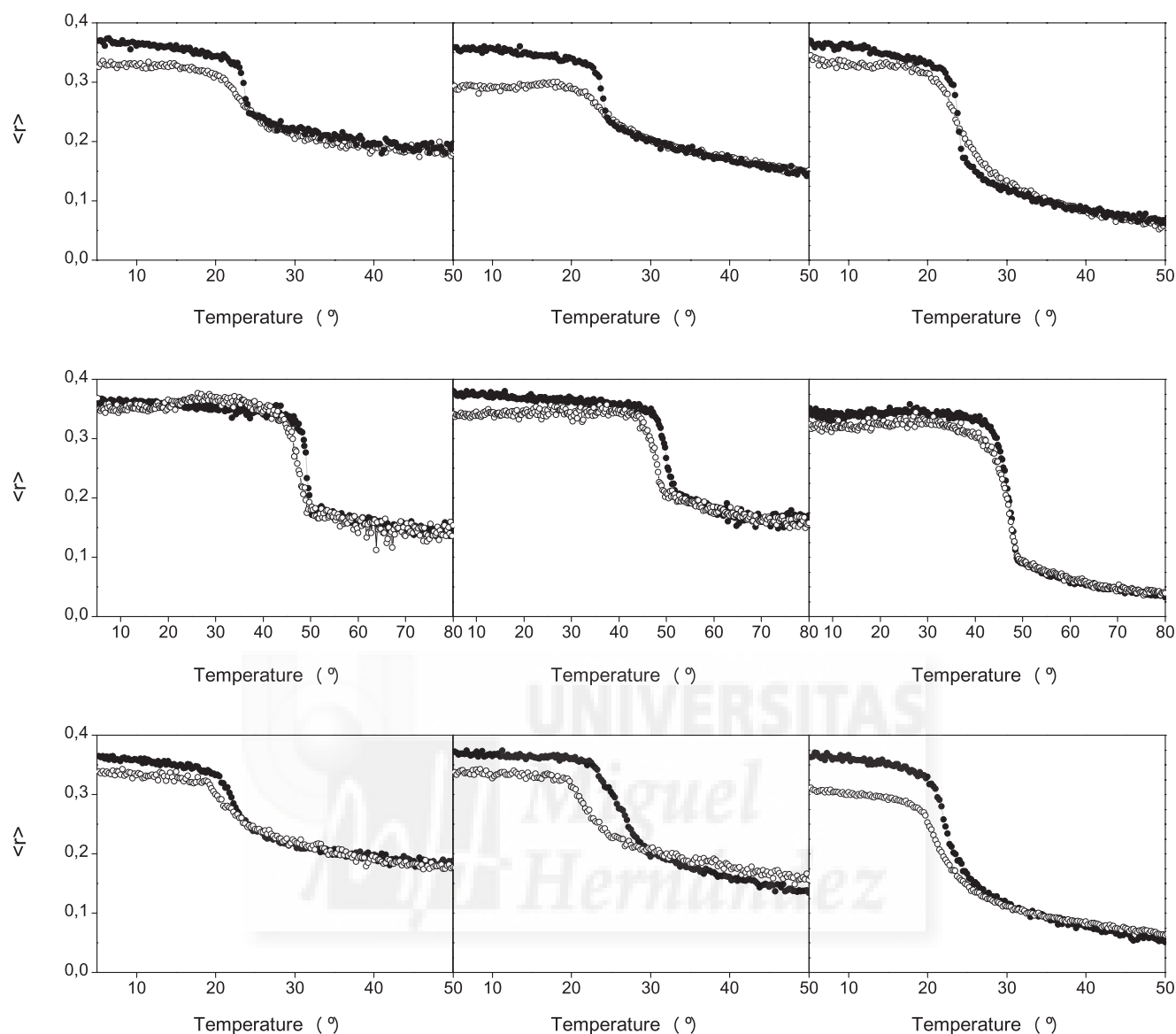


FIGURE 7. Steady-state anisotropy, $\langle r \rangle$, of TMA-DPH, PA-DPH, and DPH (left, middle, and right columns, respectively) incorporated into MLVs composed of DMPC, DMPA, and DMPA model membranes (from upper to low rows, respectively) as a function of temperature. Data correspond to vesicles in the absence (●) and presence of the p7_L peptide (○). The peptide to phospholipid molar ratio was 1:15.

ity. The narrow band at about 1624–1626 cm⁻¹ would correspond to either β -sheet structures or self-aggregated peptides forming an intermolecular network of hydrogen-bonded β -structures or both (58). In addition, we tested an increased phospholipid/peptide molar ratio of 200:1 for checking the influence of the lipid to peptide ratio on its secondary structure (Fig. 8C), being very similar to that found at higher molar ratios (Fig. 8B).

We have used MAS ³¹P NMR to observe the POPC/SM/Chol mixture at a molar ratio of 5:1:1 because the ³¹P NMR isotropic chemical shifts of both SM and POPC head groups are resolvable under MAS conditions. Furthermore, their spectral intensities reflect the molar ratio of each lipid in the mixture. This approach allows the observation of the line widths of each phospholipid component in the mixture. As observed in Fig. 9A, the chemical shift for the POPC and SM resonances were not different neither in the absence nor in the presence of the p7_L

peptide, but the line widths of the ³¹P resonances of POPC and SM were dissimilar. In the absence of p7_L, the ³¹P line width at half-height of POPC was 51 Hz and that of SM was 55 Hz. These values shifted to 118 and 101 Hz, respectively, when the peptide was present. These results show that both phospholipids, POPC and SM, exhibit a lower degree of mobility and/or an increased heterogeneity of head group environments in the presence of p7_L (59). We have also used SAXD to get information on the structural organization of the mixture containing POPC/SM/CHOL at a molar ratio of 5:1:1 in the absence and presence of the peptide (Fig. 9B). In both cases, the diffraction pattern corresponds to the liquid-crystalline L_α phase, showing an interlamellar repeat distance of 67.9 Å for the pure lipid mixture and 68.3 Å in the presence of peptide. The structural results from the global data analysis, shown in the inset of Fig. 9B, showed that the membrane thickness decreased from 55 Å in the absence of the peptide to 53.8 Å in its presence. However,

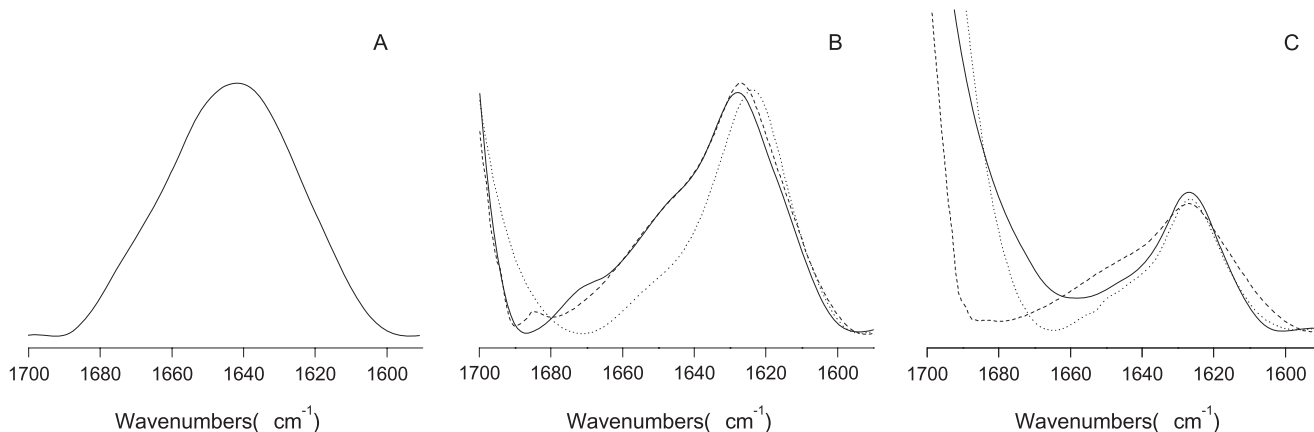


FIGURE 8. Amide I' band of the p7_L peptide in buffer (A) and in the presence of DMPC (solid line), DMPG (dashed line), and DMPA (dotted line) at a lipid/peptide molar ratio of 15:1 (B) and 200:1 (C). The spectra were taken at $T_m + 10$ °C.

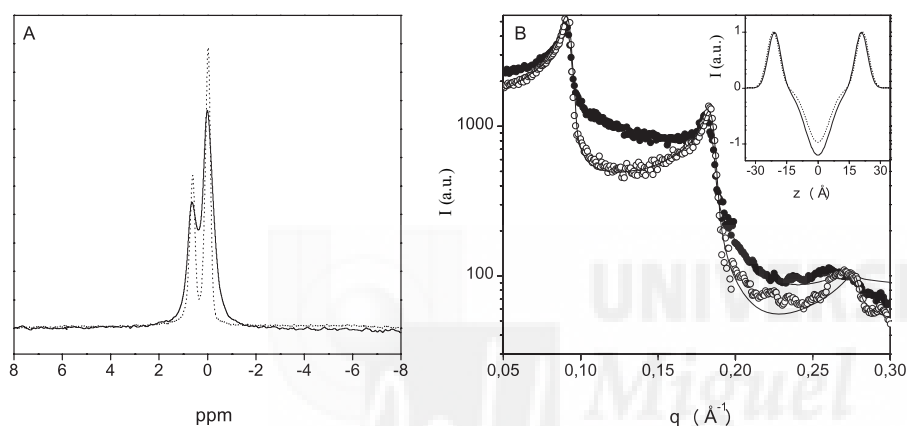


FIGURE 9. A, MAS ³¹P NMR at 25 °C and 9 kHz spinning speed (500 MHz proton frequency) spectra for POPC/SM/Chol (5:1:1 molar ratio) MLV suspension in the absence (—) and presence of p7_L at a lipid/molar ratio of 50:1 (solid line). B, small angle x-ray scattering of POPC/SM/Chol (5:1:1 molar ratio) MLV suspension in the absence (○) and presence of p7_L (●) at 25 °C in the L_α phase. Solid lines represent the best fit to the SAXD data applying a global analysis technique. The inset displays the one-dimensional electron density profiles along the bilayer normal calculated from the SAXD diffraction patterns in the absence (dotted line) and presence of p7_L (solid line).

the thickness of the water layer increased from 12.9 to 14.5 Å under the same conditions. The most significant effect was, however, the increase of the diffuse scattering in the presence of the peptide indicating that several bilayers have become positionally uncorrelated due to the influence of the peptide.

DISCUSSION

Viral morphogenesis, although one of the most important steps in the viral cycle involving lipid membranes, is not as well characterized as viral-mediated membrane fusion. The assembly of enveloped viruses takes place in the host cell membrane and in the case of HCV it has been suggested that the virus particles assembly occurs in the ER membranes (60) where different proteins, including p7, play a central role in viral particle formation and budding. HCV protein p7 is a small transmembrane protein with two TM helical domains connected by a loop, which is essential for the efficient assembly and release of infectious virions but not critical for RNA replication (10). p7 is capable of forming ion channels and mutations in the loop region abolish the channel activity of the protein, which has been described to be a viroporin-like protein (12, 15, 16). Because the biological roles of p7 can be modulated by mem-

branes, using an approach similar to that published recently (19–21), we have carried the analysis of the membrane-active regions of p7 by observing the effect of a p7-derived peptide library from HCV (strain HCV_1B4J) on the integrity of different membrane model systems. We have identified a membranotropic region in p7 coincidental with the loop domain of the protein. Consequently, we have made a comprehensive study of a peptide patterned after the p7 loop domain, p7_L, characterizing its binding and interaction with model membrane systems through a series of complementary experiments. Our findings identify a key region in the viral protein that might be implicated in the

HCV life cycle, which could be used as a new target for searching inhibitors of viral assembly, thus leading to new vaccine strategies.

We have been able to discern different regions along the p7 sequence that display distinct membranotropic properties using a peptide library derived from the p7 protein. Although the use of peptide fragments might not fully mimic the properties of the intact protein, our results give an indication of the relative propensity of the different domains to bind, interact, and affect different model membranes. When all the leakage values were taken into account for all lipid compositions assayed, one peptide displayed significant membrane rupture activity, namely the region encompassing amino acids 771–788 (Fig. 3A). Region 771–788 coincides with the p7 loop linking the two TM helices of the protein. Notably, this region displayed a high interfacial value along its sequence. This highly conserved loop seems to be necessary for homodimerization and channel forming (61). Indeed, our findings are consistent with the tenet that the interaction with lipid bilayers induces its oligomerization, as evidenced by aggregation of the p7_L peptide in the presence of model membranes. One model of p7 predicted that the

side chains of residues Lys⁷⁷⁹ and Arg⁷⁸¹ would project into the channel lumen, perhaps forming a gate controlling the flow of ions (16).

Peptide p7_L binds with high affinity to phospholipid model membranes containing negatively charged phospholipids. We and others have previously found similar binding affinities for other peptides pertaining to the loop and NHR regions of the gp41 protein (22, 23, 46, 62, 63). The p7_L peptide has a positive net formal charge of +2, implying that an electrostatic force may be responsible for the high K_p values observed for compositions containing negatively charged phospholipids. However, the peptide was also capable to bind significantly to other liposome systems composed of zwitterionic phospholipids. The peptide decreased the dipole potential of the membrane as well. Binding of p7_L to liposomes was further demonstrated by hydrophilic and lipophilic quenching probes. p7_L was less accessible for quenching by acrylamide in the presence of negatively charged phospholipids implying a buried location. A higher quenching efficiency was observed for model membranes containing negatively charged phospholipids in the presence of NS probes, suggesting that the peptide was more buried in the membrane when negatively charged phospholipids were present, but near the membrane lipid/water interface in a shallow position.

The p7_L peptide was also capable of altering the membrane stability causing the release of fluorescent probes of small size, being dependent on lipid composition and on the lipid/peptide molar ratio. The highest CF release was observed for liposomes containing negatively charged phospholipids, although significant leakage values were also observed for liposomes composed of zwitterionic phospholipids. The effect on zwitterionic vesicles should be due primarily to hydrophobic interactions within the bilayer but not to the specific charge of the phospholipid head groups. Notably, p7_L released CF but not FD10, implying that the peptide formed pores of diameter between 6 and 23 Å. The induction of hemifusion and fusion by the p7_L peptide were also studied and similar results were obtained, because specific and large membrane hemifusion and fusion values were characteristic of liposomes composed of negatively charged phospholipids. It is interesting to note that p7_L presents a CRAC motif, although we have not seen specificity of the peptide for cholesterol-rich domains.

We have also shown that the p7_L peptide is capable of affecting the steady-state fluorescence anisotropy of DPH fluorescent probes located into the palisade structure of the membrane, because the peptide increased the mobility of the phospholipid acyl chains below but not above the T_m when compared with the pure phospholipids. Additionally, by using MAS NMR, we demonstrated that the phosphate groups of the phospholipid molecules display a lower degree of mobility and/or an increased heterogeneity of head group environments in the presence of p7_L. This result strengthens that the location of the peptide is at or near the membrane interface. Moreover, the presence of p7_L slightly decreased the membrane thickness and increased its hydration layer. At the same time we found an increase of positionally uncorrelated bilayers. These data reveal that p7_L affects the elastic behavior of the membrane and further substantiates that p7_L should be located at

the lipid-water interface (23). All this information suggests that negatively charged phospholipids could play an important role in the biological function of p7. As observed by infrared, the Amide I' region of the fully hydrated peptide did not change with temperature, indicating a high stability of its conformation. In buffer, p7_L presents a high content of random structure. In marked contrast, the overall structure of the peptide in the presence of model membranes was significantly different, because it displayed a high percentage of β -sheet structures and/or self-aggregated peptides. These components were independent of the lipid-to-peptide ratio. The ThT aggregation data supports that p7_L has a tendency to oligomerize at the membrane surface.

It is interesting to note that replacement of the two conserved basic amino acids, Lys⁷⁷⁹ and Arg⁷⁸¹, pertaining to the p7 loop suppress dramatically the production of infectious viruses (12), highlighting the importance of this conserved motif as well as the relevance of the loop. Significantly, two other amino acids pertaining to the p7_L peptide, Trp⁷⁷⁶ and Tyr⁷⁸⁸, are also essential for the p7 function (12). It seems reasonable to hypothesize that the basic residues interact specifically with the phospholipid head groups of the ER. Although it could not be discarded the possibility that p7 may also interact with other proteins from HCV as it has been suggested (9). It is already known that p7 forms ionic channels in the membrane, probably forming an hexameric bundle (16). The folding of p7 could begin by forming two TM helices across the bilayer, followed by stabilization of the monomeric protein and finally the oligomerization of the monomer to form the hexameric assembly through interaction of the helices (13). The conserved positively charged loop, its location on the surface of the membrane, its tendency to oligomerize in the presence of phospholipids, as well as its specific interaction with phospholipid head groups, could be the driving force of the protein oligomerization. Therefore this protein domain may be essential for the formation of the active ion channel. Accordingly, the p7 loop appears as an attractive candidate for antiviral drug development leading to new vaccine strategies.

Acknowledgments—We are especially grateful to the National Institutes of Health AIDS Research and Reference Reagent Program, Division of AIDS, NIAID, National Institutes of Health, for the peptides used in this work; Ana I. Gómez-Sánchez for outstanding technical assistance; as well as Prof. Antonio Ferrer, IBMC-UMH, for the critical reading of the manuscript and excellent aid in correcting the English language.

REFERENCES

1. Chen, S. L., and Morgan, T. R. (2006) *Int. J. Med. Sci.* **3**, 47–52
2. Penin, F., Dubuisson, J., Rey, F. A., Moradpour, D., and Pawlotsky, J. M. (2004) *Hepatology* **39**, 5–19
3. Tan, S. L., Pause, A., Shi, Y., and Sonenberg, N. (2002) *Nat. Rev. Drug Dis.* **1**, 867–881
4. Qureshi, S. A. (2007) *Med. Res. Rev.* **27**, 353–373
5. Pozzetto, B., Bourlet, T., Grattard, F., and Bonneval, L. (1996) *Nephrol. Dial. Transplant.* **11**, Suppl. 4, 2–5
6. Vauloup-Fellous, C., Pene, V., Garaud-Aunis, J., Harper, F., Bardin, S., Suire, Y., Pichard, E., Schmitt, A., Sogni, P., Pierron, G., Briand, P., and Rosenberg, A. R. (2006) *J. Biol. Chem.* **281**, 27679–27692

7. Mizushima, H., Hijikata, M., Asabe, S., Hirota, M., Kimura, K., and Shimotohno, K. (1994) *J. Virol.* **68**, 6215–6222
8. Lin, C., Lindenbach, B. D., Pragai, B. M., McCourt, D. W., and Rice, C. M. (1994) *J. Virol.* **68**, 5063–5073
9. Sakai, A., Claire, M. S., Faulk, K., Govindarajan, S., Emerson, S. U., Purcell, R. H., and Bukh, J. (2003) *Proc. Natl. Acad. Sci. U. S. A.* **100**, 11646–11651
10. Lohmann, V., Korner, F., Koch, J., Herian, U., Theilmann, L., and Bartenschlager, R. (1999) *Science* **285**, 110–113
11. Tokita, H., Kaufmann, G. R., Matsubayashi, M., Okuda, I., Tanaka, T., Harada, H., Mukaide, M., Suzuki, K., and Cooper, D. A. (2000) *J. Clin. Microbiol.* **38**, 3450–3452
12. Steinmann, E., Penin, F., Kallis, S., Patel, A. H., Bartenschlager, R., and Pietschmann, T. (2007) *PLoS Pathog.* **3**, e103
13. Patargias, G., Zitzmann, N., Dwek, R., and Fischer, W. B. (2006) *J. Med. Chem.* **49**, 648–655
14. Carrere-Kremer, S., Montpellier-Pala, C., Cocquerel, L., Wychowski, C., Penin, F., and Dubuisson, J. (2002) *J. Virol.* **76**, 3720–3730
15. Gonzalez, M. E., and Carrasco, L. (2003) *FEBS Lett.* **552**, 28–34
16. Griffin, S. D., Beales, L. P., Clarke, D. S., Worsfold, O., Evans, S. D., Jaeger, J., Harris, M. P., and Rowlands, D. J. (2003) *FEBS Lett.* **535**, 34–38
17. Berg, T., Kronenberger, B., Hinrichsen, H., Gerlach, T., Buggisch, P., Herrmann, E., Spengler, U., Goeser, T., Nasser, S., Wursthorn, K., Pape, G. R., Hopf, U., and Zeuzem, S. (2003) *Hepatology* **37**, 1359–1367
18. Pavlovic, D., Neville, D. C., Argaud, O., Blumberg, B., Dwek, R. A., Fischer, W. B., and Zitzmann, N. (2003) *Proc. Natl. Acad. Sci. U. S. A.* **100**, 6104–6108
19. Guillen, J., Perez-Berna, A. J., Moreno, M. R., and Villalain, J. (2005) *J. Virol.* **79**, 1743–1752
20. Perez-Berna, A. J., Moreno, M. R., Guillen, J., Bernabeu, A., and Villalain, J. (2006) *Biochemistry* **45**, 3755–3768
21. Moreno, M. R., Giudici, M., and Villalain, J. (2006) *Biochim. Biophys. Acta* **1758**, 111–123
22. Pascual, R., Moreno, M. R., and Villalain, J. (2005) *J. Virol.* **79**, 5142–5152
23. Contreras, L. M., Aranda, F. J., Gavilanes, F., Gonzalez-Ros, J. M., and Villalain, J. (2001) *Biochemistry* **40**, 3196–3207
24. Surewicz, W. K., Mantsch, H. H., and Chapman, D. (1993) *Biochemistry* **32**, 389–394
25. Zhang, Y. P., Lewis, R. N., Hodges, R. S., and McElhaney, R. N. (1992) *Biochemistry* **31**, 11572–11578
26. Bretscher, M. S. (1985) *Sci. Am.* **253**, 100–108
27. Mayer, L. D., Hope, M. J., and Cullis, P. R. (1986) *Biochim. Biophys. Acta* **858**, 161–168
28. Böttcher, C. J. F., Van Gent, C. M., and Fries, C. (1961) *Anal. Chim. Acta* **1061**, 203–204
29. Edelhoch, H. (1967) *Biochemistry* **6**, 1948–1954
30. Bernabeu, A., Guillen, J., Perez-Berna, A. J., Moreno, M. R., and Villalain, J. (2007) *Biochim. Biophys. Acta* **1768**, 1659–1670
31. Moreno, M. R., Guillen, J., Perez-Berna, A. J., Amoros, D., Gomez, A. I., Bernabeu, A., and Villalain, J. (2007) *Biochemistry* **46**, 10572–10584
32. Struck, D. K., Hoekstra, D., and Pagano, R. E. (1981) *Biochemistry* **20**, 4093–4099
33. Meers, P., Ali, S., Erukulla, R., and Janoff, A. S. (2000) *Biochim. Biophys. Acta* **1467**, 227–243
34. Lentz, B. R. (1993) *Chem. Phys. Lipids* **64**, 99–116
35. Eftink, M. R., and Ghiron, C. A. (1977) *Biochemistry* **16**, 5546–5551
36. Wall, J., Ayoub, F., and O'Shea, P. (1995) *J. Cell Sci.* **108**, 2673–2682
37. Golding, C., Senior, S., Wilson, M. T., and O'Shea, P. (1996) *Biochemistry* **35**, 10931–10937
38. LeVine, H., 3rd (1993) *Protein Sci.* **2**, 404–410
39. Cladera, J., and O'Shea, P. (1998) *Biophys. J.* **74**, 2434–2442
40. Gross, E., Bedlack, R. S., Jr., and Loew, L. M. (1994) *Biophys. J.* **67**, 208–216
41. Laggner, P. (1994) *Subcell. Biochem.* **23**, 451–491
42. Pabst, G. (2006) *Biophys. Rev. Lett.* **1**, 57–84
43. Wimley, W. C., and White, S. H. (1996) *Nat. Struct. Biol.* **3**, 842–848
44. White, S. H., and Wimley, W. C. (1999) *Annu. Rev. Biophys. Biomol. Struct.* **28**, 319–365
45. Ahn, A., Gibbons, D. L., and Kielian, M. (2002) *J. Virol.* **76**, 3267–3275
46. Pascual, R., Contreras, M., Fedorov, A., Prieto, M., and Villalain, J. (2005) *Biochemistry* **44**, 14275–14288
47. Santos, N. C., Prieto, M., and Castanho, M. A. (1998) *Biochemistry* **37**, 8674–8682
48. Wall, J., Golding, C. A., Van Veen, M., and O'Shea, P. (1995) *Mol. Membr. Biol.* **12**, 183–192
49. Cladera, J., Martin, I., and O'Shea, P. (2001) *EMBO J.* **20**, 19–26
50. O'Shea, P. (2003) *Biochem. Soc. Trans.* **31**, 990–996
51. Laurent, T. C., and Granath, K. A. (1967) *Biochim. Biophys. Acta* **136**, 191–198
52. Fisher, D. B., and Cash-Clark, C. E. (2000) *Plant Physiol.* **123**, 125–138
53. Li, H., Yao, Z., Degenhardt, B., Teper, G., and Papadopoulos, V. (2001) *Proc. Natl. Acad. Sci. U. S. A.* **98**, 1267–1272
54. Veiga, A. S., and Castanho, M. A. (2007) *FEBS J.* **274**, 5096–5104
55. Davenport, L., Dale, R. E., Bisby, R. H., and Cundall, R. B. (1985) *Biochemistry* **24**, 4097–4108
56. Pebay-Peyroula, E., Dufourc, E. J., and Szabo, A. G. (1994) *Biophys. Chem.* **53**, 45–56
57. Byler, D. M., and Susi, H. (1986) *Biopolymers* **25**, 469–487
58. Arrondo, J. L., and Goni, F. M. (1999) *Prog. Biophys. Mol. Biol.* **72**, 367–405
59. Delboy, M. G., Patterson, J. L., Hollander, A. M., and Nicola, A. V. (2006) *J. Virol.* **3**, 105
60. Ait-Goughoulte, M., Hourieux, C., Patient, R., Trassard, S., Brand, D., and Roingard, P. (2006) *J. Gen. Virol.* **87**, 855–860
61. Griffin, S. D., Harvey, R., Clarke, D. S., Barclay, W. S., Harris, M., and Rowlands, D. J. (2004) *J. Gen. Virol.* **85**, 451–461
62. Korazim, O., Sackett, K., and Shai, Y. (2006) *J. Mol. Biol.* **364**, 1103–1117
63. Rabenstein, M., and Shin, Y. K. (1995) *Biochemistry* **34**, 13390–13397

Publicación 3

The Membrane-Active Regions of the Hepatitis C Virus E1 and E2 Envelope Glycoproteins

A. J. Pérez-Berná¹, J Guillén¹, M. R. Moreno¹,
A. Bernabeu¹ and J. Villalaín¹

¹Instituto de Biología Molecular y Celular, Universidad “Miguel
Hernández”, Elche-Alicante, Spain

Biochemistry 2006, 45, 3763-3776



The Membrane-Active Regions of the Hepatitis C Virus E1 and E2 Envelope Glycoproteins[†]

Ana J. Pérez-Berná, Miguel R. Moreno, Jaime Guillén, Angela Bernabeu, and José Villalain*

Instituto de Biología Molecular y Celular, Universidad Miguel Hernández, E-03202 Elche-Alicante, Spain

Received November 23, 2005; Revised Manuscript Received January 11, 2006

ABSTRACT: We have identified the membrane-active regions of the full sequences of the HCV E1 and E2 envelope glycoproteins by performing an exhaustive study of membrane leakage, hemifusion, and fusion induced by 18-mer peptide libraries on model membranes having different phospholipid compositions. The data and their comparison have led us to identify different E1 and E2 membrane-active segments which might be implicated in viral membrane fusion, membrane interaction, and/or protein–protein binding. Moreover, it has permitted us to suggest that the fusion peptide might be located in the E1 glycoprotein and, more specifically, the segment comprised by amino acid residues 265–296. The identification of these membrane-active segments from the E1 and E2 envelope glycoproteins, as well as their membranotropic propensity, supports their direct role in HCV-mediated membrane fusion, sustains the notion that different segments provide the driving force for the merging of the viral and target cell membranes, and defines those segments as attractive targets for further development of new antiviral compounds.

Hepatitis C virus (HCV)¹ is a small, enveloped RNA virus that belongs to the genus *Hepacivirus* in the family Flaviviridae (which also comprises the genera *Flavivirus* and *Pestivirus*) and is the leading cause of acute and chronic liver disease in humans, including chronic hepatitis, cirrhosis, and hepatocellular carcinoma (1, 2). There exists no vaccine to prevent HCV infection, and current therapeutic agents such as pegylated interferon and ribavirin, apart from being associated to different adverse effects, have limited success against HCV (3). Therefore, the development of effective treatments is mandatory to control HCV infection.

The HCV genome is a 9.6 kb long single-stranded RNA molecule of positive polarity that is translated into a polyprotein of approximately 3010 amino acids (4), flanked by 5' and 3' untranslated regions (Figure 1). The structural proteins include the core, which forms the viral nucleocapsid, and the envelope glycoproteins E1 (gp35) and E2 (gp70), both of them transmembrane proteins. The structural proteins are separated from the nonstructural proteins by the short

membrane peptide p7, thought to be a viroporin. The HCV genome shows a remarkable sequence variation since more than 90 genotypes distributed into six main types and subtypes have been identified (5, 6). The relationship between HCV sequence variability and liver disease status or resistance to current antivirals is unclear and likely is multifactorial (7). HCV is thought to adopt a classical icosahedral scaffold in which its two envelope glycoproteins, E1 and E2, are anchored to the host-cell-derived double-layer lipid envelope. E1 and E2 are thought to play pivotal roles at different steps of the HCV replicative cycle. There is now strong evidence that they are essential for host-cell entry, binding to receptor(s), and inducing fusion with the host-cell membrane as well as in viral particle assembly (8). These distinct functions imply that the envelope proteins adopt markedly different conformations and that the latter must be controlled tightly to occur at the appropriate phases of the replicative cycle. E1 and E2 are type I transmembrane (TM) glycoproteins, with N-terminal ectodomains and a short C-terminal TM domain. These proteins interact with each other and assemble as noncovalent heterodimers, and their TM play a major role in the E1–E2 heterodimer formation, membrane anchoring, and endoplasmic reticulum retention (9–12). Interestingly, the E2 glycoprotein has two hyper-variable regions (HVR1 and HVR2) which could function as a decoy to help the virus escape the immune system (1). Like other viral envelope proteins involved in host-cell entry, HCV envelope proteins are thought to induce fusion between the viral envelope and a host-cell membrane. The HCV envelope glycoproteins E1 and E2 are thought to be class II fusion proteins because the putative fusion peptide is supposedly localized in an internal sequence linked by antiparallel β -sheets; moreover, proteomic computational analyses suggest that HCV envelope glycoprotein E1 and

[†] This work was supported by Grant BMC2002-00158 (Ministerio de Ciencia y Tecnología, Spain) to J.V. A.J.P.-B. is a recipient of a predoctoral fellowship from G.V., Spain, and M.R.M. and A.B. are recipients of predoctoral fellowships from MEC, Spain.

* To whom correspondence should be addressed. Tel: +34 966 658 762. Fax: +34 966 658 758. E-mail: jvillalain@umh.es.

¹ Abbreviations: ANTS, 8-aminonaphthalene-1,3,6-trisulfonic acid; CF, 5-carboxyfluorescein; Chol, cholesterol; DPX, *p*-xylenebispyridinium bromide; E1, gp35 HCV envelope glycoprotein; E2, gp70 HCV envelope glycoprotein; HCV, hepatitis C virus; HVR, hypervariable region; LUV, large unilamellar vesicles; NBD-PE, *N*-(7-nitrobenz-2-oxa-1,3-diazol-4-yl)-1,2-dihexadecanoyl-*sn*-glycero-3-phosphoethanolamine; N-RhB-PE, lissamine rhodamine B 1,2-dihexadecanoyl-*sn*-glycero-3-phosphoethanolamine; PA, egg L- α -phosphatidic acid; PC, egg L- α -phosphatidylcholine; PE, egg trans-sterified L- α -phosphatidylethanolamine; PI, bovine brain L- α -phosphatidylinositol; PS, bovine brain L- α -phosphatidylserine; SM, egg sphingomyelin; TM, transmembrane domain.

pestivirus envelope glycoprotein E2 are truncated class II fusion proteins (13).

Although much information has been gathered in recent years, we do not know the processes which give place to membrane fusion. The mechanism by which proteins facilitate the formation of fusion intermediates is a complex process involving several segments of fusion proteins (14, 15). These regions, either directly or indirectly, might interact with biological membranes, contributing to the viral envelope and cell membrane merging. The existence of a quasi-species population appears to hamper the development of vaccines against HCV and favor the perpetuation of the virus in the organism. It is well-known that highly variable infectious agents can induce persistent infections, probably through generation of escape mutants (16), so that HCV infection evolves to chronicity in the majority of infected patients (17). The inability of the immune system to eliminate this virus has been ascribed to lack of immune recognition, insufficient CD4⁺ T cell help, induction of unresponsiveness in HCV-specific T cells, immune deviation, and activation of incomplete immune cell functions (18, 19). There are still many questions to be answered regarding the E1 and E2 mode of action in accelerating membrane fusion, and moreover, HCV membrane entry is an attractive target for anti-HCV therapy. To investigate the structural basis of HCV membrane fusion and identify new targets for searching new fusion inhibitors, we have carried the analysis of the different regions of HCV E1 and E2 envelope glycoproteins which might interact with phospholipid membranes using an approach similar to that used for studying HIV gp41 and SARS-CoV S proteins (20, 21), i.e., the identification of membrane-active regions of HCV E1 and E2 envelope glycoproteins by determining the effect on membrane integrity, hemifusion, and fusion of 18-mer E1 and E2 glycoprotein-derived peptide libraries. By monitoring the effect of these peptide libraries on membrane integrity, we have identified different regions on the HCV E1 and E2 envelope glycoproteins with membrane-interacting capabilities, suggest the possible location of the fusion domain plus other zones which might be implicated in oligomerization (protein-protein binding), and therefore might help in the understanding of the molecular mechanism of membrane merging as well as making possible the future development of HCV entry inhibitors which may lead to new vaccine strategies.

MATERIALS AND METHODS

Materials and Reagents. Egg L- α -phosphatidylcholine (PC), egg sphingomyelin (SM), egg trans-sterified L- α -phosphatidylethanolamine (PE), egg L- α -phosphatidic acid (PA), bovine brain L- α -phosphatidylserine (PS), bovine brain L- α -phosphatidylinositol (PI), liver lipid extract (a 2:1 chloroform:methanol extract of liver tissue), and cholesterol (Chol) were obtained from Avanti Polar Lipids (Alabaster, AL). 5-Carboxyfluorescein (CF) (>95% by HPLC), calcein, and sodium dithionite were from Sigma-Aldrich (Madrid, Spain). Lissamine rhodamine B 1,2-dihexadecanoyl-*sn*-glycero-3-phosphoethanolamine (N-RhB-PE), *N*-(7-nitrobenz-2-oxa-1,3-diazol-4-yl)-1,2-dihexadecanoyl-*sn*-glycero-3-phosphoethanolamine (NBD-PE), 8-aminonaphthalene-1,3,6-trisulfonic acid (ANTS), and *p*-xylenebispyridinium bromide (DPX) were obtained from Molecular Probes Inc. (Eugene,

OR). Three sets of 18-mer peptides derived from the E1 envelope glycoprotein (26 peptides) and from the E2 envelope glycoprotein (52 peptides) from hepatitis C virus strains 1B4J and 1AH77 having 11 amino acid overlap between sequential peptides were obtained through the NIH AIDS Research and Reference Reagent Program (Division of AIDS, NIAID, NIH, Bethesda, MD). All other reagents used were of analytical grade from Merck (Darmstadt, Germany). Water was deionized, twice distilled, and passed through Milli-Q equipment (Millipore Ibérica, Madrid, Spain) to a resistivity better than 18 M Ω cm.

Sample Preparation. Aliquots containing the appropriate amount of lipid in chloroform/methanol (2:1 v/v) were placed in a test tube, the solvents were removed by evaporation under a stream of O₂-free nitrogen, and finally traces of solvents were eliminated under vacuum in the dark for more than 3 h. For assays of vesicle leakage at pH 7.4, buffer containing 10 mM Tris-HCl, 20 mM NaCl, 40 mM CF, and 0.1 mM EDTA, pH 7.4, was used (20), whereas for assays of vesicle leakage at pH 5.4, buffer containing 20 mM citrate, 20 mM NaCl, and 40 mM calcein, pH 5.4, was used (22). To obtain multilamellar vesicles, 1 mL of buffer was added to the dry phospholipid mixture and vortexed at room temperature until a clear suspension was obtained. Large unilamellar vesicles (LUV) with a mean diameter of 90 nm were prepared from multilamellar vesicles by the extrusion method (20) using polycarbonate filters with a pore size of 0.1 μ m (Nuclepore Corp., Cambridge, CA). Breakdown of the vesicle membrane leads to content leakage, i.e., CF or calcein fluorescence. Nonencapsulated CF or calcein was separated from the vesicle suspension through a Sephadex G-75 filtration column (Pharmacia, Uppsala, Sweden) eluted with buffer containing either 10 mM Tris-HCl, 100 mM NaCl, and 0.1 mM EDTA, pH 7.4, or 20 mM citrate, 100 mM NaCl, and 0.1 mM EDTA, pH 5.4.

For assays of lipid mixing, 1 mL of buffer (10 mM Hepes, 100 mM NaCl, pH 7.4) was added to the dry phospholipid mixture (containing either 0.6 mol % NBD-PE and N-RhB-PE or 0.12 mol % NBD-PE and N-RhB-PE, or no probes), and multilamellar vesicles were obtained by vortexing at room temperature. Large unilamellar vesicles (LUV) were prepared from multilamellar vesicles by the extrusion method as above, using polycarbonate filters with a pore size of 0.2 μ m (Nuclepore Corp., Cambridge, CA). The use of 0.2 μ m pore-size filters gives place to larger liposomes and henceforth greater fluorescence intensity per surface unit. For assays of inner monolayer lipid mixing, the sample preparation was similar to lipid mixing, but sodium dithionite was added to preformed LUVs labeled with NBD-PE and N-RhB-PE at a final concentration of 100 mM. After 1 h incubation in ice, the dithionite was removed from the liposomes by size exclusion chromatography (23). For assays of vesicle fusion using the ANTS/DPX method (21), 1 mL of buffer (5 mM Hepes, pH 7.4, and either 40 mM NaCl and 25 mM ANTS or 40 mM NaCl and 90 mM DPX or 20 mM NaCl plus 12.5 mM ANTS and 45 mM DPX) was added to the dry phospholipid mixture, and multilamellar vesicles were obtained by vortexing at room temperature. Large unilamellar vesicles (LUV) were prepared from multilamellar vesicles by the extrusion method using polycarbonate filters with a pore size of 0.1 μ m (Nuclepore Corp., Cambridge, CA). Nonencapsulated ANTS and DPX were separated from the

vesicle suspension through a Sephadex G-75 filtration column (Pharmacia, Uppsala, Sweden) eluted with buffer containing 5 mM Hepes and 100 mM NaCl, pH 7.4.

All peptides were dissolved in buffer, but only those peptides which presented solubility problems were dissolved in 5% DMSO. In all cases, no aggregation was visible after DMSO addition. The phospholipid concentration was measured by methods described previously (24).

Membrane Leakage Measurement. Leakage of intraliposomal CF or calcein was assayed by treating the probe-loaded liposomes (final lipid concentration, 0.125 mM) with the appropriate amounts of peptide on microtiter plates stabilized at 25 °C using a microplate reader (FLUOstar, BMG Labtech, Germany), each well containing a final volume of 170 μ L. The medium in the microtiter plates was continuously stirred to allow the rapid mixing of peptide and vesicles. Leakage was measured at an approximate peptide-to-lipid molar ratio of 1:15. Changes in fluorescence intensity were recorded with excitation and emission wavelengths set at 492 and 517 nm, respectively. One hundred percent release was achieved by adding Triton X-100 to a final concentration of 0.5% (w/w) to the microtiter plates. Fluorescence measurements were made initially with probe-loaded liposomes and afterward by adding peptide solution and finally adding Triton X-100 to obtain 100% leakage. Leakage was quantified on a percentage basis according to the equation

$$\% \text{ release} = \frac{F_f - F_0}{F_{100} - F_0} \times 100$$

F_f being the equilibrium value of fluorescence after peptide addition, F_0 the initial fluorescence of the vesicle suspension, and F_{100} the fluorescence value after addition of Triton X-100.

Hemifusion (Outer Monolayer Phospholipid-Mixing) Measurement. Peptide-induced vesicle lipid mixing (hemifusion) was measured by resonance energy transfer (25). This assay is based on the decrease in resonance energy transfer between two probes (NBD-PE and N-RhB-PE) when the lipids of the probe-containing vesicles are allowed to mix with lipids from vesicles lacking the probes. The concentration of each of the fluorescent probes within the liposome membrane was 0.6 mol %. Liposomes were prepared as described above. Labeled and unlabeled vesicles in a proportion 1:4 were placed in a 5 mm \times 5 mm fluorescence cuvette at a final lipid concentration of 0.1 mM in a final volume of 400 μ L, stabilized at 25 °C under constant stirring. The fluorescence was measured using a Varian Cary Eclipse spectrofluorometer, using 467 and 530 nm for excitation and emission, respectively. Excitation and emission slits were set at 10 nm. Since labeled and unlabeled vesicles were mixed in a proportion of 1 to 4, respectively, 100% phospholipid mixing was estimated with a liposome preparation in which the membrane concentration of each probe was 0.12%. Phospholipid mixing was quantified on a percentage basis according to the equation

$$\% \text{ phospholipid mixing} = \frac{F_f - F_0}{F_{100} - F_0} \times 100$$

F_f being the value of fluorescence obtained 15 min after peptide addition to a liposome mixture containing liposomes

having 0.6% of each probe plus liposomes without any fluorescent probe, F_0 the initial fluorescence of the vesicles, and F_{100} is the fluorescence value of the liposomes containing 0.12% of each probe.

Membrane Fusion Measurements. Fusion of membrane vesicles was assayed using two methods, the ANTS/DPX fusion assay (21) and the dithionite fusion assay (23). For the ANTS/DPX fusion assay, LUVs containing 25 mM ANTS were mixed with LUVs containing 90 mM DPX in a 1:1 (mol/mol) portion. LUVs were placed in a 10 mm \times 10 mm fluorescence cuvette at a final lipid concentration of 0.1 mM in a final volume of 1 mL, stabilized at 25 °C under constant stirring. The fluorescence was measured using a Varian Cary Eclipse spectrofluorometer, using 353 and 520 nm for excitation and emission, respectively. Excitation and emission slits were set at 10 nm. Membrane fusion was quantified on a percentage basis according to the equation

$$\% \text{ fusion} = 100 - \left(\frac{F_f - F_0}{F_{100} - F_0} \times 100 \right)$$

F_f being the value of fluorescence obtained 15 min after peptide addition to a mixture of LUVs containing 25 mM ANTS plus LUVs containing 90 mM DPX, F_0 the initial fluorescence of the vesicles, and F_{100} is the fluorescence value of an independent LUV preparation in which the internal probe concentration was 12.5 mM ANTS and 45 mM DPX. Peptide-induced phospholipid mixing of the inner monolayer was measured by a modification of the hemifusion assay (23). LUVs were treated with sodium dithionite to completely reduce the NBD-labeled phospholipid located at the outer monolayer of the membrane. The final concentration of sodium dithionite was 100 mM (from a stock solution of 1 M dithionite in 1 M Tris-HCl, pH 10.0), and the mixture was incubated for approximately 1 h on ice in the dark. Sodium dithionite was then removed by size exclusion chromatography through a Sephadex G-75 filtration column (Pharmacia, Uppsala, Sweden) eluted with buffer containing 10 mM Tris-HCl, 100 mM NaCl, and 1 mM EDTA, pH 7.4. The proportion of labeled and unlabeled vesicles, lipid concentration, and other experimental and measurement conditions were the same as indicated above.

Hydrophobic Moments, Hydrophobicity, and Interfaciality. The scale for calculating hydrophobic moments was taken from Engelman et al. (26). Hydrophobicity and interfacial values, i.e., whole residue scales for the transfer of an amino acid of an unfolded chain into the membrane hydrocarbon palisade and the membrane interface, respectively, have been obtained from http://blanco.biomol.uci.edu/hydrophobicity_scales.html (27, 28). To detect membrane partitioning and/or membrane interacting surfaces along the whole E1 and E2 envelope glycoproteins, two-dimensional plots of the hydrophobic moments, hydrophobicity, and interfaciality have been obtained, taking into consideration the arrangement of the amino acids in the space and assuming an α -helical structure (for a detailed explanation of how to obtain the two-dimensional plots, see ref 20). Positive values represent positive bilayer-to-water transfer free energy values, and therefore, the higher the value, the greater the probability to interact with the membrane surface and/or hydrophobic core.

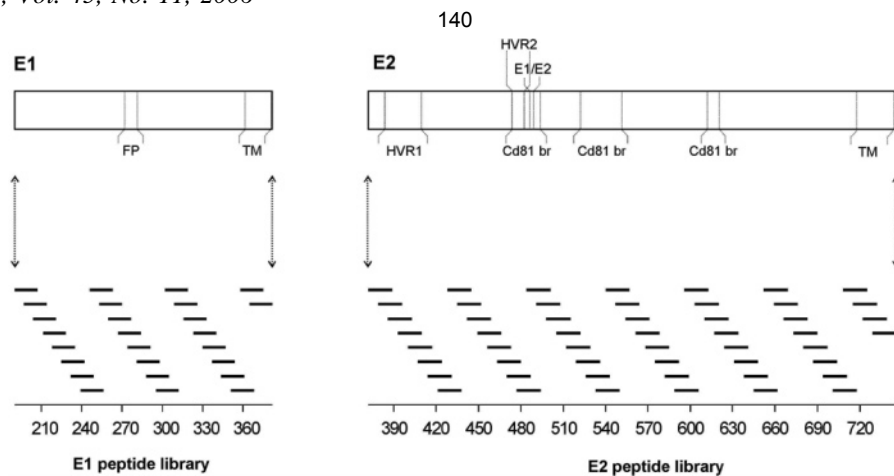


FIGURE 1: Scheme of the structure of the HCV E1 and E2 envelope glycoproteins according to literature consensus. The important supposed functional regions are highlighted, i.e., the putative fusion domain (FP), the transmembrane domain (TM), the hypervariable regions (HVR), the CD81 binding regions (CD81br), and the E1/E2 interaction domain (E1/E2). The sequence and relative location of the 18-mer peptides derived from HCV envelope glycoproteins E1 (26 peptides) and E2 (52 peptides) are shown with respect to the sequence of both proteins. Maximum overlap between adjacent peptides is 11 amino acids.

RESULTS

The peptide libraries we have used in this study and their correlation with the HCV E1 and E2 envelope glycoprotein sequences are shown in Figure 1, where it can be observed that the 18-mer peptide libraries include the whole sequence of both glycoproteins. Since two and three consecutive peptides in the library have an overlap of 11 and 4 amino acids, respectively, it seems reasonable to think on peptide-defined regions as we will present below.

Membranotropic Surfaces in E1 and E2. The E1 envelope glycoprotein is thought to be responsible for the membrane fusion process whereas the E2 envelope glycoprotein is thought to mediate the binding to the host cell, although other roles could not be ruled out (29, 30). Several hydrophobic patches have been identified in both E1 and E2 proteins which might be important, not only for modulating membrane binding and interaction but also for protein–protein interaction (29, 31, 32). To detect surfaces along the E1 and E2 envelope glycoprotein sequences which might be identified as membrane-partitioning and/or membrane-interacting zones which might be related to either tertiary or quaternary structures or both, we have plotted the average surface hydrophobic moment, hydrophobicity, and interfaciality versus the amino acid sequence of the E1 and E2 glycoprotein sequences of HCV_1B4J (the data obtained for the HCV_1AH77 strain are nearly identical), supposing it adopts an α -helical structure along the whole sequence (Figure 2; see ref 20). Although the E1 and E2 HCV glycoproteins are supposed to be class II membrane fusion proteins and therefore their α -helix content should not be as high as that of class I membrane fusion proteins, it gives us a depiction of the potential surface zones that could possibly be implicated in membranotropic action (20). As observed in Figure 2, the existence of different regions with large hydrophobic moment values along both HCV E1 and E2 envelope glycoproteins is readily evident. These sequences should show comparable capability to partition and/or interact with membranes and should be biologically functional in their roles. In addition, there are other regions which show patches of large hydrophobic moment, hydrophobicity, and/or interfaciality values. These patches of positive hydropho-

bicity and interfaciality along the surface of the protein could favor the interaction with other similar patches along these or other proteins as well as with the surface of the membrane. By observing these data, it would be possible to detect three and six distinct highly positive regions in E1 and E2, respectively (see Figure 2). In the case of E1, these regions would be comprised by amino acid residues 260–294, 316–336, and 344–382, whereas for E2 these regions would be comprised by amino acid residues 385–404, 436–446, 485–509, 548–572, 667–691, and 702–745. These data would suggest that these regions could show a tendency to partition into membranes and/or interact with the membrane surface; however, it should not be ruled out that some areas corresponding to the HCV E1 and E2 envelope glycoproteins could also be responsible for the interaction with other proteins or even between both of them as has been suggested previously (32). The generation of hydrophobic-rich surfaces along the structure of the HCV E1 and E2 envelope glycoproteins emphasizes that the actual distribution of hydrophobicity and interfaciality, i.e., structure-related factors, along E1 and E2 would affect the biological function of these sequences.

Membrane Rupture. In the first instance, we have studied the effect of the 18-mer peptide libraries derived from the HCV_1B4J E1 and E2 envelope glycoproteins and two different pH values, 7.4 and 5.4, on membrane rupture, i.e., leakage, for six different liposome compositions (Figures 3 and 4); the lipidic composition of the model membranes has been PC/Chol at a molar ratio of 5:1, PC/SM at a molar ratio of 5:1, PC/SM/Chol at a molar ratio of 5:1:1, PC/SM/Chol at a molar ratio of 26:9:15, a synthetic lipid mixture resembling the hepatocyte plasma membrane consisting of PC/PS/PI/SM/Chol at a molar ratio of 51:2.4:5.3:7.48:33.42 (33), and a lipid extract of liver membranes (containing 42% PC, 22% PE, 7% Chol, 8% PI, 1% LPC, and 21% neutral lipids).

When the 18-mer peptides from the E1 library were assayed on PC/Chol liposomes at pH 7.4, some peptides exerted an important leakage effect (Figure 3A, upper panel). The most remarkable effects were observed for peptides 14 and 18, which produced leakage values of about 20–25%. At pH 5.4 (Figure 3A, lower panel), only peptides 18 and

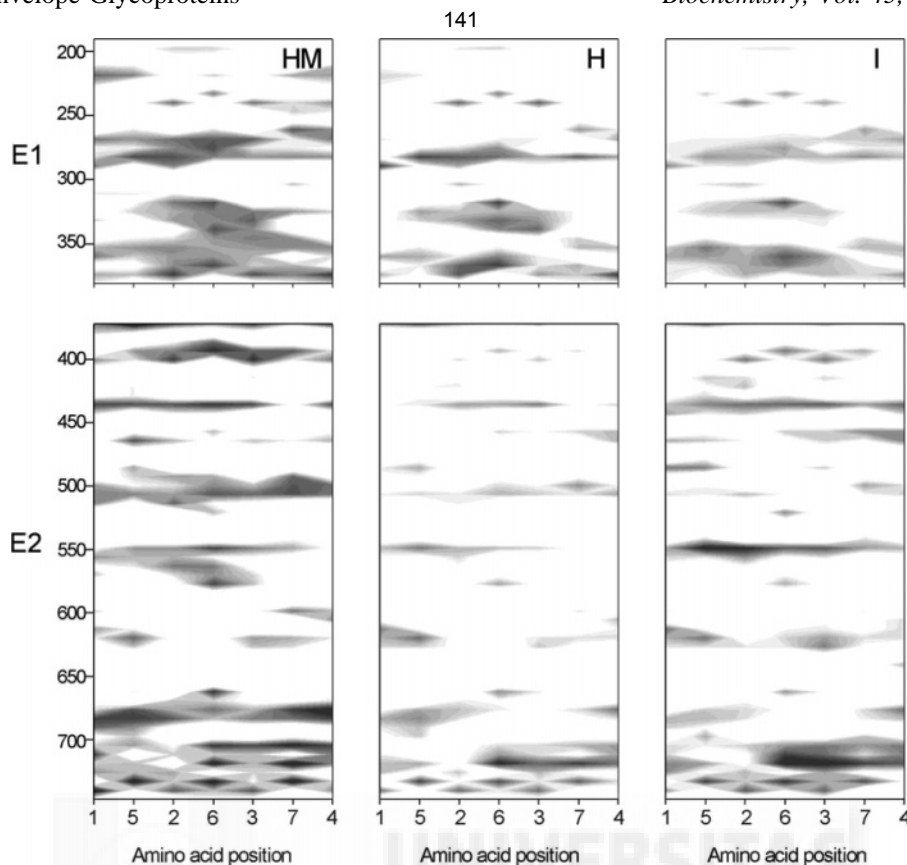


FIGURE 2: Hydrophobic moment, hydrophobicity, and interfaciality distribution of HCV E1 and E2 envelope glycoproteins assuming they form an α -helical wheel. The hydrophobic moment, hydrophobicity, and interfaciality plots show only positive bilayer-to-water transfer free energy values. The residue numbers are indicated at the left, whereas column numbers define amino acid positions (see ref 28).

24 showed relevant leakage values (about 15–23%). When liposomes composed of PC/SM at pH 7.4 were tested, the leakage pattern was different (Figure 3B, upper panel), since peptide 13 was the only one which showed a significant leakage effect (about 60%). When these liposomes were tested at pH 5.4 (Figure 3B, lower panel), peptides 18 and 19 were the ones that showed major leakage values (about 25–30%). The same peptides which, at pH 7.4, showed major effects on PC/Chol liposomes had a similar effect on PC/SM/Chol liposomes at a molar ratio of 5:1:1, but their leakage values were in general slightly higher (Figure 3C, upper panel). These were peptides 2, 14, 18, and 24 (leakage values of about 25–30%). At pH 5.4, peptides 14, 18 (about 60–65% leakage), and 19 (about 45% leakage) presented major values compared to the other ones (Figure 3C, lower panel). When liposomes composed of PC/SM/Chol at a molar ratio of 26:9:15 at pH 7.4 were assayed (Figure 3D, upper panel), peptides 14, 15, 21, 25, and 26 presented leakage values of about 10–15%. At pH 5.4 a similar pattern was found (Figure 3D, lower panel), since peptide 18 elicited a leakage value of about 20%, whereas peptides 2, 14, 19, 20, 24, and 25 showed leakage values of about 10–15%. When liposomes resembling the hepatocyte plasma membrane were assayed at pH 7.4, a completely different pattern was obtained (Figure 3E, upper panel), since peptide 25 was the only one which showed a major leakage value (about 20%). At pH 5.4 (Figure 3E, lower panel) peptides 2, 8, and 25 showed relatively higher leakage values (about 10–13%), but there was an ample region ranging from peptide 1 to peptide 11 which showed leakage values of about 5–7%. For liposomes composed of a lipid extract of liver mem-

branes at pH 7.4 (Figure 3F, upper panel), two peptides, 14 and 18, showed significant leakage values (about 65–70%), but peptides 19, 20, and 24–26 also showed major leakage values (about 15–30%). At pH 5.4 (Figure 3F, lower panel) peptides 18, 20, and 24 showed leakage values of about 30–40% whereas peptides 11, 14, 25, and 26 showed leakage values of about 20–22%.

Similarly to what was found above for E1, when the peptide library from E2 was assayed on PC/Chol liposomes at pH 7.4, some peptides induced a major effect on leakage but others did not (Figure 4A, upper panel). In this case, peptides 10, 35, and 36 showed major leakage values (about 60–80%), whereas peptides 5, 16, 17, 34, 36, 37, and 49 induced lower but important leakage values (about 15–30%). At pH 5.4, lower absolute leakage values were found, but the pattern was similar to what was found at pH 7.4 (Figure 4A, lower panel). When liposomes composed of PC/SM at pH 7.4 were used, the pattern was very similar to that found for PC/Chol liposomes (Figure 3B, upper panel), since peptides 10 and 35 were the ones which produced the major leakage values (about 40–50%). Peptides 5, 36, and 49 induced lower leakage values (about 20–25%) but significant when compared to the other ones (Figure 3B, upper panel). At pH 5.4, the absolute leakage values were higher than those found at pH 7.4, but the leakage pattern was also very similar (Figure 4B, lower panel). When leakage was assayed on PC/SM/Chol liposomes at molar ratios of 5:1:1 and 26:9:15 and pH 7.4, it was interesting to find a pattern similar to what was described above (see Figure 4C,D, upper panels). In this case, peptides 10 and 35 were again the ones which induced the higher leakage values, whereas peptides 5, 16, 17, 25,

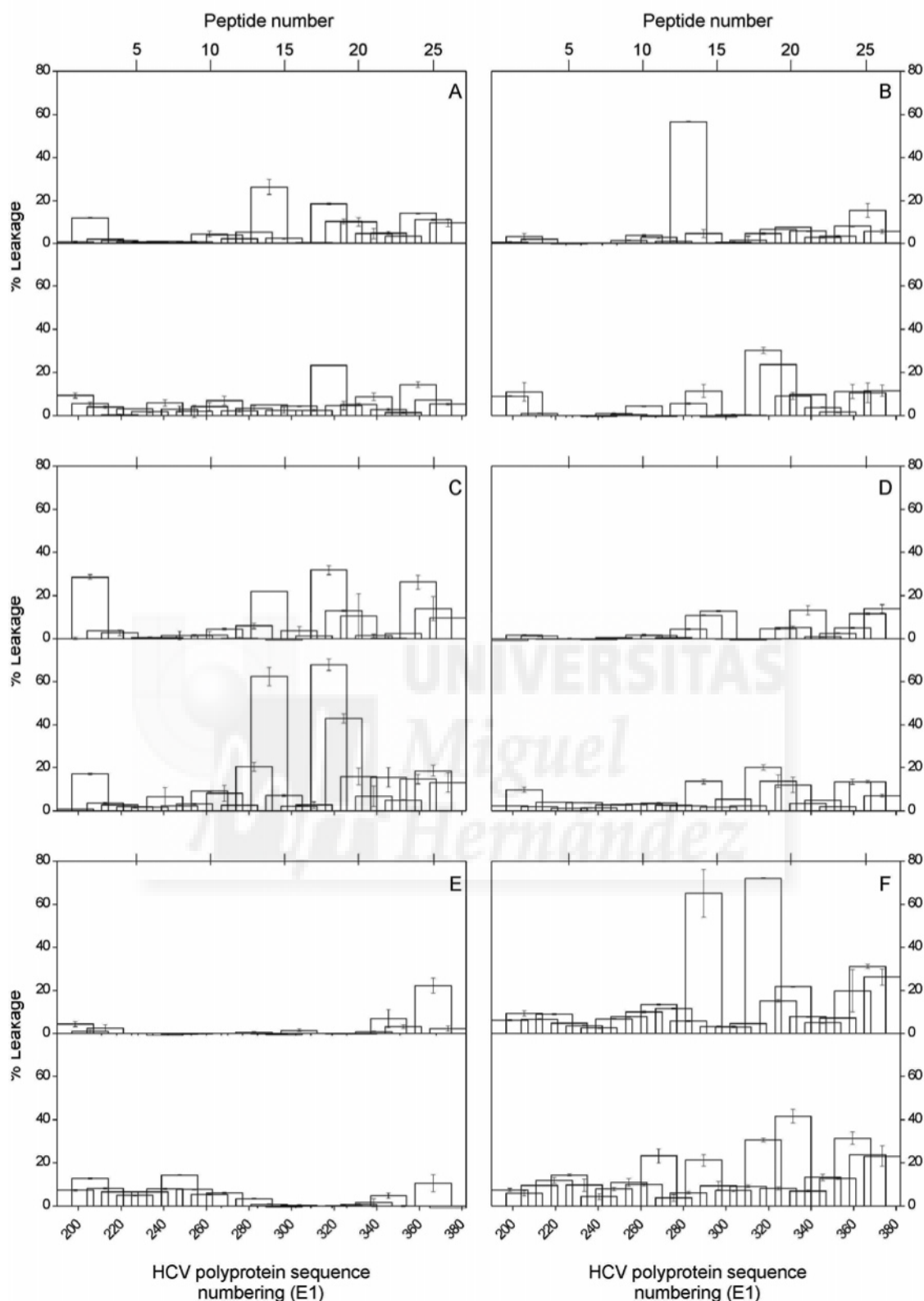


FIGURE 3: Effect of the 18-mer peptides derived from the E1 envelope glycoprotein of HCV_1B4J on the release of LUV contents for different lipid compositions and two different pH values, 7.4 and 5.4 (upper and lower panels, respectively). Leakage data for LUV composed of (A) PC/Chol at a phospholipid molar ratio of 5:1, (B) PC/SM at a phospholipid molar ratio of 5:1, (C) PC/SM/Chol at a phospholipid molar ratio of 5:1:1, (D) PC/SM/Chol at a phospholipid molar ratio of 26:9:15, (E) synthetic hepatocyte plasma membrane, and (F) lipid extract of liver membranes. Vertical bars indicate standard deviations of the mean of triplicate samples.

34, and 35 induced lower but important leakage values. It should be noted that peptide 49 induced a major leakage effect on liposomes composed of PC/SM/Chol at a molar ratio of 26:9:15 whereas it did not show any effect on

liposomes composed of PC/SM/Chol at a molar ratio of 5:1:1 (Figure 4C,D, upper panels). At pH 5.4, a similar pattern was again found, since peptides 10 and 35 were the ones which exerted the higher leakage effect, although peptides

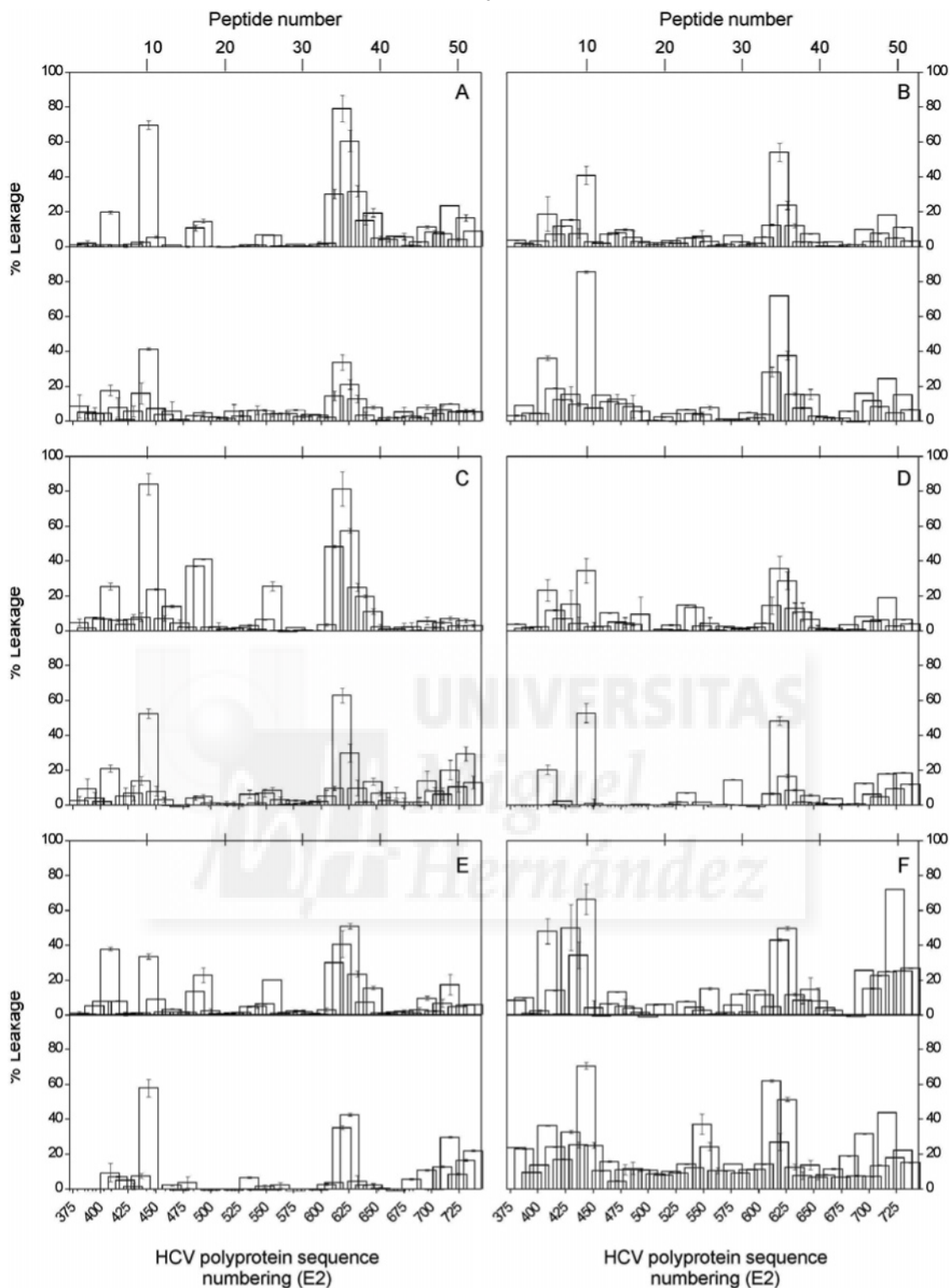


FIGURE 4: Effect of the 18-mer peptides derived from the E2 envelope glycoprotein of HCV_1B4J on the release of LUV contents for different lipid compositions and two different pH values, 7.4 and 5.4 (upper and lower panels, respectively). Leakage data for LUV composed of (A) PC/Chol at a phospholipid molar ratio of 5:1, (B) PC/SM at a phospholipid molar ratio of 5:1, (C) PC/SM/Chol at a phospholipid molar ratio of 5:1:1, (D) PC/SM/Chol at a phospholipid molar ratio of 26:9:15, (E) synthetic hepatocyte plasma membrane, and (F) liver extract of liver membranes. Vertical bars indicate standard deviations of the mean of triplicate samples.

5, 36, and 49–51 induced also relatively larger leakage values (Figure 4C,D, lower panels). It is interesting to note that peptides 16 and 17 did not show any effect at pH 5.4 but a major one at pH 7.4. When liposomes resembling the hepatocyte plasma membrane were assayed at pH 7.4, peptides 5, 10, 35, and 36 were the ones which induced a major leakage value (Figure 4E, upper panel).

Other peptides which presented relevant leakage values were peptides 16, 17, 25, and 49. At pH 5.4 a similar pattern was found, except that no leakage activity was found between peptides 10 and 35 (Figure 4E, lower panel). The pattern which was obtained for liposomes composed of a lipid extract of liver membranes at pH 7.4 and 5.4 was indeed similar to those described above, since peptide groups 5–10, 34–36,

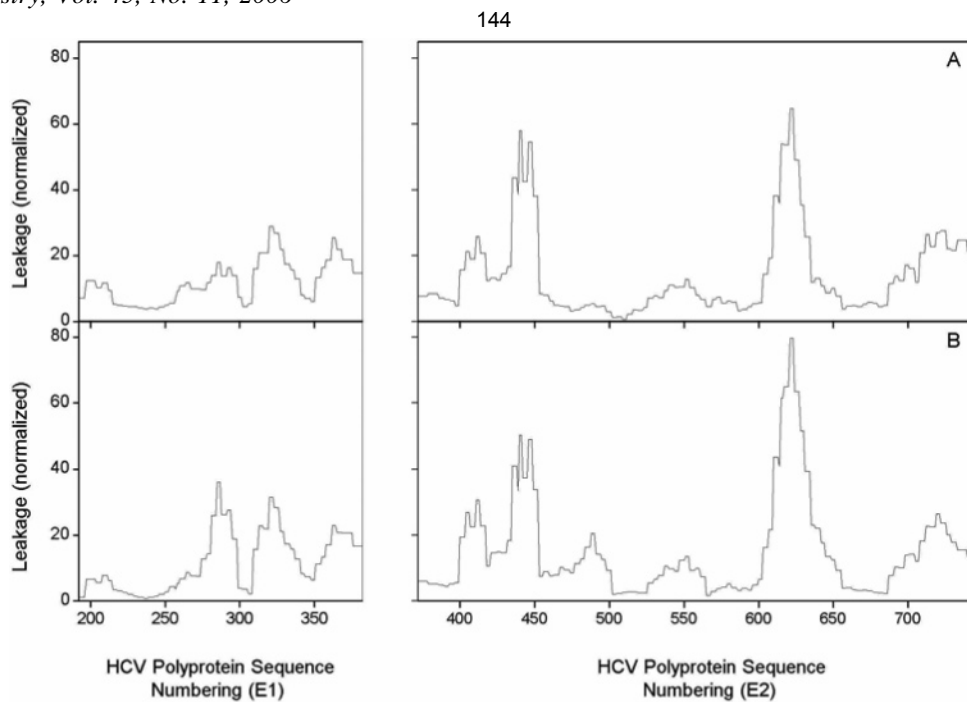


FIGURE 5: Summary of the normalized (percentage) experimental membrane rupture data (leakage) corresponding to the 18-mer peptide libraries derived from the HCV_1B4J envelope glycoproteins E1 and E2 at (A) pH 5.4 and (B) pH 7.4 for all model membranes studied.

49, and 50 were the ones which induced major leakage values (Figure 4F, upper and lower panels).

As was noted above, it seems reasonable to think on the combined effect of peptide groups or segments rather than on the effect of isolated peptides. In this context, leakage values shown in Figures 3 and 4 would define different protein segments with high relative leakage activity for both envelope glycoproteins E1 and E2. In Figure 5, we show the normalized experimental leakage data (the summation of all of the percentages of leakage for all model membranes) corresponding to the E1 and E2 derived 18-mer peptide libraries; as shown in the figure, defined leakage zones are clearly observed. For E1 and pH values 7.4 and 5.4, there are three zones having consistent relatively similar high leakage values which would approximately correspond to amino acid segments 274–298, 309–343, and 351–382. In a similar way, five zones are observed for E2 and pH 7.4, corresponding approximately to amino acid segments 394–452, 457–502, 531–565, 604–656, and 688–739. As was commented above, it is interesting to note that all of these segments show leakage at both pH values except segment 457–502 (Figure 5).

Hemifusion and Fusion. Perturbation of membranes is not sufficient to complete the process of viral and cellular membrane fusion, since it is also necessary for the merge of the monolayers and the stalk formation, according to the stalk model for membrane fusion (34). However, there is not a clear quantitative criterion to characterize fusion peptides using membrane destabilization (14). Therefore, we have also studied the effect of the peptide libraries derived from the E1 and E2 envelope glycoproteins on both membrane hemifusion and fusion using liposomes of different compositions (Figures 6 and 7). As has been shown previously (35), the energetic barrier for hemifusion and fusion is larger than for leakage (pore formation), so that peptides which might show hemifusion, and/or fusion effects in general induce leakage but peptides which induce leakage might not provoke

hemifusion and/or fusion. At the same time, leakage values, as measured here, are usually higher than hemifusion and fusion ones. Because of that, we have used two E1 and E2 envelope glycoprotein 18-mer derived libraries from two different strains of HCV, namely, HCV_1B4J and HCV_1AH77, to define more precisely the membrane-active regions of both E1 and E2 envelope glycoproteins which elicit hemifusion and fusion effects. Moreover, these studies have been made at pH 7.4 since there were no significant differences on leakage at the two pHs studied (see above).

The hemifusion pattern which was found when the E1 libraries were assayed on PC/SM/Chol liposomes defined clearly the effect induced by peptide 13 (hemifusion values of about 15–20%) and to a lesser extent peptide 14 (Figure 6A). When liposomes composed of PC/PS/Chol were used, a dramatic effect on hemifusion was observed for peptide 14, since 100% hemifusion was attained for the HCV_1AH77 strain whereas about 55% was observed for the HCV_1B4J one (Figure 6B). Similarly high hemifusion values were found when PC/PI/Chol liposomes were used (Figure 6C), since about 80% hemifusion values were found for peptides 13 (strain HCV_1AH77) and 14 (strain HCV_1B4J). Smaller but significant hemifusion values were found for peptides 18/20 and 25/26 (about 15–20%). Similar results were also found when model membranes composed of a lipid extract of liver membranes were used (Figure 6D). In the case of the HCV_1AH77 strain, peptides 14 and 19 were the ones which elicited significant hemifusion values (about 50–70%), whereas peptide 13 was the one which induced high hemifusion values (about 65%) for the HCV_1B4J strain. When fusion was assayed on liposomes composed of PC/SM/Chol and a lipid extract of liver membranes using both HCV_1AH77 and HCV_1B4J E1 libraries, similar results to those found above were obtained, since peptides 13 and 14 were the ones which induced the higher fusion values (Figure 6E–H).

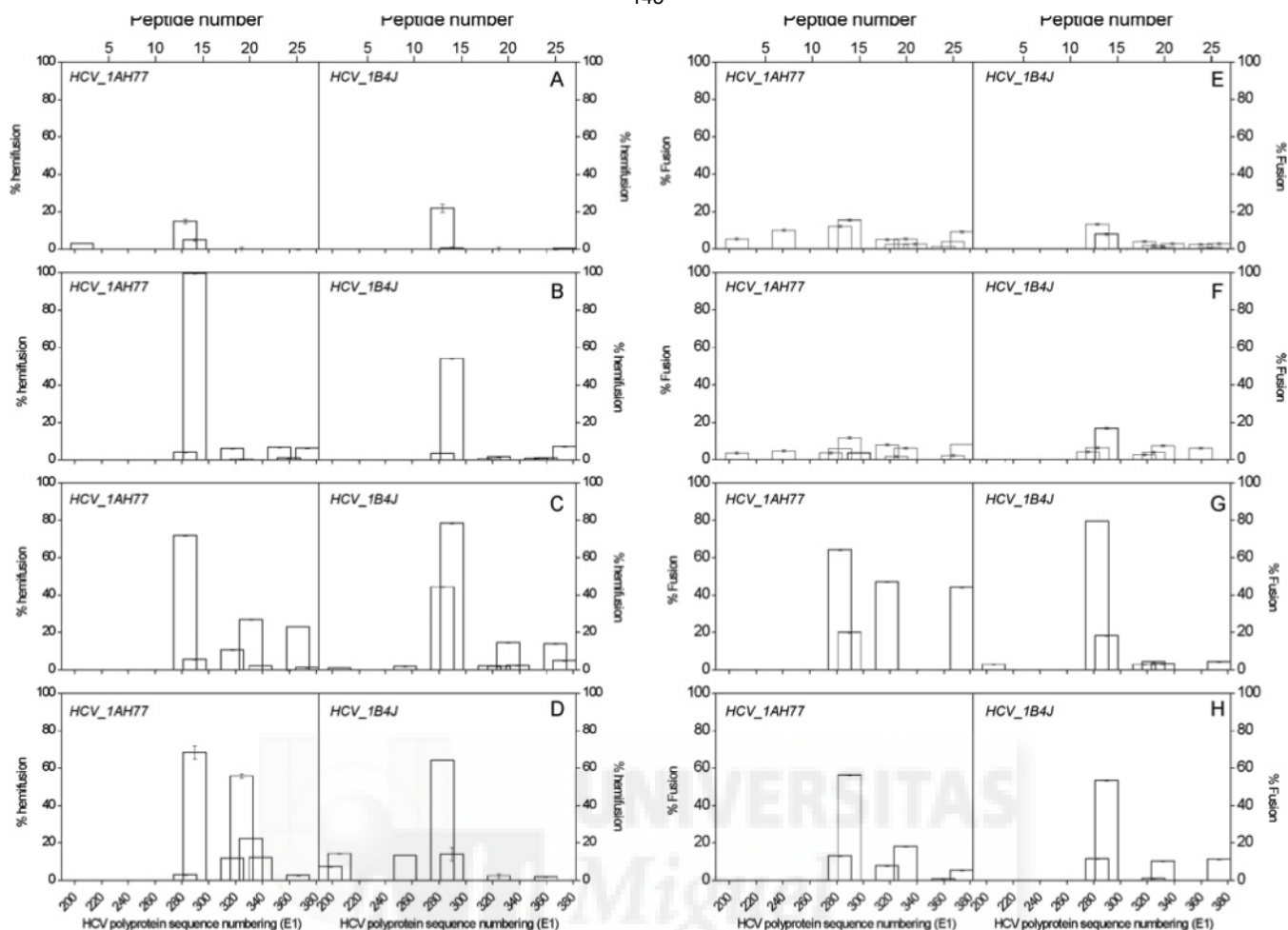


FIGURE 6: Effect of the 18-mer peptides derived from the HCV E1 envelope glycoprotein strains 1AH77 and 1B4J (left and right panels, respectively) on hemifusion (A–D) and fusion (E–H) for LUVs composed of (A, E, G) PC/SM/Chol at a phospholipid molar ratio of 5:1:1, (B) PC/PS/Chol at a phospholipid molar ratio of 5:4:1, (C) PC/PI/Chol at a phospholipid molar ratio of 5:4:1, and (D, F, H) lipid extract of liver membranes. Aqueous content fusion is shown in (E) and (F), whereas inner monolayer fusion is shown in (G) and (H). Note the different vertical scales. Vertical bars indicate standard deviations of the mean of triplicate samples.

Similarly to what was found above, when the envelope glycoprotein E2 derived libraries were assayed on PC/SM/Chol liposomes, a small number of peptides gave place to hemifusion (Figure 7A). In the case of the HCV_1AH77 library, peptide 9 was the one which induced the higher hemifusion value (about 7%) whereas from the HCV_1B4J library it was peptide 52 which induced the highest hemifusion (about 20%). When liposomes composed of PC/PS/Chol were used, peptide 36 from both HCV strains induced a relatively high hemifusion effect (Figure 7B), although peptide 10 from HCV_1B4J also elicited a major hemifusion value (about 30%). Peptide 10 from both strains was also the one which showed an important hemifusion effect (about 45–50%) when liposomes composed of PC/PI/Chol were used (Figure 7C); peptide 35 from HCV_1AH77 elicited also a major hemifusion value (about 30%). The number of peptides which induced hemifusion effects was augmented when liposomes were composed of a lipid extract of liver membranes (Figure 7D). In this case, peptides 6 and 9 (about 35–40%) from the HCV_1AH77 library and peptides 51 and 52 (about 15%) from the HCV_1B4J library were the ones which induced the higher hemifusion effects. When fusion was assayed on liposomes composed of PC/SM/Chol and a lipid extract of liver membranes, there were two main peptide groups which induced the higher relative hemifusion

values (Figure 7E–H). These groups were formed by peptides 6–10 and 35–63, whose fusion values ranged from 10% to 40%.

Following the same reasoning which was followed above, hemifusion and fusion values presented in Figures 6 and 7 would define different protein segments with high relative hemifusion and fusion activities for both envelope glycoproteins E1 and E2. To compare and relate the experimental hemifusion and fusion data with the different membranotropic segments we found by studying the hydrophobicity and interfaciality along the full E1 and E2 sequences (Figure 2), we show in Figure 8A the normalized experimental hemifusion and fusion data corresponding to the E1 and E2 derived 18-mer peptide libraries. It is possible to observe defined hemifusion and fusion zones, similarly to what was found previously for the leakage experiments, matching the segments we found previously. For E1 three zones with high hemifusion and fusion values are found, corresponding to amino acid segments 268–298, 317–339, and 360–382 (Figure 8A), which also match the ones which were detected previously by assaying membrane rupture (see Figure 5). Similarly, five zones are found for E2, which approximately correspond to amino acid segments 419–453, 453–467, 541–558, 611–628, and 713–737 (Figure 8A).

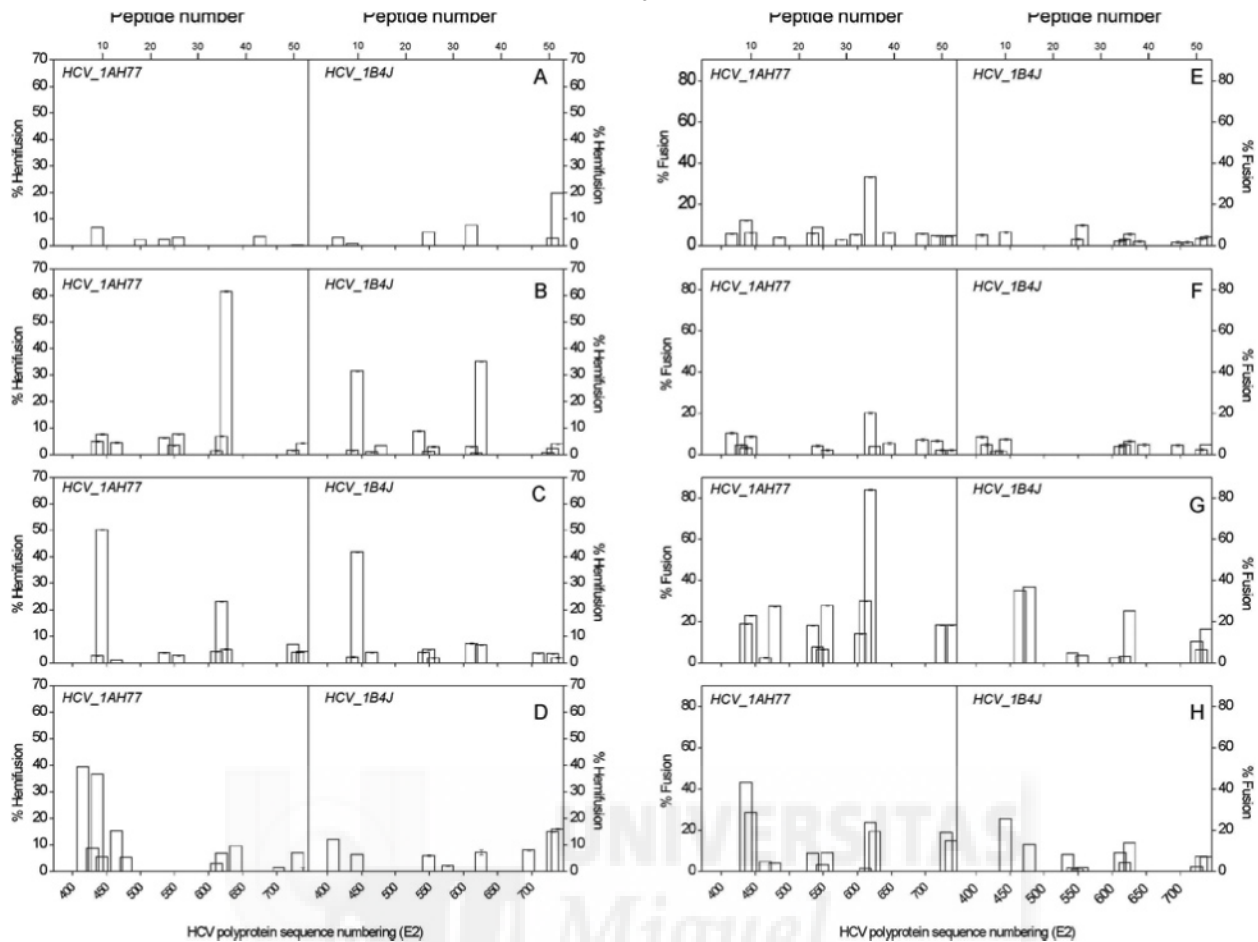


FIGURE 7: Effect of the 18-mer peptides derived from the HCV E2 envelope glycoprotein strains 1AH77 and 1B4J (left and right panels, respectively) on hemifusion (A–D) and fusion (E–H) for LUVs composed of (A, E, G) PC/SM/Chol at a phospholipid molar ratio of 5:1:1, (B) PC/PS/Chol at a phospholipid molar ratio of 5:4:1, (C) PC/PI/Chol at a phospholipid molar ratio of 5:4:1, and (D, F, H) liver extract of liver membranes. Aqueous content fusion is shown in (E) and (F), whereas inner monolayer fusion is shown in (G) and (H). Note the different vertical scales. Vertical bars indicate standard deviations of the mean of triplicate samples.

DISCUSSION

The fusion of viral and cellular membranes, the critical early events in viral infection, are mediated by class I and class II envelope fusion glycoproteins located on the outer surface of the viral membranes (14, 36, 37). Whereas class I membrane fusion proteins possess a fusion peptide at or near the amino terminus, a pair of extended α -helices, and, generally, a cluster of aromatic amino acids proximal to a hydrophobic transmembrane domain, class II fusion proteins possess an internal fusion peptide stabilized by cysteine linkages and different domains comprised mostly of anti-parallel β -sheets (38). Although their three-dimensional structure is different, their function is identical, i.e., fusion between two opposing lipid bilayers. Accumulated evidence suggests that the mechanism of membrane fusion induced by class I and class II membrane fusion proteins is similar and, in addition, requires the concerted action of different membranotropic segments of the implicated proteins (13, 38, 39). It is known that both HCV E1 and E2 envelope glycoproteins are essential for receptor binding, host-cell entry, and membrane fusion, but their specific role(s) in the different processes of the viral life cycle remain(s) uncharacterized (8, 29). The E1/E2 heterodimer is thought to be the functional unit of the HCV spike and low pH would induce its dissociation leading to homooligomerization of the active form of the fusion protein (40). However, there is

some controversy about the identity of the HCV fusion protein, either E1 or E2 or both. It was first proposed that E1 might be a good candidate, because the ectodomain of E1 might contain a putative fusion peptide (residues 265–287) (13, 41); however, structural homology with other fusion proteins suggested that E2 could be the fusion protein (29, 32).

Both E1 and E2 envelope glycoproteins possess different segments with significant properties. For example, it has been proposed that E1 could be capable of adopting a polytopic form, since, apart from containing the C-terminal membrane-spanning domain (residues 331–381), it contains a potential transmembrane one (residues 270–291) (42, 43). This segment has also been suggested to be the fusion peptide (13, 41). E2 comprises a receptor-binding domain which is connected to the transmembrane hydrophobic domain (residues 718–746) via a highly conserved sequence (residues 675–699), which seems to be necessary for heterodimerization with the E1 glycoprotein. E2 carries also regions of extreme hypervariability; while the most variable region, HVR-1, is located within the N-terminal part of E2 (residues 384–411), the HVR-2 region resides in the 476–480 segment (44). Another important E2 segment which determines the correct folding and subunit aggregation is comprised within residues 525–660 (30); different parts of this segment have also been implicated in CD81 binding (32).

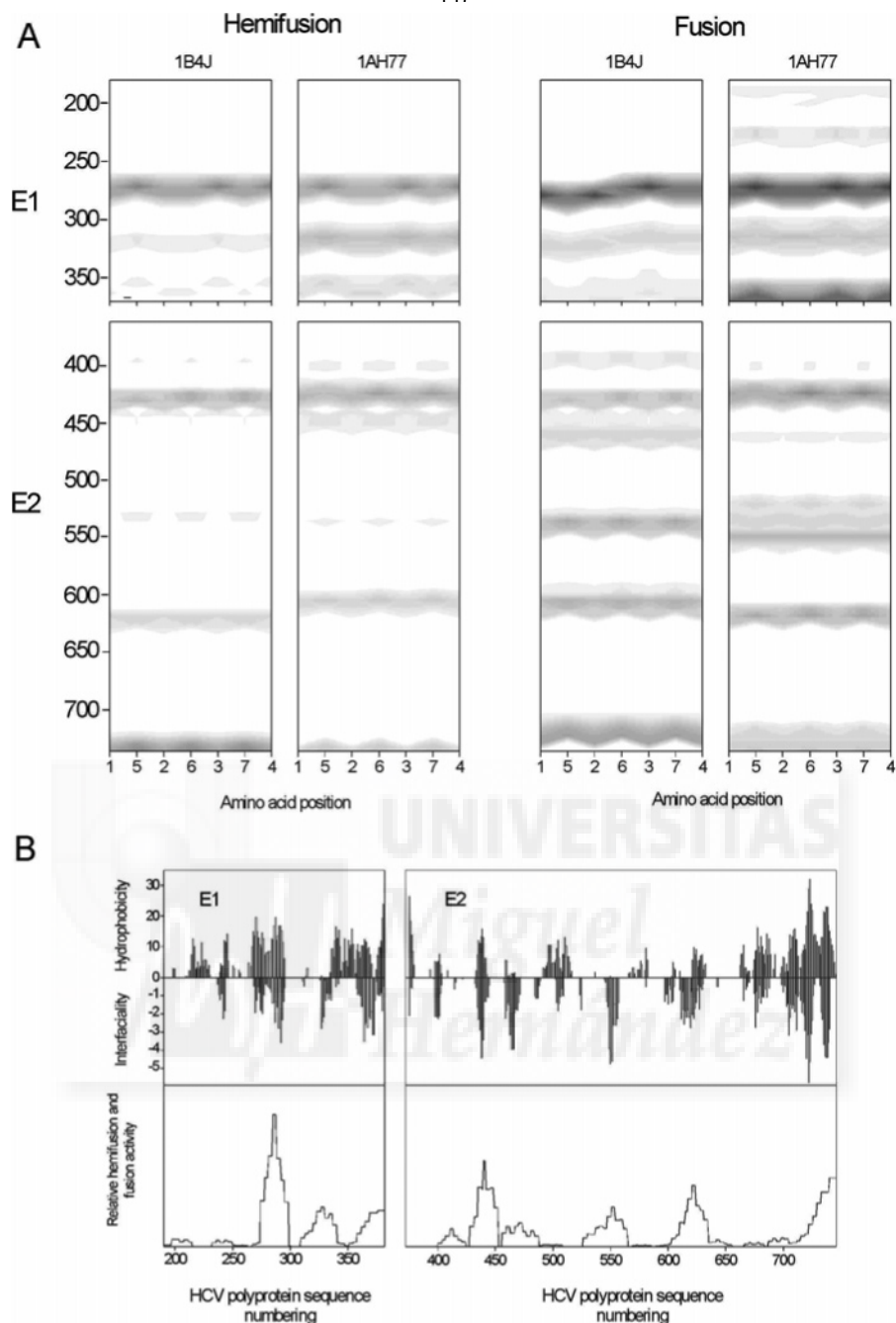


FIGURE 8: (A) Summary of the normalized (percentage) experimental membrane rupture data corresponding to the 18-mer peptide libraries derived from the envelope glycoproteins E1 and E2 corresponding to the HCV_1B4J and HCV_1AH77 strains for all model membranes studied (the darker, the higher the value). The residue numbers are indicated at the left, whereas column numbers define amino acid positions (see Figure 2). (B) Analysis of the interfacial and hydrophobic distribution for the full sequence of the envelope glycoproteins E1 and E2 using a window of 15 amino acids according to the scales of Winley and White (see text) along with the normalized hemifusion and fusion experimental data shown in (A), highlighting the relationship between the theoretical and experimentally determined membrane-active regions.

Understanding the factors that may determine the specificity and stability of the metastable native and the stable fusogenic conformations of both class I and class II membrane fusion proteins, being located on the ectodomain or endodomain or both, is required to know the mechanism of viral membrane fusion and consequent viral entry into cells.

We have previously shown the existence of different segments with membrane-interacting capabilities in the HIV gp41 and SARS S1 and S2 glycoproteins (20, 21). In this work we have made an exhaustive study of the effect on membrane integrity of a peptide scan corresponding to two peptide libraries from the HCV E1 and E2 envelope

glycoproteins of two different HCV virus strains, as well as studied their effect not only on membrane rupture but also on membrane-specific approaches such as hemifusion and fusion. Although the use of peptide fragments might not mimic the properties of the intact protein, our results give us an indication of the relative propensity of the different domains to bind, interact, and affect membranes in relation to each other, i.e., help us to classify the different regions and segments of the HCV E1 and E2 envelope glycoproteins according to their effect in an ample representation of membrane systems. As apparent from the results described above, there are different peptides corresponding to different

regions which, depending on liposome composition, sequence, and origin, have different effects on the three membrane-related items studied. It is also true that some peptides which are very active in one model membrane system are much less active in other ones, and vice versa. However, it should be noted that membrane systems having different lipid compositions have diverse properties which make them behave in a significant different way (20). For example, the presence of both SM and Chol has been related to the occurrence of laterally segregated membrane microdomains or "lipid rafts", and it has been found that there is an important relationship between membrane fusion and Chol and SM membrane content for several viruses (45, 46). In this context, it is interesting to note that it has recently been described that the presence of Chol facilitates the fusion of HCV pseudoparticles with the target membrane (47). Taking into account all of this information, we have gathered the membrane-interacting propensity of all its domains and therefore have an indication to the possible function of each segment of the HCV E1 and E2 envelope glycoproteins in each step of the fusion process. This information could provide us with an outline of the possible mechanism of membrane fusion as driven by this membrane fusion protein.

As we have shown above, different segments of both E1 and E2 present high positive values of hydrophobic moment, hydrophobicity, and interfaciality (Figure 2). It is very interesting to note that these segments match exceedingly well with segments showing major leakage and fusion values for all liposome types and conditions (Figures 5 and 8). As is already known, the fusion peptide is an essential factor in viral fusion proteins; however, there exists some controversy about its exact identification. The E1 envelope glycoprotein segment comprising residues 265–296 has a significant theoretical and experimental membranotropic effect as shown here and, therefore, should be the candidate to contain the fusion peptide domain. This sequence possesses a high degree of hydrophobicity and interfaciality, essential properties for membrane-interacting segments in proteins (Figure 8B). The other two membrane-active regions of E1, though showing less membranotropic activity than the first one, possess also a significant effect. Since the C-terminal transmembrane domain is comprised by residues 331–381, the segment comprising residues 310–331 could be involved in promotion of membrane destabilization, as well as pore formation and enlargement, in a manner similar to that of the pretransmembrane and/or loop domains of class I fusion proteins (15, 48–51). Similarly to E1, there are different segments on E2, which show major positive values of hydrophobic moments, hydrophobicity, and interfaciality, that also show major leakage and fusion values. From the theoretical point of view, six zones could be identified (Figure 2) but five from experimental data (Figures 5 and 8). One of the most membranotropic regions of E2 is comprised by residues 715–746, which corresponds to the C-terminal transmembrane domain of the protein (Figure 8B). Consecutively to this one, we found two membranotropic regions comprised by residues 603–635 and 525–565, which have been implicated in folding and receptor binding. Following these, we found the segment comprised by residues 455–489 which includes the hypervariable HVR-2 region. Adjacent to this one we find the most membranotropic region of E2, that comprising residues 423–453. While this region is signifi-

cantly more membranotropic than the other E2 regions, it is not as membrane active as region 265–296 from E1 (Figure 8B). If the fusion peptide were located in E2, this region should be the candidate to contain it. Similarly to what was noted above, the different membrane-active segments found in E2 could be involved in promotion of membrane destabilization, pore formation, and/or enlargement, probably in combination with other E1 regions. It is interesting to note that two significant regions of E2, the highly conserved sequence necessary for heterodimerization with E1 (residues 675–699) and the hypervariable HVR-1 region (residues 384–411), have no or very limited membranotropic activity (Figures 5 and 8A,B). This is in contrast with hydrophobicity analysis that revealed the highly hydrophobic domain of HVR-1 (44).

For membrane fusion to occur, fusion proteins must pull the viral and cellular membranes, create membrane defects, induce hemifusion and fusion, and, last but not least, induce pore formation, stabilization, and enlargement (52). The fusion domain is mainly responsible for the first steps of membrane fusion, but in the last instance other HCV E1 and E2 envelope glycoprotein segments, in combination with the previous one, drive and accomplish membrane fusion. The binding to the surface and the modulation of the phospholipid biophysical properties which take place when the HCV E1 and E2 envelope glycoprotein domains bind to the membrane could be related to the conformational changes which occur upon binding of the envelope glycoprotein to its receptors. The change in conformation and the possible formation of oligomeric forms in the presence of membranes could indicate the propensity of the protein to self-assemble and suggest that these changes might be part of the structural transition that transform HCV E1 and E2 envelope glycoproteins from the inactive to the active state, being most probably the dominant form during membrane fusion and, probably, driven by the interaction of the different segments indicated in this work. The destabilization of the phospholipid bilayer as a result of the interaction of the HCV E1 and E2 envelope glycoprotein segments would provide a way to lower the energy barrier necessary for fusion. The change in free energy associated with the structural changes taking place should be sufficient to cause phospholipid mixing and membrane fusion. In addition, the knowledge of all membrane-active regions of HCV E1 and E2 envelope glycoproteins could aid in the search for molecules which could revert or reduce the action of those specific membrane-active peptides; i.e., those molecules which inhibit peptide-induced membrane leakage, hemifusion, or fusion could be potential candidates as inhibitors of membrane fusion, as has been done successfully for class I fusion inhibitors.

CONCLUDING REMARKS

The HCV entry process is considered to be an attractive target for chemotherapeutic intervention, as blocking HCV entry into its target cell leads to suppression of viral infectivity, replication, and the cytotoxicity induced by virus-cell contacts. Therefore, the inhibition of membrane fusion by direct action on either E1 or E2 or both is increasing in importance as an additional approach either to combat directly against HCV infection or to prevent its spread. An understanding of the structural features of the fusogenic intermediates is essential because they are attractive drug

targets. The results reported in this work sustain the notion that different membranotropic segments of both HCV E1 and E2 provide the driving force for the merging of the viral and target cell membranes, as well as they could help us to develop inhibitors of HCV infection in a similar way as HIV peptide inhibitors have been generated.

ACKNOWLEDGMENT

We are especially grateful to the National Institutes of Health AIDS Research and Reference Reagent Program, Division of AIDS, NIAID, NIH, for the peptides used in this work, as well as to Ana M. Gómez for expert technical assistance.

REFERENCES

- Penin, F., Dubuisson, J., Rey, F. A., Moradpour, D., and Pawlotsky, J. M. (2004) Structural biology of hepatitis C virus, *Hepatology* 39, 5–19.
- Tan, S. L., Pause, A., Shi, Y., and Sonenberg, N. (2002) Hepatitis C therapeutics: current status and emerging strategies, *Nat. Rev. Drug Discovery*, 867–881.
- Wong, V. K., Cheong-Lee, C., Ford, J. A., and Yoshida, E. M. (2005) Acute sensorineural hearing loss associated with peginterferon and ribavirin combination therapy during hepatitis C treatment: Outcome after resumption of therapy, *World J. Gastroenterol.* 11, 5392–5393.
- Reed, K. E., and Rice, C. M. (2000) Overview of hepatitis C virus genome structure, polyprotein processing, and protein properties, *Curr. Top. Microbiol. Immunol.* 242, 55–84.
- Simmonds, P., Alberti, A., Alter, H. J., Bonino, F., Bradley, D. W., Brechot, C., et al. (1994) A proposed system for the nomenclature of hepatitis C viral genotypes, *Hepatology* 19, 1321–1324.
- Tokita, H., Okamoto, H., Iizuka, H., Kishimoto, J., Tsuda, F., Miyakawa, Y., and Mayumi, M. (1998) The entire nucleotide sequences of three hepatitis C virus isolates in genetic groups 7–9 and comparison with those in the other eight genetic groups, *J. Gen. Virol.* 79, 1847–1857.
- Pawlotsky, J. M. (2003) Mechanisms of antiviral treatment efficacy and failure in chronic hepatitis C, *Antiviral Res.* 59, 1–11.
- Bartosch, B., Dubuisson, J., and Cosset, F.-L. (2003) Infectious hepatitis C pseudoviruses containing functional E1E2 envelope protein complexes, *J. Exp. Med.* 197, 633–642.
- Cocquerel, L., Duvet, S., Meunier, J. C., Pillez, A., Cacan, R., Wychowski, C., and Dubuisson, J. (1999) The transmembrane domain of hepatitis C virus glycoprotein E1 is a signal for static retention in the endoplasmic reticulum, *J. Virol.* 73, 2641–2649.
- Cocquerel, L., Meunier, J. C., Pillez, A., Wychowski, C., and Dubuisson, J. (1998) A retention signal necessary and sufficient for endoplasmic reticulum localization maps to the transmembrane domain of hepatitis C virus glycoprotein E2, *J. Virol.* 72, 2183–2191.
- Deleersnyder, V., Pillez, A., Wychowski, C., Blight, K., Xu, J., Hahn, Y. S., Rice, C. M., and Dubuisson, J. (1997) Formation of native hepatitis C virus glycoprotein complexes, *J. Virol.* 71, 697–704.
- Op De Beeck, A., Montserret, R., Duvet, S., Cocquerel, L., Cacan, R., Barberot, B., Le Maire, M., Penin, F., and Dubuisson, J. (2000) The transmembrane domains of hepatitis C virus envelope glycoproteins E1 and E2 play a major role in heterodimerization, *J. Biol. Chem.* 275, 31428–31437.
- Garry, R. F., and Dash, S. (2003) Proteomics computational analyses suggest that hepatitis C virus E1 and pestivirus E2 envelope glycoproteins are truncated class II fusion proteins, *Virology* 307, 255–265.
- Epand, R. M. (2003) Fusion peptides and the mechanism of viral fusion, *Biochim. Biophys. Acta* 1614, 116–121.
- Peisajovich, S. G., and Shai, Y. (2003) Viral fusion proteins: multiple regions contribute to membrane fusion, *Biochim. Biophys. Acta* 1614, 122–129.
- Hahn, Y. S. (2003) Subversion of immune responses by hepatitis C virus: immunomodulatory strategies beyond evasion?, *Curr. Opin. Immunol.* 15, 443–449.
- Alter, H. (1995) To C or not to C: these are the questions, *Blood* 85, 1681–1695.
- Grakoui, A., Shoukry, N. H., Woollard, D. J., Han, J. H., Hanson, H. L., Ghayeb, J., Murthy, K. K., Rice, C. M., and Walker, C. M. (2003) HCV persistence and immune evasion in the absence of T cell help, *Science* 302, 659–662.
- Racanello, V., and Rehermann, B. (2003) Hepatitis C virus infection: when silence is deception, *Trends Immunol.* 24, 456–464.
- Guillén, J., Pérez-Berná, A. J., Moreno, M. R., and Villalaín, J. (2005) Identification of the membrane-active regions of the severe acute respiratory syndrome coronavirus spike membrane glycoprotein using a 16/18-mer peptide scan: implications for the viral fusion mechanism, *J. Virol.* 79, 1743–1752.
- Moreno, M. R., Pascual, R., and Villalaín, J. (2004) Identification of membrane-active regions of the HIV-1 envelope glycoprotein gp41 using a 15-mer gp41-peptide scan, *Biochim. Biophys. Acta* 1661, 97–105.
- Shin, J., Shum, P., and Thompson, D. H. (2003) Acid-triggered release via dePEGylation of DOPE liposomes containing acid-labile vinyl ether PEG-lipids, *J. Control Release* 91, 187–200.
- Meers, P., Ali, S., Erukulla, R., and Janoff, A. S. (2000) Novel inner monolayer fusion assays reveal differential monolayer mixing associated with cation-dependent membrane fusion, *Biochim. Biophys. Acta* 1467, 227–243.
- Böttcher, C. S. F., Van Gent, C. M., and Fries, C. (1961) A rapid and sensitive submicro phosphorous determination, *Anal. Chim. Acta* 24, 203–204.
- Struck, D. K., Hoekstra, D., and Pagano, R. E. (1981) Use of resonance energy transfer to monitor membrane fusion, *Biochemistry* 20, 4093–4099.
- Engelman, D. M., Steitz, T. A., and Goldman, A. (1986) Identifying nonpolar transbilayer helices in amino acid sequences of membrane proteins, *Annu. Rev. Biophys. Chem.* 15, 321–353.
- White S. H., and Wimley, W. C. (1999) Membrane protein folding and stability: physical principles, *Annu. Rev. Biophys. Biomol. Struct.* 28, 319–365.
- Wimley, W. C., and White, S. H. (1996) Experimentally determined hydrophobicity scale for proteins at membrane interfaces, *Nat. Struct. Biol.* 3, 842–848.
- Drummer, H. E., and Pountourios, P. (2004) Hepatitis C virus glycoprotein E2 contains a membrane-proximal heptad repeat sequence that is essential for E1E2 glycoprotein heterodimerization and viral entry, *J. Biol. Chem.* 279, 30066–30072.
- Patel, A. H., Wood, J., Penin, F., Dubuisson, J., and McKeating, J. A. (2000) Construction and characterization of chimeric hepatitis C virus E2 glycoproteins: analysis of regions critical for glycoprotein aggregation and CD81 binding, *J. Gen. Virol.* 81, 2873–2883.
- Brazzoli, M., Helenius, A., Fong, S. K., Houghton, M., Abrignani, S., and Merola, M. (2005) Folding and dimerization of hepatitis C virus E1 and E2 glycoproteins in stably transfected CHO cells, *Virology* 332, 438–453.
- Yagnik, A. T., Lahm, A., Meola, A., Roccasecca, R. M., Ercole, B. B., Nicosia, A., and Tramontano, A. (2000) A model for the hepatitis C virus envelope glycoprotein E2, *Proteins* 40, 355–366.
- Bretscher, M. S. (1985) The molecules of the cell membrane, *Sci. Am.* 253, 100–109.
- Jahn, R., and Grubmüller, H. (2002) Membrane fusion, *Curr. Opin. Cell Biol.* 14, 488–495.
- Nieva, J. L., Gofñi, F. M., and Alonso, A. (1989) Liposome fusion catalytically induced by phospholipase C, *Biochemistry* 28, 7364–7367.
- Blumenthal, R., Clague, M. J., Durell, S. R., and Epand, R. M. (2003) Membrane fusion, *Chem. Rev.* 103, 53–69.
- Chernomordik, L. V., and Kozlov, M. M. (2005) Membrane hemifusion: Crossing a chasm in two leaps, *Cell* 123, 375–382.
- Schibli, D. J., and Weissenhorn, W. (2004) Class I and class II viral fusion protein structures reveal similar principles in membrane fusion, *Mol. Membr. Biol.* 21, 361–371.
- Gallo, S. A., Finnegan, C. M., Viard, M., Raviv, Y., Dimitrov, A. S., Rawat, S. S., Puri, A., Durell, S., and Blumenthal, R. (2003) The HIV Env-mediated fusion reaction, *Biochim. Biophys. Acta* 1614, 36–50.
- Op De Beeck, A., Voisset, C., Bartosch, B., Ciczora, Y., Cocquerel, L., Keck, Z., Fong, S., Cosset, F. L., and Dubuisson, J. (2004)

- Characterization of functional hepatitis C virus envelope glycoproteins, *J. Virol.* 78, 2994–3002.
41. Flint, M., Thomas, J. M., Maidens, C. M., Shotton, C., Levy, S., Barclay, W. S., and McKeating, J. A. (1999) Functional analysis of cell surface-expressed hepatitis C virus E2 glycoprotein, *J. Virol.* 73, 6782–6790.
 42. Ciccaglione, A. R., Costantino, A., Marcantonio, C., Equestre, M., Geraci, A., and Rapicetta, M. (2001) Mutagenesis of hepatitis C virus E1 protein affects its membrane-permeabilizing activity, *J. Gen. Virol.* 82, 2243–2250.
 43. Migliaccio, C. T., Follis, K. E., Matsuura, Y., and Nunberg, J. H. (2004) Evidence for a polytopic form of the E1 envelope glycoprotein of hepatitis C virus, *Virus Res.* 105, 47–57.
 44. Kurihara, C., Tsuzuki, Y., Hokari, R., Nakashima, H., Mataka, N., Kuroki, M., Kawaguchi, A., Nagao, S., Kondo, T., and Miura, S. (2004) A highly hydrophobic domain within hypervariable region 1 may be related to the entry of hepatitis C virus into cultured human hepatoma cells, *J. Med. Virol.* 74, 546–555.
 45. Ahn, A., Gibbons, D. L., and Kielian, M. (2002) The fusion peptide of Semliki Forest virus associates with sterol-rich membrane domain, *J. Virol.* 76, 3267–3275.
 46. Nguyen, D. H., and Hildreth, J. E. K. (2000) Evidence for budding of human immunodeficiency virus type 1 selectively from glycolipid-enriched membrane lipid rafts, *J. Virol.* 74, 3264–3272.
 47. Lavillette, D., Bartosch, B., Nourrisson, D., Verney, G., Cosset, F. L., Penin, F., and Pécheur, E. I. (2005) Hepatitis C virus glycoproteins mediate low pH-dependent membrane fusion with liposomes, *J. Biol. Chem.* (in press).
 48. Contreras, L. M., Aranda, F. J., Gavilanes, F., González-Ros, J. M., and Villalán, J. (2001) Structure and interaction with membrane model systems of a peptide derived from the major epitope region of HIV protein gp41: implications on viral fusion mechanism, *Biochemistry* 40, 3196–3207.
 49. Pascual, R., Moreno, M. R., and Villalán, J. (2005) A peptide pertaining to the loop segment of human immunodeficiency virus gp41 binds and interacts with model biomembranes: implications for the fusion mechanism, *J. Virol.* 79, 5142–5152.
 50. Pascual, R., Contreras, M., Fedorov, A., Prieto, M. J. E., and Villalán, J. (2005) Interaction of a peptide derived from the N-heptad repeat region of gp41 env ectodomain with model membranes. Modulation of phospholipid phase behavior, *Biochemistry* 44, 14275–14288.
 51. Sáez-Cirión, A., Arrondo, J. L., Gomara, M. J., Lorizate, M., Iloro, I., Melikyan, G., and Nieva, J. L. (2003) Structural and functional roles of HIV-1 gp41 pretransmembrane sequence segmentation, *Biophys. J.* 85, 3769–3780.
 52. Earp, L. J., Delos, S. E., Park, H. E., and White, J. M. (2004) The many mechanisms of viral membrane fusion proteins, *Curr. Top. Microbiol. Immunol.* 285, 25–66.

BI0523963



Publicación 4

Interaction of the Most Membranotropic Region of the HCV E2 Envelope Glycoprotein with Membranes. Biophysical Characterization

A. J. Pérez-Berná¹, J Guillén¹, M. R. Moreno¹, A. I.
Gómez-Sánchez¹, G. Pabst², P. Laggner² and J.
Villalaín¹

¹Instituto de Biología Molecular y Celular, Universidad “Miguel
Hernández”, Elche-Alicante, Spain

²Biophysics and Nanosystems Research, Austrian Academy of Sciences,
Graz A-8042, Austria

Biophysical Journal Volume 94 June 2008 4737–4750



Interaction of the Most Membrantropic Region of the HCV E2 Envelope Glycoprotein with Membranes. Biophysical Characterization

Ana J. Pérez-Berná,* Jaime Guillén,* Miguel R. Moreno,* Ana I. Gómez-Sánchez,* George Pabst,[†] Peter Laggner,[†] and José Villalain*

*Instituto de Biología Molecular y Celular, Universidad “Miguel Hernández”, Elche-Alicante, Spain; and [†]Institute of Biophysics and Nanosystems Research, Austrian Academy of Sciences, Graz, Austria

ABSTRACT The previously identified membrane-active regions of the hepatitis C virus (HCV) E1 and E2 envelope glycoproteins led us to identify different segments that might be implicated in viral membrane fusion, membrane interaction, and/or protein-protein binding. HCV E2 glycoprotein contains one of the most membrantropic segments, segment 603–634, which has been implicated in CD81 binding, E1/E2 and E2/E2 dimerization, and membrane interaction. Through a series of complementary experiments, we have carried out a study of the binding and interaction with the lipid bilayer of a peptide corresponding to segment 603–634, peptide E2_{FP}, as well as the structural changes induced by membrane binding that take place in both the peptide and the phospholipid molecules. Here, we demonstrate that peptide E2_{FP} binds to and interacts with phospholipid model membranes, modulates the polymorphic phase behavior of membrane phospholipids, is localized in a shallow position in the membrane, and is probably oligomerized in the presence of membranes. These data support the role of E2_{FP} in HCV-mediated membrane fusion, and sustain the notion that this segment of the E2 envelope glycoprotein, together with other segments of E2 and E1 glycoproteins, provides the driving force for the merging of the viral and target cell membranes.

INTRODUCTION

Hepatitis C virus (HCV), an enveloped positive single-stranded RNA virus of the *Flaviviridae* family, has an important impact on public health since it is the leading cause of acute and chronic liver disease in humans, including chronic hepatitis, cirrhosis, and hepatocellular carcinoma (1–3). At the moment, there exists no vaccine to prevent HCV infection, and current therapeutic agents have limited success against HCV (4). The HCV genome consists of one translational open reading frame encoding a polyprotein precursor of ~3010 amino acids in length, including structural and nonstructural proteins, that is cleaved by host and viral proteases (5). The polyprotein precursor is cotranslationally and posttranslationally processed by both cellular and viral proteases at the level of the endoplasmic reticulum membrane to yield 10 mature structural and nonstructural proteins. The structural proteins include the core, which forms the viral nucleocapsid, and the envelope transmembrane glycoproteins E1 and E2. The structural proteins are separated from the nonstructural proteins by the short membrane protein p7. HCV entry into the cell is achieved by the fusion of viral and cellular membranes, and morphogenesis and budding has been suggested to take place in the endoplasmic reticulum (6). Therefore, the protein regions implicated in fusion and/or budding must interact with the biological membrane and should be conser-

vative membrantropic sequences. The variability of the HCV proteins gives the virus the ability to escape the host's immune surveillance system and the development of a vaccine proves to be a difficult task (7). Furthermore, HCV proteins are very sensitive to folding, assembly, mutations, and deletions. Finding protein-membrane and protein-protein interaction inhibitors could be a good strategy against HCV infection, since they might prove to be potential therapeutic agents.

The viral structure of HCV is thought to adopt a classical icosahedral scaffold in which the E1 and E2 envelope glycoproteins are anchored to the host-cell-derived double-layer lipid envelope. Both of them are essential for host-cell entry, binding to receptor(s), and fusion with the host cell membrane, as well as in viral particle assembly (8). E1 and E2 are type I transmembrane glycoproteins, with an N-terminal ectodomain and a short C-terminal transmembrane domain. They interact with each other and assemble as noncovalent heterodimers. It is significant that their transmembrane domains play a major role in the E1/E2 heterodimer formation, membrane anchoring, and endoplasmic reticulum retention (9–12). The HCV envelope glycoproteins E1 and E2 are included in the class II fusion proteins, because the putative fusion peptide is localized in an internal sequence linked by antiparallel β -sheets; moreover, proteomics computational analyses suggest that HCV envelope glycoprotein E1 is a truncated class II fusion protein (13). The HCV membrane fusion process is pH-dependent, and low endosomal pH promotes the arrangement of E1/E2 to its active form (14). Many aspects regarding the function and properties of both HCV E1 and E2 glycoproteins still remain unresolved; even so, the location of the fusion peptide is controversial, since several data suggest that it could be located in either E1 or E2.

Submitted December 3, 2007, and accepted for publication February 21, 2008.

Address reprint requests to Dr. José Villalain, Instituto de Biología Molecular y Celular, Campus de Elche, Universidad “Miguel Hernández”, E-03202 Elche-Alicante, Spain. Tel.: 34-966-658-762; Fax: 34-966-658-758; E-mail: jvillalain@umh.es.

Editor: Mark Girvin.

© 2008 by the Biophysical Society
0006-3495/08/06/4737/14 \$2.00

doi: 10.1529/biophysj.107.126896

Although previous data have proposed a direct role of HCV E1 in membrane fusion, whereas HCV E2 should mediate the binding with receptor CD81, and should also be responsible for heterodimerization with E1, recent data suggest that indeed both E1 and E2 glycoproteins participate in the membrane fusion mechanism (14–18).

We have recently identified the membrane-active regions of the HCV E1 and E2 glycoproteins by observing the effect of E1 and E2 glycoprotein-derived peptide libraries on model membrane integrity, and have found different segments that present high positive values of hydrophobic moment, hydrophobicity, and interfaciality (19). These results permit us to suggest the possible location of different segments in these proteins that might be implicated in protein-lipid and protein-protein interactions, helping us to understand the processes that give rise to the interaction between the different proteins and the membrane. The most membranotropic regions of E2 are made up of segments comprising residues 455–489, which include the hypervariable HVR-2 region, 525–565 and 603–634 (19). Region 603–634 shows a very high hydrophobicity and interfaciality, as well as significant leakage, hemifusion, and fusion effects in membrane model systems (19). Of significance is the demonstration, using infectious HCV pseudoparticles, that mutations in this region abolished infectivity and membrane fusion, demonstrating that this segment of the E2 glycoprotein participates in the viral fusion process (15). It is known that the mechanism by which proteins facilitate the formation of fusion intermediates is a complex process involving several segments of fusion proteins (20,21), and at the same time, there are still many questions to be answered regarding the E1 and E2 mode of action in HCV and cell host membrane fusion. Since the 603–634 region of the HCV E2 envelope glycoprotein might be involved in membrane destabilization and at the same time take part in the fusion events as a helper for the fusion peptide and/or the pretransmembrane regions, as well as other segments, we have made an in-depth study of the 603–634 HCV E2 region, peptide E2_{FP}, patterned after peptides ⁶⁰³-LTPRCLVDYPYRLWHYPC-⁶²⁰, ⁶¹⁰-DYPYRLWHYPC⁶²⁷, and ⁶¹⁷-HYPCTLNFSIFKVRMYVG-⁶³⁴ (peptides 34–36 from the original HCV E1/E2 peptide library, respectively (19)). We have studied the binding and interaction of E2_{FP} with membrane model systems, as well as the structural changes that take place in both the peptide and phospholipid molecules induced by membrane binding through a series of complementary experiments. In this work, we show that peptide E2_{FP} strongly partitions and buries into phospholipid membranes, interacts with negatively charged phospholipids, and modulates the phase polymorphic behavior of model membranes.

MATERIALS AND METHODS

Materials and reagents

The peptide E2_{FP}, corresponding to the sequence ⁶⁰³-LTPRCLVDYPYRLWHYPC⁶²⁷ from HCV strain 1B4J (with N-terminal

acetylation and C-terminal amidation) was obtained from Genemed Synthesis, San Francisco, CA. The peptide E2_{FP} was purified by reverse-phase high-performance liquid chromatography (C-8 column (Vydac, Hesperia, CA), 250 × 4.6 mm, flow rate 1 ml/min; solvent A, 0.1% trifluoroacetic acid; solvent B, 99.9% acetonitrile, and 0.1% trifluoroacetic acid) to >95% purity, and its composition and molecular mass were confirmed by amino acid analysis and mass spectroscopy. Since trifluoroacetate has a strong infrared absorbance at ~1673 cm⁻¹, which interferes with the characterization of the peptide amide I band (22), residual trifluoroacetic acid, used both in peptide synthesis and in the high-performance liquid chromatography mobile phase, was removed by several lyophilization/solubilization cycles in 10 mM HCl (23). Egg L- α -phosphatidylcholine (EPC), egg L- α -phosphatidic acid (EPA), egg sphingomyelin (SM), bovine brain phosphatidylserine (BPS), egg transsterified L- α -phosphatidylethanolamine (TPE), lyso- α -phosphatidylcholine (LPC), 1,2-dimyristoylphosphatidylcholine (DMPC), 1,2-dimyristoylphosphatidylglycerol (DMPG), 1,2-dimyristoylphosphatidylserine, 1,2-dimyristoylphosphatidic acid (DMPA), 1,2-dielaidoyl-*sn*-glycero-3-phosphatidylethanolamine (DEPE), 1-palmitoyl, 2-oleoyl-*sn*-glycero-3-phosphatidylethanolamine, liver lipid extract, cholesterol (Chol), Lissamine rhodamine B 1,2-dihexadecanoyl-*sn*-glycero-3-phosphoethanolamine, and *N*-(7-nitrobenz-2-oxa-1,3-diazol-4-yl)-1,2-dihexadecanoyl-*sn*-glycero-3-phosphatidylethanolamine (NBD-PE) were obtained from Avanti Polar Lipids (Alabaster, AL). 5-Carboxyfluorescein (CF) (>95% by high-performance liquid chromatography), 5-doxy-stearic acid (5NS), 16-doxy-stearic acid (16NS), dehydroergosterol (ergosta-5,7,9(11),22-tetraen-3 β -ol), sodium dithionite, deuterium oxide (99.9% by atom), Triton X-100, EDTA, and HEPES were purchased from Sigma-Aldrich (Madrid, Spain). 1,6-Diphenyl-1,3,5-hexatriene (DPH), 1-(4-trimethylammoniumphenyl)-6-phenyl-1,3,5-hexatriene (TMA-DPH), and 4-(2-(6-(dioctylamino)-2-naphthalenyl)(ethenyl)-1-(3-sulfopropyl)-pyridinium inner salt (di-8-ANEPPS) were obtained from Molecular Probes (Eugene, OR). All other reagents used were of analytical grade from Sigma-Aldrich. Water was deionized, twice distilled, and passed through a Milli-Q equipment (Millipore Ibérica, Madrid, Spain) to a resistivity better than 18 M Ω cm.

Vesicle preparation

Aliquots containing the appropriate amount of lipid in chloroform/methanol (2:1, v/v) were placed in a test tube, the solvents removed by evaporation under a stream of O₂-free nitrogen, and finally, traces of solvents were eliminated under vacuum in the dark for >3 h. The lipid films were re-suspended in an appropriate buffer and incubated either at 25°C or 10°C above the gel-to-liquid-crystal-phase transition temperature (*T_m*) with intermittent vortexing for 30 min to hydrate the samples and obtain multilamellar vesicles (MLV). The samples were frozen and thawed five times to ensure complete homogenization and maximization of peptide/lipid contacts, with occasional vortexing. Large unilamellar vesicles (LUV) with mean diameter 0.1 and 0.2 μ m for leakage or hemifusion and fusion experiments, respectively, were prepared from multilamellar vesicles by the extrusion method (24), using polycarbonate filters with a pore size of 0.1 and 0.2 μ m (Nuclepore Corp., Cambridge, CA). The phospholipid and peptide concentration were measured by methods described previously (25,26).

Membrane leakage measurement

LUVs with a mean diameter of 0.1 μ m were prepared as indicated above in buffer containing 10 mM Tris, 20 mM NaCl, pH 7.4, and CF at a concentration of 40 mM. Nonencapsulated CF was separated from the vesicle suspension through a Sephadex G-75 filtration column (Pharmacia, Uppsala, Sweden) eluted with buffer containing 10 mM TRIS, 100 mM NaCl, 1 mM EDTA, pH 7.4. Membrane rupture (leakage) of intraliposomal CF was assayed by treating the probe-loaded liposomes (final lipid concentration, 0.125 mM) with the appropriate amounts of peptide using a 5 × 5 mm fluorescence cuvette on a Cary Eclipse spectrofluorometer (Varian, San Carlos, CA), stabilized at 25°C with the appropriate amounts of peptide, each well containing a final volume of 400 μ l. The medium in the cuvettes was continuously stirred to allow the rapid

mixing of peptide and vesicles. Leakage was assayed until no more change in fluorescence was obtained. The fluorescence was measured using a Varian Cary Eclipse spectrofluorometer. Changes in fluorescence intensity were recorded with excitation and emission wavelengths set at 492 and 517 nm, respectively. Excitation and emission slits were set at 5 nm. One hundred percent release was achieved by adding Triton X-100 to the cuvette to a final concentration of 0.5% (w/w). Fluorescence measurements were made initially with probe-loaded liposomes, afterward by adding peptide solution, and finally by adding Triton X-100 to obtain 100% leakage. Leakage was quantified on a percentage basis according to the equation, $\%L = [(F_f - F_0) \times 100] / (F_{100} - F_0)$, where F_f is the equilibrium value of fluorescence after peptide addition, F_0 is the initial fluorescence of the vesicle suspension, and F_{100} is the fluorescence value after the addition of Triton X-100.

Phospholipid-mixing measurement

Peptide-induced vesicle lipid mixing was measured by resonance energy transfer (27). This assay is based on the decrease in resonance energy transfer between two probes (NBD-PE and Lissamine rhodamine B 1,2-dihexadecanoyl-*sn*-glycero-3-phosphoethanolamine) when the lipids of the probe-containing vesicles are allowed to mix with lipids from vesicles lacking the probes. The concentration of each of the fluorescent probes within the liposome membrane was 0.6% mol. LUVs with a mean diameter of 0.2 μm were prepared as described above. Labeled and unlabeled vesicles in the proportion 1:4 were placed in a 5 \times 5-mm fluorescence cuvette at a final lipid concentration of 100 μM in a final volume of 400 μl , stabilized at 25°C under constant stirring. The fluorescence was measured using a Varian Cary Eclipse fluorescence spectrometer using 467 nm and 530 nm for excitation and emission, respectively. Excitation and emission slits were set at 10 nm. Since labeled/unlabeled vesicles were mixed in a proportion of 1:4, 100% phospholipid mixing was estimated with a liposome preparation in which the membrane concentration of each probe was 0.12%. Phospholipid mixing was quantified on a percentage basis according to the equation, $\%PM = [(F_f - F_0) \times 100] / (F_{100} - F_0)$, where F_f is the value of fluorescence obtained 15 min after peptide addition to a liposome mixture containing liposomes with 0.6% of each probe plus liposomes without any fluorescent probe, F_0 is the initial fluorescence of the vesicles, and F_{100} is the fluorescence value of the liposomes containing 0.12% of each probe.

Inner-monolayer phospholipid-mixing (fusion) measurement

Peptide-induced phospholipid-mixing of the inner monolayer was measured by a modification of the phospholipid-mixing measurement stated above (28). This assay is based on the decrease in resonance energy transfer between two probes (NBD-PE and Lissamine rhodamine B 1,2-dihexadecanoyl-*sn*-glycero-3-phosphoethanolamine) when the lipids of the probe-containing vesicles are allowed to mix with lipids from vesicles lacking the probes. The concentration of each of the fluorescent probes within the liposome membrane was 0.6 mol %. LUVs with a mean diameter of 0.2 μm were prepared as described above. LUVs were treated with sodium dithionite to completely reduce the NBD-labeled phospholipid located at the outer monolayer of the membrane. Final concentration of sodium dithionite was 100 mM (from a stock solution of 1 M dithionite in 1 M TRIS, pH 10.0) and incubated for \sim 1 h on ice in the dark. Sodium dithionite was then removed by size-exclusion chromatography through a Sephadex G-75 filtration column (Pharmacia) eluted with buffer containing 10 mM TRIS, 100 mM NaCl, 1 mM EDTA, pH 7.4. The proportion of labeled and unlabeled vesicles, lipid concentration, and other experimental and measurement conditions were the same as indicated above for the phospholipid mixing assay.

Peptide binding to vesicles

The partitioning of the peptide into the phospholipid bilayer was monitored by the fluorescence enhancement of tryptophan. Fluorescence spectra were

recorded in an SLM Aminco 8000C spectrofluorometer with excitation and emission wavelengths of 290 and 348 nm, respectively, and 4-nm spectral bandwidths. Measurements were carried out in 20 mM HEPES, 50 mM NaCl, EDTA 0.1 mM, pH 7.4. Intensity values were corrected for dilution, and the scatter contribution was derived from lipid titration of a vesicle blank. Partitioning coefficients were obtained using (29)

$$\frac{I}{I_0} = 1 + \left[\left(\frac{I_{\max}}{I_0} - 1 \right) \times \left(\frac{K_p[L]}{[W] + K_p[L]} \right) \right],$$

where I and I_0 are the final and the initial intensities respectively, k_p is a mole fraction partition coefficient that represents the amount of peptide in the bilayers as a fraction of the total peptide present in the system, I_{\max} is a variable value for the fluorescence enhancement at complete partitioning determined by fitting the equation to the experimental data, $[L]$ is the lipid concentration, and $[W]$ is the concentration of water (55.3 M). The peptide concentration in the assays was 30 μM .

Steady-state fluorescence anisotropy

MLVs were formed in 100 mM NaCl, 0.05 mM EDTA, 25 mM HEPES, pH 7.4. Aliquots of TMA-DPH or DPH in N,N' -dimethylformamide (2×10^{-4} M) were directly added into the lipid dispersion to obtain a probe/lipid molar ratio of 1:500. Samples were incubated for 15 or 60 min for TMA-DPH and DPH, respectively, 10°C above the T_m of the phospholipid mixture. Afterward, the peptides were added to obtain a peptide/lipid molar ratio of 1:15 and incubated at 10°C above the T_m of each lipid for 1 h, with occasional vortexing. All fluorescence studies were carried using 5 \times 5-mm quartz cuvettes in a final volume of 400 μl (315 μM lipid concentration). All the data were corrected for background intensities and progressive dilution. The steady-state fluorescence anisotropy, $\langle r \rangle$, was measured with an automated polarization accessory using a Varian Cary Eclipse fluorescence spectrometer, coupled to a Peltier device (Varian) for automatic temperature change. The vertically and horizontally polarized emission intensities, elicited by vertically polarized excitation, were corrected for background scattering by subtracting the corresponding polarized intensities of a phospholipid preparation lacking probes. The G-factor, accounting for differential polarization sensitivity, was determined by measuring the polarized components of the fluorescence of the probe with horizontally polarized excitation ($G = I_{\text{HV}} / I_{\text{HH}}$). Samples were excited at 360 nm (slit width, 5 nm) and fluorescence emission was recorded at 430 nm (slit width, 5 nm). The values were calculated from the equation (30). The steady-state anisotropy was defined by equation $\langle r \rangle = (I_{\text{VV}} - GI_{\text{VH}}) / (I_{\text{VV}} + 2GI_{\text{VH}})$, where I_{VV} and I_{VH} are the measured fluorescence intensities (after appropriate background subtraction) with the excitation polarizer vertically oriented and the emission polarizer vertically and horizontally oriented, respectively.

Fluorescence quenching of Trp emission by water-soluble and lipophilic probes

For acrylamide quenching assays, aliquots from a 4 M solution of the water-soluble quencher were added to the solution-containing peptide in the presence and absence of liposomes at a peptide/lipid molar ratio of 1:100. The results obtained were corrected for dilution and the scatter contribution was derived from acrylamide titration of a vesicle blank. The data were analyzed according to the Stern-Volmer equation (31), $F_0/F = 1 + K_{\text{sv}}[Q]$, where I_0 and I represent the fluorescence intensities in the absence and presence of the quencher $[Q]$, respectively, and K_{sv} is the Stern-Volmer quenching constant, which is a measure of the accessibility of Trp to acrylamide. Quenching studies with lipophilic probes were performed by successive addition of small amounts of 5NS or 16NS in ethanol to the samples of the peptide incubated with LUV. The final concentration of ethanol was kept below 2.5% (v/v) to avoid any significant bilayer alterations. After each addition, there was an incubation period of 15 min before the measurement. The effective quencher concentration in the membrane, $[Q]_L$, was calculated using the relationship (32)

$$[Q]_L = [Q]_T \left(1 - \frac{K_{PQ} \gamma_L [L]}{1 - \gamma_L [L] + K_{PQ} \gamma_L [L]} \right) \frac{K_{PQ}}{1 - \gamma_L [L]}$$

where γ_L is the phospholipid molar volume, $[Q]_T$ is the total quencher concentration, $[L]$ is the lipid molar concentration, and K_{PQ} is the partition coefficient of the quencher. The K_{PQ} values for 5NS and 16NS were as reported previously (33). The fluorescence data were analyzed using a direct fit according to the relationship (34)

$$\frac{I_0}{I} = \frac{1 + K_{SV}[Q]_L}{(1 + K_{SV}[Q]_L)(1 - f_B) + f_B}$$

where I_0 is the fluorescence intensity in the absence of quencher, K_{SV} is the Stern-Volmer quenching constant, and $f_B = I_{0,B}/I_0$, where $I_{0,B}$ is the fluorescence intensity of the fluorophore population accessible to the quencher. The excitation and emission wavelengths were 290 and 348 nm, respectively.

Fluorescence measurements using FPE-labeled membranes

LUVs with a mean diameter of 0.1 μm were prepared in buffer containing 10 mM TRIS-HCl, pH 7.4. The vesicles were labeled exclusively in the outer bilayer leaflet with fluoresceinphosphatidylethanolamine (FPE), as described previously (35). Briefly, LUVs were incubated with 0.1 mol % FPE dissolved in ethanol (never more than 0.1% of the total aqueous volume) at 37°C for 1 h in the dark. Any remaining unincorporated FPE was removed by gel filtration on a Sephadex G-25 column equilibrated with the appropriate buffer. FPE-vesicles were stored at 4°C until use in an oxygen-free atmosphere. Fluorescence time courses of FPE-labeled vesicles were measured after the desired amount of peptide was added into 400 μl of lipid suspensions (200 μM lipid) using a Varian Cary Eclipse fluorescence spectrometer. Excitation and emission wavelengths were set at 490 and 520 nm, respectively, using excitation and emission slits set at 5 nm. Temperature was controlled with a thermostatic bath at 25°C. The contribution of light scattering to the fluorescence signals was measured in experiments without the dye and was subtracted from the fluorescence traces. Data were fitted to a hyperbolic binding model (36) using the equation $F = (F_{\max}[P])/(K_d + [P])$, where F is the fluorescence variation, F_{\max} the maximum fluorescence variation, $[P]$ the peptide concentration, and K_d the dissociation constant of the membrane binding process.

Measurement of the membrane dipole potential using di-8-ANEPPS-labeled membranes

Aliquots containing the appropriate amount of lipid in chloroform-methanol (2:1 v/v) and di-8-ANEPPS were placed in a test tube to obtain a probe/lipid molar ratio of 1:100 and LUVs, with a mean diameter of 90 nm, were prepared as described previously. Steady-state fluorescence measurements were recorded with a Varian Cary Eclipse spectrofluorometer. Dual wavelength recordings with the dye di-8-ANEPPS were obtained by exciting the samples at two different wavelengths (450 and 520 nm) and measuring their intensity ratio, $R_{450/520}$, at an emission wavelength of 620 nm (37,38). By exciting the membrane suspensions at two different wavelengths corresponding to the maximum and the minimum of the difference spectrum, a fluorescence intensity ratio R can be calculated, which can be used as a measure of the relative changes in the magnitude of the dipole potential. The fluorescence ratio R is defined as the ratio of the fluorescence intensity at an excitation wavelength of 450 nm divided by the intensity at 520 nm. The lipid concentration was 200 μM , and all experiments were performed at 25°C.

Infrared spectroscopy

For IR spectroscopy, the samples were prepared as above but in D_2O buffer; $\sim 25 \mu\text{l}$ of a pelleted sample in D_2O was placed between two CaF_2 windows

separated by 50- μm thick Teflon spacers in a liquid demountable cell (Harrick, Ossining, NY). The spectra were obtained in a Bruker IFS55 spectrometer (Bruker Biospin, Rheinstetten, Germany) using a deuterated triglycine sulfate detector. Each spectrum was obtained by collecting 200 interferograms with a nominal resolution of 2 cm^{-1} , transformed using triangular apodization, and a sample shuttle accessory was used to obtain sample and background spectra to average background spectra between sample spectra over the same time period. The spectrometer was continuously purged with dry air at a dew point of -40°C . All samples were equilibrated at the lowest temperature for 20 min before acquisition. An external bath circulator, connected to the infrared spectrometer, controlled the sample temperature. For temperature studies, samples were scanned using 2°C intervals with a 2-min delay between consecutive scans. Subtraction of buffer spectra taken at the same temperature as the samples, center-of-gravity frequencies, and band-narrowing methods were performed interactively using either GRAMS/32 or Spectra-Calc (Galactic Industries, Salem, MA), as described previously (39,40).

Differential scanning calorimetry

MLVs were formed as described above in 100 mM NaCl, 0.05 mM EDTA and 25 mM HEPES, pH 7.4. The peptides were added to obtain a peptide/lipid molar ratio of 1:15. The final volume was 1.2 ml (500 μM lipid concentration), and was incubated 10°C above the T_m of each phospholipid for 1 h, with occasional vortexing. Samples were degassed under vacuum for 10–15 min with gentle stirring, before being loaded into the calorimetric cell. Differential scanning calorimetry (DSC) experiments were performed in a VP-DSC differential scanning calorimeter (MicroCal) under a constant external pressure of 30 psi to avoid bubble formation, and samples were heated at a constant scan rate of 60°C/h. Experimental data were corrected from small mismatches between the two cells by subtracting a buffer baseline before data analysis. The excess heat capacity functions were analyzed using Origin 7.0 (Microcal). The errors in determination of T_c and ΔH were 0.2°C and 0.5 kJ/mol, respectively. The thermograms were defined by the onset and completion temperatures of the transition peaks obtained from heating scans. To avoid artifacts due to the thermal history of the sample, the first scan was never considered; second and further scans were carried out until a reproducible and reversible pattern was obtained.

³¹P NMR

Samples were prepared as described above at a lipid/peptide molar ratio of 50:1 and concentrated by centrifugation (14,000 rpm for 15 min). ³¹P NMR spectra were recorded at different temperatures in the Fourier transform mode in a Bruker Avance 500 MHz NMR (Bruker BioSpin) spectrometer operating at a resonance frequency of 202.38 MHz for ³¹P-nuclei and using a 5 mm probe BBO BB-1H. Probe temperature was maintained at $\pm 0.2^\circ\text{C}$ by a Bruker BVT 3000 variable digital temperature unit. Measurements, spectra acquisition, and calibration were essentially performed as previously described (41). Typical acquisition parameters: spectral width of 30 kHz in 16 K data points, $\pi/2$ pulse widths of typically 6.5 μs , and relaxation delays of 5 s. Typically, 1600 scans were recorded with deuterium (D_2O) lock.

Small-angle x-ray scattering experiments

MLVs at a concentration of 5% (w/w) prepared without or with the peptide at a lipid/peptide molar ratio of 50:1 were prepared as stated above and submitted to 15 temperature cycles (heating at 45°C and cooling at -20°C). Small-angle x-ray diffraction (SAXD) measurements were carried out using a Hecus SWAX-camera (Hecus X-ray Systems, Graz, Austria), as described previously (42), with Ni-filtered Cu-K_α radiation ($\lambda = 1542 \text{ \AA}$) originating from a sealed-tube x-ray generator (GE-Seifert, Ahrensburg, Germany) operating at a power of 2 kW (50 kV, 4 mA). Sample-to-detector distance was

27.8 cm. A linear-position-sensitive detector was used with 1024-channel resolution. SAXD angle calibration was done with silver stearate. The measurements were performed with the sample placed in a thin-walled 1-mm diameter quartz capillary held in a steel cuvette holder at different temperatures with an exposure time of 1 h. The SAXD curves were analyzed after background subtraction and normalization in terms of a full q -range model using the program GAP (43).

RESULTS

The HCV E1 envelope glycoprotein is thought to be responsible for the membrane fusion process, whereas the HCV E2 envelope glycoprotein is thought to mediate the binding to the host cell, although other roles could not be ruled out (14,15,44). It is interesting that several hydrophobic patches have been identified in the E2 protein that might be important for modulating membrane binding and interaction (17,19). In Fig. 1, we present the analysis of the hydrophobic moment, hydrophobicity, and interfaciality distribution along the E2 envelope glycoprotein sequence of the HCV_1B4J strain, assuming it forms an α -helical wheel along the whole sequence (19). Although the E1 and E2 HCV envelope glycoproteins are supposed to be class II membrane fusion proteins and therefore their α -helix content should not be as high as that of class I membrane fusion proteins, these data give us a depiction of the potential surface zones that could be implicated in the modulation of membrane binding. As we have shown previously, the sequence comprising residues 603–634 is one of the most membranotropic regions of HCV E2 (19). Furthermore, it has been shown recently that this segment participates in the viral fusion process (15). Because of that, we present here the results of the study of the interaction with model membranes of a peptide derived from this region, the E2_{FP} peptide, comprising residues 603–634 (see Fig. 1). Peptide E2_{FP} has been patterned after peptides 34 (⁶⁰³-LTPRCLVDYPYRL-

WHYPC-⁶²⁰), 35 (⁶¹⁰-DYPYRLWHYPCTLNFSIF-⁶²⁷), and 36 (⁶¹⁷-HYPCTLNFSIFKVRMYVG-⁶³⁴), from the original HCV E2 peptide library (19).

The ability of the E2_{FP} peptide to interact with membranes was determined from the increase in fluorescence emission intensity of its Trp residues in the presence of model membranes (45) containing different phospholipid compositions at different lipid/peptide ratios (Fig. 2A). It should be recalled that HCV pseudoparticle membrane fusion does not require any protein or receptor at the membrane surface, and it has been shown as well that the presence of Chol enhances it (14). The fluorescence emission of the peptide in buffer had a maximum at 344 nm, typical for Trp in a polar environment, whereas in the presence of liposomes it decreased to 333 nm, implying binding of the peptide to the membrane bilayer (a low-polarity environment was sensed by Trp). These results were further corroborated when the Trp fluorescence intensity of the E2_{FP} peptide increased when the lipid/peptide ratio was increased, indicating a significant change in the environment of the Trp moiety of the peptide (Fig. 2A). From fitting, K_p values in the range 10^5 – 10^6 were obtained for different phospholipid compositions (Table 1), indicating that the peptide was bound to the membrane surface with very high affinity (39,45–47). Slightly higher K_p values were obtained for negatively charged phospholipid-containing bilayers; the E2_{FP} peptide has a positive net formal charge, so that an electrostatic effect might be the reason to observe higher- K_p -value compositions containing negatively charged phospholipids. Furthermore, in the presence of model membranes, the anisotropy values of the peptide Trp increased upon increasing the lipid/peptide ratio, with the limiting value being ~ 0.125 for liver membranes (not shown), indicating a significant motional restriction of the Trp moieties of the peptide at a relatively high lipid/protein ratio (30). We have also used the electrostatic surface potential probe FPE

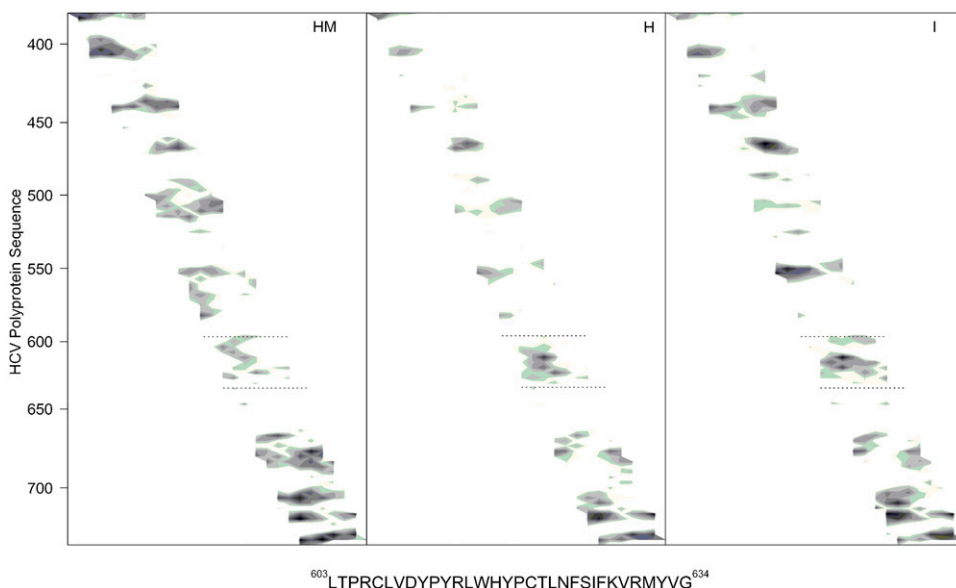


FIGURE 1 Hydrophobic moment (*HM*), hydrophobicity (*H*), and interfaciality (*I*) distributions for HCV E2 envelope glycoprotein (19), assuming it forms an α -helical wheel (71). Only positive bilayer-to-water transfer free-energy values are shown (the darker, the greater). The residue numbers are indicated at the left. The sequence of the E2_{FP} peptide studied in this work is shown and highlighted in the figure with dotted lines.

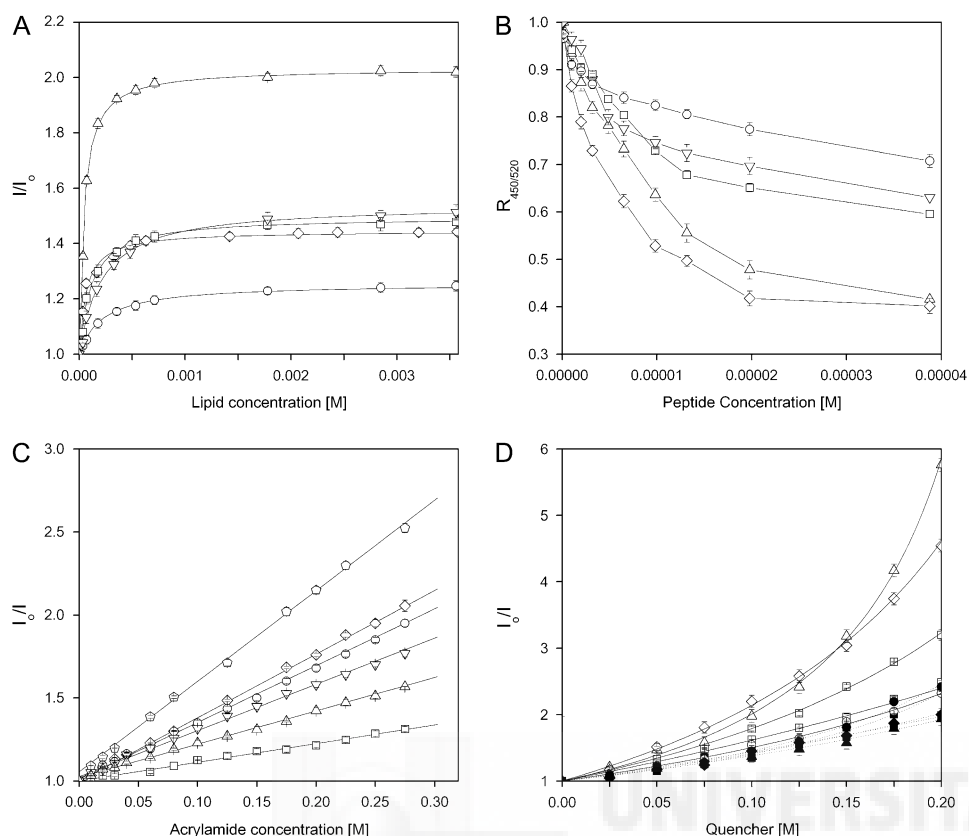


FIGURE 2 (A) Determination of the partition constant, K_p , of E2_{FP} through the change of the intrinsic tryptophan fluorescence in the presence of increasing lipid concentrations. (B) Effect of E2_{FP} on the membrane dipole potential monitored through the fluorescence ratio (R) of di-8-ANEPPS. (C) Stern-Volmer plots of the quenching of the Trp fluorescence emission of E2_{FP} by acrylamide. (D) Depth-dependent quenching of the Trp fluorescence emission of E2_{FP} by 5NS (solid symbols) and 16NS (open symbols) in LUVs. Peptide in buffer is represented in B as an open pentagon. LUVs were composed of EPC/Chol at a molar ratio of 5:1 (○), BPS/Chol at a molar ratio of 5:1 (◇), EPG/Chol at a molar ratio of 5:1 (□), EPA/Chol at a molar ratio of 5:1 (△) and liver extract lipids (▽). In C and D, the lipid/peptide ratio was 100:1, whereas the lipid concentration was 200 μ M in B–D. Vertical bars indicate standard deviations of the mean of triplicate samples.

(48) to monitor the binding of the E2_{FP} peptide to model membranes composed of different lipid compositions at different lipid/peptide ratios (not shown). Supporting the previous data, E2_{FP} had a high affinity for model membranes, higher for liposomes composed of the liver lipid extract than for the others. Changes in the membrane dipole potential magnitude elicited by E2_{FP} were monitored by means of the spectral shift of the fluorescence probe di-8-ANEPPS (37,49,50). The variation of the fluorescence intensity ratio $R_{450/520}$ normalized as a function of the peptide concentration for different membrane compositions is shown in Fig. 2 B. In the presence of the peptide, the greater decrease in $R_{450/520}$ value was measured in the presence of negatively charged lipid compositions, confirming again the presence of a specific interaction of the peptide with vesicles bearing negatively charged phospholipids.

We also studied the accessibility of the Trp residue of membrane-bound E2_{FP} peptide toward acrylamide, a neutral, water-soluble, highly efficient quenching molecule. The quenching data is presented in Fig. 2 C and the lower K_{SV} values obtained in the presence of lipids, compared with the measurements in their absence (Table 1), suggest that the E2_{FP} peptide is buried in the membrane, becoming less accessible for quenching by acrylamide. Linear Stern-Volmer plots are indicative of the Trp residue being accessible to acrylamide, and in all cases, the quenching of the peptide Trp residues showed acrylamide-dependent concentration behavior. It is interesting that the K_{SV} values in the presence of EPG- and EPA-containing vesicles were slightly lower than in the presence of the other vesicles, indicating that the peptide was slightly more buried inside the membrane in the presence of those phospholipids. The transverse location

TABLE 1 Partition coefficients, Stern-Volmer quenching constants, and maximal leakage, hemifusion, and fusion values at a phospholipid/peptide ratio of 15:1 for the E2_{FP} peptide incorporated in LUVs of different compositions

LUV compositions	K_p (Trp)	K_{sv} (M^{-1}) Acrylamide	K_{sv} (M^{-1}) 5NS	K_{sv} (M^{-1}) 16NS	Leakage (max %)	Hemifusion (max %)	Fusion (max %)
EPG/Chol, 5:1	4.85×10^5	1.124	4.44435	3.119	100	100	59
EPA/Chol, 5:1	1.24×10^6	2.006	2.69487	1.708	100	100	55
BPS/Chol, 5:1	8.6×10^5	3.826	5.65617	1.979	100	100	56
EPC/Chol, 5:1	2.49×10^5	3.418	2.16296	0.550	78	69	50
Liver extract	2.57×10^5	2.782	3.84889	0.131	46	46	40
E2 _{FP} in buffer	—	5.456	—	—	—	—	—

(penetration) of the E2_{FP} peptide into the lipid bilayer was evaluated by monitoring the relative quenching of the fluorescence of the Trp residues by the lipophylic spin probes 5NS and 16NS when the peptide was incorporated into vesicles with different phospholipid compositions (Fig. 2 D and Table 1). It can be seen that, in general and for each one of the different membrane compositions studied, the E2_{FP} peptide was quenched more efficiently by 5NS, a quencher for molecules near or at the interface, than by 16NS, a quencher for molecules buried deep in the membrane, suggesting that E2_{FP} remained close to the lipid/water interface.

To further explore the effect of the E2_{FP} peptide in the destabilization of membrane vesicles, we studied their effect on the release of encapsulated fluorophores in model membranes of various compositions. The extent of leakage observed at different peptide/lipid molar ratios and the effect on different phospholipid compositions is shown in Fig. 3 A (see also Table 1). The E2_{FP} peptide induced the highest percentage of leakage (leakage values between 90 and 100%), even at lipid/peptide ratios as high as 15:1, for liposomes containing negatively charged phospholipids (Fig. 3 A). Lower, but significant, leakage values were obtained for liposomes composed of EPC alone, EPC plus Chol, EPC plus TPE, and EPC/SM/Chol at a molar ratio of 52:18:30, since at a lipid/peptide ratio of 30:1, leakage values >60% were observed. Liposomes composed of lipid liver extract and liposomes composed of EPC/SM/Chol at a molar ratio of 5:1:1 were the ones that elicited the lowest leakage values, i.e., ~50% (Fig. 3 A). The induction of outer-monolayer lipid mixing (hemifusion) by the E2_{FP} peptide was tested with several types of vesicles utilizing the probe dilution assay (27,28), and the results are shown in Fig. 3 B. The higher hemifusion values were found for liposomes containing negatively charged phospholipids (liposomes containing EPG, EPA, and BPS), as well as liposomes containing TPE, which showed high hemifusion values near 100% at a lipid/peptide molar ratio of 5:1. Lower hemifusion values were

observed for liposomes containing either EPC or EPC plus Chol (~78% leakage). Liposomes containing complex mixtures of lipids, i.e., the liver extract and EPC/SM/Chol, showed ~40% leakage at the lowest lipid/peptide molar ratio used. It is interesting that liposomes containing LPC displayed the least leakage values (~20%). Inner-monolayer lipid-mixing (fusion) results induced by the E2_{FP} peptide in liposomes of different compositions are shown in Fig. 3 C. In contrast to the results shown above, the highest fusion values were found for the complex mixture containing EPC/SM/Chol at a molar ratio of 52:18:30 (leakage values of ~70% at a lipid/peptide molar ratio of 5:1) Leakage values between 60% and 50% were found for liposomes containing negatively charged phospholipids, as well as for liposomes containing TPE, whereas leakage values between 50% and 40% were found for liposomes composed of EPC, either pure or with added Chol, EPC/SM/Chol at a molar ratio of 5:1:1, and liposomes composed of the liver lipid extract.

The effect of the E2_{FP} peptide on the structural and thermotropic properties of phospholipid membranes was investigated by measuring the steady-state fluorescence anisotropy of the fluorescent probes DPH and TMA-DPH (51–53) incorporated into model membranes composed of saturated synthetic phospholipids as a function of temperature (Fig. 4). In general, E2_{FP} was capable of decreasing the cooperativity of the transition T_m for all phospholipids, as observed by both types of probes. With respect to the anisotropy, at temperatures above, but not below, the T_m for liposomes composed of DMPG, E2_{FP} induced a greater increase in the anisotropy values for DPH (Fig. 4 B) than for TMA-DPH (Fig. 4 A). This effect was similar to that found for DMPA (Fig. 4, C and D), DMPC (Fig. 4, E and F) and the complex mixture EPC/SM/Chol at a molar ratio of 5:1:1 (Fig. 4, G and H). In contrast, there was no significant change in the anisotropy either below or above T_m for DEPE liposomes (Fig. 4, I and J). These data would suggest that E2_{FP} was capable of decreasing the mobility of the phospholipid acyl chains when compared to the

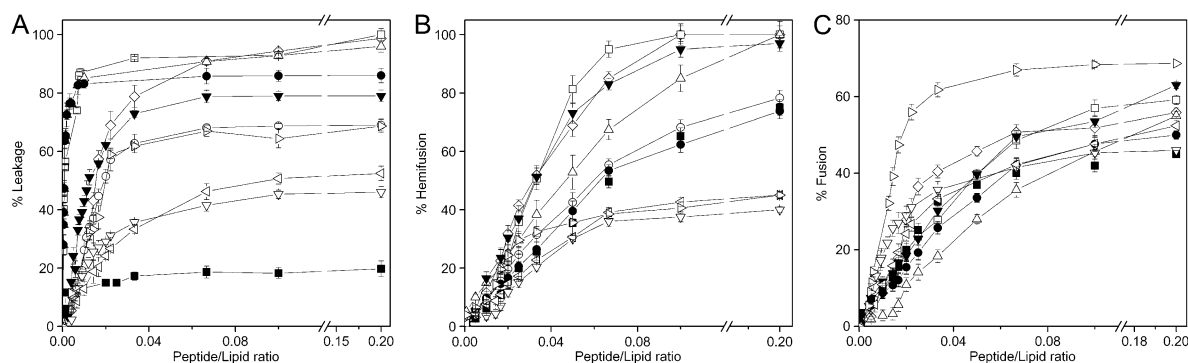


FIGURE 3 Effect of the E2_{FP} peptide on (A) membrane rupture, i.e., leakage, (B) membrane phospholipid mixing of the outer monolayer, i.e., hemifusion, and (C) membrane phospholipid mixing of the inner monolayer, i.e., fusion, of fluorescent probes encapsulated in LUVs containing different lipid compositions at different lipid/peptide molar ratios. The lipid compositions used were EPC/Chol at a molar ratio of 5:1 (○), BPS/Chol at a molar ratio of 5:1 (◇), EPG/Chol at a molar ratio of 5:1 (□), EPA/Chol at a molar ratio of 5:1 (△), liver extract lipids (▽), EPC/SM/Chol at a molar ratio of 5:1:1 (◁), EPC/SM/Chol at a molar ratio of 52.18.30 (◊), EPC (●), EPC/LPC at a molar ratio of 5:1 (■), and EPC/TPE at a molar ratio of 5:1 (▼).

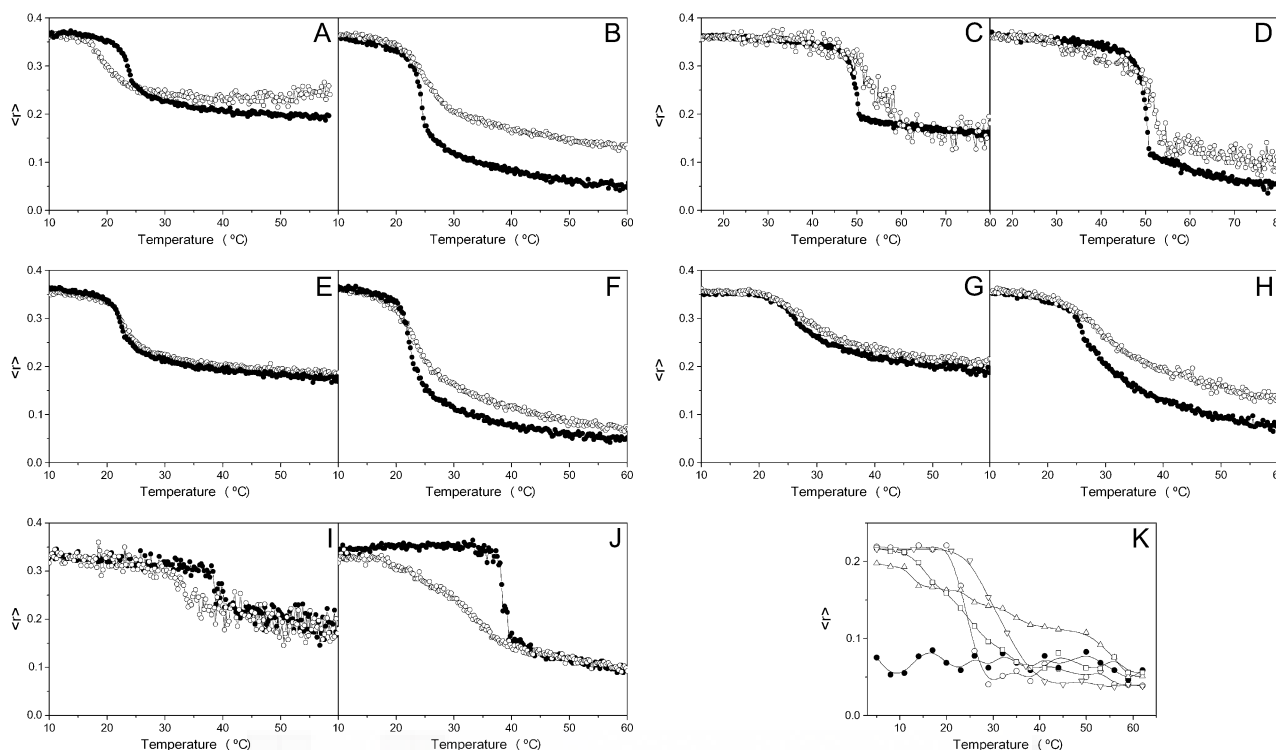


FIGURE 4 Steady-state anisotropy, $\langle r \rangle$, as a function of temperature of TMA-DPH (A, C, E, G, and I) and DPH (B, D, F, H, and J) incorporated into MLVs composed of DMPG (A and B), DMPA (C and D), DMPC (E and F), EPC/SM/Chol at a lipid molar ratio of 5:1:1 (G and H), and DEPE (I and J). Data correspond to vesicles in the absence (●) and presence (○) of the E2_{FP} peptide. (K) Intrinsic steady-state anisotropy of the E2_{FP} peptide as a function of temperature in solution (●) and incorporated into MLVs composed of DMPC (○), DMPA (△), DMPG (□), and DEPE (▽). The peptide/lipid molar ratio in all cases was 1:15.

pure phospholipid (except in the case of DEPE). These results suggest that the E2_{FP} peptide, although interacting with the membrane, should be located at the lipid-water interface, and that its incorporation should not be affected significantly by differences in headgroup charge (41). It is of interest that E2_{FP} is capable of decreasing significantly the cooperativity of DEPE (Fig. 4, I and J; see below). We have also studied the intrinsic anisotropy of the peptide Trp residues in the presence of liposomes composed of pure synthetic phospholipids (Fig. 4 K). In solution, the anisotropy value was ~ 0.3 along the whole range of temperatures studied. However, in the presence of the phospholipids, the anisotropy values differed depending on temperature: they were higher below the T_m of each specific phospholipid, but lower above it (Fig. 4 K). More important, the change in anisotropy occurred coincidentally when the main gel-to-liquid phase transition of the phospholipids took place; these data implied, first, that the peptide was effectively incorporated into the membrane palisade, and, second, that the peptide was capable of sensing the phase transition of each one of the phospholipids.

It is well known that the capability of phosphatidylethanolamines in general, and DEPE in particular, to display, apart from the main gel-to-liquid crystalline phase transition, L_β - L_α , a liquid-to-hexagonal phase transition, L_α - H_{II} (54). To observe any effect of E2_{FP} on the phase polymorphism

behavior of DEPE, we have assayed the thermotropic phase behavior of DEPE by differential scanning calorimetry (DSC) (Fig. 5 A). As observed in Fig. 5 A, pure DEPE displays the main gel-to-liquid crystalline phase transition at $\sim 38^\circ\text{C}$, whereas the lamellar-to-hexagonal phase transition is observed at $\sim 64^\circ\text{C}$ (54). In the presence of the peptide at a lipid/peptide molar ratio of 50:1, the main gel-to-liquid crystalline transition was broadened and slightly shifted to lower temperatures, whereas the liquid-to-hexagonal phase transition was completely abolished (Fig. 5 A). ^{31}P NMR spectrometry, sensitive to local motion and orientation of the phosphate group in membrane phospholipids (55), is suitable for following structural changes in membranes. DEPE and other phosphatidylethanolamines, when organized in bilayer structures, give rise to an asymmetrical ^{31}P NMR line shape with a high-field peak and a low-field shoulder, presenting a residual chemical shift anisotropy, $\Delta\sigma$, of 36–40 ppm in the gel state and 27–30 ppm in the liquid-crystalline state (Fig. 5 B). In the H_{II} phase, the chemical shift anisotropy is further averaged due to rapid lateral diffusion of the phospholipid around the tubes of which this phase is composed, resulting in a line-shape with reverse symmetry, i.e., a high-field shoulder and a low-field peak, accompanied by a twofold reduction in the absolute value of $\Delta\sigma$ (Fig. 5 B). This is the behavior we found for pure DEPE as expected (Fig. 5 B).

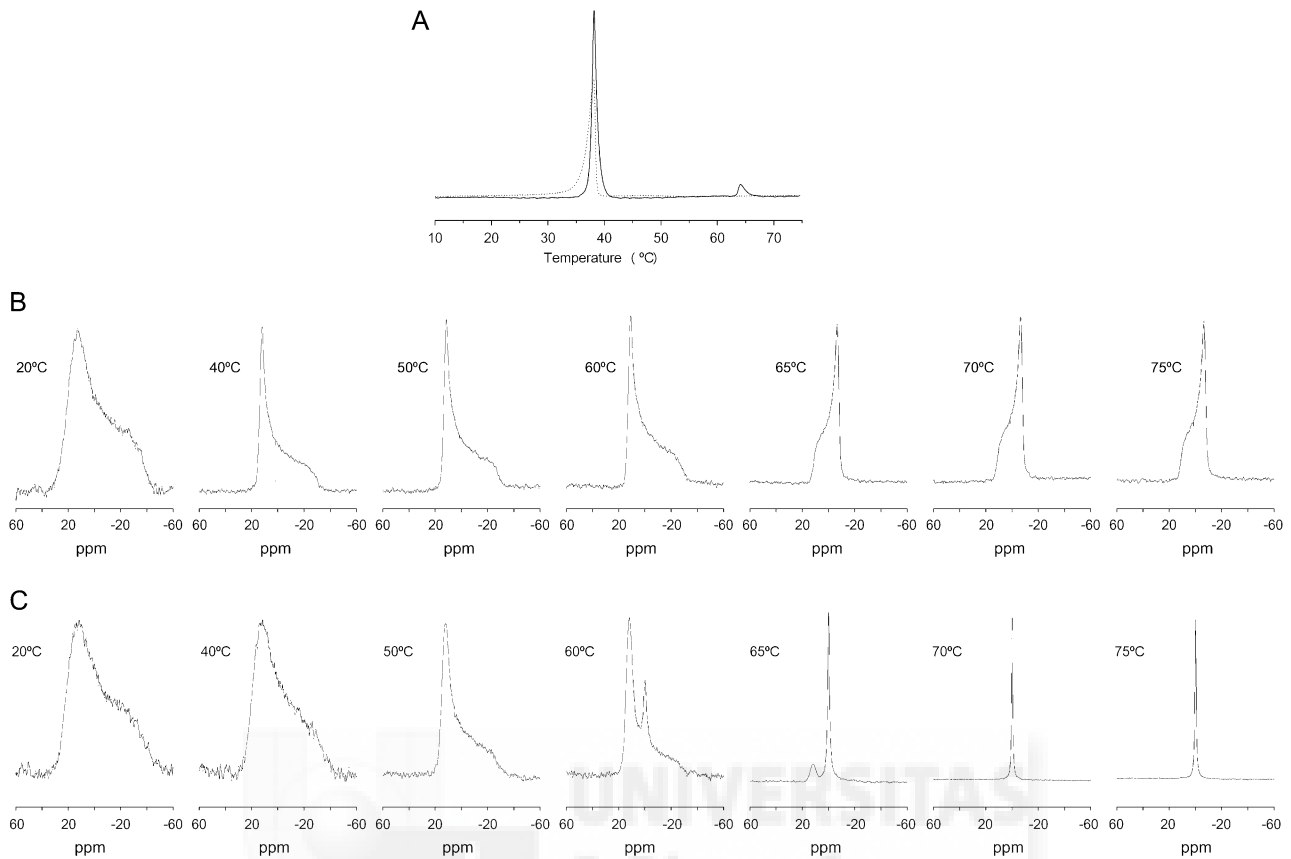


FIGURE 5 (A) DSC heating thermograms of DEPE in the absence (solid line) and presence (dashed line) of the E2_{FP} peptide. (B and C) ³¹P NMR spectra of DEPE phospholipid dispersions in the absence (B) and presence (C) of the E2_{FP} peptide at a phospholipid/peptide molar ratio of 15:1 at different temperatures, as stated. The ³¹P NMR spectra have been normalized.

However, when E2_{FP} was added to attain a lipid/peptide molar ratio of 50:1, the NMR profile of DEPE was completely different, since, beginning at ~60°C, an isotropic peak at 0 ppm was apparent. This peak, which should correspond to another phase induced by the presence of the E2_{FP} peptide (see below), increased in intensity at increasing temperatures, being the only component present at high temperatures (Fig. 5 C).

Information on the structural organization of DEPE and DEPE in the presence of E2_{FP} was obtained by the use of SAXD. This technique defines the nanoscopic structure and provides the interlamellar repeat distance in the lamellar phase, which comprises both the bilayer and the water layer thickness. The diffraction patterns of pure DEPE and DEPE in the presence of E2_{FP} are shown in Fig. 6. The figure illustrates the diffraction patterns collected at 25°C, 45°C, and 70°C, i.e., in the L_β, in the L_α, and in the H_{II} phases, respectively, for pure DEPE (Fig. 6, A–C, respectively). In the presence of the peptide, the diffraction patterns showed an increase in membrane disorder, and also indicated that several bilayers had become positionally uncorrelated due to the peptide's presence; at the same time, the scattering and the fluctuation increased, and the membranes showed a slight

increase in membrane thickness (from 66 Å and 54 Å in the absence of peptide to 69 Å and 59 Å in its presence, at 25°C and 45°C, respectively). Pure DEPE, when organized in the hexagonal H_{II} structure, showed a first-order diffraction at 66 Å; however, the presence of the E2_{FP} peptide induced the disappearance of the reflections characteristic of the phospholipid in the hexagonal phase (Fig. 6 C). The new pattern observed in the presence of the peptide showed the occurrence of a lamellar structure with a spacing and membrane thickness similar to that found in the L_α phase at 45°C.

The existence of structural changes on the E2_{FP} peptide induced by membrane binding was studied by analyzing the infrared amide I' band located between 1700 and 1600 cm⁻¹ in membranes by Fourier transformed infrared spectroscopy. The amide I' band of the peptide in the presence of DMPC, DMPG, and DMPA in D₂O buffer at a lipid/peptide molar ratio of 15:1 displayed a maximum at 1626 cm⁻¹, 1621 cm⁻¹, and 1618 cm⁻¹, respectively (not shown in the interests of brevity). The maximum of the band did not change significantly upon increasing the temperature (not shown), which suggests a high degree of conformational stability of the peptide in solution. The assignment of the amide I' component bands to specific structural features has been described

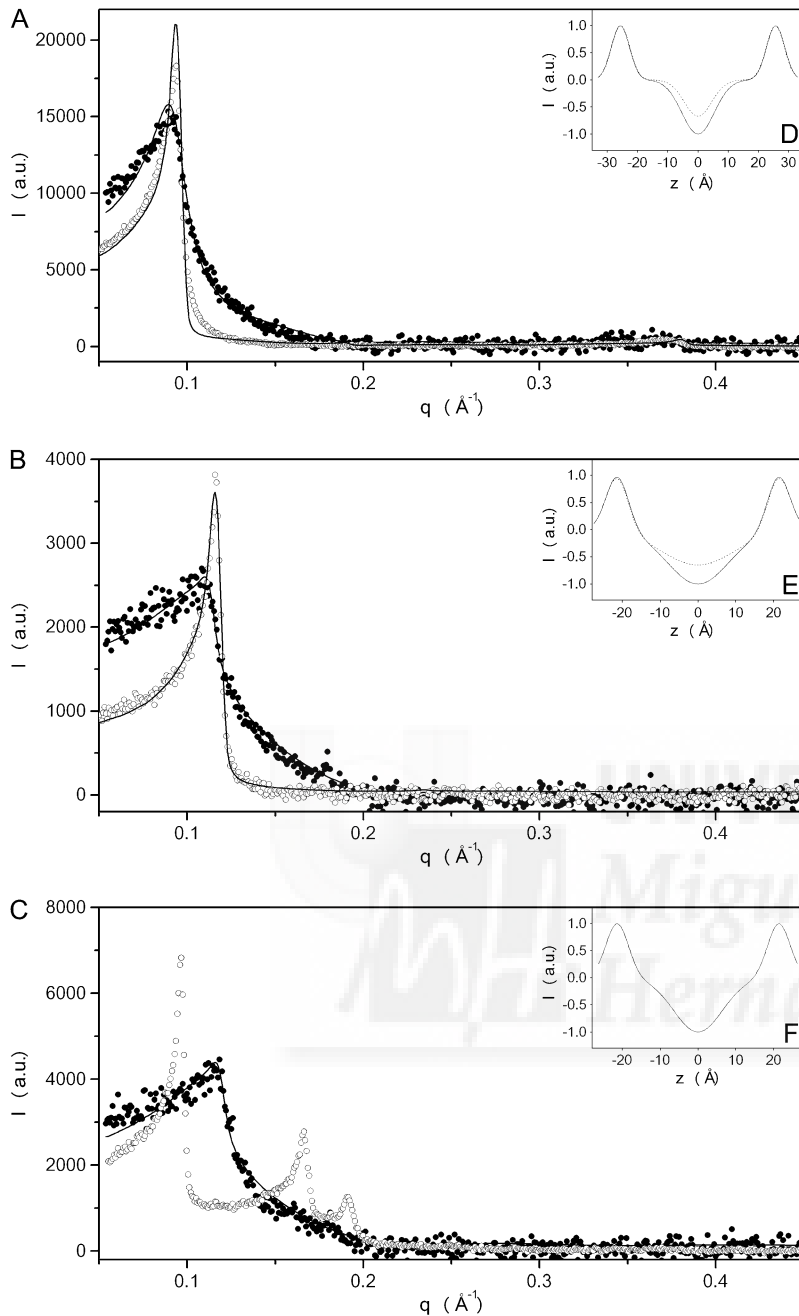


FIGURE 6 Small angle x-ray scattering of DEPE MLV suspension in the absence (○) and presence (●) of the E2_{FP} peptide in (A) the gel phase at 25°C, (B) the crystalline liquid phase at 45°, and (C) the hexagonal phase at 70°. Solid lines represent the best fit to the SAXD data applying a global analysis technique. The insets (D–F) display the one-dimensional electron density profiles along the bilayer normal calculated from the SAXD diffraction patterns in the absence (dotted lines) and presence (solid lines) of the peptide.

previously (45). Bands at $\sim 1620\text{--}1626\text{ cm}^{-1}$ would correspond to either β -sheet structures or self-aggregated peptides forming a intermolecular network of hydrogen-bonded β -structures or both (56), so that those structures should be the main ones of E2_{FP} in the presence of membranes.

DISCUSSION

The fusion of viral and cellular membranes, the critical early events in viral infection, are mediated by class I and II envelope fusion glycoproteins located on the outer surface of the viral membranes (21,57–60). Whereas class I membrane

fusion proteins possess a fusion peptide at or near the amino terminus that is critical for fusion, a pair of extended α -helices and, generally, a cluster of aromatic amino acids proximal to a hydrophobic transmembrane domain, class II fusion proteins possess an internal fusion peptide located at a distal location from the transmembrane anchor, as well as different domains comprised mostly of antiparallel β -sheets (58,61). Although their three-dimensional structure is different, their function is identical, and therefore they must share structural and/or functional characteristics in the specific domains, which interact with and disrupt biological membranes (13,61,62). It is known that both HCV E1 and E2 envelope

glycoproteins are essential for receptor binding, host-cell entry, and membrane fusion, but their specific roles in the different processes of the viral life cycle are not known (8,15,44,57,63). The E1/E2 heterodimer is thought to be the functional unit, and low pH would induce its dissociation leading to homooligomerization of the active form of the fusion protein (15,63–65). It is already known that, apart from the fusion peptide and the pre- and transmembrane domains, there exist other membranotropic segments along the sequence of membrane fusion proteins which, under a concerted action, are essential for membrane fusion (20). In this context, several hydrophobic patches have been identified in both E1 and E2 envelope glycoproteins which might be important in the mechanism of membrane fusion, not only for modulating membrane binding and interaction, but also for protein-protein interaction (17–19,44,66). These regions should be decisive for membrane fusion to take place, since destabilization of the lipid bilayer and membrane fusion are the result of the binding and interaction of these segments with biological membranes. Recently, it was shown that different segments from E2 participate in the viral fusion process, one of them a segment comprised by residues 600–620 (15). As we showed in a previous work, one of the most membranotropic regions of E2 belongs to the region comprising residues 603–634 (19). In that work, we analyzed the effect of two peptide libraries from HCV E1 and E2 on leakage, hemifusion, and fusion, using model membranes composed of EPC/SM/Chol and liver extract lipids. In this work, we have made an in-depth study of peptide E2_{FP}, which is the combination of the sequence of the previously studied peptides ⁶⁰³-LTPRCLVDYPYRLWHYPC-⁶²⁰, ⁶¹⁰-DYPYRLWHYPCTLNFSIF-⁶²⁷, and ⁶¹⁷-HYPCTLNFSIFKVRMYVG-⁶³⁴. In this context, the work described here is the natural extension of the previous study, since we have studied the binding and interaction of a new peptide, peptide E2_{FP}, with membrane model systems composed not only of EPC/SM/Chol and liver extract lipids, but also of phospholipids containing specific hydrocarbon acyl chains and headgroups, as well as phospholipids inducing both negative and positive bilayer curvature. We describe leakage, hemifusion, and fusion induced by peptide E2_{FP}, but also its binding, transverse location, aggregation state, and phospholipid polymorphic phase behavior, as well as its structure in the presence of a number of model membrane systems. It should be noted also that this E2 region includes the sequence 613–618, which is supposed to be involved in CD81 binding, and E1/E2 and E2/E2 dimerization (15). Therefore, we present here the results of the study of the interaction of a peptide derived from this region, the E2_{FP} peptide, with model membrane systems.

Peptide E2_{FP} is one of the most membranotropic sequences of HCV E2; accordingly, the E2_{FP} peptide studied in this work displays a high binding constant to model membranes having different phospholipid compositions, as has been found for other peptides (39,46). After binding, the Trp res-

idue of the peptide resides in an environment with a low dielectric constant, showing a significant motional restriction. E2_{FP} showed a slightly higher affinity for anionic-phospholipid compositions than for those containing zwitterionic phospholipids; this difference should be due to the fact that the peptide has a positive net charge at pH 7.4. The existence of a specific interaction with liposomes containing negatively charged phospholipids was corroborated by the change of the dipole potential at the membrane surface, as well as by hydrophilic and lipophilic probe quenching, suggesting that the E2_{FP} peptide was effectively incorporated in the membranes, located in a shallow position but nearer to the interface in the presence of zwitterionic phospholipids than in the presence of negatively charged ones. Nevertheless, the E2_{FP} peptide is capable of binding with high affinity to model membranes containing both negatively charged and zwitterionic phospholipids.

The E2_{FP} peptide was also capable of disrupting the membrane bilayer, causing the release of fluorescent probes. This effect is dependent on lipid composition and on the lipid/peptide molar ratio. The highest effect was observed for liposomes containing negatively charged phospholipids, but leakage values observed for liposomes composed of zwitterionic phospholipids, although lower, were also significant. Although the specific disrupting effect should be due primarily to hydrophobic interactions within the bilayer, the specific charge of the phospholipid headgroups affect the extent of membrane leakage, albeit slightly. The induction of hemifusion and fusion by E2_{FP} were also studied, and similar results were obtained: specific and large membrane hemifusion and fusion values were found in the presence of liposomes composed of both negatively charged and zwitterionic phospholipids. It is interesting that liposomes containing TPE (phospholipid inducing negative curvature) displayed relatively high hemifusion and fusion values, whereas liposomes containing LPC (phospholipid inducing positive curvature) were the ones that elicited the lowest values. This inhibitory effect produced by inverted-cone-shaped phospholipids has been previously observed in some viral and nonviral fusion systems (67–70). This effect could be due to the fact that E2_{FP}, located at the bilayer interface and interacting with the phospholipid headgroups, could be capable of changing the polymorphic phase behavior of the membrane bilayer, since it was able to inhibit the presence of hexagonal phases but induce the presence of other lamellar phases (isotropic ³¹P-NMR signal, but lamellar SAXD diffraction pattern). As observed by SAXD, the presence of the peptide increased slightly the membrane thickness and increased the disorder of the membrane. The increase in the membrane thickness, the increase in lateral tension within the membrane, and the packing stress could disorder the lipid molecules in a way that could be detected by NMR as an isotropic signal. These data reveal that E2_{FP} affects the fluidity behavior of the phospholipids in the membrane, suggesting, as commented previously, that the E2_{FP} peptide,

although interacting with the membrane, should be located at the lipid-water interface (41).

We have also shown that E2_{FP} peptide is capable of affecting the steady-state fluorescence anisotropy of fluorescent probes located in the palisade structure of the membrane, since the peptide, in general, was able of decreasing the mobility of the phospholipid acyl chains above but not below the T_m when compared to the pure phospholipids. It is significant that the peptide sensed the phospholipid main phase transition, indicating its incorporation into the palisade structure of the membrane. The infrared spectra of the amide I' region of the fully hydrated peptide did not change with temperature, indicating a high stability of its conformation, where extended β -strands with strong intermolecular interactions predominated. The binding to the surface and the modulation of the phospholipid biophysical properties that take place when E2_{FP} is bound to the membrane, i.e., partitioning into the membrane surface and perturbation of the bilayer architecture, could be related to the conformational changes that might occur during the activity of the HCV E2 glycoprotein. For all assayed phospholipids, and at increasing peptide concentrations, we observed a decrease in cooperativity and mobility. These features would indicate that E2_{FP} would interact with the membrane through both electrostatic and hydrophobic effects, and that it would be adsorbed at the membrane interface; however, it is possible that part of the peptide could be inserted deeper than the membrane interface, in this way increasing the membrane permeability, as we have already shown. These and previous data suggest the notion that the E2 region where E2_{FP} resides might be a fusion determinant and have an essential role in the membrane fusion process. If that is true, it would imply that both HCV E1 and E2 glycoproteins are directly implicated in the mechanism that makes possible the entry of the HCV virus into its cellular host: in this way, fusion peptides would be implicated in the very first steps of membrane fusion, whereas other membranotropic segments would be implicated in membrane destabilization, pore formation, and enlargement. All these sequences should be attractive candidates for antiviral drug development, since they could be targets for antiviral compounds that may lead to new vaccine strategies

This work was supported by grant BFU2005-00186-BMC (Ministerio de Ciencia y Tecnología, Madrid, Spain) to J.V. A.J.P. and J.G. are recipients of predoctoral fellowships from the Autonomous Government of the Comunidad Valenciana, Valencia, Spain.

REFERENCES

- Chen, S. L., and T. R. Morgan. 2006. The natural history of hepatitis C virus (HCV) infection. *Int. J. Med. Sci.* 3:47–52.
- Penin, F., J. Dubuisson, F. A. Rey, D. Moradpour, and J. M. Pawlowsky. 2004. Structural biology of hepatitis C virus. *Hepatology*. 39:5–19.
- Tan, S. L., A. Pause, Y. Shi, and N. Sonenberg. 2002. Hepatitis C therapeutics: current status and emerging strategies. *Nat. Rev. Drug Discov.* 1:867–881.
- Qureshi, S. A. 2007. Hepatitis C virus: biology, host evasion strategies, and promising new therapies on the horizon. *Med. Res. Rev.* 27:353–373.
- Reed, K. E., and C. M. Rice. 2000. Overview of hepatitis C virus genome structure, polyprotein processing, and protein properties. *Curr. Top. Microbiol. Immunol.* 242:55–84.
- Vauloup-Fellous, C., V. Pene, J. Garraud-Aunis, F. Harper, S. Bardin, Y. Suire, E. Pichard, A. Schmitt, P. Sogni, G. Pierron, P. Briand, and A. R. Rosenberg. 2006. Signal peptide peptidase-catalyzed cleavage of hepatitis C virus core protein is dispensable for virus budding but destabilizes the viral capsid. *J. Biol. Chem.* 281:27679–27692.
- Pozzetto, B., T. Bourlet, F. Grattard, and L. Bonneval. 1996. Structure, genomic organization, replication and variability of hepatitis C virus. *Nephrol. Dial. Transplant.* 11(Suppl. 4):2–5.
- Bartosch, B., J. Dubuisson, and F. L. Cosset. 2003. Infectious hepatitis C virus pseudo-particles containing functional E1–E2 envelope protein complexes. *J. Exp. Med.* 197:633–642.
- Cocquerel, L., J. C. Meunier, A. Pillez, C. Wychowski, and J. Dubuisson. 1998. A retention signal necessary and sufficient for endoplasmic reticulum localization maps to the transmembrane domain of hepatitis C virus glycoprotein E2. *J. Virol.* 72:2183–2191.
- Cocquerel, L., C. Wychowski, F. Minner, F. Penin, and J. Dubuisson. 2000. Charged residues in the transmembrane domains of hepatitis C virus glycoproteins play a major role in the processing, subcellular localization, and assembly of these envelope proteins. *J. Virol.* 74:3623–3633.
- Cocquerel, L., A. Op de Beeck, M. Lambot, J. Roussel, D. Delgrange, A. Pillez, C. Wychowski, F. Penin, and J. Dubuisson. 2002. Topological changes in the transmembrane domains of hepatitis C virus envelope glycoproteins. *EMBO J.* 21:2893–2902.
- Op De Beeck, A., R. Montserret, S. Duvet, L. Cocquerel, R. Cacan, B. Barberot, M. Le Maire, F. Penin, and J. Dubuisson. 2000. The transmembrane domains of hepatitis C virus envelope glycoproteins E1 and E2 play a major role in heterodimerization. *J. Biol. Chem.* 275:31428–31437.
- Garry, R. F., and S. Dash. 2003. Proteomics computational analyses suggest that hepatitis C virus E1 and pestivirus E2 envelope glycoproteins are truncated class II fusion proteins. *Virology*. 307:255–265.
- Lavillette, D., B. Bartosch, D. Nourrisson, G. Verney, F. L. Cosset, F. Penin, and E. I. Pecheur. 2006. Hepatitis C virus glycoproteins mediate low pH-dependent membrane fusion with liposomes. *J. Biol. Chem.* 281:3909–3917.
- Lavillette, D., E. I. Pecheur, P. Donot, J. Fresquet, J. Molle, R. Corbau, M. Dreux, F. Penin, and F. L. Cosset. 2007. Characterization of fusion determinants points to the involvement of three discrete regions of both E1 and E2 glycoproteins in the membrane fusion process of hepatitis C virus. *J. Virol.* 81:8752–8765.
- Bartosch, B., and F. L. Cosset. 2006. Cell entry of hepatitis C virus. *Virology*. 348:1–12.
- Yagnik, A. T., A. Lahm, A. Meola, R. M. Roccasecca, B. B. Ercole, A. Nicosia, and A. Tramontano. 2000. A model for the hepatitis C virus envelope glycoprotein E2. *Proteins*. 40:355–366.
- Roccasecca, R., H. Ansuini, A. Vitelli, A. Meola, E. Scarselli, S. Acali, M. Pezzanera, B. B. Ercole, J. McKeating, A. Yagnik, A. Lahm, A. Tramontano, R. Cortese, and A. Nicosia. 2003. Binding of the hepatitis C virus E2 glycoprotein to CD81 is strain specific and is modulated by a complex interplay between hypervariable regions 1 and 2. *J. Virol.* 77:1856–1867.
- Perez-Berna, A. J., M. R. Moreno, J. Guillen, A. Bernabeu, and J. Villalain. 2006. The membrane-active regions of the hepatitis C virus E1 and E2 envelope glycoproteins. *Biochemistry*. 45:3755–3768.
- Peisajovich, S. G., and Y. Shai. 2003. Viral fusion proteins: multiple regions contribute to membrane fusion. *Biochim. Biophys. Acta.* 1614:122–129.
- Epand, R. M. 2003. Fusion peptides and the mechanism of viral fusion. *Biochim. Biophys. Acta.* 1614:116–121.

22. Surewicz, W. K., H. H. Mantsch, and D. Chapman. 1993. Determination of protein secondary structure by Fourier transform infrared spectroscopy: a critical assessment. *Biochemistry*. 32:389–394.
23. Zhang, Y. P., R. N. Lewis, R. S. Hodges, and R. N. McElhaney. 1992. FTIR spectroscopic studies of the conformation and amide hydrogen exchange of a peptide model of the hydrophobic transmembrane α -helices of membrane proteins. *Biochemistry*. 31:11572–11578.
24. Mayer, L. D., M. J. Hope, and P. R. Cullis. 1986. Vesicles of variable sizes produced by a rapid extrusion procedure. *Biochim. Biophys. Acta*. 858:161–168.
25. Böttcher, C. S. F., C. M. Van Gent, and C. Fries. 1961. A rapid and sensitive sub-micro phosphorus determination. *Anal. Chim. Acta*. 1061: 203–204.
26. Edelhoch, H. 1967. Spectroscopic determination of tryptophan and tyrosine in proteins. *Biochemistry*. 6:1948–1954.
27. Struck, D. K., D. Hoekstra, and R. E. Pagano. 1981. Use of resonance energy transfer to monitor membrane fusion. *Biochemistry*. 20:4093–4099.
28. Meers, P., S. Ali, R. Erukulla, and A. S. Janoff. 2000. Novel inner monolayer fusion assays reveal differential monolayer mixing associated with cation-dependent membrane fusion. *Biochim. Biophys. Acta*. 1467:227–243.
29. Sainz, B., Jr., J. M. Rausch, W. R. Gallaher, R. F. Garry, and W. C. Wimley. 2005. Identification and characterization of the putative fusion peptide of the severe acute respiratory syndrome-associated coronavirus spike protein. *J. Virol.* 79:7195–7206.
30. Lakowicz, J. 1999. Principles of Fluorescence Spectroscopy. Kluwer-Plenum Press, New York.
31. Eftink, M. R., and C. A. Ghiron. 1977. Exposure of tryptophanyl residues and protein dynamics. *Biochemistry*. 16:5546–5551.
32. Castanho, M., and M. Prieto. 1995. Filipin fluorescence quenching by spin-labeled probes: studies in aqueous solution and in a membrane model system. *Biophys. J.* 69:155–168.
33. Wardlaw, J. R., W. H. Sawyer, and K. P. Ghiggino. 1987. Vertical fluctuations of phospholipid acyl chains in bilayers. *FEBS Lett.* 223:20–24.
34. Santos, N. C., M. Prieto, and M. A. Castanho. 1998. Interaction of the major epitope region of HIV protein gp41 with membrane model systems. A fluorescence spectroscopy study. *Biochemistry*. 37:8674–8682.
35. Wall, J., F. Ayoub, and P. O'Shea. 1995. Interactions of macromolecules with the mammalian cell surface. *J. Cell Sci.* 108:2673–2682.
36. Golding, C., S. Senior, M. T. Wilson, and P. O'Shea. 1996. Time resolution of binding and membrane insertion of a mitochondrial signal peptide: correlation with structural changes and evidence for cooperativity. *Biochemistry*. 35:10931–10937.
37. Cladera, J., and P. O'Shea. 1998. Intramembrane molecular dipoles affect the membrane insertion and folding of a model amphiphilic peptide. *Biophys. J.* 74:2434–2442.
38. Gross, E., R. S. Bedlack, Jr., and L. M. Loew. 1994. Dual-wavelength ratiometric fluorescence measurement of the membrane dipole potential. *Biophys. J.* 67:208–216.
39. Bernabeu, A., J. Guillen, A. J. Perez-Berna, M. R. Moreno, and J. Villalain. 2007. Structure of the C-terminal domain of the pro-apoptotic protein Hrk and its interaction with model membranes. *Biochim. Biophys. Acta*. 1768:1659–1670.
40. Giudici, M., J. A. Poveda, M. L. Molina, L. de la Canal, J. M. Gonzalez-Ros, K. Fuller, U. Fuller, and J. Villalain. 2006. Antifungal effects and mechanism of action of viscotoxin A3. *FEBS J.* 273:72–83.
41. Contreras, L. M., F. J. Aranda, F. Gavilanes, J. M. Gonzalez-Ros, and J. Villalain. 2001. Structure and interaction with membrane model systems of a peptide derived from the major epitope region of HIV protein gp41: implications on viral fusion mechanism. *Biochemistry*. 40:3196–3207.
42. Laggner, P. 1994. X-ray diffraction on biomembranes with emphasis on lipid moiety. *Subcell. Biochem.* 23:451–491.
43. Pabst, G. 2006. Global properties of biomimetic membranes: perspectives on molecular features. *Biophys. Rev. Lett.* 1:57–84.
44. Drummer, H. E., and P. Poubourios. 2004. Hepatitis C virus glycoprotein E2 contains a membrane-proximal heptad repeat sequence that is essential for E1E2 glycoprotein heterodimerization and viral entry. *J. Biol. Chem.* 279:30066–30072.
45. Pascual, R., M. Contreras, A. Fedorov, M. Prieto, and J. Villalain. 2005. Interaction of a peptide derived from the N-heptad repeat region of gp41 Env ectodomain with model membranes. Modulation of phospholipid phase behavior. *Biochemistry*. 44:14275–14288.
46. Moreno, M. R., J. Guillen, A. J. Perez-Berna, D. Amoros, A. I. Gomez, A. Bernabeu, and J. Villalain. 2007. Characterization of the interaction of two peptides from the N terminus of the NHR domain of HIV-1 gp41 with phospholipid membranes. *Biochemistry*. 46: 10572–10584.
47. Pascual, R., M. R. Moreno, and J. Villalain. 2005. A peptide pertaining to the loop segment of human immunodeficiency virus gp41 binds and interacts with model biomembranes: implications for the fusion mechanism. *J. Virol.* 79:5142–5152.
48. Wall, J., C. A. Golding, M. Van Veen, and P. O'Shea. 1995. The use of fluoresceinphosphatidylethanolamine (FPE) as a real-time probe for peptide-membrane interactions. *Mol. Membr. Biol.* 12:183–192.
49. Cladera, J., I. Martin, and P. O'Shea. 2001. The fusion domain of HIV gp41 interacts specifically with heparan sulfate on the T-lymphocyte cell surface. *EMBO J.* 20:19–26.
50. O'Shea, P. 2003. Intermolecular interactions with/within cell membranes and the trinity of membrane potentials: kinetics and imaging. *Biochem. Soc. Trans.* 31:990–996.
51. Davenport, L., R. E. Dale, R. H. Bisby, and R. B. Cundall. 1985. Transverse location of the fluorescent probe 1,6-diphenyl-1,3,5-hexatriene in model lipid bilayer membrane systems by resonance excitation energy transfer. *Biochemistry*. 24:4097–4108.
52. Lentz, B. R. 1993. Use of fluorescent probes to monitor molecular order and motions within liposome bilayers. *Chem. Phys. Lipids*. 64: 99–116.
53. Pebay-Peyroula, E., E. J. Dufourc, and A. G. Szabo. 1994. Location of diphenyl-hexatriene and trimethylammonium-diphenyl-hexatriene in dipalmitoylphosphatidylcholine bilayers by neutron diffraction. *Biophys. Chem.* 53:45–56.
54. Epand, R. M. 1998. Lipid polymorphism and protein-lipid interactions. *Biochim. Biophys. Acta*. 1376:353–368.
55. Killian, J. A., and B. de Kruijff. 1986. The influence of proteins and peptides on the phase properties of lipids. *Chem. Phys. Lipids*. 40: 259–284.
56. Arrondo, J. L., and F. M. Goni. 1999. Structure and dynamics of membrane proteins as studied by infrared spectroscopy. *Prog. Biophys. Mol. Biol.* 72:367–405.
57. Kielian, M. 2006. Class II virus membrane fusion proteins. *Virology*. 344:38–47.
58. Kielian, M., and F. A. Rey. 2006. Virus membrane-fusion proteins: more than one way to make a hairpin. *Nat. Rev. Microbiol.* 4:67–76.
59. Eckert, D. M., and P. S. Kim. 2001. Mechanisms of viral membrane fusion and its inhibition. *Annu. Rev. Biochem.* 70:777–810.
60. Blumenthal, R., M. J. Clague, S. R. Durell, and R. M. Epand. 2003. Membrane fusion. *Chem. Rev.* 103:53–69.
61. Schibli, D. J., and W. Weissenhorn. 2004. Class I and class II viral fusion protein structures reveal similar principles in membrane fusion. *Mol. Membr. Biol.* 21:361–371.
62. Gallo, S. A., C. M. Finnegan, M. Viard, Y. Raviv, A. Dimitrov, S. S. Rawat, A. Puri, S. Durell, and R. Blumenthal. 2003. The HIV Env-mediated fusion reaction. *Biochim. Biophys. Acta*. 1614:36–50.
63. Ciczora, Y., N. Callens, F. Penin, E. I. Pecheur, and J. Dubuisson. 2007. Transmembrane domains of hepatitis C virus envelope glycoproteins: residues involved in E1E2 heterodimerization and involvement of these domains in virus entry. *J. Virol.* 81:2372–2381.
64. Ciczora, Y., N. Callens, C. Montpellier, B. Bartosch, F. L. Cosset, A. Op de Beeck, and J. Dubuisson. 2005. Contribution of the charged residues of hepatitis C virus glycoprotein E2 transmembrane domain

- to the functions of the E1E2 heterodimer. *J. Gen. Virol.* 86:2793–2798.
65. Keck, Z. Y., A. Op De Beeck, K. G. Hadlock, J. Xia, T. K. Li, J. Dubuisson, and S. K. Fong. 2004. Hepatitis C virus E2 has three immunogenic domains containing conformational epitopes with distinct properties and biological functions. *J. Virol.* 78:9224–9232.
66. Brazzoli, M., A. Helenius, S. K. Fong, M. Houghton, S. Abrignani, and M. Merola. 2005. Folding and dimerization of hepatitis C virus E1 and E2 glycoproteins in stably transfected CHO cells. *Virology.* 332:438–453.
67. Stiasny, K., and F. X. Heinz. 2004. Effect of membrane curvature-modifying lipids on membrane fusion by tick-borne encephalitis virus. *J. Virol.* 78:8536–8542.
68. Baljinnyam, B., B. Schroth-Diez, T. Korte, and A. Herrmann. 2002. Lysolipids do not inhibit influenza virus fusion by interaction with hemagglutinin. *J. Biol. Chem.* 277:20461–20467.
69. Chernomordik, L., E. Leikina, M. S. Cho, and J. Zimmerberg. 1995. Control of baculovirus gp64-induced syncytium formation by membrane lipid composition. *J. Virol.* 69:3049–3058.
70. Gaudin, Y. 2000. Rabies virus-induced membrane fusion pathway. *J. Cell Biol.* 150:601–612.
71. Guillen, J., A. J. Perez-Berna, M. R. Moreno, and J. Villalain. 2005. Identification of the membrane-active regions of the severe acute respiratory syndrome coronavirus spike membrane glycoprotein using a 16/18-mer peptide scan: implications for the viral fusion mechanism. *J. Virol.* 79:1743–1752.



Publicación 5

The pre-transmembrane region of the HCV E1 envelope glycoprotein Interaction with model membranes

A. J. Pérez-Berná¹, A. Bernabeu¹, J. Guillén¹, M. R.
Moreno¹, and J. Villalaín¹

¹Instituto de Biología Molecular y Celular, Universidad “Miguel
Hernández”, Elche-Alicante, Spain

Biochimica et Biophysica Acta





Contents lists available at ScienceDirect

Biochimica et Biophysica Acta

journal homepage: www.elsevier.com/locate/bbamem

The pre-transmembrane region of the HCV E1 envelope glycoprotein Interaction with model membranes

Ana J. Pérez-Berná, Angela Bernabeu, Miguel R. Moreno, Jaime Guillén, José Villalain *

Instituto de Biología Molecular y Celular, Edf. Torregaitán, Campus de Elche, Universidad "Miguel Hernández", E-03202 Elche-Alicante, Spain

ARTICLE INFO

Article history:

Received 29 January 2008
Received in revised form 22 March 2008
Accepted 24 March 2008
Available online xxxx

Keywords:

Peptide–lipid interaction
E1 glycoprotein
HCV
Pre-transmembrane

ABSTRACT

The previously identified membranotropic regions of the HCV E1 envelope glycoprotein, a class II membrane fusion protein, permitted us to identify different sequences which might be implicated in viral membrane fusion, membrane interaction and/or protein–protein binding. HCV E1 glycoprotein presents a membranotropic region immediately adjacent to the transmembrane segment, which could be involved in membrane destabilization similarly to the pre-transmembrane domains of class I fusion proteins. Consequently, we have carried out a study of the binding and interaction with the lipid bilayer of a peptide corresponding to segment 309–340, peptide E1_{PTM}, as well as the structural changes which take place in both the peptide and the phospholipid molecules induced by the binding of the peptide to the membrane. Here we demonstrate that peptide E1_{PTM} strongly partitions into phospholipid membranes, interacts with negatively-charged phospholipids and locates in a shallow position in the membrane. These data support its role in HCV-mediated membrane fusion and suggest that the mechanism of membrane fusion elicited by class I and II fusion proteins might be similar.

© 2008 Elsevier B.V. All rights reserved.

1. Introduction

Hepatitis C virus (HCV) has an important impact on public health since it is the leading cause of acute and chronic liver disease, such as chronic hepatitis, cirrhosis, and hepatocellular carcinoma [1–3]. The HCV genome is widely heterogeneous and replication errors cause a high rate of mutations [4]. There exists no vaccine to prevent HCV infection and current therapeutic agents have limited efficacy against the virus [5]. The variability of the HCV proteins gives the virus the ability to escape the host immune surveillance system and notably

hampers the development of an efficient vaccine. The HCV genome encodes a polyprotein precursor that is cleaved by host and viral proteases to yield ten mature structural and non-structural proteins [6]. HCV entry into the cell is achieved by the fusion of viral and cellular membranes, and morphogenesis and budding has been suggested to take place in the endoplasmic reticulum, ER [7]. Therefore, the viral region implicated in fusion to and/or budding from the cells must interact with the membrane and should be a conserved sequence. Thus, finding inhibitors of protein–membrane and protein–protein interactions involved in virus fusion and/or budding could be an alternative and valuable strategy against HCV infection since they could be potential therapeutic agents.

The fusion of viral and cellular membranes, the critical early events in viral infection, are mediated by class I, II and III envelope fusion glycoproteins located on the outer surface of the viral membranes [8–12]. Whereas class I membrane fusion proteins possess a fusion peptide at or near the amino terminus, a pair of extended α -helices and, generally, a cluster of aromatic amino acids proximal to a hydrophobic transmembrane domain, class II fusion proteins possess an internal fusion peptide located at a distal location from the transmembrane anchor, as well as different domains comprised mostly of antiparallel β -sheets [9,13]. Class III fusion proteins have features in common to both class I and II proteins [14]. Their three dimensional structure is different but their function is identical, so that they must share structural and functional characteristics in specific domains which interact with and disrupt biological membranes [13,15,16]. HCV E1 and E2 envelope glycoproteins are essential for receptor binding, host cell entry and membrane fusion,

Abbreviations: 5NS, 5-Doxyl-stearic acid; 16NS, 16-Doxyl-stearic acid; BPS, Bovine brain L- α -phosphatidylserine; CF, 5-Carboxyfluorescein; Chol, Cholesterol; di-8-ANEPPS, 4-(2-(6-(Diocetyl amino)-(2-naphthalenyl)-(ethenyl)-1-(3-sulfopropyl)-pyridinium inner salt; DMPA, 1,2-Dimyristoyl-*sn*-glycero-phosphatidic acid; DMPC, 1,2-Dimyristoyl-*sn*-glycero-phosphatidylcholine; DMPG, 1,2-Dimyristoyl-*sn*-glycero-phosphatidylglycerol; DMPS, 1,2-Dimyristoyl-*sn*-glycero-3-phosphatidylserine; DPH, 1,6-Diphenyl-1,3,5-hexatriene; EPA, Egg L- α -phosphatidic acid; EPC, Egg L- α -phosphatidylcholine; EPG, Egg L- α -phosphatidylglycerol; ER, Endoplasmic reticulum; FD10/20, Fluorescein isothiocyanate dextran with an average molecular weight of 10,000/20,000; FPE, fluorescein-phosphatidylethanolamine; HCV, Hepatitis C virus; HIV, Human immunodeficiency virus; LPC, Lyso- α -phosphatidylcholine; LUV, Large Unilamellar Vesicles; MLV, Multilamellar Vesicles; NBD-PE, N-(7-Nitrobenz-2-oxa-1,3-diazol-4-yl)-1,2-dihexadecanoyl-*sn*-glycero-phosphoethanolamine; N-RhB-PE, Lissamine™ rhodamine B 1,2-dihexadecanoyl-*sn*-glycero-3-phosphoethanolamine; PTM, Pre-transmembrane domain; SM, Egg sphingomyelin; T_m , Temperature of the gel-to-liquid crystalline phase transition; TM, Transmembrane domain; TMA-DPH, 1-(4-trimethylammoniumphenyl)-6-phenyl-1,3,5-hexatriene; TPE, Egg trans-esterified L- α -phosphatidylethanolamine

* Corresponding author. Tel.: +34 966 658 762; fax +34 966 658 758.

E-mail address: jvillalain@umh.es (J. Villalain).

0005-2736/\$ – see front matter © 2008 Elsevier B.V. All rights reserved.
doi:10.1016/j.bbamem.2008.03.018

Please cite this article as: A.J. Pérez-Berná, et al., The pre-transmembrane region of the HCV E1 envelope glycoprotein, Biochimica et Biophysica Acta (2008), doi:10.1016/j.bbamem.2008.03.018

but their specific roles in the different processes of the viral life cycle are not known [8,17–20]. E1 and E2 are type I transmembrane (TM) glycoproteins, with an N-terminal ectodomain and a short C-terminal TM domain and assemble as non-covalent heterodimers. Their TM domains play a major role in the E1/E2 heterodimer formation, membrane anchoring, and ER retention [21–24]. The HCV envelope glycoproteins E1 and E2 are included in the class II fusion proteins, and the putative fusion peptide is localized in an internal sequence linked by antiparallel β -sheets [8,9]. The HCV membrane fusion process is pH-dependent, and low endosomal pH promotes the arrangement of E1/E2 to its active form [25]. Many aspects regarding the function and properties of both HCV E1 and E2 glycoproteins still remain unresolved; even so, the location of the fusion peptide is controversial since several data suggest that it could be located in either E1 or E2. Although previous data have proposed a direct role of HCV E1 on membrane fusion whereas HCV E2 should mediate the binding with receptor CD81 as well as be responsible of heterodimerization with E1, recent data suggest that indeed both E1 and E2 glycoproteins participate in the membrane fusion mechanism [17,25–28]. Several hydrophobic patches have been identified in both E1 and E2 envelope glycoproteins which might be important in the mechanism of membrane fusion, not only for modulating membrane binding and interaction, but also for protein–protein interaction [19,27–30].

Studies with a number of viral fusion proteins have showed that the region immediately adjacent to the membrane-spanning domain plays an essential role in the fusogenic activities of these proteins, being a common characteristic to viral fusion proteins of several virus families [31–33]. These pre-transmembrane (PTM) domains would function as promoters of membrane destabilization [34–36]. We have recently identified the membrane-active regions of the HCV E1 and E2 glycoproteins by observing the effect of E1 and E2 glycoprotein-derived peptide libraries on model membrane integrity [29]. These results have permitted us to suggest the possible location of different segments in these proteins which might be implicated in protein–lipid and protein–protein interactions. In particular, E1 presents three membranotropic segments encompassing approximately residues 265–296, 310–348 and 349–381 (Fig. 1) [16,20,29]. Segment 265–296 has been suggested to be the putative fusion peptide, whereas segment 349–381 defines the E1 TM domain. The region encompassing residues 310–348 is located immediately adjacent to the TM domain, presents a localized

high hydrophobic moment surface area and is capable of destabilizing model membranes. Although its sequence does not present a high content of aromatic amino acids as membrane fusion proteins of class I have, it could be involved in membrane destabilization similarly to the PTM domains of class I fusion proteins.

It is known that the mechanism by which proteins facilitate the formation of fusion intermediates is a complex process involving several segments of fusion proteins [11,37]. However, there are still many questions to be answered regarding the E1 and E2 mode of action in HCV and cell host membrane fusion. Since the PTM region of the HCV E1 envelope glycoprotein might take part in the fusion mechanism like the PTM regions found in other proteins, we have focused on the possible functional roles of the E1 PTM-like domain by an in-depth study of a peptide patterned after this domain, peptide E1_{PTM}. This peptide encompasses the 309–340 region of HCV E1 and is the combination of the sequence of peptides 18 (³⁰⁹-YPGHVSGHRMAWDMMMNW-³²⁶), 19 (³¹⁶-HRMAWDMMMNWSPTTALV-³³³) and 20 (³²³-MMNWSPTTALVVSQLLRI-³⁴⁰) from the original HCV E1 peptide library [29]. We have studied the binding and interaction of E1_{PTM} with the lipid bilayer, as well as the structural changes induced in both the peptide and phospholipid molecules upon membrane binding. We show that E1_{PTM} strongly partitions into phospholipid membranes, interacts with negatively-charged phospholipids and locates in a shallow position in the membrane. These results would suggest that the PTM domain of HCV E1 could be involved in the merging of the viral and target cell membranes working synergistically with other membrane-active regions of the protein.

2. Materials and methods

2.1. Materials and reagents

The peptide E1_{PTM} corresponding to the sequence ³⁰⁹-YPGHVSGHRMAWDMMMNWSPTTALVVSQLLRI-³⁴⁰ from HCV strain 1B4J, with N-terminal acetylation and C-terminal amidation, was obtained from Genemed Synthesis, San Francisco, Calif. The peptide E1_{PTM} was purified by reverse-phase HPLC to better than 95% purity, and its composition and molecular mass were confirmed by amino acid analysis and mass spectroscopy. Since trifluoroacetate has a strong

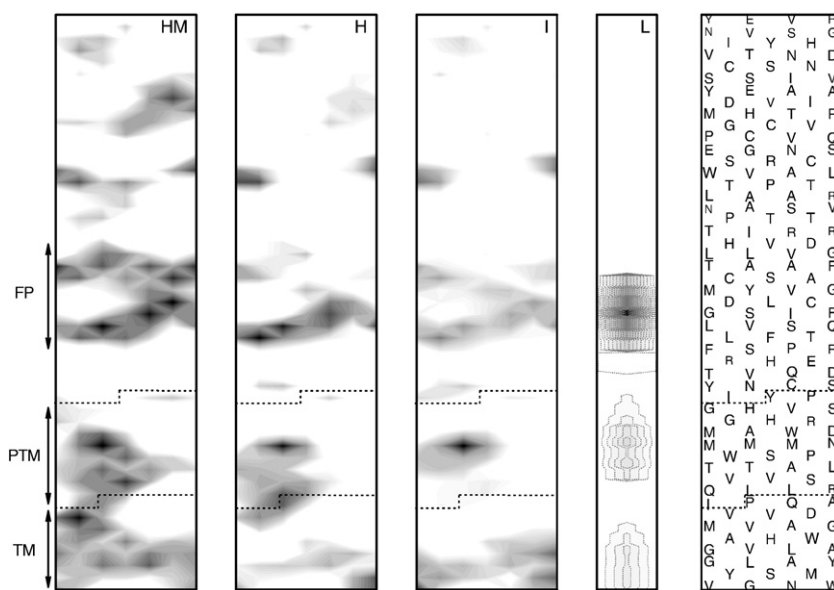


Fig. 1. Schematic view of the organization of the whole sequence of HCV E1 glycoprotein showing the approximate structural and functional regions (fusion peptide, FP, pre-transmembrane, PTM, and transmembrane, TM), as well as the corresponding hydrophobic moment (HM), hydrophobicity (H), interfaciality distribution (I), and experimental average leakage (L) (for details see Refs. [29,55]). Only positive bilayer-to-water transfer free-energy values are shown (the darker, the greater). The sequence of the E1_{PTM} peptide studied in this work is shown and highlighted in the figure with dotted lines.

infrared absorbance at approximately 1673 cm^{-1} , which interferes with the characterization of the peptide Amide I band [38], residual trifluoroacetic acid, used both in peptide synthesis and in the high-performance liquid chromatography mobile phase, was removed by several lyophilization/solubilisation cycles in 10 mM HCl [39]. Egg L- α -phosphatidylcholine (EPC), egg L- α -phosphatidic acid (EPA), lyso- α -phosphatidylcholine (LPC), egg trans-esterified L- α -phosphatidylethanolamine (TPE), egg sphingomyelin (SM), bovine brain L- α -phosphatidylserine (BPS), 1,2-dimyristoyl-*sn*-glycero-3-phosphocholine (DMPC), 1,2-dimyristoyl-*sn*-glycero-3-[phospho-*rac*-(1-glycerol)] (DMPG), 1,2-dimyristoyl-*sn*-glycero-3-[phospho-L-serine] (DMPS), 1,2-dimyristoyl-*sn*-glycero-3-phosphate (DMPA), cholesterol (Chol), liver lipid extract, lissamine rhodamine B 1,2-dihexadecanoyl-*sn*-glycero-3-phosphoethanolamine (N-RhB-PE), and *N*-(7-nitrobenz-2-oxa-1,3-diazol-4-yl)-1,2-dihexadecanoyl-*sn*-glycero-3-phosphatidylethanolamine (NBD-PE) were obtained from Avanti Polar Lipids (Alabaster, AL, USA). 5-Carboxyfluorescein, CF, (>95% by HPLC), fluorescein isothiocyanate labeled dextrans FD10 and FD20, 5-doxyl-stearic acid (5NS), 16-doxyl-stearic acid (16NS), sodium dithionite, deuterium oxide (99.9% by atom), Triton X-100, sodium dodecyl sulfate (SDS), EDTA, and HEPES were purchased from Sigma-Aldrich (Madrid, ES, EU). 1,6-Diphenyl-1,3,5-hexatriene (DPH), 1-(4-trimethylammoniumphenyl)-6-phenyl-1,3,5-hexatriene (TMA-DPH), fluorescein-phosphatidylethanolamine (FPE), and 4-(2-(6-(dioctylamino)-(2-naphthalenyl) (ethenyl)-1-(3-sulfopropyl)-pyridinium inner salt (di-8-ANEPPS) were obtained from Molecular Probes (Eugene, OR). All other reagents used were of analytical grade from Sigma-Aldrich (Madrid, ES, EU). Water was deionized, twice-distilled and passed through a Milli-Q equipment (Millipore Ibérica, Madrid, ES, EU) to a resistivity better than 18 M Ω cm.

2.2. Vesicle preparation

Aliquots containing the appropriate amount of lipid in chloroform/methanol (2:1, v/v) were placed in a test tube, the solvents removed by evaporation under a stream of O₂-free nitrogen, and finally, traces of solvents were eliminated under vacuum in the dark for more than 3 h. The lipid films were resuspended in an appropriate buffer and incubated either at 25 °C or 10 °C above the phase transition temperature (T_m) with intermittent vortexing for 30 min to hydrate the samples and obtain multilamellar vesicles (MLV). The samples were frozen and thawed five times to ensure complete homogenization and maximization of peptide/lipid contacts with occasional vortexing. Large unilamellar vesicles (LUV) with a mean diameter of 0.1 μm for CF leakage and 0.2 μm for dextran leakage, hemifusion and fusion experiments were prepared from multilamellar vesicles by the extrusion method [40] using polycarbonate filters with a pore size of 0.1 and 0.2 μm (Nuclepore Corp., Cambridge, CA, USA). The phospholipid and peptide concentrations were measured by methods described previously [41,42].

2.3. Membrane leakage measurement

LUVs with a mean diameter of 0.1 μm were prepared as indicated above in buffer containing 10 mM TRIS, 20 mM NaCl, pH 7.4, and either CF at a concentration of 40 mM or fluorescein-labeled dextran at a concentration of 100 mg/ml. Non-encapsulated CF or dextran were separated from the vesicle suspension through a filtration column containing Sephadex G-75 or Sephadex S500HR Sephacryl, respectively (Pharmacia, Uppsala, SW, EU), eluted with buffer containing 10 mM TRIS, 100 mM NaCl, and 0.1 mM EDTA, pH 7.4. Membrane rupture (leakage) of intraliposomal fluorescent probes was carried out using 5 mM \times 5 mm quartz cuvettes stabilized at 25 °C under constant stirring in a final volume of 400 μl (100 μM lipid concentration). Leakage was assayed until no more change in fluorescence was obtained. The fluorescence was measured using a Varian Cary Eclipse spectrofluorimeter. Changes in fluorescence intensity were recorded

with excitation and emission wavelengths set at 492 and 517 nm, respectively. Excitation and emission slits were set at 5 nm. The peptide, dissolved in buffer containing 5% trifluoroethanol, was added to attain the suitable peptide/lipid molar ratio. One hundred percent release was achieved by adding Triton X-100 to a final concentration of 0.5% (wt/wt). For details see Refs. [43,44].

2.4. Phospholipid-mixing measurement

Peptide-induced vesicle lipid mixing (hemifusion) was measured by resonance energy transfer [45]. This assay is based on the decrease in resonance energy transfer between two probes (NBD-PE and N-RhB-PE) when the lipids of the probe-containing vesicles are allowed to mix with lipids from vesicles lacking the probes. The concentration of each of the fluorescent probes within the liposome membrane was 0.6% mol. LUVs with a mean diameter of 0.2 μm were prepared as described above. Labeled and unlabeled vesicles in a proportion 1:4 were placed in a 5 mm \times 5 mm fluorescence cuvette at a final lipid concentration of 100 μM in a final volume of 400 μl , stabilized at 25 °C under constant stirring. The fluorescence was measured using a Varian Cary Eclipse fluorescence spectrometer using 467 nm and 530 nm for excitation and emission, respectively. Excitation and emission slits were set at 5 nm. Since labeled and unlabeled vesicles were mixed in a proportion of 1 to 4, respectively, 100% phospholipid-mixing was estimated with a liposome preparation in which the membrane concentration of each probe was 0.12%. Phospholipid-mixing was quantified on a percentage basis according to $\%PM = (F_f - F_0) / (F_{100} - F_0) \cdot 100$, F_f being the equilibrium value of fluorescence after peptide addition to a liposome mixture containing liposomes having 0.6% of each probe plus liposomes without any fluorescent probe, F_0 the initial fluorescence of the vesicles and F_{100} is the fluorescence value of the liposomes containing 0.12% of each probe. The peptide, dissolved in buffer containing 5% trifluoroethanol, was added to attain the suitable peptide/lipid molar ratio. Other experimental and measurement conditions were the same as indicated previously [44].

2.5. Inner-monolayer phospholipid-mixing (fusion) measurement

Peptide-induced phospholipid-mixing of the inner monolayer was measured by a modification of the phospholipid-mixing measurement stated above [46]. The concentration of each of the fluorescent probes within the liposome membrane was 0.6% mol. LUVs with a mean diameter of 0.2 μm were prepared as described above. LUVs were treated with sodium dithionite to completely reduce the NBD-labeled phospholipid located at the outer monolayer of the membrane. The final concentration of sodium dithionite was 100 mM (from a stock solution of 1 M dithionite in 1 M TRIS, pH 10.0) and incubated for approximately 1 h on ice in the dark. Sodium dithionite was then removed by size exclusion chromatography through a Sephadex G-75 filtration column (Pharmacia, Uppsala, Sweden) eluted with buffer containing 10 mM TRIS, 100 mM NaCl, and 1 mM EDTA, pH 7.4. The proportion of labeled and unlabeled vesicles, lipid concentration and other experimental and measurement conditions were the same as indicated above for the phospholipid-mixing assay.

2.6. Peptide binding to vesicles

The partitioning of the peptide into the phospholipid bilayer was monitored by the fluorescence enhancement of tryptophan. Fluorescence emission spectra were recorded in a SLM Aminco 8000C spectrofluorometer with excitation wavelength of 290 and a 4 nm spectral bandwidth. Measurements were carried out in 20 mM HEPES, 50 mM NaCl, and EDTA 0.1 mM, pH 7.4. Intensity values were corrected for dilution, and the scatter contribution was derived from lipid titration of a vesicle blank. The peptide, dissolved in buffer containing 5% trifluoroethanol, was added to attain the suitable

Table 1

Result of the alignment (CLUSTALW) of residues 309–340 from reference strains representing the six major genotypes of hepatitis C virus as well as the E1^{PTM} sequence examined in this work

Genotype	Virus strain	Sequence
1A	H77	YPGHITGHRMAWDMMNWSPPTAALVVAQLLRI
1B	HC-J4	YPGHLISGHRMA-DMMNWSPTTALVVSQQLLRI
1A	HC-TN	YPGHISGHRMAWDMMNWSPPTAALLVAQLLRI
2A	HC-J6	YPGTITGHRMAWDMMNWSPATMILAYAMRV
3A	S52	YPGHVSGHRMAWDMMNWSPAVGMVVAHILRL
4A	ED43	YTGHITGHRMAWDMMNWSPPTTLVLAQVMRI
5A	SA13	YSGHITGHRMAWDMMNWSPPTALVMAQLLRI
6A	HK	YIGHVTGHRMAWDMMNWSPPTTLVLSLILRV
	E1 ^{PTM}	YPGHVSGHRMAWDMMNWSPPTALVVSQQLLRI
2B	HC-J8	YQGHITGHRMAWDMMLWSPTLTMILAYAARV
Consensus sequence		* * : : * * * * * * * * : : * * : : : : * :

The consensus sequence is shown beneath the alignment.

peptide/lipid molar ratio. The data were analyzed as previously described [44].

2.7. Steady-state fluorescence anisotropy

MLVs were formed in 100 mM NaCl, 0.05 mM EDTA and 25 mM HEPES, pH 7.4. Aliquots of TMA-DPH or DPH in *N,N'*-dimethylformamide (2×10^{-4} M) were directly added into the lipid dispersion to obtain a probe/lipid molar ratio of 1/500. Samples were incubated for 15 or 60 min when TMA-DPH or DPH were used, respectively, 10 °C above the gel-to-liquid crystalline phase transition temperature T_m of the phospholipid mixture. Afterwards, the peptide dissolved in buffer containing 5% trifluoroethanol, was added to obtain a peptide/lipid molar ratio of 1:15 and incubated 10 °C above the T_m of each lipid for 1 h, with occasional vortexing. All fluorescence studies were carried using 5 mm × 5 mm quartz cuvettes in a final volume of 400 μ l (315 μ M lipid concentration). All the data were corrected for background intensities and progressive dilution. The steady-state fluorescence anisotropy, $\langle r \rangle$, was measured with an automated polarization accessory using a Varian Cary Eclipse fluorescence spectrometer, coupled to a Peltier device for automatic temperature change. The data were analyzed as previously described [44].

2.8. Fluorescence quenching of Trp emission by water-soluble and lipophilic probes

For acrylamide quenching assays, aliquots from a 4 M solution of the water-soluble quencher were added to the solution-containing peptide in the presence and absence of liposomes at a peptide/lipid molar ratio of 1:100. The results obtained were corrected for dilution and the scatter contribution was derived from acrylamide titration of a vesicle blank. The data were analyzed according to the Stern–Volmer equation [47], $I_0/I = 1 + K_{sv}[Q]$, where I_0 and I represent the fluorescence intensities in the absence and the presence of the quencher [Q], respectively, and K_{sv} is the Stern–Volmer quenching constant, which is a measure of the accessibility of Trp to acrylamide. Quenching studies with lipophilic probes were performed by successive addition of small amounts of 5NS or 16NS in ethanol to the samples of the peptide incubated with LUV. The final concentration of ethanol was kept below 2.5% (v/v) to avoid any significant bilayer alterations. After each addition an incubation period of 15 min was kept before the measurement. The data were analyzed as previously described [44].

2.9. Fluorescence measurements using FPE-labeled membranes

LUVs with a mean diameter of 0.1 μ m were prepared in buffer containing 10 mM TRIS-HCl, pH 7.4. The vesicles were labeled

exclusively in the outer bilayer leaflet with FPE as described previously [48]. Briefly, LUVs were incubated with 0.1 mol % FPE dissolved in ethanol (never more than 0.1% of the total aqueous volume) at 37 °C for 1 h in the dark. Any remaining unincorporated FPE was removed by gel filtration on a Sephadex G-25 column equilibrated with the appropriate buffer. FPE-vesicles were stored at 4 °C until use in an oxygen-

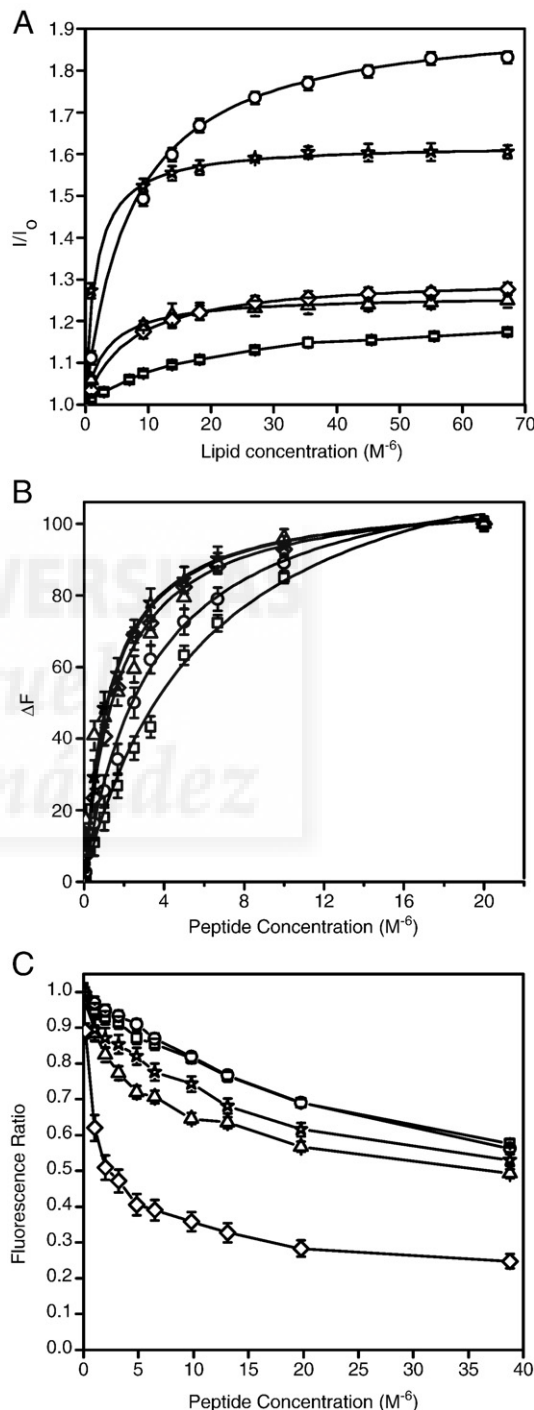


Fig. 2. (A) Determination of the partition constant, K_p , of E1^{PTM} through the change of the intrinsic tryptophan fluorescence in the presence of increasing lipid concentrations, (B) determination of the dissociation constant (K_d) of E1^{PTM} through the change of the fluorescence signal amplitude of FPE, and (C) Effect of E1^{PTM} on the membrane dipole potential monitored through the fluorescence ratio (R) of di-8-ANEPPS. The lipid compositions used were EPC/Chol at a molar ratio of 5:1 (\circ), BPS/Chol at a molar ratio of 5:1 (\diamond), EPG/Chol at a molar ratio of 5:1 (\star), EPA/Chol at a molar ratio of 5:1 (\triangle) and lipid liver extract (\square).

Table 2Partition coefficients, Stern–Volmer quenching constants and maximal leakage, hemifusion and fusion values for the E1_{PTM} peptide incorporated in LUVs of different compositions

LUV compositions	K_p Trp	K_d (μM) FPE	K_{sv} (M^{-1}) Acrylamide	K_{sv} (M^{-1}) 5-NS	K_{sv} (M^{-1}) 16-NS	Leakage (max%)	Hemifusion (max%)	Fusion (max%)
EPG/Chol 5:1	$4.40 \pm 0.1 \cdot 10^7$	$1.4 \pm 0.1 \cdot 10^6$	4.82	2.34	2.02	92	33	19
EPA/Chol 5:1	$1.60 \pm 0.1 \cdot 10^7$	$1.3 \pm 0.1 \cdot 10^6$	2.39	6.23	4.47	91	23	14
BPS/Chol 5:1	$8.03 \pm 0.5 \cdot 10^6$	$1.6 \pm 0.1 \cdot 10^6$	6.51	1.51	1.66	98	35	28
EPC/Chol 5:1	$7.10 \pm 0.4 \cdot 10^6$	$3.4 \pm 0.1 \cdot 10^6$	5.58	2.06	1.63	96	19	12
LIVER EXTRACT	$3.02 \pm 0.4 \cdot 10^6$	$6.2 \pm 0.2 \cdot 10^6$	8.43	7.85	3.76	45	15	9
EPC/TPE 4:1	–	–	–	–	–	61	50	39
EPC/LPC 4:1	–	–	–	–	–	100	98	45
E1 _{PTM} in buffer	–	–	17.87	–	–	–	–	–

free atmosphere. Fluorescence time courses of FPE-labeled vesicles were measured after the desired amount of peptide, dissolved in buffer containing 5% trifluoroethanol, was added into 400 μl of lipid suspensions (200 μM lipid) using a Varian Cary Eclipse fluorescence spectrometer. Excitation and emission wavelengths were set at 490 and 520 nm, respectively, using excitation and emission slits set at 5 nm. Temperature was controlled with a thermostatic bath at 25 °C. The contribution of light scattering to the fluorescence signals was measured in experiments without the dye and was subtracted from the fluorescence traces. Data were fitted either to a hyperbolic binding model [49] using the following equation, $F = (F_{\text{max}}[P]) / (K_d + [P])$, where F is the fluorescence variation, F_{max} the maximum fluorescence variation, $[P]$ the peptide concentration, and K_d the dissociation constant of the membrane binding process. The experimental points shown in the figures are the mean values of at least three measurements.

2.10. Measurement of the membrane dipole potential using Di-8-ANEPPS-labeled membranes

Aliquots containing the appropriate amount of lipid in chloroform-methanol (2:1 vol/vol) and di-8-ANEPPS were placed in a test tube to obtain a probe/lipid molar ratio of 1/100 and LUVs, with a mean diameter of 90 nm, were prepared as described previously. Steady-state fluorescence measurements were recorded with a Varian Cary Eclipse spectrofluorimeter. Dual wavelength recordings with the dye di-8-ANEPPS were obtained by exciting the samples at two different wavelengths (450 and 520 nm) and measuring their intensity ratio, $R_{450/520}$, at an emission wavelength of 620 nm [50,51]. Changes in the total membrane dipole moment cause a shift in the excitation spectrum maximum of di-8-ANEPPS. By exciting the membrane suspensions at two different wavelengths corresponding to the maximum and the minimum of the difference spectrum, a fluorescence intensity ratio R can be calculated, which can be used as a measure of the relative changes in the magnitude of the dipole potential. The fluorescence ratio R is defined as the ratio of the fluorescence intensity at an excitation wavelength of 450 nm divided by that at 520 nm. The peptide, dissolved in buffer containing 5% trifluoroethanol, was added to attain the suitable peptide/lipid molar ratio. The lipid concentration was 200 μM , and all experiments were performed at 25 °C.

2.11. Infrared spectroscopy

For infrared spectroscopy, liposomes prepared as above but in D₂O buffer, were added to a vial containing lyophilized peptide and resuspended with intermittent vortexing for 30 min. The samples were frozen and thawed five times to ensure complete homogenization and maximization of peptide/lipid contacts with occasional vortexing. Approximately 25 μl of a pelleted sample were placed between two CaF₂ windows separated by 50- μm thick Teflon spacers in a liquid demountable cell (Harrick, Ossining, NY). The spectra were obtained in a Bruker IFS55 spectrometer using a deuterated

triglycine sulfate detector. Each spectrum was obtained by collecting 200 interferograms with a nominal resolution of 2 cm^{-1} , transformed using triangular apodization and, in order to average background spectra between sample spectra over the same time period, a sample shuttle accessory was used to obtain sample and background spectra. The spectrometer was continuously purged with dry air at a dew point of -40 °C in order to remove atmospheric water vapor from the bands of interest. All samples were equilibrated at the lowest temperature for 20 min before acquisition. An external bath circulator, connected to the infrared spectrometer, controlled the sample temperature. For temperature studies, samples were scanned

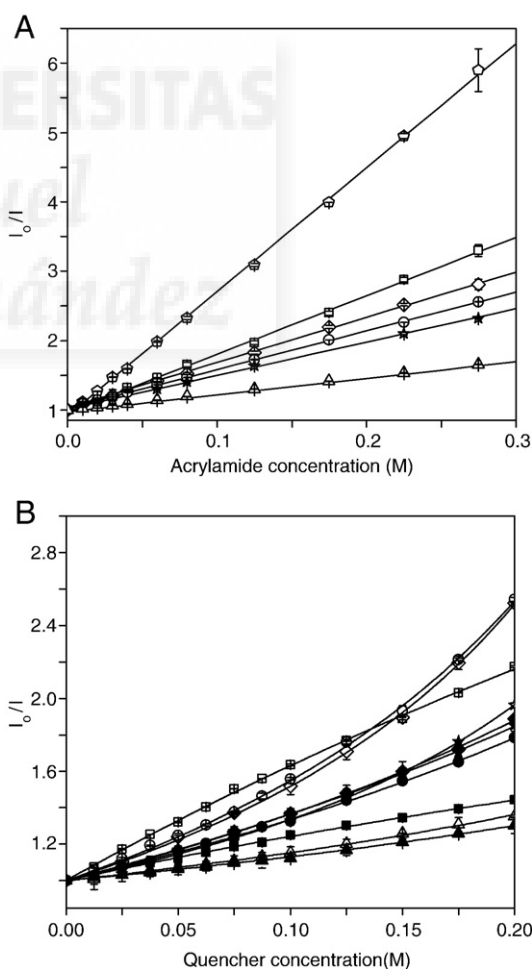


Fig. 3. Stern–Volmer plots of the quenching of the Trp fluorescence emission of E1_{PTM} by (A) acrylamide and (B) 5NS (filled symbols) and 16NS (empty symbols) in the presence of LUVs. Quenching of the Trp fluorescence emission by acrylamide in aqueous buffer (\circ) and in the presence of LUVs composed of EPC/Chol at a molar ratio of 5:1 (\bullet), BPS/Chol at a molar ratio of 5:1 (\diamond), EPG/Chol at a molar ratio of 5:1 (\star), EPA/Chol at a molar ratio of 5:1 (\triangle) and lipid liver extract (\square). The lipid to peptide ratio was 50:1.

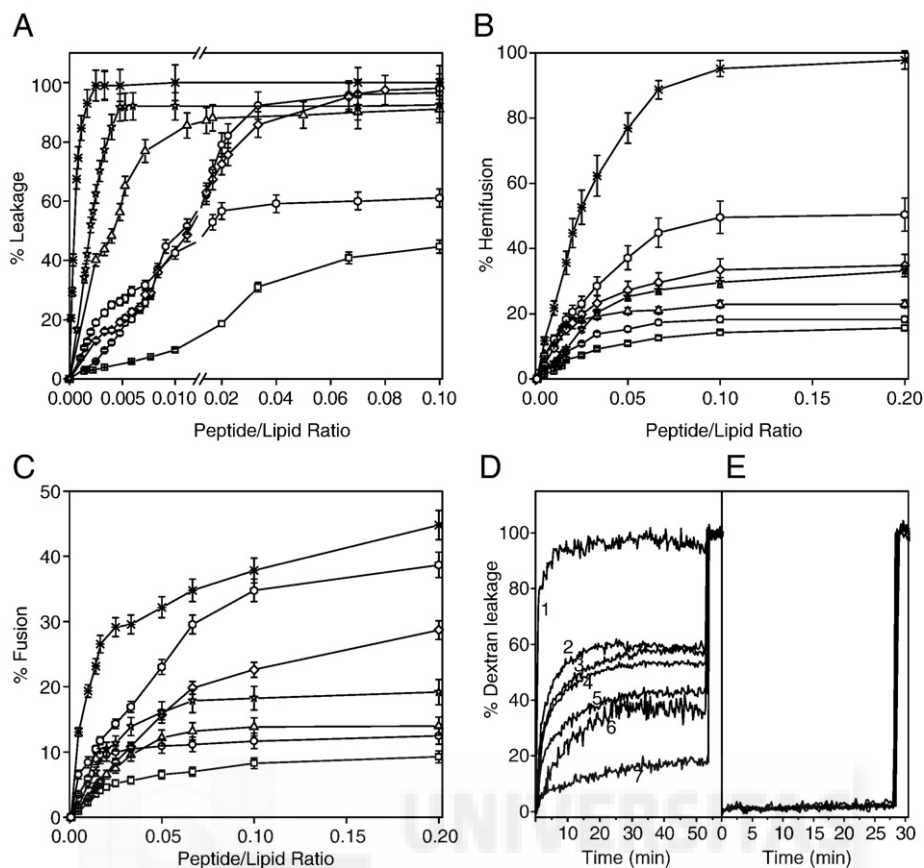


Fig. 4. Effect of the E1_{PTM} peptide on (A) membrane rupture, (B) hemifusion, (C) fusion of fluorescent probes encapsulated in LUVs containing different lipid compositions at different lipid-to-peptide molar ratios. The lipid compositions used were EPC/Chol at a molar ratio of 5:1 (○), BPS/Chol at a molar ratio of 5:1 (◇), EPG/Chol at a molar ratio of 5:1 (☆), EPA/Chol at a molar ratio of 5:1 (△), lipid liver extract (□), EPC/LPC at a molar ratio of 4:1 (∗) and EPC/TPE at a molar ratio of 4:1 (○). The lines connecting the experimental data are merely guides to the eye. Release of (D) FD10 and (E) FD20 after addition of the E1_{PTM} peptide from LUVs composed of (1) EPC/LPC at a molar ratio of 4:1, (2) EPG/Chol at a molar ratio of 5:1, (3) EPA/Chol at a molar ratio of 5:1, (4) BPS/Chol at a molar ratio of 5:1, (5) EPC/Chol at a molar ratio of 5:1, (6) lipid liver extract and (7) EPC/TPE at a molar ratio of 4:1. The lipid to peptide ratio was 15:1.

using 2 °C intervals and a 2-min delay between each consecutive scan. The data were analyzed as previously described [43,44].

2.12. Hydrophobic moment, hydrophobicity, and interfaciality

The hydrophobic moment calculations were carried out according to Eisenberg et al. [52] and the scale for calculating hydrophobic moments was taken from Engelman et al. [53]. Hydrophobicity and interfacial values, i.e., whole residue scales for the transfer of an amino acid of an unfolded chain into the membrane hydrocarbon palisade and the membrane interface respectively, have been obtained from http://blanco.biomol.uci.edu/hydrophobicity_scales.html [54]. Each specific value in the two-dimensional plot represents the mean of the values pertaining to the hydrophobic moment, hydrophobicity and interfaciality of the amino acid at that position and its neighbours [55]. Positive values correspond to positive bilayer-to-water transfer free-energy values and therefore, the higher the value, the greater the probability to interact with the membrane surface and/or the hydrophobic core.

3. Results

The HCV E1 envelope glycoprotein is thought to be responsible for the membrane fusion process whereas the HCV E2 envelope glycoprotein is thought to mediate the binding to the host cell, although other roles could not be ruled out [17,19,25]. In Fig. 1 we present the analysis of the hydrophobic moment, hydrophobicity and interfaciality distribution along the E1 envelope glycoprotein sequence of HCV_1B4J strain as-

suming it forms an α -helical wheel along the whole sequence [29]. Although the E1 and E2 HCV envelope glycoproteins are supposed to be class II membrane fusion proteins and therefore their α -helix content should not be as high as that of class I membrane fusion proteins, these data display the potential surface zones that could be implicated in the modulation of membrane binding and/or protein interaction. As we have shown previously, HCV E1 includes a highly membranotropic region immediately adjacent to the E1 TM domain (Fig. 1). As shown in Table 1, this region is significantly conserved among the major genotypes of HCV. Since this region, similarly to other pre-transmembrane regions of other fusion proteins, could be important in the membrane fusion process [56], we present here the results of the study of the interaction of a peptide derived from this region with model membranes, the E1_{PTM} peptide, comprising residues 309–340 (Fig. 1). Peptide E1_{PTM} has been patterned after peptides 18 (³⁰⁹-YPGHVSGHR-MAWDMMMNW-³²⁶), 19 (³¹⁶-HRMAWDMMMNWSPTTALV-³³³) and 20 (³²³-MMNWSPTTALVVSQQLRI-³⁴⁰) from the original HCV E1 peptide library [29].

The interaction of the E1_{PTM} peptide with membrane vesicles was followed by the change of the fluorescence emission of the two Trp residues in the presence of model membranes containing different phospholipid compositions at different lipid/peptide ratios [57]. Upon the addition of liposomes, a concomitant blue shift and an increase of the fluorescence emission maximum were observed, indicating that the Trp residues of the peptide were in a hydrophobic environment (Fig. 2A). K_p values in the range 10^7 – 10^6 were obtained for the different phospholipid compositions studied (Table 2). These K_p values show that the peptide was bound to the membrane surface with high affinity

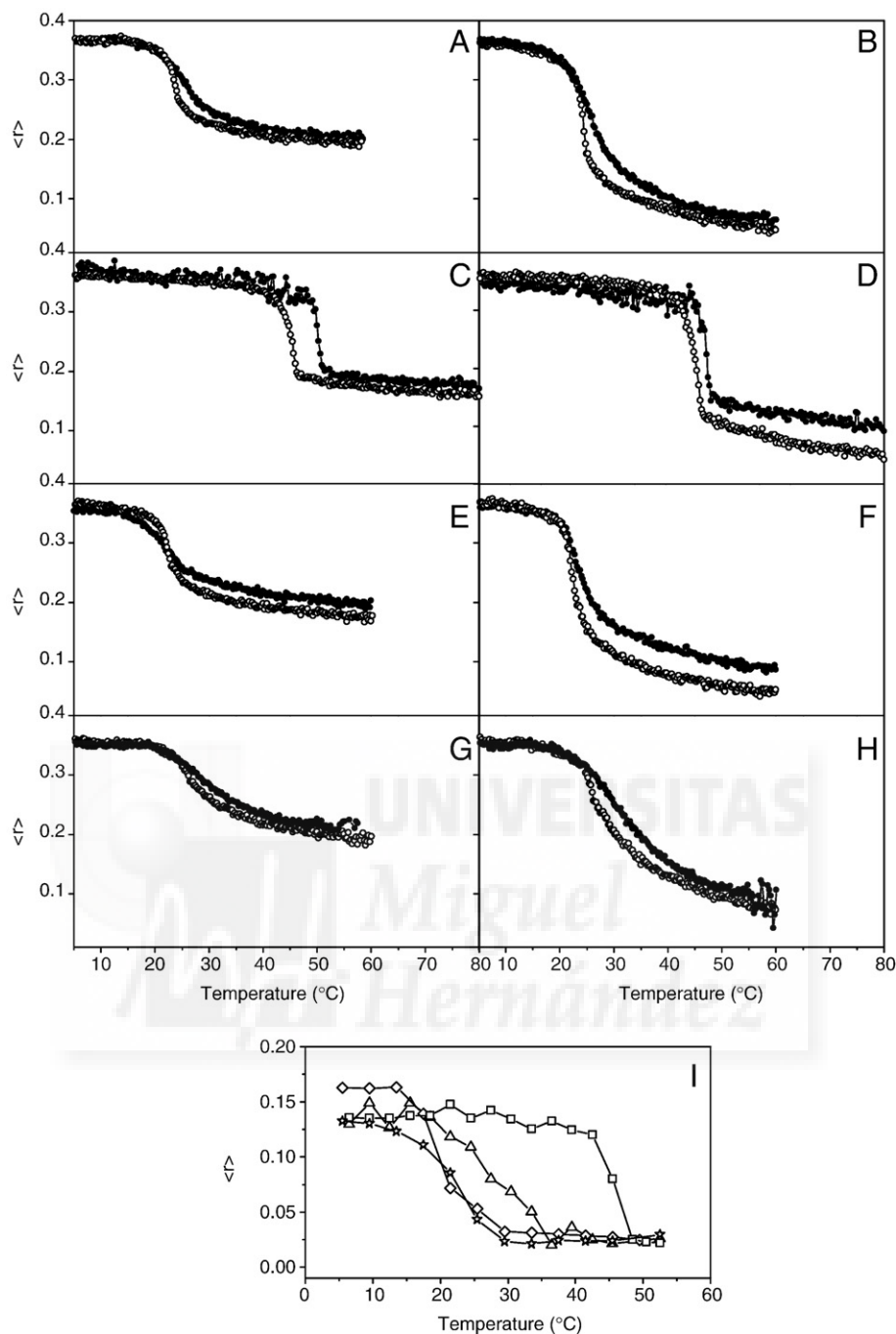


Fig. 5. Steady-state anisotropy values, $\langle r \rangle$, as a function of temperature of (A, C, E, G) TMA-DPH and (B, D, F, H) DPH incorporated into MLVs composed of (A and B) DMPC, (C and D) DMPA, (E and F) DMPG, and (G and H) EPC/SM/Chol at a lipid molar ratio of 5:1:1. Data correspond to vesicles in the absence (○) and in the presence of the E1_{PTM} peptide (●). (I) Intrinsic steady-state anisotropy of the E1_{PTM} peptide as a function of temperature in solution (●) and incorporated into MLVs composed of (◇) DMPC, (□) DMPA, (☆) DMPG and (△) DMPS. The peptide-to-lipid molar ratio was 1:15.

[57–60]. Concomitantly, there was a large displacement of the Trp emission frequency maximum of the Trp residues in the presence of LUVs. In solution the peptide had an emission maximum centered at 345 nm, typical for Trp in a polar environment, whereas in the presence of increasing concentrations of liposomes the emission maximum of the Trp residues presented a shift of about 10–11 nm to lower wavelengths depending on liposome composition (data not shown), implying that the Trp residues sensed a low-polarity environment upon interaction with the membrane. We have also used the electrostatic surface potential probe FPE [61] to confirm the binding of the E1_{PTM} peptide to model membranes composed of different

lipid compositions at different lipid/peptide ratios (Fig. 2B). As observed in the figure, E1_{PTM} had a higher affinity for model membranes containing negatively-charged phospholipids than for the other compositions, including the liver lipid extract (Table 2). Changes in the magnitude of the membrane dipole potential elicited by E1_{PTM} were monitored by means of the spectral shift of the fluorescence probe di-8-ANEPPS [50,62,63]. The variation of the fluorescence intensity ratio $R_{450/520}$ normalized as a function of the peptide concentration for different membrane compositions is shown in Fig. 2C, demonstrating that the peptide was capable of inserting into the lipid bilayer and modifying the dipole potential. In the presence of the

peptide, the greater decrease in the $R_{450/520}$ value was measured in bilayers with negatively-charged lipids. Taking together all these data, the peptide interacted strongly with membranes containing negatively-charged phospholipids but also with zwitterionic ones.

Stern–Volmer plots for the quenching of Trp by acrylamide, recorded in the absence and presence of lipid vesicles, are shown in Fig. 3A. Linear Stern–Volmer plots indicate that the Trp residues are fairly accessible to acrylamide, and in all cases, the quenching of the peptide Trp residue showed an acrylamide dependent concentration behavior. In aqueous solution the Trp residues were highly exposed to the solvent that led to a more efficient quenching. However, in the presence of the phospholipid membranes, the extent of quenching was significantly reduced, indicating a poor accessibility of the Trp residues to the aqueous phase, consistent with the incorporation of the E1_{PTM} peptide into the lipid bilayer. This notion is substantiated by the lower K_{sv} values obtained from the Stern–Volmer plots (Table 2). As expected, K_{sv} values were lower in the presence of negatively-charged phospholipids, consistent with a deeper location in negative bilayers. The transverse location of the peptide in the lipid bilayer was investigated by monitoring the relative quenching of the Trp fluorescence by the lipophilic spin probes 5NS and 16NS. The variation of the fluorescence intensity as a function of the effective concentration of both 5NS and 16NS probes is shown in Fig. 3B, whereas the K_{sv} values for both probes are presented in Table 2. It is observed that, in general, 16NS quenches the peptide fluorescence less efficiently than 5NS. Although it should be taken into account that the E1_{PTM} peptide has two Trp residues in the middle of the peptide sequence separated by five amino acids, these data suggest that it is localized in a shallow position in the membrane, but deeper in model membranes composed of negatively-charged phospholipids.

To examine the effect of the E1_{PTM} peptide in the destabilization of membrane vesicles, we studied the extent of CF leakage, i.e., membrane rupture, at different peptide-to-lipid molar ratios and different phospholipid compositions (Fig. 4A). It is interesting to note that the E1_{PTM} peptide induced 100% of leakage, even at peptide-to-lipid ratios as low as 0.0025, for liposomes composed of EPC/LPC (Fig. 4A). Significant leakage values between were observed for liposomes composed of EPC/Chol, BPS/Chol, EPG/Chol and EPA/Chol (at the highest peptide-to-lipid ratio studied, i.e., 1:10, leakage values were about 90–100%). Lower leakage values of about 60% and 40% were obtained for liposomes

composed of EPC/TPE and the lipid liver extract, respectively (Fig. 4A). Perturbation of membranes is not sufficient to complete the process of viral and cellular membrane fusion, since it is also necessary for the merge of the monolayers and the stalk formation, according to the stalk model for membrane fusion [11]. However, there is not a clear quantitative criterion to characterize fusion peptides using membrane destabilization. Therefore, we have also studied the effect of the peptide on both hemifusion and fusion using liposomes of different compositions. As it has been shown previously [64], the energetic barrier for hemifusion and fusion is larger than for leakage (pore formation). At the same time, leakage values, as measured here, are usually higher than hemifusion and fusion ones. The induction of outer and inner-monolayer lipid mixing (hemifusion and true fusion, respectively) by the E1_{PTM} peptide was tested with several types of vesicles utilizing a probe dilution assay [45,46]. As shown in Fig. 4B and C and Table 2, the higher hemifusion and fusion values were found for liposomes containing EPC/LPC (about 100% hemifusion and 45% fusion, respectively, at a peptide-to-lipid ratio of 1:5), whereas liposomes composed of EPC/TPE displayed also significant values (about 45% hemifusion and 35% fusion). Lower but significant hemifusion and fusion values were observed for the other liposome compositions tested, the higher hemifusion and fusion values were found for liposomes containing negatively-charged phospholipids (Fig. 4B and C).

Two main models of induced pores by peptides have been described: the barrel-stave model and the toroidal model [65,66], which in principle could be distinguished from each other by performing leakage assays using liposomes with different membrane curvature propensity [67,68]. As commented above, the maximum leakage induced by the E1_{PTM} peptide was different depending on the specific phospholipid composition of the liposomes, i.e., leakage was greater for LPC-containing liposomes than for TPE-containing ones. It is known that peptides which form toroidal pores tend to impose a positive curvature tension on the membrane that apparently facilitates the formation of the pores [69]. The presence of lipid or molecules that facilitate a positive curvature on the membrane, such as LPC, could then aid the formation of toroidal pores, whereas the presence of lipid or molecules in the membrane that facilitate a negative curvature, such as TPE, could inhibit the formation of toroidal pores. According to the observed results (Fig. 3B), it could then be possible that the E1_{PTM} peptide might form toroidal pores in the membrane. In order to characterize the pore size of

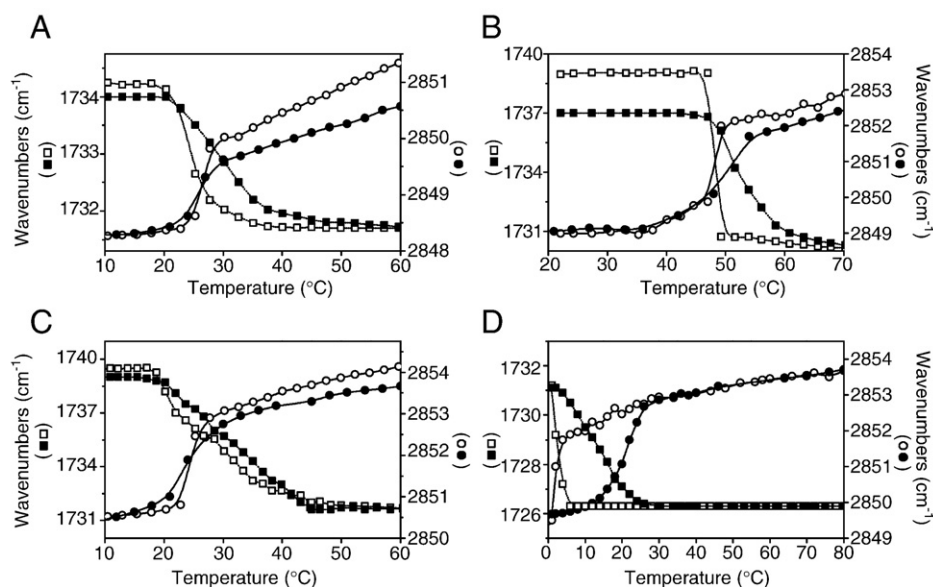


Fig. 6. Temperature dependency of the phospholipid CH₂ (○, ●) and C=O ester group (□, ■) stretching frequency values of (A) DMPC, (B) DMPA, (C) DMPG and (D) LPC in the absence (□, ○) and in the presence (■, ●) of the E1_{PTM} peptide at a lipid-to-peptide molar ratio of 15:1.

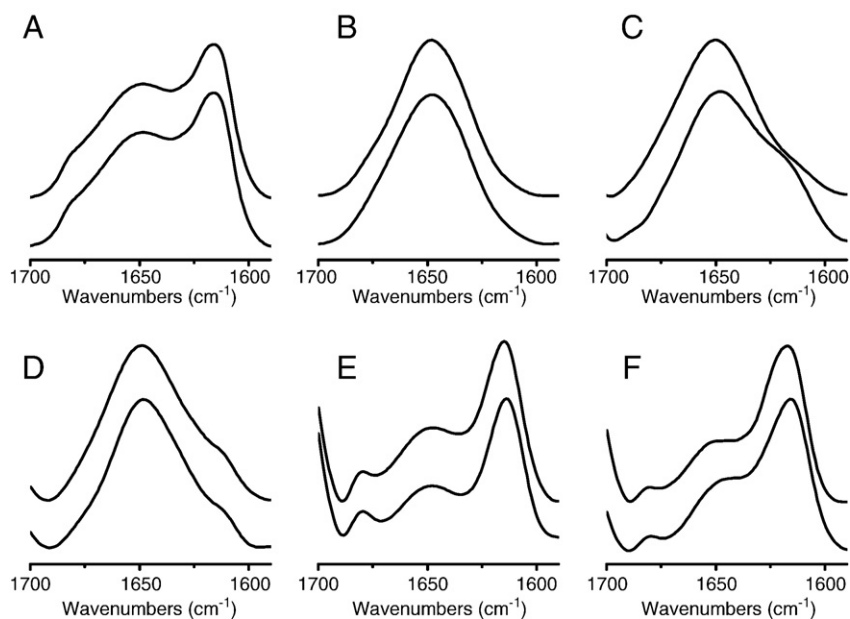


Fig. 7. Amide I' band of the E1_{PTM} peptide in (A) solution, and in the presence of (B) 40% of TFE, (C) LPC, (D) DMPC, (E), DMPG, and (F) DMPA at a lipid-to-peptide molar ratio of 15:1. Spectra are displayed at two temperatures, 2 °C (---) and 50 °C (—).

the pores which would be formed by the peptide, we carried out a series of experiments using FITC-dextran of different sizes entrapped in liposomes with different compositions (FD-10 and FD-20, having Stoke radii around 23 Å and 33 Å, respectively [70]). As observed in Fig. 4D and E, the E1_{PTM} peptide was able to induce the leakage of FD10 entrapped in liposomes but not of FD20. Since E1_{PTM} promoted the leakage of CF (Fig. 4A) and FD10 (Fig. 4D) but not of FD20 (Fig. 4E), the pore size which would be formed by the peptide should be comprised between 23 Å and 30 Å. In accordance with the CF data shown above, EPC/LPC liposomes displayed a high FD10 leakage, but a low one in liposomes composed of EPC/TPE (about 98% and 15% leakage, respectively). Apart from that, the ability of E1_{PTM} to induce leakage of encapsulated FD10 was larger in model membranes composed of negatively-charged phospholipids.

The effect of the E1_{PTM} peptide on the structural and thermotropic properties of phospholipid membranes was investigated by measuring the steady-state fluorescence anisotropy of the fluorescent probes DPH and TMA-DPH incorporated into model membranes composed of saturated synthetic phospholipids as a function of temperature (Fig. 5). For DMPC bilayers, E1_{PTM} decreased the cooperativity of the thermal transition as well as induced a slight increase of the anisotropy of all types of probes above the T_m of the phospholipid (Fig. 5A and B). In the case of DMPA, E1_{PTM} did not affect significantly the cooperativity of the main gel-to-liquid transition but elicited a shift to higher temperatures of about 4 °C and 2 °C for DPH and TMA-DPH, respectively (Fig. 5C and D). Similarly to what was observed for DMPC, a small increase in anisotropy was observed above T_m of the phospholipid. For vesicles composed of DMPG, the E1_{PTM} peptide slightly decreased the cooperativity of the thermal transition, as well as it increased the anisotropy above the T_m of the phospholipid (Fig. 5E and F). A relatively complex lipid mixture, EPC/SM/Chol at a molar ratio of 5:1:1, was also studied and similarly to what was observed above, i.e., the peptide decreased the cooperativity of the main transition and a slightly increased of the anisotropy above but not below T_m (Fig. 5G and H). These results suggest that the difference in the charge between the phospholipid headgroups affect, but slightly, the peptide incorporation into the lipid bilayer as well as that it should be located at the lipid-water interface influencing the fluidity of the phospholipids [58]. We have also studied the intrinsic anisotropy of the Trp residues of the peptide in the presence of liposomes composed of pure synthetic phospholipids (Fig. 5I). In the presence of the phospholipids, the

anisotropy values were different depending on temperature: they were higher below the T_m of each specific phospholipid, whereas they were lower above it. More important, the change in anisotropy occurred coincidentally when the main gel-to-liquid phase transition of each specific phospholipid took place; these data implied, first, that the peptide was effectively incorporated into the membrane palisade and second, the peptide was capable of sensing the phase transition of each one of the phospholipids.

Although it has been shown that the incorporation of transmembrane peptides in the phospholipid palisade of the membrane can affect not only the phospholipid chain order but also inter-chain coupling, a shift in the frequency of the CH₂ symmetric stretching band is a reliable index of the phase behavior of phospholipid dispersions [71]. The temperature dependence of the CH₂ symmetric frequency of pure DMPC is shown in Fig. 6A, where a highly cooperative change at approximately 23 °C was observed, corresponding to the gel-to-liquid crystalline phase transition, T_m , of the phospholipid. In the presence of E1_{PTM}, the cooperativity of the gel-to-liquid crystalline phase transition of DMPC was reduced, and the frequency of the CH₂ symmetric frequency decreased above but not below the T_m when compared with the pure phospholipid. The frequency at the maximum of the C=O vibration band for DMPC in the presence of the peptide, similarly to what was observed for the CH₂ frequency, displayed a less cooperative transition than the pure phospholipid, but it was shifted to higher temperatures (Fig. 6A). In the case of DMPA a highly cooperative change corresponding to the main transition T_m of the phospholipid was observed at approximately 48 °C (Fig. 6B). The presence of the E1_{PTM} peptide induced a shift of the T_m to higher temperatures as well as a slight decrease in the cooperativity of the transition. Significantly, the frequency of the CH₂ symmetric frequency decreased above but not below the T_m when compared with the pure phospholipid, indicating that the peptide induced an increase in the proportion of *trans* isomers when compared with the pure phospholipid. The frequency at the maximum of the C=O vibration band displayed a large cooperative transition corresponding to the gel-to-liquid crystalline phase transition of the phospholipid, but the intensity of the hydrated C=O group in the presence of the peptide was higher than in its absence at temperatures below but not above the T_m (Fig. 6B). When the peptide was incorporated in DMPG, a slight decrease in the cooperativity of the transition was observed (Fig. 6C). The frequency of the CH₂ symmetric

frequency decreased above the T_m , when compared with the pure phospholipid, indicating that the proportion of *trans* isomers was higher above the T_m . The frequency at the maximum of the C=O vibration band of DMPG was not significantly affected by the presence of the peptide, as observed in Fig. 6C. We have also examined the temperature dependence of the stretching vibration bands of LPC in the presence of the peptides, as observed in Fig. 6D. Interestingly, the phase transition observed at about 4 °C for the pure phospholipid was shifted to about 20 °C without any effect on the frequency neither below nor above the transition (it should be recalled that pure LPC has a transition from an interdigitated phase to a micellar one). The same effect was observed when observing the C=O vibration band frequency (Fig. 6C). These results confirm that the E1_{PTM} peptide is capable of inserting into the palisade structure of the membrane affecting the phospholipid acyl chains packing, as well as altering the order degree of the bilayer.

The existence of structural changes on the E1_{PTM} peptide induced by membrane binding was studied by analyzing the infrared Amide I' band located between 1700 and 1600 cm⁻¹ in membranes by infrared spectroscopy (Fig. 7). The Amide I' region of the fully hydrated peptide in buffer is shown in Fig. 7A. Two main bands are apparent, a broad one with a maximum at about 1648 cm⁻¹ and a narrow band with a maximum at about 1616 cm⁻¹. The band with the intensity maxima at about 1648 cm⁻¹ would correspond to a mixture of unordered but also helical structures, whereas the band with the intensity maxima at about 1616 cm⁻¹ would correspond to aggregated structures [72,73]. The maximum of the bands did not change significantly upon increasing the temperature, suggesting a high degree of conformational stability of the peptide. The Amide I' band of the peptide in the presence of TFE and LPC displayed a maximum at about 1648 cm⁻¹ and 1649 cm⁻¹, respectively, indicating that the structure of the peptide corresponds to a mixture of unordered and helical structures (Fig. 7B and C). The band envelope of the Amide I' region of the peptide bound to DMPC model membranes at a phospholipid/peptide molar ratio of 15:1 was different from that seen for the pure peptide in solution but similar to the Amide I' band observed in the presence of TFE and LPC, displaying a maximum at about 1648 cm⁻¹ (Fig. 7D). However, the band envelope of the Amide I' region of the peptide bound to DMPG and DMPA membranes was significantly different from that seen for the pure peptide in solution (Fig. 7E and F), since the intensity maxima were 1615 cm⁻¹ and 1617 cm⁻¹, respectively. In this case, the structure of the peptide corresponds mainly to aggregated structures. As it was found for the peptide in solution, the maximum of the band did not change significantly upon increasing the temperature in the presence of the membranes, indicating also a high degree of conformational stability.

4. Discussion

It is known that the region immediately adjacent to the membrane-spanning domain of different membrane fusion proteins plays an essential role in the fusogenic activities of these proteins [31–33,74–76]. The segment encompassing residues 309–340 of HCV E1 glycoprotein is located immediately adjacent to the TM domain, is capable of destabilizing model membranes, presents a localized high hydrophobic moment surface area, could be involved in membrane destabilization similarly to the PTM domain of class I fusion proteins and is highly conserved in all strains of HCV [34–36]. Interestingly, part of the E1_{PTM} sequence is a conserved hydrophobic-heptad repeat and site-directed mutagenesis of this sequence affects significantly viral entry [77]. Consequently, we have made a comprehensive study of a peptide patterned after the E1 region, E1_{PTM}, characterizing its binding and interaction with model membrane systems.

Peptide E1_{PTM} has a significant membranotropic activity and displays a high binding constant in the presence of model membranes having different phospholipid compositions, similarly to what has been found for other peptides [43,44]. After binding, the Trp residues of

the peptide reside in an environment with a low dielectric constant showing a significant motional restriction. E1_{PTM} showed a slightly higher affinity for anionic-phospholipid compositions, possibly due to the fact that the peptide has a positive net charge at pH 7.4. The existence of a specific interaction with liposomes containing negatively-charged phospholipids was corroborated by the change of the dipole potential at the membrane surface, as well as by hydrophilic and lipophilic probe quenching, suggesting that the E1_{PTM} peptide was effectively incorporated into the membranes, but located nearer to the membrane surface in the presence of zwitterionic phospholipids than in the presence of negatively-charged ones.

The E1_{PTM} peptide was also capable of disrupting the membrane bilayer causing the release of fluorescent probes, this effect being dependent on lipid composition and on the lipid/peptide molar ratio. The highest effect was observed for liposomes containing negatively-charged phospholipids, but significant leakage values were also observed for liposomes composed of zwitterionic phospholipids. The induction of hemifusion and fusion by E1_{PTM} were also studied and similar results were obtained, since specific and large membrane hemifusion and fusion values were found in the presence of liposomes composed of both negatively-charged phospholipids and zwitterionic ones. Interestingly, liposomes containing TPE (phospholipid inducing negative curvature) displayed relatively low hemifusion and fusion values, whereas, on the contrary, liposomes containing LPC (phospholipid inducing positive curvature) were the ones that elicited the most. These data reveal that E1_{PTM} affects the fluidity behavior of the phospholipids in the membrane suggesting that the E1_{PTM} peptide, although interacting with the membrane, should be located at the lipid–water interface [58]. Notably, E1_{PTM} released CF and FD10 but not FD20, implying that the peptide formed pores with diameter between 23 Å and 30 Å. The induction of hemifusion and fusion by the E1_{PTM} peptide were also studied and similar results were obtained, since specific and large membrane hemifusion and fusion values were characteristic of liposomes composed of negatively-charged phospholipids.

We have also shown that E1_{PTM} peptide is capable of affecting the steady-state fluorescence anisotropy of fluorescent probes located in the membrane, since the peptide, in general, was able of decreasing the mobility of the phospholipid acyl chains above but not below T_m when compared to the pure phospholipids. Significantly, the peptide sensed the phospholipid main phase transition indicating its incorporation into the membrane bilayer. The infrared spectra of the Amide I' region of the fully hydrated peptide did not change with temperature, indicating a high stability of its conformation, where a mixture of α -helix, random and aggregated structures coexisted. However we have observed differences on the proportion of the different secondary elements when the peptide was incorporated into membranes of different phospholipid compositions. Whereas the α -helix and random content was similar in the presence of TFE, LPC or DMPC, they changed significantly in the presence of DMPG and DMPA, where aggregated structures predominated. These data would suggest that the presence of different phospholipid headgroups would modulate the secondary structure of the peptide as it has been suggested for other peptides [57,58,60].

The binding to the surface and the modulation of the phospholipid biophysical properties which take place when E1_{PTM} is bound to the membrane, i.e., partitioning into the membrane surface and perturbation of the bilayer architecture, could be related to the conformational changes which might occur during the activity of the HCV E1 glycoprotein. These features would indicate that E1_{PTM} would interact with the membrane through both electrostatic and hydrophobic effects, as well as it would be adsorbed at the membrane interface. The capacity of E1_{PTM} to induce an enhanced release of CF from liposomes containing positive curvature-inducing phospholipids, such as LPC, could indicate that this peptide would form pores, possibly through the formation of toroidal-like structures [78]. These data suggest that the E1 region where the E1_{PTM} peptide resides might be a fusion determinant and have

an essential role in the membrane fusion process, overall in the destabilization of the viral envelope membrane. If that were true, it would imply that both HCV E1 and E2 glycoproteins are directly implicated in the mechanism that makes possible the entry of the HCV virus into its cellular host. Because this HCV E1 segment presents many similarities with other domains from class I membrane fusion proteins, it is a potential target for the development of inhibitor molecules of HCV entry and/or membrane fusion.

Acknowledgements

This work was supported by grant BFU2005-00186-BMC (Ministerio de Ciencia y Tecnología, Spain) to J.V. A.J.P. and J.G. are recipients of pre-doctoral fellowships from the Autonomous Government of the Comunidad Valenciana, Spain. We are especially grateful to Ana I. Gómez-Sánchez for her excellent technical assistance.

References

- [1] S.L. Chen, T.R. Morgan, The natural history of hepatitis C virus (HCV) infection, *Int. J. Med. Sci.* 3 (2006) 47–52.
- [2] F. Penin, J. Dubuisson, F.A. Rey, D. Moradpour, J.M. Pawlotsky, Structural biology of hepatitis C virus, *Hepatology* 39 (2004) 5–19.
- [3] S.L. Tan, A. Pause, Y. Shi, N. Sonenberg, Hepatitis C therapeutics: current status and emerging strategies, *Nat. Rev. Drug Discov.* 1 (2002) 867–881.
- [4] B. Pozzetto, T. Bourlet, F. Grattard, L. Bonneval, Structure, genomic organization, replication and variability of hepatitis C virus, *Nephrol. Dial. Transplant.* 11 (Suppl 4) (1996) 2–5.
- [5] S.A. Qureshi, Hepatitis C virus-biology, host evasion strategies, and promising new therapies on the horizon, *Med. Res. Rev.* 27 (2007) 353–373.
- [6] K.E. Reed, C.M. Rice, Overview of hepatitis C virus genome structure, polyprotein processing, and protein properties, *Curr. Top. Microbiol. Immunol.* 242 (2000) 55–84.
- [7] C. Vauloup-Fellous, V. Pene, J. Garaud-Aunis, F. Harper, S. Bardin, Y. Suire, E. Pichard, A. Schmitt, P. Sogni, G. Pierron, P. Briand, A.R. Rosenberg, Signal peptide peptidase-catalyzed cleavage of hepatitis C virus core protein is dispensable for virus budding but destabilizes the viral capsid, *J. Biol. Chem.* 281 (2006) 27679–27692.
- [8] M. Kielian, Class II virus membrane fusion proteins, *Virology* 344 (2006) 38–47.
- [9] M. Kielian, F.A. Rey, Virus membrane-fusion proteins: more than one way to make a hairpin, *Nat. Rev. Microbiol.* 4 (2006) 67–76.
- [10] D.M. Eckert, P.S. Kim, Mechanisms of viral membrane fusion and its inhibition, *Annu. Rev. Biochem.* 70 (2001) 777–810.
- [11] R.M. Epanand, Fusion peptides and the mechanism of viral fusion, *Biochim. Biophys. Acta* 1614 (2003) 116–121.
- [12] R. Blumenthal, M.J. Clague, S.R. Durell, R.M. Epanand, Membrane fusion, *Chem. Rev.* 103 (2003) 53–69.
- [13] D.J. Schibli, W. Weissenhorn, Class I and class II viral fusion protein structures reveal similar principles in membrane fusion, *Mol. Membr. Biol.* 21 (2004) 361–371.
- [14] E. Teissier, E.I. Pecheur, Lipids as modulators of membrane fusion mediated by viral fusion proteins, *Eur. Biophys. J.* 36 (2007) 887–899.
- [15] S.A. Gallo, C.M. Finnegan, M. Viard, Y. Raviv, A. Dimitrov, S.S. Rawat, A. Puri, S. Durell, R. Blumenthal, The HIV Env-mediated fusion reaction, *Biochim. Biophys. Acta* 1614 (2003) 36–50.
- [16] R.F. Garry, S. Dash, Proteomics computational analyses suggest that hepatitis C virus E1 and pestivirus E2 envelope glycoproteins are truncated class II fusion proteins, *Virology* 307 (2003) 255–265.
- [17] D. Lavillette, E.I. Pecheur, P. Donot, J. Fresquet, J. Molle, R. Corbau, M. Dreux, F. Penin, F.L. Cosset, Characterization of fusion determinants points to the involvement of three discrete regions of both E1 and E2 glycoproteins in the membrane fusion process of hepatitis C virus, *J. Virol.* 81 (2007) 8752–8765.
- [18] B. Bartosch, J. Dubuisson, F.L. Cosset, Infectious hepatitis C virus pseudo-particles containing functional E1–E2 envelope protein complexes, *J. Exp. Med.* 197 (2003) 633–642.
- [19] H.E. Drummer, P. Pombourios, Hepatitis C virus glycoprotein E2 contains a membrane-proximal heptad repeat sequence that is essential for E1E2 glycoprotein heterodimerization and viral entry, *J. Biol. Chem.* 279 (2004) 30066–30072.
- [20] Y. Ciczora, N. Callens, F. Penin, E.I. Pecheur, J. Dubuisson, Transmembrane domains of hepatitis C virus envelope glycoproteins: residues involved in E1E2 heterodimerization and involvement of these domains in virus entry, *J. Virol.* 81 (2007) 2372–2381.
- [21] L. Cocquerel, J.C. Meunier, A. Pillez, C. Wychowski, J. Dubuisson, A retention signal necessary and sufficient for endoplasmic reticulum localization maps to the transmembrane domain of hepatitis C virus glycoprotein E2, *J. Virol.* 72 (1998) 2183–2191.
- [22] L. Cocquerel, C. Wychowski, F. Minner, F. Penin, J. Dubuisson, Charged residues in the transmembrane domains of hepatitis C virus glycoproteins play a major role in the processing, subcellular localization, and assembly of these envelope proteins, *J. Virol.* 74 (2000) 3623–3633.
- [23] L. Cocquerel, A. Op de Beeck, M. Lambot, J. Roussel, D. Delgrange, A. Pillez, C. Wychowski, F. Penin, J. Dubuisson, Topological changes in the transmembrane domains of hepatitis C virus envelope glycoproteins, *Embo J.* 21 (2002) 2893–2902.
- [24] A. Op De Beeck, R. Montserret, S. Duvet, L. Cocquerel, R. Cacan, B. Barberot, M. Le Maire, F. Penin, J. Dubuisson, The transmembrane domains of hepatitis C virus envelope glycoproteins E1 and E2 play a major role in heterodimerization, *J. Biol. Chem.* 275 (2000) 31428–31437.
- [25] D. Lavillette, B. Bartosch, D. Nourrisson, G. Verney, F.L. Cosset, F. Penin, E.I. Pecheur, Hepatitis C virus glycoproteins mediate low pH-dependent membrane fusion with liposomes, *J. Biol. Chem.* 281 (2006) 3909–3917.
- [26] B. Bartosch, F.L. Cosset, Cell entry of hepatitis C virus, *Virology* 348 (2006) 1–12.
- [27] A.T. Yagnik, A. Lahm, A. Meola, R.M. Roccasecca, B.B. Ercole, A. Nicosia, A. Tramontano, A model for the hepatitis C virus envelope glycoprotein E2, *Proteins* 40 (2000) 355–366.
- [28] R. Roccasecca, H. Ansuini, A. Vitelli, A. Meola, E. Scarselli, S. Acali, M. Pezzanera, B.B. Ercole, J. McKeating, A. Yagnik, A. Lahm, A. Tramontano, R. Cortese, A. Nicosia, Binding of the hepatitis C virus E2 glycoprotein to CD81 is strain specific and is modulated by a complex interplay between hypervariable regions 1 and 2, *J. Virol.* 77 (2003) 1856–1867.
- [29] A.J. Perez-Berna, M.R. Moreno, J. Guillen, A. Bernabeu, J. Villalain, The membrane-active regions of the hepatitis C virus E1 and E2 envelope glycoproteins, *Biochemistry* 45 (2006) 3755–3768.
- [30] M. Brazzoli, A. Helenius, S.K. Fong, M. Houghton, S. Abrignani, M. Merola, Folding and dimerization of hepatitis C virus E1 and E2 glycoproteins in stably transfected CHO cells, *Virology* 332 (2005) 438–453.
- [31] T. Suarez, S. Nir, F.M. Goni, A. Saez-Cirion, J.L. Nieva, The pre-transmembrane region of the human immunodeficiency virus type-1 glycoprotein: a novel fusogenic sequence, *FEBS Lett.* 477 (2000) 145–149.
- [32] A. Saez-Cirion, M.J. Gomara, A. Agirre, J.L. Nieva, Pre-transmembrane sequence of Ebola glycoprotein. Interfacial hydrophobicity distribution and interaction with membranes, *FEBS Lett.* 533 (2003) 47–53.
- [33] S. Tong, F. Yi, A. Martin, Q. Yao, M. Li, R.W. Compans, Three membrane-proximal amino acids in the human parainfluenza type 2 (HPV2) F protein are critical for fusogenic activity, *Virology* 280 (2001) 52–61.
- [34] T. Suarez, W.R. Gallaher, A. Agirre, F.M. Goni, J.L. Nieva, Membrane interface-interacting sequences within the ectodomain of the human immunodeficiency virus type 1 envelope glycoprotein: putative role during viral fusion, *J. Virol.* 74 (2000) 8038–8047.
- [35] B. Sainz Jr., J.M. Rausch, W.R. Gallaher, R.F. Garry, W.C. Wimley, The aromatic domain of the coronavirus class I viral fusion protein induces membrane permeabilization: putative role during viral entry, *Biochemistry* 44 (2005) 947–958.
- [36] J. Guillen, M.R. Moreno, A.J. Perez-Berna, A. Bernabeu, J. Villalain, Interaction of a peptide from the pre-transmembrane domain of the severe acute respiratory syndrome coronavirus spike protein with phospholipid membranes, *J. Phys. Chem. B* 111 (2007) 13714–13725.
- [37] S.G. Peisajovich, Y. Shai, Viral fusion proteins: multiple regions contribute to membrane fusion, *Biochim. Biophys. Acta* 1614 (2003) 122–129.
- [38] W.K. Surewicz, H.H. Mantsch, D. Chapman, Determination of protein secondary structure by Fourier transform infrared spectroscopy: a critical assessment, *Biochemistry* 32 (1993) 389–394.
- [39] Y.P. Zhang, R.N. Lewis, R.S. Hodges, R.N. McElhaney, FTIR spectroscopic studies of the conformation and amide hydrogen exchange of a peptide model of the hydrophobic transmembrane alpha-helices of membrane proteins, *Biochemistry* 31 (1992) 11572–11578.
- [40] L.D. Mayer, M.J. Hope, P.R. Cullis, Vesicles of variable sizes produced by a rapid extrusion procedure, *Biochim. Biophys. Acta* 858 (1986) 161–168.
- [41] C.S.F. Böttcher, C.M. Van Gent, C. Fries, A rapid and sensitive sub-micro phosphorus determination, *Anal. Chim. Acta* 1061 (1961) 203–204.
- [42] H. Edelhoch, Spectroscopic determination of tryptophan and tyrosine in proteins, *Biochemistry* 6 (1967) 1948–1954.
- [43] A. Bernabeu, J. Guillen, A.J. Perez-Berna, M.R. Moreno, J. Villalain, Structure of the C-terminal domain of the pro-apoptotic protein Hrk and its interaction with model membranes, *Biochim. Biophys. Acta* 1768 (2007) 1659–1670.
- [44] M.R. Moreno, J. Guillen, A.J. Perez-Berna, D. Amorós, A.I. Gomez, A. Bernabeu, J. Villalain, Characterization of the interaction of two peptides from the N terminus of the NHR domain of HIV-1 gp41 with phospholipid membranes, *Biochemistry* 46 (2007) 10572–10584.
- [45] D.K. Struck, D. Hoekstra, R.E. Pagano, Use of resonance energy transfer to monitor membrane fusion, *Biochemistry* 20 (1981) 4093–4099.
- [46] P. Meers, S. Ali, R. Erukulla, A.S. Janoff, Novel inner monolayer fusion assays reveal differential monolayer mixing associated with cation-dependent membrane fusion, *Biochim. Biophys. Acta* 1467 (2000) 227–243.
- [47] M.R. Eftink, C.A. Chiron, Exposure of tryptophanyl residues and protein dynamics, *Biochemistry* 16 (1977) 5546–5551.
- [48] J. Wall, F. Ayoub, P. O'Shea, Interactions of macromolecules with the mammalian cell surface, *J. Cell Sci.* 108 (Pt 7) (1995) 2673–2682.
- [49] C. Golding, S. Senior, M.T. Wilson, P. O'Shea, Time resolution of binding and membrane insertion of a mitochondrial signal peptide: correlation with structural changes and evidence for cooperativity, *Biochemistry* 35 (1996) 10931–10937.
- [50] J. Cladera, P. O'Shea, Intramembrane molecular dipoles affect the membrane insertion and folding of a model amphiphilic peptide, *Biophys. J.* 74 (1998) 2434–2442.
- [51] E. Gross, R.S. Bedlack Jr., L.M. Loew, Dual-wavelength ratiometric fluorescence measurement of the membrane dipole potential, *Biophys. J.* 67 (1994) 208–216.
- [52] D. Eisenberg, E. Schwarz, M. Komaromy, R. Wall, Analysis of membrane and surface protein sequences with the hydrophobic moment plot, *J. Mol. Biol.* 179 (1984) 125–142.

- [53] D.M. Engelman, T.A. Steitz, A. Goldman, Identifying nonpolar transbilayer helices in amino acid sequences of membrane proteins, *Annu. Rev. Biophys. Biophys. Chem.* 15 (1986) 321–353.
- [54] W.C. Wimley, S.H. White, Experimentally determined hydrophobicity scale for proteins at membrane interfaces, *Nat. Struct. Biol.* 3 (1996) 842–848.
- [55] J. Guillen, A.J. Pérez-Berná, M.R. Moreno, J. Villalain, Identification of the membrane-active regions of the severe acute respiratory syndrome coronavirus spike membrane glycoprotein using a 16/18-mer peptide scan: implications for the viral fusion mechanism, *J. Virol.* 79 (2005) 1743–1752.
- [56] K.S. Yeung, G.A. Yamanaka, N.A. Meanwell, Severe acute respiratory syndrome coronavirus entry into host cells: opportunities for therapeutic intervention, *Med. Res. Rev.* 26 (2006) 414–433.
- [57] R. Pascual, M. Contreras, A. Fedorov, M. Prieto, J. Villalain, Interaction of a peptide derived from the N-heptad repeat region of gp41 Env ectodomain with model membranes. Modulation of phospholipid phase behavior, *Biochemistry* 44 (2005) 14275–14288.
- [58] L.M. Contreras, F.J. Aranda, F. Gavilanes, J.M. Gonzalez-Ros, J. Villalain, Structure and interaction with membrane model systems of a peptide derived from the major epitope region of HIV protein gp41: implications on viral fusion mechanism, *Biochemistry* 40 (2001) 3196–3207.
- [59] N.C. Santos, M. Prieto, M.A. Castanho, Interaction of the major epitope region of HIV protein gp41 with membrane model systems. A fluorescence spectroscopy study, *Biochemistry* 37 (1998) 8674–8682.
- [60] R. Pascual, M.R. Moreno, J. Villalain, A peptide pertaining to the loop segment of human immunodeficiency virus gp41 binds and interacts with model biomembranes: implications for the fusion mechanism, *J. Virol.* 79 (2005) 5142–5152.
- [61] J. Wall, C.A. Golding, M. Van Veen, P. O'Shea, The use of fluoresceinphosphatidylethanolamine (FPE) as a real-time probe for peptide-membrane interactions, *Mol. Membr. Biol.* 12 (1995) 183–192.
- [62] J. Cladera, I. Martin, P. O'Shea, The fusion domain of HIV gp41 interacts specifically with heparan sulfate on the T-lymphocyte cell surface, *Embo J.* 20 (2001) 19–26.
- [63] P. O'Shea, Intermolecular interactions with/within cell membranes and the trinity of membrane potentials: kinetics and imaging, *Biochem. Soc. Trans.* 31 (2003) 990–996.
- [64] J.L. Nieva, F.M. Goni, A. Alonso, Liposome fusion catalytically induced by phospholipase C, *Biochemistry* 28 (1989) 7364–7367.
- [65] L. Yang, T.A. Harroun, T.M. Weiss, L. Ding, H.W. Huang, Barrel-stave model or toroidal model? A case study on melittin pores, *Biophys. J.* 81 (2001) 1475–1485.
- [66] D. Allende, S.A. Simon, T.J. McIntosh, Melittin-induced bilayer leakage depends on lipid material properties: evidence for toroidal pores, *Biophys. J.* 88 (2005) 1828–1837.
- [67] G. Basanez, Membrane fusion: the process and its energy suppliers, *Cell. Mol. Life Sci.* 59 (2002) 1478–1490.
- [68] A. Janowska-Wieczorek, A. Matsuzaki, A.M. L. The hematopoietic microenvironment: matrix metalloproteinases in the hematopoietic microenvironment, *Hematol.* 4 (2000) 515–527.
- [69] S.R. Durell, I. Martin, J.M. Ruyschaert, Y. Shai, R. Blumenthal, What studies of fusion peptides tell us about viral envelope glycoprotein-mediated membrane fusion (review), *Mol. Membr. Biol.* 14 (1997) 97–112.
- [70] T.C. Laurent, K.A. Granath, Fractionation of dextran and Ficoll by chromatography on Sephadex G-200, *Biochim. Biophys. Acta* 136 (1967) 191–198.
- [71] H.H. Mantsch, R.N. McElhaney, Phospholipid phase transitions in model and biological membranes as studied by infrared spectroscopy, *Chem. Phys. Lipids* 57 (1991) 213–226.
- [72] J.L. Arrondo, F.M. Goni, Structure and dynamics of membrane proteins as studied by infrared spectroscopy, *Prog. Biophys. Mol. Biol.* 72 (1999) 367–405.
- [73] D.M. Byler, H. Susi, Examination of the secondary structure of proteins by deconvolved FTIR spectra, *Biopolymers* 25 (1986) 469–487.
- [74] K. Salzwedel, J.T. West, E. Hunter, A conserved tryptophan-rich motif in the membrane-proximal region of the human immunodeficiency virus type 1 gp41 ectodomain is important for Env-mediated fusion and virus infectivity, *J. Virol.* 73 (1999) 2469–2480.
- [75] I. Munoz-Barroso, K. Salzwedel, E. Hunter, R. Blumenthal, Role of the membrane-proximal domain in the initial stages of human immunodeficiency virus type 1 envelope glycoprotein-mediated membrane fusion, *J. Virol.* 73 (1999) 6089–6092.
- [76] J. Zhou, R.E. Dutch, R.A. Lamb, Proper spacing between heptad repeat B and the transmembrane domain boundary of the paramyxovirus SV5 F protein is critical for biological activity, *Virology* 239 (1997) 327–339.
- [77] H.E. Drummer, I. Boo, P. Pountourios, Mutagenesis of a conserved fusion peptide-like motif and membrane-proximal heptad-repeat region of hepatitis C virus glycoprotein E1, *J. Gen. Virol.* 88 (2007) 1144–1148.
- [78] A.J. Garcia-Saez, S. Chiantia, P. Schwille, Effect of line tension on the lateral organization of lipid membranes, *J. Biol. Chem.* 282 (2007) 33537–33544.



CAPÍTULO V

ANEXO DE PUBLICACIONES

EN PROCESO DE ACEPTACIÓN



Publicación 6

Biophysical characterization of the fusogenic region of HCV E1 envelope glycoprotein

A. J. Pérez-Berná¹, G. Pabst², P. Laggner² and J. Villalaín¹

¹Instituto de Biología Molecular y Celular, Universidad “Miguel
Hernández”, Elche-Alicante, Spain

²Biophysics and Nanosystems Research, Austrian Academy of Sciences, Graz
A-8042, Austria



Publicación 7

Effect of the pre-transmembrane region of the HCV E1 envelope glycoprotein on DEPE polymorphism

A. J. Pérez-Berná¹, A. González-Álvarez¹, G. Pabst², P.
Laggner² and J. Villalaín¹

¹Instituto de Biología Molecular y Celular, Universidad “Miguel
Hernández”, Elche-Alicante, Spain

²Biophysics and Nanosystems Research, Austrian Academy of Sciences, Graz
A-8042, Austria



Publicación 8

Searching of HCV inhibition viral-cell fusion

A. J. Pérez-Berná¹, D. Lavillette² and J. Villalaín¹

¹Instituto de Biología Molecular y Celular, Universidad “Miguel Hernández”, Elche-Alicante, Spain

²Laboratoire de Vectorologie Retrovirale et Therapie Genique, INSERM U412, Ecole Normale Supérieure de Lyon and IFR 74, Lyon, France





CAPÍTULO VI

RESULTADOS



RESULTADOS

El virus de la hepatitis C (HCV) es un virus con envuelta lipídica que presenta como material genético una hebra sencilla y positiva de RNA. El HCV pertenece al género *Hepacivirus* dentro de la familia *Flaviviridae*. Este virus es el agente causal de enfermedades hepáticas humanas (Penin et al., 2004; Tan et al., 2002). No existe vacuna para evitar la infección viral ni agentes terapéuticos eficientes para contrarrestar la enfermedad (Qureshi, 2007). El genoma viral del HCV consiste en un único marco de lectura abierta que codifica una poliproteína precursora. Ésta incluye las proteínas estructurales y no estructurales que se procesan por medio de proteasas virales y celulares. Las proteínas estructurales son: la proteína *core*, la cual forma la nucleocápsida viral y las glicoproteínas de la envuelta *E1* y *E2*, ambas proteínas transmembranas. Las proteínas estructurales están separadas de las no estructurales por una pequeña proteína transmembrana, *p7*.

La entrada del virus a la célula se lleva a cabo por medio de la fusión de la membrana de la envuelta viral y la membrana celular; en cambio la morfogénesis del virión y la salida se lleva a cabo en el retículo endoplasmático (Vauloup-Fellous et al., 2006). El genoma viral del HCV es muy heterogéneo debido a que los errores durante la replicación causan un alto número de mutaciones, por ello las regiones implicadas en la entrada o salida del virus cobran en este virus más importancia, ya que suelen estar más conservadas en todas las estirpes. Por tanto en primer lugar nos propusimos encontrar las regiones membranotrópicas de las proteínas estructurales del HCV que posiblemente estuvieran implicadas en procesos de fusión, morfogénesis y salida viral, para utilizarlas como dianas terapéuticas contra las que buscar moléculas que evitaran la interacción entre las proteínas y las membranas. Esta nueva estrategia puede permitir el encontrar nuevos agentes terapéuticos contra la infección del HCV.

Intentamos localizar en la proteína *core* las regiones membranotrópicas. La proteína *core* es una proteína básica que muestra una alta homología con las proteínas de la nucleocápsida de otros flavivirus. Esta proteína está muy conservada entre las diferentes estirpes de HCV (Cha et al., 1992). Tiene muchas funciones, sin embargo su misión más

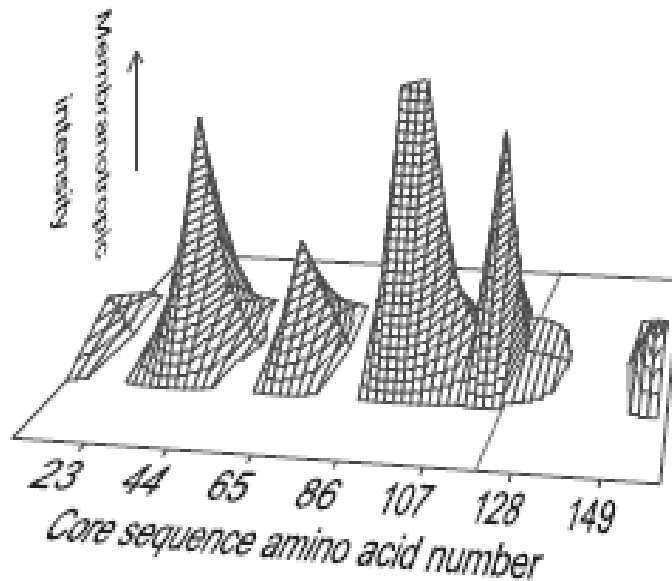


Figura 6.1. Resumen del porcentaje normalizado de liberación de contenidos de todos los sistemas lipídicos estudiados, correspondientes a las librerías peptídicas 18-mer de la proteína *core* sobre la secuencia lineal de la proteína.

molecular de la morfogénesis viral hemos estudiado la estructura secundaria de estas regiones en presencia y ausencia de membranas modelo basadas en RAFT y extracto lipídico de hígado. Para completar el estudio de las regiones membranotrópicas de la proteína *core* del HCV, realizamos un estudio por rayos X con sistemas modelo de membranas constituidas por el fosfolípido DEPE. Se ensayaron las principales regiones membranotrópicas de la proteína *core* de HCV a tres temperaturas diferentes: 25°C, 45°C y 70°C. La región 29-46 desestabiliza la membrana y su interacción provoca la aparición de un patrón de interacción propio de membranas desordenadas, así como un estrechamiento la membrana. La región 155-172 en cambio impide la aparición de formas no lamelares, por lo que estabiliza la fase bicapa de la membrana. Futuros estudios tomando como dianas estas regiones pueden permitir el desarrollo de nuevas estrategias antivirales basadas en inhibidores del ensamblaje viral.

La siguiente proteína estructural en la que intentamos localizar las regiones membranotrópicas fue la proteína *p7*. La proteína *p7* está localizada dentro de la poliproteína precursora entre las proteínas estructurales y no estructurales, específicamente entre las proteínas *E2* y la *NS2*. *p7* es esencial para el ensamblaje y la

importante es la morfogénesis viral. Hemos analizado e identificado diferentes regiones dentro de la proteína que interaccionan con sistemas modelo de membrana. Para ello hemos utilizado librerías peptídicas de 18 aminoácidos, derivadas de dos estirpes, 1AH77 y 1B4J, de la proteína *core*. Las regiones membranotrópicas se localizan en las regiones 29-46, 57-74, 85-123 y 155-172 (Figura 6.1). Intentando explicar el mecanismo

salida eficiente de los viriones, indicando que *p7* está involucrada en la fase tardía del ciclo de replicación viral (Steinmann et al., 2007). A nivel molecular, *p7* es una proteína transmembrana de 63 aminoácidos con 2 dominios transmembrana, TM1 y TM2, conectados por un bucle que modula la actividad del canal. (Gonzalez and Carrasco, 2003; Griffin et al., 2003; Steinmann et al., 2007). *p7* oligomeriza en hexámeros de hélices diméricas con un diámetro interno de poro de 15Å (Griffin et al., 2003). Esta proteína implicada en el proceso de salida del virus puede ser también un candidato para desarrollar nuevos fármacos antivirales. Hemos llevado a cabo una búsqueda de las regiones membranotrópicas de la proteína *p7*, investigando el efecto en la liberación de contenidos liposomas compuestos por diferentes sistemas modelo de membrana, de una librería peptídica derivada de las estirpes 1AH77 y 1B4J. Hemos identificado el dominio del bucle entre las hélices como la región más membranotrópica de la proteína. Además hemos realizado una caracterización biofísica de la interacción de un péptido sintético derivado de esta región, *p7L*, con sistemas modelo de membrana (Figura 6.2). Hemos demostrado que *p7L* tiene una alta constante de partición con fosfolípidos, sobre todo con aquellos sistemas modelo de membrana que contienen carga negativa. Está localizado en la superficie de la membrana y oligomeriza en presencia de ellas. *p7L* forma poros cuyo tamaño está comprendido entre 6 y 23 Å, el mismo diámetro de poro que debería tener la proteína nativa. Por ello esta región puede ser esencial para la actividad del canal.

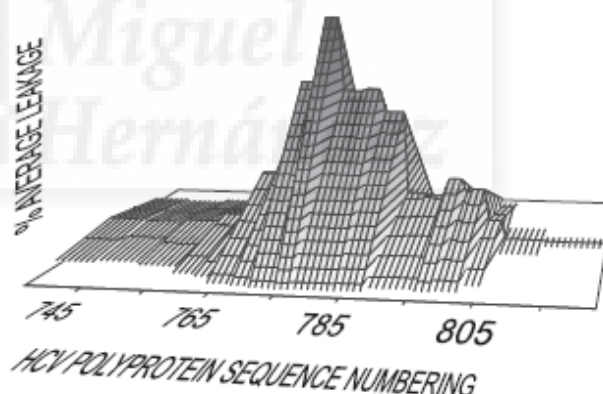


Figura 6.2. Resumen del porcentaje normalizado de liberación de contenidos de todos los sistemas lipídicos estudiados con las librerías 18-mer correspondientes proteína *p7* sobre la secuencia lineal de la proteína.

Las glicoproteínas de la envuelta viral *E1* y *E2* son proteínas de fusión de clase II truncadas (Garry and Dash, 2003). Para estudiar las bases estructurales de la fusión de membranas del HCV e identificar nuevas dianas para buscar inhibidores de fusión hemos realizado un análisis de las diferentes regiones de las glicoproteínas de la envuelta *E1* y *E2*, las cuales interaccionan *in vivo* con las membranas fosfolipídicas (Lavillette et al., 2006).

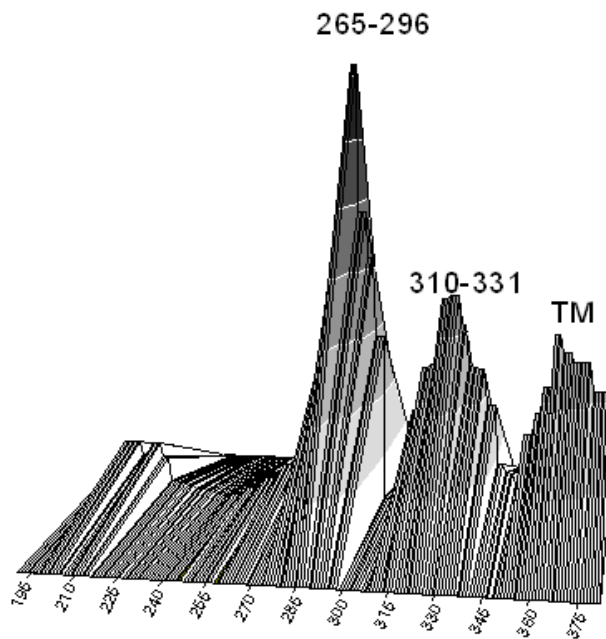


Figura 6.3. Resumen del porcentaje normalizado de liberación de contenidos, hemifusión y fusión de todos los sistemas lipídicos estudiados con las librerías 18-mer correspondientes proteína *E1* sobre la secuencia lineal de la proteína.

Las regiones membranotrópicas de las glicoproteínas *E1* y *E2* se determinaron por medio de ensayos de liberación de contenidos de liposomas, ensayos de hemifusión y fusión de una librería de péptidos de 18 aminoácidos derivados de las glicoproteínas *E1* y *E2* de las estirpes 1AH77 y 1B4J. Por medio de estos ensayos hemos identificado las regiones 265-296 como la región fusogénica, el segmento 310-331 localizado cerca de la region transmembrana y que muestra un grado de desestabilización de membranas parecido al que se ha descrito para las regiones pretransmembrana de las proteínas de fusión de clase I (Figura 6.3). La región 603-635 que es una de las regiones más membranotrópicas de la proteína *E2* y la región 525-565 la cual se ha descrito como región de unión al receptor, el segmento 455-489 que incluye la región hipervariable 2 y la región 423-453 que es una región necesaria para el plegamiento de la proteína (Figura 6.4). Hemos seleccionado entre las zonas membranotrópicas de

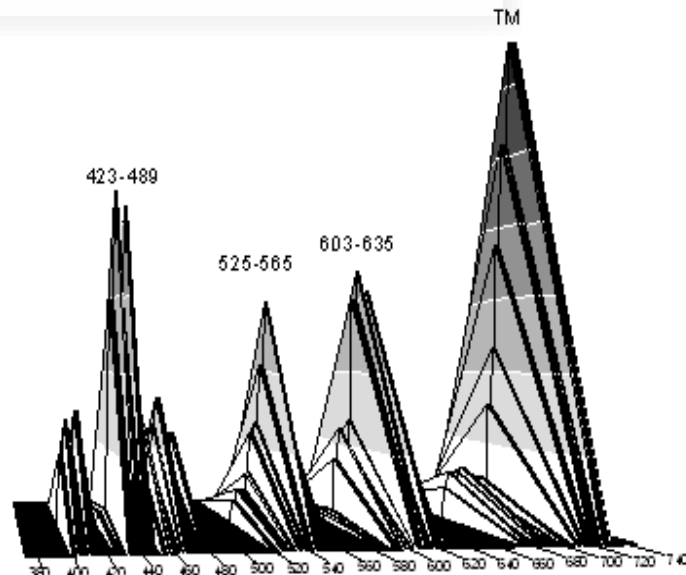


Figura 6.4. Resumen del porcentaje normalizado de liberación de contenidos, hemifusión y fusión de todos los sistemas lipídicos estudiados con las librerías 18-mer correspondientes proteína *E2* sobre la secuencia lineal de la proteína.

E1 y *E2* las regiones que pueden estar implicadas en el proceso de fusión de membranas para realizar una caracterización biofísica de la interacción lipido-péptido y así poder explicar la fusión de membranas necesaria para la entrada del virus. Las regiones caracterizadas han sido la región del péptido de fusión, la región pretransmembrana y la zona más membranotrópica de la proteína *E2*.



Figura 6.5. Localización de la región estudiada dentro de la glicoproteína *E2*

La región más fusogénica de la proteína *E2* es la región 603-634 (Figura 6.5). Hemos estudiado la interacción y unión de un péptido derivado de esta región con sistemas modelo de membrana. La constante de partición de este péptido es alta para todos los sistemas lipídicos estudiados. El péptido se encuentra localizado en la superficie de la membrana cercana al carbono 5. El péptido provoca liberación de contenidos, hemifusión y fusión de sistemas modelo de membrana. Los residuos fluorescentes del péptido aumentan su anisotropía de fluorescencia en presencia de sistemas modelo de membrana, así como la anisotropía de sondas extrínsecas localizadas a diferentes profundidades en la membrana, por lo que el péptido está incorporándose en las membranas y sintiendo los cambios transicionales que ocurren en el lípido. El péptido en presencia de membranas mostró una conformación en lámina- β . El péptido muestra las

constantes de partición y los efectos más significativos en presencia de sistemas modelo de membrana con carga negativa, indicando que la interacción del péptido con la membrana tiene una componente mayoritaria electrostática y otra hidrofóbica. Hemos estudiado también la estructura de la membrana tras la inserción del péptido en sistemas modelo de membranas basados en DEPE. Este fosfolípido tiene la capacidad de formar estructuras no lamelares a altas temperaturas, ya que una de las características principales de los regiones fusogénicas es la de estabilizar estructuras no lamelares. La presencia de péptido imposibilita la formación de fase hexagonal a altas temperaturas, lo cual es importante para la fusión de membranas. La limitación de este péptido para estabilizar fases no

lamelares imposibilita a esta región convertirse en el péptido de fusión de HCV, aunque no descartamos que este péptido esté implicado en la fusión de membranas desestabilizando y afectando a la estructura de la membrana de la célula diana para ayudar a la interacción del péptido de fusión.

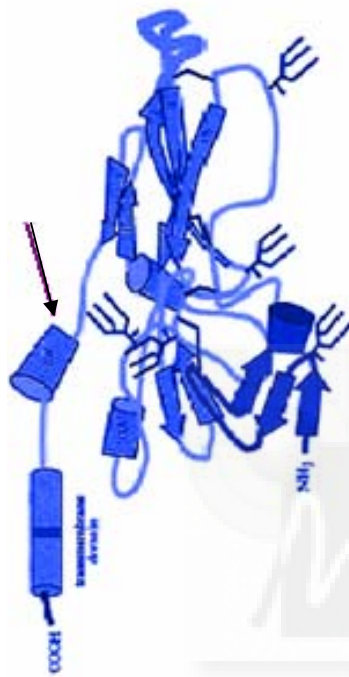


Figura 6.6 Localización de la región estudiada dentro de la glicoproteína *E1*.

Otra región estudiada fue la zona 309-340, cercana a la región transmembrana de la proteína *E1* (Figura 6.6). La región inmediatamente adyacente a la región transmembrana de las proteínas de fusión de clase I juega un papel esencial en la actividad fusogénica de estas proteínas (Munoz-Barroso et al., 1999; Saez-Cirion et al., 2003; Salzwedel et al., 1999; Suarez et al., 2000; Tong et al., 2001; Zhou et al., 1997). Un péptido derivado de la región 309-340 de *E1* de HCV, es capaz de unirse a membranas con alta afinidad, desestabilizar sistemas modelo de membrana provocando la formación de poros, liberación de contenido, hemifusión y fusión de membranas, sobretodo en fosfolípidos que tiene carga negativa y en fosfolípidos que forman curvaturas positivas como el LPC. Esta capacidad podría indicar que el péptido podría formar poros con estructuras toroidales. El péptido tiene conformación en lámina β en disolución acuosa y en presencia de sistema modelo de

membrana. El péptido se une a la superficie de la membrana y perturba la arquitectura de la membrana. También hemos estudiado la interacción del péptido con sistemas modelo de membrana basados en DEPE. La presencia del péptido en este sistema modelo de membrana provoca una disminución en la temperatura de la transición a fase hexagonal. Esto podría ser consecuencia de la estabilización por la presencia del péptido de estructuras no lamelares. Todos estos datos sugieren que esta región de *E1* podría desempeñar una función importante en el proceso de fusión, como la desempeñada por las regiones pretransmembrana de la proteínas de fusión de clase I. Teniendo en cuenta la situación donde se encuentra este péptido, su función en la proteína nativa podría ser la de desestabilizar la envuelta viral para que el proceso de fusión se pueda llevar a cabo.

La otra región implicada en el proceso de fusión es la zona del péptido de fusión. No está claro el papel que los péptidos de fusión desempeñan en la fusión de membranas. Una hipótesis sugiere que actúan como centros activos que median la fusión de la membrana celular y la envuelta viral, por tanto los péptidos de fusión deben de tener la capacidad de perturbar biomembranas (Nieva and Agirre, 2003). La región del péptido de fusión de HCV está compuesta por una región hidrofóbica seguida de una región polar con carga

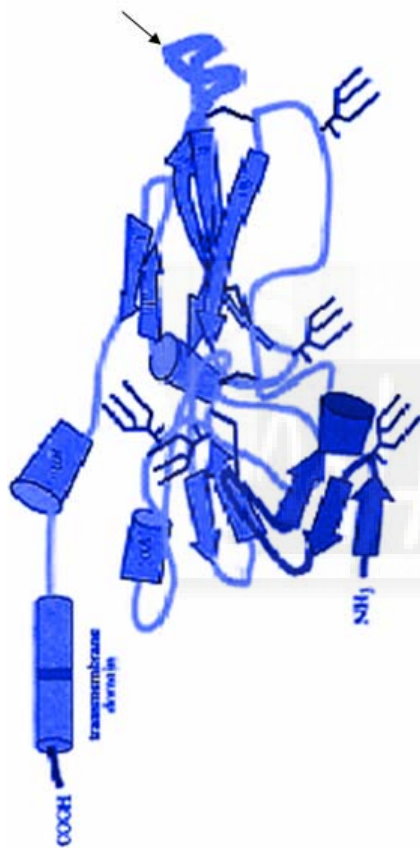


Figura 6.7 Localización de la región estudiada dentro de la glicoproteína E1.

positiva compuesta por los residuos RRH que se encuentra entre láminas β (Figura 6.7). Ante la imposibilidad de estudiar estas dos regiones juntas, ya que la síntesis química falló tras sucesivos intentos por compañías diferentes y la toxicidad del péptido limitaba la expresión del mismo en bacterias utilizando incluso construcciones diseñadas para la expresión de péptidos con toxicidad alta, decidimos estudiar la interacción de esta región por medio de dos péptidos diferentes de 18 aminoácidos de longitud donde uno contenía la región hidrofóbica y otro la polar. En esta tesis incluimos sólo los estudios realizados a la región hidrofóbica de la región fusogénica. El péptido 274-291 se une a sistemas modelo de membrana con alta afinidad. Hemos observado que el péptido induce un alto grado de liberación de contenidos, hemifusión y fusión en todos los sistemas de membrana estudiados. El péptido se inserta en la superficie de la membrana cercano al carbono 5.

Teniendo en cuenta que HCVpp muestran un aumento en la fusión ante la presencia de colesterol, ensayamos si el péptido de fusión presentaba similar afinidad por sistemas modelo de membrana basados en POPC/SM/CHOL a relaciones determinadas para que en las fases líquido-cristalina aparecen microdominios líquido-ordenados de

esfingomielina-colesterol llamados *Raft*. El péptido mostró una dependencia exponencial entre la concentración de colesterol y los niveles de hemifusión. También por medio de ensayos de FRET entre la tirosina del péptido y el dihidroergosterol, un análogo fluorescente de colesterol, encontramos que el péptido interacciona y particiona preferencialmente a los dominios ricos en colesterol. El péptido mostró una interacción preferencial por sistemas modelo de membrana zwitteriónicos, extracto lipídico hepático y sistemas modelo de membrana enriquecidos en colesterol. Sin embargo el péptido también mostró afinidad por sistemas modelo basados en PS. Se ha observado que este fosfolípido puede migrar a la hemicapa externa durante los procesos de fusión (Estepa et al., 2001). También se ha visto que el péptido de fusión del HIV provoca la formación de “nipples” (abultamientos redondeados) locales en la membrana plasmática celular (Dimitrov et al., 2001) permitiendo la formación de plegamientos locales que finalmente inducen zonas de fase no lamelares en la hemicapa externa. El desequilibrio producido por el diferente ensamblaje fosfolipídico entre la hemicapa interna y externa produce flip-flop de la hemicapa interna a la externa para satisfacer las restricciones de empaquetamiento (Janmey and Kinnunen, 2006). De acuerdo con estos datos, se puede considerar que la interacción de las regiones fusogénicas con membranas enriquecidas en dominios enriquecidos con PS o colesterol desestabilizaría la membrana y podrían estabilizar la formación de estructuras no lamelares. También hemos observado por SAXD, RMN y DSC que la presencia del péptido induce la aparición de fases hexagonales en el lípido DEPE a temperaturas más bajas, indicando que el péptido estabiliza y permite la formación de estructuras no lamelares a menores temperaturas. Por tanto esta región puede jugar un papel importante en el mecanismo de fusión. También es importante la dependencia exponencial de interacción que hemos encontrado entre el péptido de fusión y el colesterol, sobre todo teniendo en cuenta que las glicoproteínas *E1* y *E2 in vitro* han mostrado que la presencia de colesterol facilita el proceso de fusión (Lavillette et al., 2005). Este efecto se podría explicar por la dependencia exponencial en el efecto que el péptido de fusión presenta ante la presencia de colesterol.

Los resultados mas significativos de esta tesis se hayan en el estudio de los péptidos derivados de las regiones 274-298. Éste péptido permite la aparición de estructuras hexagonales en el lípido DEPE a temperaturas menores de lo esperado, esto

significa que esta región peptídica estabiliza estructuras no lamelares necesarias para la función de fusionar, lo que confirma nuestros resultados anteriores de localización del péptido de fusión de la hepatitis C en esta región. Otras regiones que también han mostrado unos resultados significativos han sido las regiones 309-326 y 603-629. Estas regiones desestabilizan las membranas dando lugar a perfiles de difracción propios de membranas desordenadas tanto a baja como alta temperatura. Para sistemas modelo de membranas de DEPE en presencia del péptido 309-326, la fase hexagonal puede ser detectada a temperaturas menores de lo esperado. En cambio en el lípido DEPE en presencia de un péptido derivado de la región 603-629, la fase hexagonal no aparece en ninguno de los perfiles estudiados. Podemos sugerir que el péptido de fusión de HCV se encuentra situado en las regiones 274-298. La región 603-629 también podría estar implicada en el proceso de desestabilización de membrana previo a la fusión, ayudando así a la inserción del péptido de fusión localizado en la región 274-298.

Tras la identificación de las regiones membranotrópicas implicadas en el proceso de fusión, hemos tomado estas regiones como dianas, ya que si estas regiones que se hayan altamente conservadas en todas las estirpes de HCV no interaccionan con membrana, el proceso de fusión no ocurriría y por ello el virus no podría entrar ni infectar a las células. Hemos intentado evitar la interacción de péptidos derivados de estas regiones con otros péptidos provenientes de librerías de las proteínas *E1* y *E2* de la envuelta viral, ya que pensamos que los péptidos diana, regiones altamente hidrofóbicas deben de estar cubiertos con otras partes de la proteína y sólo se encontrarían expuestas en el momento de la fusión tras el cambio conformacional producido en el endosoma como consecuencia del cambio de pH. Después de varios barridos hemos encontrado dos péptidos dirigidos contra la región del péptido de fusión que redujeron un 93% y 98% respectivamente, la liberación de contenidos y la hemifusión del péptido de fusión *in vitro* a relación molar 1/1 diana/inhibidor.

Ensayamos *in vivo* la neutralización de la infección viral que estos péptidos mostraban frente a HCVpp que expresan en la envuelta

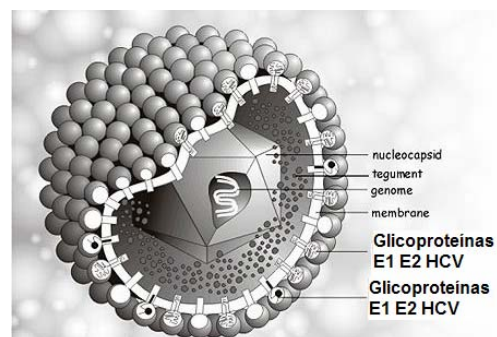


Figura 6.8. Esquema de las HCVpp

viral las glicoproteínas *E1* y *E2* del HCV con células hepáticas (Figura 6.8). Los péptidos inhibidores mostraron una neutralización de la entrada viral del 51% y del 36% a una concentración 0.1mM con HCVpp de la estirpe 1B4J. La concentración a la que los péptidos muestran un efecto significativo de neutralización de la infección es muy alto, por lo que debemos intentar incrementar la afinidad del inhibidor por la diana. Sin embargo el resultado más importante de estos ensayos es que tras un exhaustivo estudio de interacción lípido-péptido hemos encontrado nuevas dianas terapéuticas basadas en regiones membrano-trópicas conservadas que han resultado ser efectivas contra la entrada del HCV a la célula, lo que abre las puertas para el desarrollo de nuevas estrategias de búsqueda de nuevos fármacos y vacunas contra el HCV.



CAPÍTULO VII

DISCUSIÓN



7. DISCUSIÓN GENERAL

Los procesos de entrada y salida de los virus con envuelta lipídica a la célula huésped son, junto con la replicación del material genético viral los acontecimientos más importantes en el ciclo viral. Sin embargo, hay muy pocos fármacos antivirales desarrollados para impedir estos eventos. Esto se debe en gran medida al desconocimiento que se tiene de la complejidad de estos procesos de membrana. Ambos son procesos energéticamente desfavorables por lo que es necesaria la participación de una maquinaria especializada en el virus para facilitar estos procesos. La morfogénesis de los viriones del HCV se lleva a cabo en el retículo endoplasmático, y la proteína *core* es la encargada de interactuar con el RNA, con las proteínas de la envuelta y finalmente con la membrana para formar la envuelta viral. Nosotros hemos encontrado diferentes regiones capaces de interactuar con membranas dentro de esta proteína; sin embargo teniendo en cuenta los resultados obtenidos mediante difracción de rayos X, DSC, FTIR y la bibliografía existente de esta proteína, proponemos la región 29-46 como la región membranotrópica más importante implicada en la morfogénesis viral.

La proteína *p7* es una proteína de la familia de las vioporinas. Recientemente han

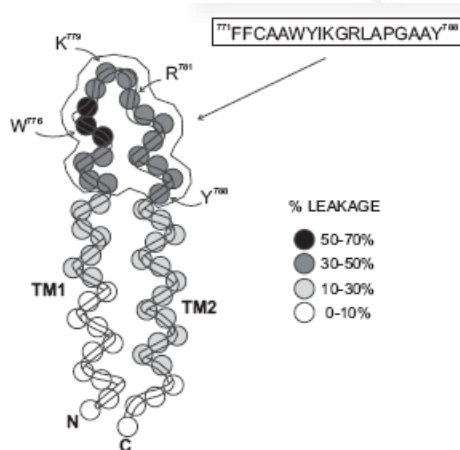


Figura 7.1. Esquema de la proteína *p7*, reseñando los resultados de liberación de contenidos

aparecido trabajos donde mutaciones en el bucle que une sus dos regiones transmembrana provoca una liberación viral 100 veces inferior, por tanto compuestos que bloqueen este canal podría convertirse en otra terapia antiviral. Nosotros hemos observado que la región del bucle es también la región más membranotrópica de la proteína. Un péptido de 18 aminoácidos derivado de esta región no cambia la arquitectura global de la membrana pero permite la formación de poros de un tamaño semejante al que la proteína nativa formaría. Por tanto, para realizar una búsqueda

de agentes que bloqueen el canal podría realizarse con tan sólo péptidos similares al que nosotros hemos estudiado sin necesidad de expresar la proteína *p7*, proteína altamente hidrofóbica, entera.

Las proteínas de fusión son máquinas especializadas que a lo largo de la evolución han sido seleccionadas por su habilidad para ayudar al virus a sortear la barrera que supone la membrana celular. En los últimos años se ha observado que dentro de las proteínas de fusión pueden existir varias regiones capaces de interactuar con la membrana, ayudando así a superar las barreras energéticas impuestas por la membrana celular. En los trabajos presentados en esta tesis se han identificado varias secuencias dentro de las glicoproteínas *E1* y *E2* del HCV, que son las responsables de los proceso de fusión. Aunque todas las regiones membranotrópicas dentro de las glicoproteínas *E1* y *E2* estudiadas, presentan características comunes, de interacción y unión con membranas, se han visto diferencias sobre todo en la arquitectura de las membranas biológicas tras la interacción de estas regiones, que podrían dar idea de sus diferentes papeles en el proceso de fusión. Según los datos obtenidos y la posible localización de las regiones membranotrópicas en las proteínas *E1* y *E2* hemos desarrollado un posible mecanismo de fusión de membranas para el HCV. La sucesión de pasos sería el siguiente (Figura 7.2).

Tras la interacción con el receptor (Figura 7.2 B) y endocitosis del virus en endosomas, el cambio de pH provocaría un cambio conformacional en las proteínas *E1* y *E2* (figura 7.2.C) exponiendo las regiones fusogénicas o permitiendo que éstas se aproximen a la membrana. En primer lugar la región 603-635 de *E2* interactuaría con la membrana del endosoma desestabilizándola y permitiría la inserción del péptido de fusión, región 274-298 en *E1* (Figura 7.2.D). Ambos producirían una desestabilización de la membrana. Teniendo en cuenta la interacción preferencial que la región del péptido de fusión muestra por el colesterol si éste estuviera en la membrana este proceso sería más eficiente. Posteriormente se produciría un contacto con los fosfolípidos negativos de la hemicapa interna, bien por movimientos de flip-flop de los lípidos o por huecos formados en la membrana. Este contacto con los fosfolípidos negativos facilitaría la oligomerización de los péptido, acercando las hemicapas externas de las membranas huésped y viral,

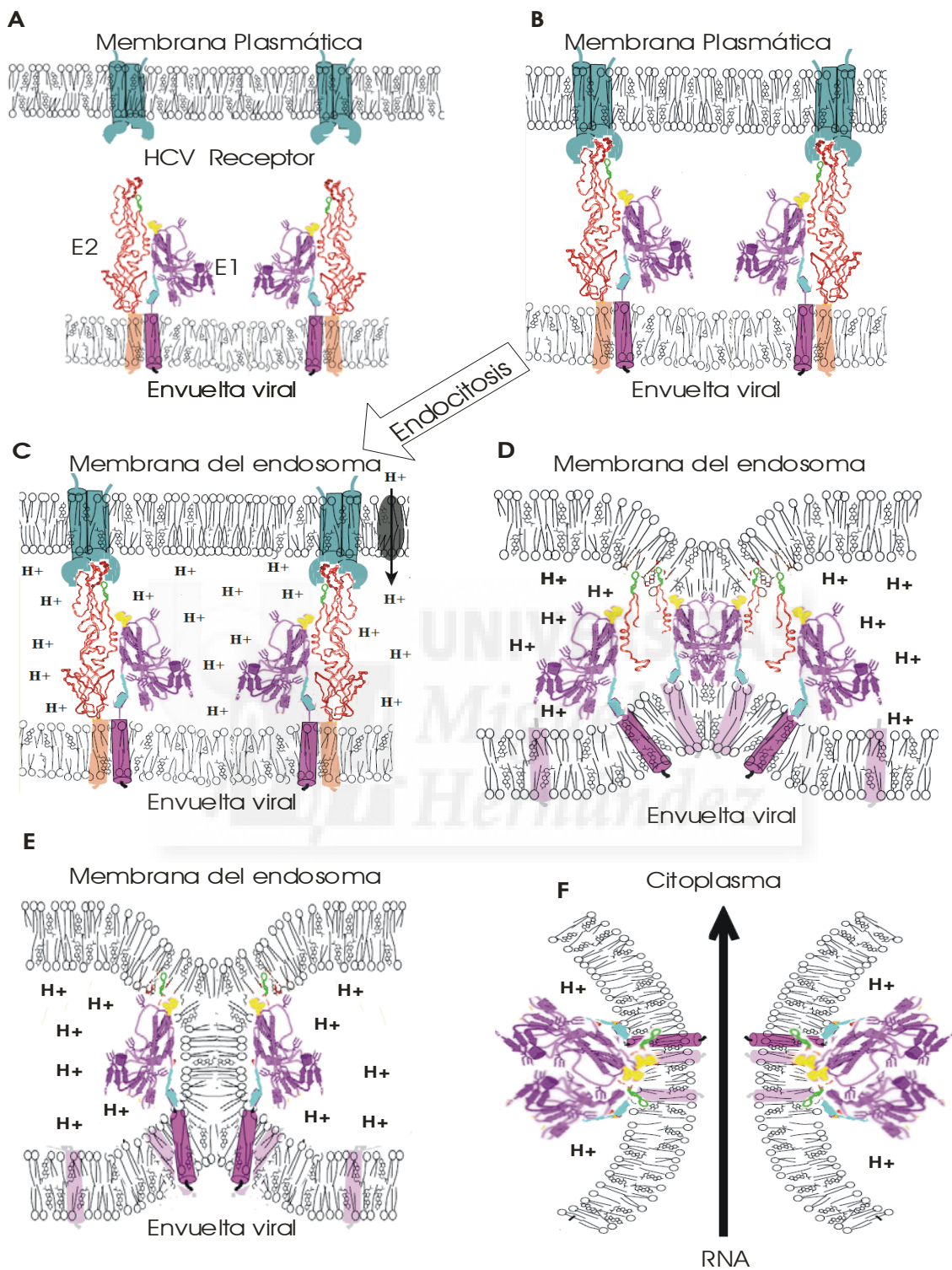


Figura 7.2. Hipótesis de fusión de membranas del HCV. Las regiones membranotrópicas se encuentran señaladas, en amarillo se resalta la región fusogénica de la glicoproteína *E1*, en verde la región fusogénica de *E2* y en azul la región pretransmembrana de *E1*. En las figuras D, E y F se ha eliminado partes de la glicoproteína *E2* para simplificar el modelo. (A) Modelo de las membranas celulares, con los receptores de HCV y de la envuelta viral con las glicoproteínas *E1* y *E2*. (B) Glicoproteína *E2* unida al receptor de HCV. (C) Acidificación de la vesícula de endocitosis por la acción de los transportadores de protones del endosoma, (D) Cambio conformacional en las proteínas *E1* y *E2* exponiendo las regiones membranotrópicas de ambas proteínas. (E) Las regiones membranotrópicas se hallan insertadas interfacialmente desestabilizando y permitiendo la interacción entre las membranas del endosoma y viral. (F) Formación del poro de fusión y liberación el RNA al citoplasma celular.

tendrían y posteriormente induciendo el contacto de las hemicapas internas con la consiguiente fusión (Figura 7.2.E). Mientras tanto el péptido pretransmembrana, situado cercano a la membrana de la envuelta viral, realizaría la misma función que los anteriores pero desestabilizando la membrana de la envuelta vira. La desestabilización de ambas membranas, la de la envuelta viral y la del endosoma, unido a los cambio conformacionales que tendría lugar en estas regiones de las proteínas al interaccionar con la membrana podrían ayudar a superar las barreras energéticas del proceso de fusión. Tras la formación del poro de fusión, estas regiones fusogénicas podrían contactar con los lípidos negativos provocando una estabilización en la membrana de las estructuras no lamelares formadas y con ello el ensanchamiento del poro de fusión que daría lugar a la entrada del virus a la célula huésped (Figura 7.2.F).

Durante los últimos años un gran número de investigaciones se han llevado a cabo para intentar encontrar compuestos terapéuticos contra la infección del HCV. De momento las dianas más importantes a las que se han dirigido estas investigaciones se han basado en evitar la replicación viral. Nosotros, con nuestro trabajo, hemos propuesto nuevas dianas contra la entrada, el ensamblaje y la salida del virus. Además hemos comprobado que las dianas elegidas para entrada viral tienen efecto neutralizante en la infección entrada viral consiguiendo dos nuevos compuestos basados en péptidos que a concentración milimolar neutralizan la infección viral. Sabemos que debemos seguir trabajando para aumentar la afinidad de estos fármacos por sus dianas pero pueden ser el inicio de una nueva generación de medicamentos dirigidos a evitar el paso más importante de la infección, la entrada viral.

CAPÍTULO VIII

UNIVERSITAS

Miguel

Hernández

CONCLUSIONES



8.1. CONCLUSIONES


1. Hemos identificado varias regiones membranotrópicas en la proteína core del HCV. De entre ellas, la región 29-46 es capaz de perturbar la arquitectura de la membrana. Esta región podría jugar un papel importante en el ensamblaje y morfogénesis viral.
2. Hemos identificado la región del bucle como la parte más membranotrópica de la proteína p7 del HCV. Un péptido de 18 aminoácidos derivado de esta región es capaz de formar poros del mismo tamaño que los formados por la proteína nativa.
3. Hemos identificado diferentes regiones fusogénicas dentro de las proteínas E1 y E2 de HCV. Extrapolando los resultados obtenidos con los péptidos sintéticos a las proteínas nativas hemos propuesto un modelo para explicar la fusión de membranas producida por el HCV.
4. Hemos encontrado un péptido derivado de la región 309-340 de la proteína E1, localizado cerca de la región transmembrana que podría desempeñar una función parecida a la que ejercen las regiones pretransmembrana de las proteínas de clase I. Esta región perturba y modifica la arquitectura de la membrana. Interacciona con fosfolípidos que modifican la curvatura de la membrana y estabiliza estructuras no lamelares necesarias para la fusión de membranas.
5. La región fusogénica de la glicoproteína E2, localizada entre los residuos 603-634, desestabiliza altamente la membrana y modifica su arquitectura pero evita la formación de fases no lamelares.
6. Hemos propuesto la región 274-298 de la proteína E1 como péptido de fusión de HCV. Esta región de la glicoproteína E1 desestabiliza la membrana, muestra un aumento del efecto fusogénico correlacionado exponencialmente con la concentración de colesterol, y estabiliza estructuras no lamelares necesarias en el proceso de fusión.
7. Tomando diferentes regiones membranotrópicas de las glicoproteínas E1 y E2 del virus del HCV como diana, hemos encontrado dos péptidos que *in vitro* inhiben la actividad del péptido de fusión un 97% e *in vivo* neutralizan un 50% la infección de HCVpp de la estirpe 1BCG a las células hepáticas a una concentración 0.1mM.



8.2 CONCLUSIONS

1. We have identified several membrano-active regions in the HCV structural core protein; among them, the region 29-46 significantly perturbs the membrane architecture. This region might play an important role in the viral assembly and morphogenesis.
2. We have identified the loop region in the HCV p7 protein as the most membranotropic domain in the protein. One 18-mer peptide that mimics the loop region forms pores with a similar size than those formed by the native protein.
3. We have identified several fusogenic regions along the E1 and E2 glycoproteins. We have extrapolated the biophysical characterization obtained for the synthetic peptides and we have proposed a fusion model to explain how the HCV might enter into the cell.
4. We have found one peptide derived from the region 309-340 of the E1 glycoprotein, located near the transmembrane domain that could play a similar function that are played by the pretransmembrane region in the Class I fusion proteins. This region disturbs the membrane and modifies the membrane architecture, it interacts with phospholipids that modify the membrane curvature and it stabilizes non-lamellar structures needed for the fusion process.
5. The fusogenic region in the protein E2 is located between the residues 603-634. This region desestabilizes the membrane and modify the membrane architecture, although it prevents the formation of non-lamellar structures.
6. We have proposed the region 274-298 in the E1 protein as a fusion peptide. This region perturbs the membrane and shows a fusion facilitation correlated with the cholesterol concentration. This peptide stabilizes non-lamellar structures needed for the fusion process.
7. We have used several membranotropic regions along the E1 and E2 glycoproteins as targets to find potential therapeutical targets. We have found two peptides that *in vitro* inhibit a 97% the fusogenic effect of the fusion peptide and *in vivo* one peptide neutralises about 50% of entry of HCVpp strain 1BCG in hepatic cells at a concentration about 0.1mM.



The background of the page is a dense field of purple and yellow flowers, possibly lavender and marigolds, with a soft, out-of-focus effect. The colors are vibrant and create a warm, natural atmosphere.

CAPÍTULO IX

UNIVERSITAS
Miguel

BIBLIOGRAFÍA



9. BIBLIOGRAFÍA

- Acosta-Rivero, N., Alvarez-Obregon, J. C., Musacchio, A., Falcon, V., Duenas-Carrera, S., Marante, J., Menendez, I., and Morales, J. (2002). In vitro self-assembled HCV core virus-like particles induce a strong antibody immune response in sheep. *Biochem Biophys Res Commun* **290**, 300-4.
- Acton, S. L., Scherer, P. E., Lodish, H. F., and Krieger, M. (1994). Expression cloning of SR-BI, a CD36-related class B scavenger receptor. *J Biol Chem* **269**, 21003-9.
- Aman, M. J., Bosio, C. M., Panchal, R. G., Burnett, J. C., Schmaljohn, A., and Bavari, S. (2003). Molecular mechanisms of filovirus cellular trafficking. *Microbes Infect* **5**, 639-49.
- Argenziano, G., Puig, S., Zalaudek, I., Sera, F., Corona, R., Alsina, M., Barbato, F., Carrera, C., Ferrara, G., Guilabert, A., Massi, D., Moreno-Romero, J. A., Munoz-Santos, C., Petrillo, G., Segura, S., Soyer, H. P., Zanchini, R., and Malveyh, J. (2006). Dermoscopy improves accuracy of primary care physicians to triage lesions suggestive of skin cancer. *J Clin Oncol* **24**, 1877-82.
- Arrondo, J. L., and Goni, F. M. (1999). Structure and dynamics of membrane proteins as studied by infrared spectroscopy. *Prog Biophys Mol Biol* **72**, 367-405.
- Arrondo, J. L., Muga, A., Castresana, J., and Goni, F. M. (1993). Quantitative studies of the structure of proteins in solution by Fourier-transform infrared spectroscopy. *Prog Biophys Mol Biol* **59**, 23-56.
- Bangham, A. D., and Horne, R. W. (1964). Negative Staining of Phospholipids and Their Structural Modification by Surface-Active Agents as Observed in the Electron Microscope. *J Mol Biol* **8**, 660-8.
- Bangham, A. D., Standish, M. M., and Watkins, J. C. (1965a). Diffusion of univalent ions across the lamellae of swollen phospholipids. *J Mol Biol* **13**, 238-52.
- Bangham, A. D., Standish, M. M., and Weissmann, G. (1965b). The action of steroids and streptolysin S on the permeability of phospholipid structures to cations. *J Mol Biol* **13**, 253-9.
- Bartenschlager, R., and Pietschmann, T. (2005). Efficient hepatitis C virus cell culture system: what a difference the host cell makes. *Proc Natl Acad Sci U S A* **102**, 9739-40.
- Barth, A. (2007). Infrared spectroscopy of proteins. *Biochim Biophys Acta* **1767**, 1073-101.
- Bartosch, B., Dubuisson, J., and Cosset, F. L. (2003). Infectious hepatitis C virus pseudo-particles containing functional E1-E2 envelope protein complexes. *J Exp Med* **197**, 633-42.
- Basanez, G. (2002). Membrane fusion: the process and its energy suppliers. *Cell Mol Life Sci* **59**, 1478-90.
- Basanez, G., Shinnar, A. E., and Zimmerberg, J. (2002). Interaction of hagfish cathelicidin antimicrobial peptides with model lipid membranes. *FEBS Lett* **532**, 115-20.
- Bavari, S., Bosio, C. M., Wiegand, E., Ruthel, G., Will, A. B., Geisbert, T. W., Hevey, M., Schmaljohn, C., Schmaljohn, A., and Aman, M. J. (2002). Lipid raft microdomains: a gateway for compartmentalized trafficking of Ebola and Marburg viruses. *J Exp Med* **195**, 593-602.
- Bender, F. C., Whitbeck, J. C., Ponce de Leon, M., Lou, H., Eisenberg, R. J., and Cohen, G. H. (2003). Specific association of glycoprotein B with lipid rafts during herpes simplex virus entry. *J Virol* **77**, 9542-52.

- Blumenthal, R., Clague, M. J., Durell, S. R., and Eband, R. M. (2003). Membrane fusion. *Chem Rev* **103**, 53-69.
- Boucheix, C., and Rubinstein, E. (2001). Tetraspanins. *Cell Mol Life Sci* **58**, 1189-205.
- Brockman, H. (1994). Dipole potential of lipid membranes. *Chem Phys Lipids* **73**, 57-79.
- Brown, D. A., and London, E. (2000). Structure and function of sphingolipid- and cholesterol-rich membrane rafts. *J Biol Chem* **275**, 17221-4.
- Brown, R. E. (1998). Sphingolipid organization in biomembranes: what physical studies of model membranes reveal. *J Cell Sci* **111** (Pt 1), 1-9.
- Cafiso, D., McLaughlin, A., McLaughlin, S., and Winiski, A. (1989). Measuring electrostatic potentials adjacent to membranes. *Methods Enzymol* **171**, 342-64.
- Carrere-Kremer, S., Montpellier-Pala, C., Cocquerel, L., Wychowski, C., Penin, F., and Dubuisson, J. (2002). Subcellular localization and topology of the p7 polypeptide of hepatitis C virus. *J Virol* **76**, 3720-30.
- Casal, H. L., and Mantsch, H. H. (1984). Polymorphic phase behaviour of phospholipid membranes studied by infrared spectroscopy. *Biochim Biophys Acta* **779**, 381-401.
- Cevc, G. (1990). Membrane electrostatics. *Biochim Biophys Acta* **1031**, 311-82.
- Cladera, J., Martin, I., Ruysschaert, J. M., and O'Shea, P. (1999). Characterization of the sequence of interactions of the fusion domain of the simian immunodeficiency virus with membranes. Role of the membrane dipole potential. *J Biol Chem* **274**, 29951-9.
- Cladera, J., and O'Shea, P. (1998). Intramembrane molecular dipoles affect the membrane insertion and folding of a model amphiphilic peptide. *Biophys J* **74**, 2434-42.
- Cladera, J., Rigaud, J. L., Villaverde, J., and Dunach, M. (1997). Liposome solubilization and membrane protein reconstitution using Chaps and Chapso. *Eur J Biochem* **243**, 798-804.
- Clarke, R. J., and Kane, D. J. (1997). Optical detection of membrane dipole potential: avoidance of fluidity and dye-induced effects. *Biochim Biophys Acta* **1323**, 223-39.
- Cocquerel, L., Wychowski, C., Minner, F., Penin, F., and Dubuisson, J. (2000). Charged residues in the transmembrane domains of hepatitis C virus glycoproteins play a major role in the processing, subcellular localization, and assembly of these envelope proteins. *J Virol* **74**, 3623-33.
- Cullis, P. R., and de Kruijff, B. (1979). Lipid polymorphism and the functional roles of lipids in biological membranes. *Biochim Biophys Acta* **559**, 399-420.
- Cullis, P. R., van Dijck, P. W., de Kruijff, B., and de Gier, J. (1978). Effects of cholesterol on the properties of equimolar mixtures of synthetic phosphatidylethanolamine and phosphatidylcholine. A ³¹P NMR and differential scanning calorimetry study. *Biochim Biophys Acta* **513**, 21-30.
- Cha, T. A., Beall, E., Irvine, B., Kolberg, J., Chien, D., Kuo, G., and Urdea, M. S. (1992). At least five related, but distinct, hepatitis C viral genotypes exist. *Proc Natl Acad Sci U S A* **89**, 7144-8.
- Chambers, T. J., Hahn, C. S., Galler, R., and Rice, C. M. (1990). Flavivirus genome organization, expression, and replication. *Annu Rev Microbiol* **44**, 649-88.
- Chen, Z., and Rand, R. P. (1997). The influence of cholesterol on phospholipid membrane curvature and bending elasticity. *Biophys J* **73**, 267-76.
- Chernomordik, L. V., and Kozlov, M. M. (2003). Protein-lipid interplay in fusion and fission of biological membranes. *Annu Rev Biochem* **72**, 175-207.
- Chernomordik, L. V., and Kozlov, M. M. (2005). Membrane hemifusion: crossing a chasm in two leaps. *Cell* **123**, 375-82.

- Choo, Q. L., Richman, K. H., Han, J. H., Berger, K., Lee, C., Dong, C., Gallegos, C., Coit, D., Medina-Selby, R., Barr, P. J., and et al. (1991). Genetic organization and diversity of the hepatitis C virus. *Proc Natl Acad Sci U S A* **88**, 2451-5.
- Chung, C. S., Huang, C. Y., and Chang, W. (2005). Vaccinia virus penetration requires cholesterol and results in specific viral envelope proteins associated with lipid rafts. *J Virol* **79**, 1623-34.
- De Francesco, R., and Migliaccio, G. (2005). Challenges and successes in developing new therapies for hepatitis C. *Nature* **436**, 953-60.
- de Kruijff, B. (1997). Lipid polymorphism and biomembrane function. *Curr Opin Chem Biol* **1**, 564-9.
- Di Bisceglie, A. M., Conjeevaram, H. S., Fried, M. W., Sallie, R., Park, Y., Yurdaydin, C., Swain, M., Kleiner, D. E., Mahaney, K., and Hoofnagle, J. H. (1995). Ribavirin as therapy for chronic hepatitis C. A randomized, double-blind, placebo-controlled trial. *Ann Intern Med* **123**, 897-903.
- Dimitrov, A. S., Xiao, X., Dimitrov, D. S., and Blumenthal, R. (2001). Early intermediates in HIV-1 envelope glycoprotein-mediated fusion triggered by CD4 and co-receptor complexes. *J Biol Chem* **276**, 30335-41.
- Dowhan, W. (1997). Molecular basis for membrane phospholipid diversity: why are there so many lipids? *Annu Rev Biochem* **66**, 199-232.
- Dreux, M., Pietschmann, T., Granier, C., Voisset, C., Ricard-Blum, S., Mangeot, P. E., Keck, Z., Fong, S., Vu-Dac, N., Dubuisson, J., Bartenschlager, R., Lavillette, D., and Cosset, F. L. (2006). High density lipoprotein inhibits hepatitis C virus-neutralizing antibodies by stimulating cell entry via activation of the scavenger receptor BI. *J Biol Chem* **281**, 18285-95.
- Drummer, H. E., and Pountourios, P. (2004). Hepatitis C virus glycoprotein E2 contains a membrane-proximal heptad repeat sequence that is essential for E1E2 glycoprotein heterodimerization and viral entry. *J Biol Chem* **279**, 30066-72.
- Eftink, M. R., and Ghiron, C. A. (1976). Exposure of tryptophanyl residues in proteins. Quantitative determination by fluorescence quenching studies. *Biochemistry* **15**, 672-80.
- Eickmann, M., Becker, S., Klenk, H. D., Doerr, H. W., Stadler, K., Censini, S., Guidotti, S., Maignani, V., Scarselli, M., Mora, M., Donati, C., Han, J. H., Song, H. C., Abrignani, S., Covacci, A., and Rappuoli, R. (2003). Phylogeny of the SARS coronavirus. *Science* **302**, 1504-5.
- Epanand, R. M. (1998). Lipid polymorphism and protein-lipid interactions. *Biochim Biophys Acta* **1376**, 353-68.
- Estepa, A. M., Rocha, A. I., Mas, V., Perez, L., Encinar, J. A., Nunez, E., Fernandez, A., Gonzalez Ros, J. M., Gavilanes, F., and Coll, J. M. (2001). A protein G fragment from the salmonid viral hemorrhagic septicemia rhabdovirus induces cell-to-cell fusion and membrane phosphatidylserine translocation at low pH. *J Biol Chem* **276**, 46268-75.
- Evans, M. J., von Hahn, T., Tscherne, D. M., Syder, A. J., Panis, M., Wolk, B., Hatzioannou, T., McKeating, J. A., Bieniasz, P. D., and Rice, C. M. (2007). Claudin-1 is a hepatitis C virus co-receptor required for a late step in entry. *Nature* **446**, 801-5.
- Fernandes, M. X., Garcia de la Torre, J., and Castanho, M. A. (2002). Joint determination by Brownian dynamics and fluorescence quenching of the in-depth location profile of biomolecules in membranes. *Anal Biochem* **307**, 1-12.
- Florine-Casteel, K. (1990). Phospholipid order in gel- and fluid-phase cell-size liposomes measured by digitized video fluorescence polarization microscopy. *Biophys J* **57**, 1199-215.

- Furuse, M., Fujita, K., Hiiragi, T., Fujimoto, K., and Tsukita, S. (1998). Claudin-1 and -2: novel integral membrane proteins localizing at tight junctions with no sequence similarity to occludin. *J Cell Biol* **141**, 1539-50.
- Garry, R. F., and Dash, S. (2003). Proteomics computational analyses suggest that hepatitis C virus E1 and pestivirus E2 envelope glycoproteins are truncated class II fusion proteins. *Virology* **307**, 255-65.
- Goffard, A., Lazrek, M., Schanen, C., Lobert, P. E., Bocket, L., Dewilde, A., and Hober, D. (2006). [Emergent viruses: SARS-associate coronavirus and H5N1 influenza virus]. *Ann Biol Clin (Paris)* **64**, 195-208.
- Gonzalez, M. E., and Carrasco, L. (2003). Viroporins. *FEBS Lett* **552**, 28-34.
- Grakoui, A., McCourt, D. W., Wychowski, C., Feinstone, S. M., and Rice, C. M. (1993). Characterization of the hepatitis C virus-encoded serine proteinase: determination of proteinase-dependent polyprotein cleavage sites. *J Virol* **67**, 2832-43.
- Griffin, S. D., Beales, L. P., Clarke, D. S., Worsfold, O., Evans, S. D., Jaeger, J., Harris, M. P., and Rowlands, D. J. (2003). The p7 protein of hepatitis C virus forms an ion channel that is blocked by the antiviral drug, Amantadine. *FEBS Lett* **535**, 34-8.
- Griffin, S. D., Harvey, R., Clarke, D. S., Barclay, W. S., Harris, M., and Rowlands, D. J. (2004). A conserved basic loop in hepatitis C virus p7 protein is required for amantadine-sensitive ion channel activity in mammalian cells but is dispensable for localization to mitochondria. *J Gen Virol* **85**, 451-61.
- Guillen, J., Moreno, M. R., Perez-Berna, A. J., Bernabeu, A., and Villalain, J. (2007). Interaction of a Peptide from the Pre-transmembrane Domain of the Severe Acute Respiratory Syndrome Coronavirus Spike Protein with Phospholipid Membranes. *J Phys Chem B* **111**, 13714-25.
- Hafez, I. M., and Cullis, P. R. (2001). Roles of lipid polymorphism in intracellular delivery. *Adv Drug Deliv Rev* **47**, 139-48.
- Helle, F., Goffard, A., Morel, V., Duverlie, G., McKeating, J., Keck, Z. Y., Foung, S., Penin, F., Dubuisson, J., and Voisset, C. (2007). The neutralizing activity of anti-hepatitis C virus antibodies is modulated by specific glycans on the E2 envelope protein. *J Virol* **81**, 8101-11.
- Hijikata, M., Kato, N., Ootsuyama, Y., Nakagawa, M., and Shimotohno, K. (1991). Gene mapping of the putative structural region of the hepatitis C virus genome by in vitro processing analysis. *Proc Natl Acad Sci U S A* **88**, 5547-51.
- Hope, R. G., and McLauchlan, J. (2000). Sequence motifs required for lipid droplet association and protein stability are unique to the hepatitis C virus core protein. *J Gen Virol* **81**, 1913-25.
- Houghton, M., Weiner, A., Han, J., Kuo, G., and Choo, Q. L. (1991). Molecular biology of the hepatitis C viruses: implications for diagnosis, development and control of viral disease. *Hepatology* **14**, 381-8.
- Huang, C., and Li, S. (1999). Calorimetric and molecular mechanics studies of the thermotropic phase behavior of membrane phospholipids. *Biochim Biophys Acta* **1422**, 273-307.
- Jahn, R., and Grubmuller, H. (2002). Membrane fusion. *Curr Opin Cell Biol* **14**, 488-95.
- Jahn, R., and Sudhof, T. C. (1999). Membrane fusion and exocytosis. *Annu Rev Biochem* **68**, 863-911.
- Janmey, P. A., and Kinnunen, P. K. (2006). Biophysical properties of lipids and dynamic membranes. *Trends Cell Biol* **16**, 538-46.
- Jardetzky, T. S., and Lamb, R. A. (2004). Virology: a class act. *Nature* **427**, 307-8.

- Jelesarov, I., and Bosshard, H. R. (1999). Isothermal titration calorimetry and differential scanning calorimetry as complementary tools to investigate the energetics of biomolecular recognition. *J Mol Recognit* **12**, 3-18.
- Jolivet-Reynaud, C., Dalbon, P., Viola, F., Yvon, S., Paranhos-Baccala, G., Piga, N., Bridon, L., Trabaud, M. A., Battail, N., Sibai, G., and Jolivet, M. (1998). HCV core immunodominant region analysis using mouse monoclonal antibodies and human sera: characterization of major epitopes useful for antigen detection. *J Med Virol* **56**, 300-9.
- Jones, M. N. (1995). The surface properties of phospholipid liposome systems and their characterisation. *Adv Colloid Interface Sci* **54**, 93-128.
- Kaiser, R. D., and London, E. (1998). Location of diphenylhexatriene (DPH) and its derivatives within membranes: comparison of different fluorescence quenching analyses of membrane depth. *Biochemistry* **37**, 8180-90.
- Kaiser, R. D., and London, E. (1999). Location of diphenylhexatriene (DPH) and its derivatives within membranes: comparison of different fluorescence quenching analyses of membrane depth. *Biochemistry* **38**, 2610.
- Kato, N., Hijikata, M., Ootsuyama, Y., Nakagawa, M., Ohkoshi, S., Sugimura, T., and Shimotohno, K. (1990). Molecular cloning of the human hepatitis C virus genome from Japanese patients with non-A, non-B hepatitis. *Proc Natl Acad Sci U S A* **87**, 9524-8.
- Kelly, S. M., Jess, T. J., and Price, N. C. (2005). How to study proteins by circular dichroism. *Biochim Biophys Acta* **1751**, 119-39.
- Kielian, M. (2006). Class II virus membrane fusion proteins. *Virology* **344**, 38-47.
- Koynova, R., and Caffrey, M. (1995). Phases and phase transitions of the sphingolipids. *Biochim Biophys Acta* **1255**, 213-36.
- Koziel, M. J., Dudley, D., Wong, J. T., Dienstag, J., Houghton, M., Ralston, R., and Walker, B. D. (1992). Intrahepatic cytotoxic T lymphocytes specific for hepatitis C virus in persons with chronic hepatitis. *J Immunol* **149**, 3339-44.
- Kozlov, M. M., Leikin, S. L., Chernomordik, L. V., Markin, V. S., and Chizmadzhev, Y. A. (1989). Stalk mechanism of vesicle fusion. Intermixing of aqueous contents. *Eur Biophys J* **17**, 121-9.
- Laggner, P. (1988). X-ray studies on biological membrane using synchrotron radiation. *Topic in current Chemistry* **145**.
- Lakowicz, J. R. (2006). "Principles of fluorescence spectroscopy," 3rd/Ed. Springer, New York ; Berlin.
- Langmuir, I. (1917). Constitution and fundamental properties of solids and liquids. II. Liquids. *J.Am.Chem.Soc.* **39**, 1848-1906.
- Lavillette, D., Bartosch, B., Nourrisson, D., Verney, G., Cosset, F. L., Penin, F., and Pecheur, E. I. (2006). Hepatitis C virus glycoproteins mediate low pH-dependent membrane fusion with liposomes. *J Biol Chem* **281**, 3909-17.
- Lavillette, D., Tarr, A. W., Voisset, C., Donot, P., Bartosch, B., Bain, C., Patel, A. H., Dubuisson, J., Ball, J. K., and Cosset, F. L. (2005). Characterization of host-range and cell entry properties of the major genotypes and subtypes of hepatitis C virus. *Hepatology* **41**, 265-74.
- Loew, G. H., Phillips, J., and Pack, G. (1979). Quantum chemical studies of the metabolism of polycyclic aromatic amines and the stabilities and electrophilicities of their arylnitrenium ions in relation to their mutagenic/carcinogenic potencies. *Cancer Biochem Biophys* **3**, 101-10.
- Luzzati, V. (1997). Biological significance of lipid polymorphism: the cubic phases. *Curr Opin Struct Biol* **7**, 661-8.
- Luzzati, V., and Husson, F. (1962). The structure of the liquid-crystalline phasis of lipid-water systems. *J Cell Biol* **12**, 207-19.

- Maillard, P., Huby, T., Andreo, U., Moreau, M., Chapman, J., and Budkowska, A. (2006). The interaction of natural hepatitis C virus with human scavenger receptor SR-BI/Cla1 is mediated by ApoB-containing lipoproteins. *Faseb J* **20**, 735-7.
- Majeau, N., Gagne, V., Bolduc, M., and Leclerc, D. (2005). Signal peptide peptidase promotes the formation of hepatitis C virus non-enveloped particles and is captured on the viral membrane during assembly. *J Gen Virol* **86**, 3055-64.
- Mantsch, H. H., and McElhaney, R. N. (1991). Phospholipid phase transitions in model and biological membranes as studied by infrared spectroscopy. *Chem Phys Lipids* **57**, 213-26.
- Marsh, D. (1980). Molecular motion in phospholipid bilayers in the gel phase: long axis rotation. *Biochemistry* **19**, 1632-1637.
- Matto, M., Rice, C. M., Aroeti, B., and Glenn, J. S. (2004). Hepatitis C virus core protein associates with detergent-resistant membranes distinct from classical plasma membrane rafts. *J Virol* **78**, 12047-53.
- Mayer, L. D., Hope, M. J., and Cullis, P. R. (1986). Vesicles of variable sizes produced by a rapid extrusion procedure. *Biochim Biophys Acta* **858**, 161-8.
- McHutchison, J. G., and Poynard, T. (1999). Combination therapy with interferon plus ribavirin for the initial treatment of chronic hepatitis C. *Semin Liver Dis* **19 Suppl 1**, 57-65.
- Meertens, L., Bertaux, C., and Dragic, T. (2006). Hepatitis C virus entry requires a critical postinternalization step and delivery to early endosomes via clathrin-coated vesicles. *J Virol* **80**, 11571-8.
- Miyayari, Y., Atsuzawa, K., Usuda, N., Watashi, K., Hishiki, T., Zayas, M., Bartenschlager, R., Wakita, T., Hijikata, M., and Shimotohno, K. (2007). The lipid droplet is an important organelle for hepatitis C virus production. *Nat Cell Biol* **9**, 1089-97.
- Munoz-Barroso, I., Salzwedel, K., Hunter, E., and Blumenthal, R. (1999). Role of the membrane-proximal domain in the initial stages of human immunodeficiency virus type 1 envelope glycoprotein-mediated membrane fusion. *J Virol* **73**, 6089-92.
- Nakai, K., Okamoto, T., Kimura-Someya, T., Ishii, K., Lim, C. K., Tani, H., Matsuo, E., Abe, T., Mori, Y., Suzuki, T., Miyamura, T., Nunberg, J. H., Moriishi, K., and Matsuura, Y. (2006). Oligomerization of hepatitis C virus core protein is crucial for interaction with the cytoplasmic domain of E1 envelope protein. *J Virol* **80**, 11265-73.
- Neumann, A. U., Lam, N. P., Dahari, H., Davidian, M., Wiley, T. E., Mika, B. P., Perelson, A. S., and Layden, T. J. (2000). Differences in viral dynamics between genotypes 1 and 2 of hepatitis C virus. *J Infect Dis* **182**, 28-35.
- Neumann N, S. G. (1990). Circular Dichroism of proteins. *Bradshaw*, 107-117.
- New (1990). Liposomes, a practical approach. *IRI Press, Oxford*
- Nieva, J. L., and Agirre, A. (2003). Are fusion peptides a good model to study viral cell fusion? *Biochim Biophys Acta* **1614**, 104-15.
- Ohvo-Rekila, H., Ramstedt, B., Leppimaki, P., and Slotte, J. P. (2002). Cholesterol interactions with phospholipids in membranes. *Prog Lipid Res* **41**, 66-97.
- Okada, A., Miura, T., and Takeuchi, H. (2001). Protonation of histidine and histidine-tryptophan interaction in the activation of the M2 ion channel from influenza A virus. *Biochemistry* **40**, 6053-60.
- Op De Beeck, A., Voisset, C., Bartosch, B., Ciczora, Y., Cocquerel, L., Keck, Z., Fong, S., Cosset, F. L., and Dubuisson, J. (2004). Characterization of functional hepatitis C virus envelope glycoproteins. *J Virol* **78**, 2994-3002.

- Patargias, G., Zitzmann, N., Dwek, R., and Fischer, W. B. (2006). Protein-protein interactions: modeling the hepatitis C virus ion channel p7. *J Med Chem* **49**, 648-55.
- Pawlotsky, J. M. (2003). Hepatitis C virus genetic variability: pathogenic and clinical implications. *Clin Liver Dis* **7**, 45-66.
- Peng, Y., Akmentin, W., Connelly, M. A., Lund-Katz, S., Phillips, M. C., and Williams, D. L. (2004). Scavenger receptor BI (SR-BI) clustered on microvillar extensions suggests that this plasma membrane domain is a way station for cholesterol trafficking between cells and high-density lipoprotein. *Mol Biol Cell* **15**, 384-96.
- Penin, F., Dubuisson, J., Rey, F. A., Moradpour, D., and Pawlotsky, J. M. (2004). Structural biology of hepatitis C virus. *Hepatology* **39**, 5-19.
- Perez-Berna, A. J., Guillen, J., Moreno, M. R., Bernabeu, A., Pabst, G., Laggner, P., and Villalain, J. (2008a). Identification of the Membrane-active Regions of Hepatitis C Virus p7 Protein: BIOPHYSICAL CHARACTERIZATION OF THE LOOP REGION. *J Biol Chem* **283**, 8089-101.
- Perez-Berna, A. J., Guillen, J., Moreno, M. R., Gomez-Sanchez, A. I., Pabst, G., Laggner, P., and Villalain, J. (2008b). Interaction of the most membranotropic region of the HCV E2 envelope glycoprotein with membranes. Biophysical characterization. *Biophys J*.
- Perez-Berna, A. J., Moreno, M. R., Guillen, J., Bernabeu, A., and Villalain, J. (2006). The membrane-active regions of the hepatitis C virus E1 and E2 envelope glycoproteins. *Biochemistry* **45**, 3755-68.
- Perez-Berna, A. J., Veiga, A. S., Castanho, M. A., and Villalain, J. (2007). Hepatitis C virus core protein binding to lipid membranes: the role of domains 1 and 2. *J Viral Hepat*.
- Perez-Berna, A. J., Veiga, A. S., Castanho, M. A., and Villalain, J. (2008c). Hepatitis C virus core protein binding to lipid membranes: the role of domains 1 and 2. *J Viral Hepat* **15**, 346-56.
- Qureshi, S. A. (2007). Hepatitis C virus—biology, host evasion strategies, and promising new therapies on the horizon. *Med Res Rev* **27**, 353-73.
- Ramstedt, B., and Slotte, J. P. (2002). Membrane properties of sphingomyelins. *FEBS Lett* **531**, 33-7.
- Rhinds, D., and Brissette, L. (2004). The role of scavenger receptor class B type I (SR-BI) in lipid trafficking: defining the rules for lipid traders. *Int J Biochem Cell Biol* **36**, 39-77.
- Roche, S., Bressanelli, S., Rey, F. A., and Gaudin, Y. (2006). Crystal structure of the low-pH form of the vesicular stomatitis virus glycoprotein G. *Science* **313**, 187-91.
- Roche, S., Rey, F. A., Gaudin, Y., and Bressanelli, S. (2007). Structure of the prefusion form of the vesicular stomatitis virus glycoprotein G. *Science* **315**, 843-8.
- Saez-Cirion, A., Gomara, M. J., Agirre, A., and Nieva, J. L. (2003). Pre-transmembrane sequence of Ebola glycoprotein. Interfacial hydrophobicity distribution and interaction with membranes. *FEBS Lett* **533**, 47-53.
- Sainz, B., Jr., Rausch, J. M., Gallaher, W. R., Garry, R. F., and Wimley, W. C. (2005). The aromatic domain of the coronavirus class I viral fusion protein induces membrane permeabilization: putative role during viral entry. *Biochemistry* **44**, 947-58.
- Salzwedel, K., West, J. T., and Hunter, E. (1999). A conserved tryptophan-rich motif in the membrane-proximal region of the human immunodeficiency virus type 1 gp41 ectodomain is important for Env-mediated fusion and virus infectivity. *J Virol* **73**, 2469-80.

- Santos, N. C., Prieto, M., and Castanho, M. A. (2003). Quantifying molecular partition into model systems of biomembranes: an emphasis on optical spectroscopic methods. *Biochim Biophys Acta* **1612**, 123-35.
- Schamberger, J., and Clarke, R. J. (2002). Hydrophobic ion hydration and the magnitude of the dipole potential. *Biophys J* **82**, 3081-8.
- Schmidt-Mende, J., Bieck, E., Hugle, T., Penin, F., Rice, C. M., Blum, H. E., and Moradpour, D. (2001). Determinants for membrane association of the hepatitis C virus RNA-dependent RNA polymerase. *J Biol Chem* **276**, 44052-63.
- Seeger, C. (2005). Salient molecular features of hepatitis C virus revealed. *Trends Microbiol* **13**, 528-34.
- Seigneuret, M. (2006). Complete predicted three-dimensional structure of the facilitator transmembrane protein and hepatitis C virus receptor CD81: conserved and variable structural domains in the tetraspanin superfamily. *Biophys J* **90**, 212-27.
- Shah, W. A., Peng, H., and Carbonetto, S. (2006). Role of non-raft cholesterol in lymphocytic choriomeningitis virus infection via alpha-dystroglycan. *J Gen Virol* **87**, 673-8.
- Siegel, D. P. (1993). Energetics of intermediates in membrane fusion: comparison of stalk and inverted micellar intermediate mechanisms. *Biophys J* **65**, 2124-40.
- Siegel, D. P. (1999). The modified stalk mechanism of lamellar/inverted phase transitions and its implications for membrane fusion. *Biophys J* **76**, 291-313.
- Siegel, D. P., and Epan, R. M. (1997). The mechanism of lamellar-to-inverted hexagonal phase transitions in phosphatidylethanolamine: implications for membrane fusion mechanisms. *Biophys J* **73**, 3089-111.
- Simmonds, P., Bukh, J., Combet, C., Deleage, G., Enomoto, N., Feinstone, S., Halfon, P., Inchauspe, G., Kuiken, C., Maertens, G., Mizokami, M., Murphy, D. G., Okamoto, H., Pawlotsky, J. M., Penin, F., Sablon, E., Shin, I. T., Stuyver, L. J., Thiel, H. J., Viazov, S., Weiner, A. J., and Widell, A. (2005). Consensus proposals for a unified system of nomenclature of hepatitis C virus genotypes. *Hepatology* **42**, 962-73.
- Somerharju, P., Virtanen, J. A., and Cheng, K. H. (1999). Lateral organisation of membrane lipids. The superlattice view. *Biochim Biophys Acta* **1440**, 32-48.
- Song, H. C., Seo, M. Y., Stadler, K., Yoo, B. J., Choo, Q. L., Coates, S. R., Uematsu, Y., Harada, T., Greer, C. E., Polo, J. M., Pileri, P., Eickmann, M., Rappuoli, R., Abrignani, S., Houghton, M., and Han, J. H. (2004). Synthesis and characterization of a native, oligomeric form of recombinant severe acute respiratory syndrome coronavirus spike glycoprotein. *J Virol* **78**, 10328-35.
- Steinmann, E., Penin, F., Kallis, S., Patel, A. H., Bartenschlager, R., and Pietschmann, T. (2007). Hepatitis C virus p7 protein is crucial for assembly and release of infectious virions. *PLoS Pathog* **3**, e103.
- Struck, D. K., Hoekstra, D., and Pagano, R. E. (1981). Use of resonance energy transfer to monitor membrane fusion. *Biochemistry* **20**, 4093-9.
- Suarez, T., Gallaher, W. R., Agirre, A., Goni, F. M., and Nieva, J. L. (2000a). Membrane interface-interacting sequences within the ectodomain of the human immunodeficiency virus type 1 envelope glycoprotein: putative role during viral fusion. *J Virol* **74**, 8038-47.
- Suarez, T., Nir, S., Goni, F. M., Saez-Cirion, A., and Nieva, J. L. (2000b). The pre-transmembrane region of the human immunodeficiency virus type-1 glycoprotein: a novel fusogenic sequence. *FEBS Lett* **477**, 145-9.
- Suomalainen, M. (2002). Lipid rafts and assembly of enveloped viruses. *Traffic* **3**, 705-9.

- Surewicz, W. K., Mantsch, H. H., and Chapman, D. (1993). Determination of protein secondary structure by Fourier transform infrared spectroscopy: a critical assessment. *Biochemistry* **32**, 389-94.
- Szoka, F., Jr., and Papahadjopoulos, D. (1980). Comparative properties and methods of preparation of lipid vesicles (liposomes). *Annu Rev Biophys Bioeng* **9**, 467-508.
- Takamizawa, A., Mori, C., Fuke, I., Manabe, S., Murakami, S., Fujita, J., Onishi, E., Andoh, T., Yoshida, I., and Okayama, H. (1991). Structure and organization of the hepatitis C virus genome isolated from human carriers. *J Virol* **65**, 1105-13.
- Tan, S. L., Pause, A., Shi, Y., and Sonenberg, N. (2002). Hepatitis C therapeutics: current status and emerging strategies. *Nat Rev Drug Discov* **1**, 867-81.
- Thayer, A. M., and Kohler, S. J. (1981). Phosphorus-31 nuclear magnetic resonance spectra characteristic of hexagonal and isotropic phospholipid phases generated from phosphatidylethanolamine in the bilayer phase. *Biochemistry* **20**, 6831-4.
- Thomssen, R., Bonk, S., Propfe, C., Heermann, K. H., Kochel, H. G., and Uy, A. (1992). Association of hepatitis C virus in human sera with beta-lipoprotein. *Med Microbiol Immunol* **181**, 293-300.
- Thorp, E. B., and Gallagher, T. M. (2004). Requirements for CEACAMs and cholesterol during murine coronavirus cell entry. *J Virol* **78**, 2682-92.
- Tong, S., Yi, F., Martin, A., Yao, Q., Li, M., and Compans, R. W. (2001). Three membrane-proximal amino acids in the human parainfluenza type 2 (HPIV 2) F protein are critical for fusogenic activity. *Virology* **280**, 52-61.
- Van Itallie, C. M., and Anderson, J. M. (2006). Claudins and epithelial paracellular transport. *Annu Rev Physiol* **68**, 403-29.
- Vauloup-Fellous, C., Pene, V., Garaud-Aunis, J., Harper, F., Bardin, S., Suire, Y., Pichard, E., Schmitt, A., Sogni, P., Pierron, G., Briand, P., and Rosenberg, A. R. (2006). Signal peptide peptidase-catalyzed cleavage of hepatitis C virus core protein is dispensable for virus budding but destabilizes the viral capsid. *J Biol Chem* **281**, 27679-92.
- Viard, M., Blumenthal, R., and Raviv, Y. (2002). Improved separation of integral membrane proteins by continuous elution electrophoresis with simultaneous detergent exchange: application to the purification of the fusion protein of the human immunodeficiency virus type 1. *Electrophoresis* **23**, 1659-66.
- Villalain, J. (1996). Location of cholesterol in model membranes by magic-angle-sample-spinning NMR. *Eur J Biochem* **241**, 586-93.
- Vincent, N., Genin, C., and Malvoisin, E. (2002). Identification of a conserved domain of the HIV-1 transmembrane protein gp41 which interacts with cholesterol groups. *Biochim Biophys Acta* **1567**, 157-64.
- Vitovic, P., Alakoskela, J. M., and Kinnunen, P. K. (2008). Assessment of drug-lipid complex formation by a high-throughput langmuir-balance and correlation to phospholipidosis. *J Med Chem* **51**, 1842-8.
- Wakita, T., Pietschmann, T., Kato, T., Date, T., Miyamoto, M., Zhao, Z., Murthy, K., Habermann, A., Krausslich, H. G., Mizokami, M., Bartenschlager, R., and Liang, T. J. (2005). Production of infectious hepatitis C virus in tissue culture from a cloned viral genome. *Nat Med* **11**, 791-6.
- Wall, J., Golding, C. A., Van Veen, M., and O'Shea, P. (1995). The use of fluoresceinphosphatidylethanolamine (FPE) as a real-time probe for peptide-membrane interactions. *Mol Membr Biol* **12**, 183-92.
- Weegink, C. J., Sentjens, R. E., Beld, M. G., Dijkgraaf, M. G., and Reesink, H. W. (2003). Chronic hepatitis C patients with a post-treatment virological relapse re-treated with an induction dose of 18 MU interferon-alpha in combination with ribavirin and amantadine: a two-arm randomized pilot study. *J Viral Hepat* **10**, 174-82.

- Weissenhorn, W., Hinz, A., and Gaudin, Y. (2007). Virus membrane fusion. *FEBS Lett* **581**, 2150-5.
- Wiener, M. C., and White, S. H. (1992). Structure of a fluid dioleoylphosphatidylcholine bilayer determined by joint refinement of x-ray and neutron diffraction data. II. Distribution and packing of terminal methyl groups. *Biophys J* **61**, 428-33.
- Yasui, K., Wakita, T., Tsukiyama-Kohara, K., Funahashi, S. I., Ichikawa, M., Kajita, T., Moradpour, D., Wands, J. R., and Kohara, M. (1998). The native form and maturation process of hepatitis C virus core protein. *J Virol* **72**, 6048-55.
- Yonezawa, A., Cavrois, M., and Greene, W. C. (2005). Studies of ebola virus glycoprotein-mediated entry and fusion by using pseudotyped human immunodeficiency virus type 1 virions: involvement of cytoskeletal proteins and enhancement by tumor necrosis factor alpha. *J Virol* **79**, 918-26.
- Zampighi, G. A., Zampighi, L. M., Fain, N., Lanzavecchia, S., Simon, S. A., and Wright, E. M. (2006). Conical electron tomography of a chemical synapse: vesicles docked to the active zone are hemi-fused. *Biophys J* **91**, 2910-8.
- Zhong, J., Gastaminza, P., Cheng, G., Kapadia, S., Kato, T., Burton, D. R., Wieland, S. F., Uprichard, S. L., Wakita, T., and Chisari, F. V. (2005). Robust hepatitis C virus infection in vitro. *Proc Natl Acad Sci U S A* **102**, 9294-9.
- Zhou, J., Dutch, R. E., and Lamb, R. A. (1997). Proper spacing between heptad repeat B and the transmembrane domain boundary of the paramyxovirus SV5 F protein is critical for biological activity. *Virology* **239**, 327-39.
- Zignego, A. L., Macchia, D., Monti, M., Thiers, V., Mazzetti, M., Foschi, M., Maggi, E., Romagnani, S., Gentilini, P., and Brechot, C. (1992). Infection of peripheral mononuclear blood cells by hepatitis C virus. *J Hepatol* **15**, 382-6.



Trabajos realizados a lo largo de esta tesis:

- *The membrane-active regions of the Hepatitis C virus E1 and E2 envelope Glycoproteins.* Pérez-Berná AJ, Miguel R. Moreno, Jaime Guillén, Angela Bernabeu, and José Villalaín. *Biochemistry*, 45, 3755-3768. 2006
- *Identification of the membrane-active regions of HCV p7 protein. Biophysical characterization of the loop region.* Pérez-Berná AJ, Guillén J, Moreno MR, Bernabeu A, Pabst G, Laggner P and Villalaín J. *Journal of Biological Chemistry*. 283, 8089-101, 2008.
- *Hepatitis C virus core protein binding to lipid membranes: the role of domains 1 and 2.* Pérez-Berná AJ, Veiga AS, Castanho MA and Villalaín J. *Journal of Viral Hepatitis*; 15, 346-56, 2008
- *Interaction of the most membranotropic region of the HCV E2 envelope glycoprotein with membranes.* Pérez-Berná AJ, Moreno MR, Guillén J, Gomez-Sanchez AI, Pabst G, Laggner P and Villalaín J. *Biophysical Journal*, 94, 4737-50, 2008.
- *The pre-transmembrane region of the HCV E1 envelope glycoprotein. Interaction with model membranes.* Pérez-Berná AJ, Guillén J, Moreno MR, Bernabeu A and Villalaín J. *Biochimica et Biophysica Acta*. 18424260, Aceptado en abril del 2008.
- *Identification of the membrane-active regions implicated in the viral fusion and budding mechanism of the HCV structural proteins using a 18-mer peptide scan with Differential scanning calorimetry and Small-angle x-ray scattering (SAXs) screening* Perez-Berna AJ, Pabst G, Laggner P, Villalain J En elaboración
- *Biophysical characterization of the fusogenic region of HCV E1 envelope glycoprotein.* Pérez-Berná AJ, J. Guillén, Pabst G, Laggner P and Villalaín J. En elaboración
- *Effect of the pre-transmembrane region of the HCV E1 envelope glycoprotein on DEPE polymorphism.* Pérez-Berná AJ, González-Álvarez A, Pabst G, Laggner P and Villalaín J. En elaboración
- *Biophysical characterization of the region 274-298 of E1 envelope glycoproteins from HCV: Interaction with model biomembranes.* Pérez-Berná AJ, GuillénJ, Pabst G, Laggner P and Villalaín J. En elaboración
- *Searching of HCV inhibition viral-cell fusion* Pérez-Berná AJ, Lavillette D and Villalaín J. En elaboración
- *Identification of the Membrane-Active Regions of the Severe Acute Respiratory Syndrome Coronavirus Spike Membrane Glycoprotein. Using a 16/18-Mer Peptide*

Scan: Implications for the Viral Fusion Mechanism. Guillén J, Pérez-Berná AJ, Moreno MR and Villalaín J. *Journal of Virology*, p. 1743–1752, 2005

- *Biophysical characterization and membrane interaction of the most membranotropic region of the HIV-1 gp41 endodomain.* Moreno MR, Pérez-Berná AJ, Guillén J, Villalaín J. *Biochimica et Biophysica Acta*;1778, 1298-307, 2008
- *A second SARS-COV S2 Glycoprotein internal membrana-active peptide. Biophysical characterization and membrana interaction.* Guillén J; Pérez-Berná AJ.; Moreno MR and Villalaín J. *Biochemistry*, Aceptado Junio 2008.
- *Structure of the C-terminal domain of the pro-apoptotic protein Hrk and its interaction with model membranes.* Bernabeu A, Guillen J, Perez-Berna AJ, Moreno MR and Villalain J. *Biochimica et Biophysica Acta*;1768, 1659-70, 2007
- *Characterization of the Interaction of Two Peptides from the N Terminus of the NHR Domain of HIV-1 gp41 with Phospholipid Membranes.* Moreno MR, Guillen J, Perez-Berna AJ, Amoros D, Gomez-Sanchez AI, Bernabeu A and Villalain J. *Biochemistry*;46, 10572-84, 2007.
- *Interaction of a peptide from the pre-transmembrane domain of the severe acute respiratory syndrome coronavirus spike protein with phospholipid membranes.* Guillén J, Moreno MR, Pérez-Berna AJ, Bernabeu A and Villalaín J. *The Journal of Physical Chemistry. B*; 111, 13714-25, 2007.
- *Membranotropic regions of membrane-fusion proteins. The use of peptide libraries.* Pérez-Berná AJ, Guillén J, Moreno MR and Villalaín J. *Libro: Membrane-active peptides: methods and results on structure and function.*(Ed. M.R.C. Castanho), IUL La Jolla, California. 2008

CURRICULUM VITAE

DATOS PERSONALES

Nombre: Ana Joaquina Pérez Berná

E-mail: ajperezberna@umh.es

Fecha de nacimiento: 19 – Septiembre- 1981

Nacionalidad: Española

Teléfono: 627155042

DATOS ACADÉMICOS Y PREMIOS

- 2003: Licenciada en Bioquímica por la “Universidad Miguel Hernández”, Elche (España). Nota Media: 9.08 sobre 10.
- 2003: Premio extraordinario fin de carrera en la licenciatura en Bioquímica (Universidad Miguel Hernández 2003).
- 2004: Premio Estudiante Cinco Estrellas de la Universidad Miguel Hernández.
- 2005: Realiza los cursos de doctorado del programa Biología Molecular y celular con nota media Sobresaliente
- 19-10-2006: Obtiene la suficiencia investigadora
- 19-09-2008: Lectura y defensa de tesis

EXPERIENCIA PROFESIONAL

- 2002. Estancia investigadora en el “Instituto de Bioingeniería” de la “Universidad Miguel Hernández” para el aprendizaje de biología molecular, cultivos celulares, preparación de células madre, inmunoprecipitación, Western blot, microscopía de fluorescencia y transfecciones celulares.
- 2003 hasta la actualidad: Investigadora en el Grupo de Biomembranas del “Instituto de Bioquímica y Biología Molecular y Celular” de la “Universidad Miguel Hernández” de Elche para el aprendizaje de técnicas biofísicas como calorimetría diferencial de barrido, espectroscopia de infrarrojo por transformada de Fourier (IR, ATR, 2D-IR), espectroscopia de absorción, dicroísmo circular, fluorescencia, resonancia magnética nuclear (^{31}P y ^2H -NMR, y solid-state NMR, CP/MAS y HR/MAS) y biología molecular, tal como ingeniería de vectores, transfección en eucariotas/bacterias, expresión y purificación de proteínas.
- 2007: Estancia investigadora en el “Institute of Biophysics and Nanosystems Research” de la “Austrian Academy of Sciences” en Graz, Austria para el aprendizaje de difracción de rayos X de ángulo pequeño (SAXS) y de ángulo grande (WAXS); así como la técnica de análisis global.

SITUACIÓN ACTUAL

Actualmente estoy contratada por la “Universidad Miguel Hernández” como personal docente investigador en prácticas en el “Instituto de Biología Molecular y Celular”. Estoy terminando mi tesis doctoral que lleva por título “Búsqueda y caracterización biofísica de regiones membranotrópicas de las proteínas estructurales de HCV. Búsqueda de inhibidores de la entrada del virus”, dirigida por Profesor Dr José Villalaín. La fecha de lectura prevista es el 19 de septiembre del 2008

BECAS DISFRUTADAS:

- 2003: Beca de colaboración del “Ministerio de Educación y Ciencia”
- 2004: Beca europea asociada al proyecto integrado: “Targeting Replication and Integration of HIV (TRIOH).
- 2004-2008: Beca para la formación de personal investigador para alcanzar el grado de doctor de la “Consellería de Educación y Ciencia” de la “Generalitat Valenciana”.

PUBLICACIONES

- *The membrane-active regions of the Hepatitis C virus E1 and E2 envelope Glycoproteins.* Pérez-Berná AJ, Miguel R. Moreno, Jaime Guillén, Angela Bernabeu, and José Villalaín. *Biochemistry*, 45, 3755-3768, 2006
- *Identification of the membrane-active regions of HCV p7 protein. Biophysical characterization of the loop region.* Pérez-Berná AJ, Guillén J, Moreno MR, Bernabeu A, Pabst G, Laggner P and Villalaín J. *Journal of Biological Chemistry*. 283, 8089-101, 2008.
- *Hepatitis C virus core protein binding to lipid membranes: the role of domains 1 and 2.* Pérez-Berná AJ, Veiga AS, Castanho MA and Villalaín J. *Journal of Viral Hepatitis*;15, 346-56, 2008
- *Interaction of the most membranotropic region of the HCV E2 envelope glycoprotein with membranes.* Pérez-Berná AJ, Moreno MR, Guillén J, Gomez-Sanchez AI, Pabst G, Laggner P and Villalaín J. *Biophysical Journal*, 94,4737-50, 2008.
- *The pre-transmembrane region of the HCV E1 envelope glycoprotein. Interaction with model membranes.* Pérez-Berná AJ, Guillén J, Moreno MR, Bernabeu A and

Villalaín J. *Biochimica et Biophysica Acta*. Doi: 18424260, Aceptado en abril del 2008.

- *Identification of the membrane-active regions implicated in the viral fusion and budding mechanism of the HCV structural proteins using a 18-mer peptide scan with Differential scanning calorimetry and Small-angle x-ray scattering (SAXs) screening* Pérez-Berna AJ, Pabst G, Laggner P, Villalain J. En elaboración
- *Biophysical characterization of the fusogenic region of HCV E1 envelope glycoprotein.* Pérez-Berná AJ, J. Guillén, Pabst G, Laggner P and Villalaín J. En elaboración
- *Effect of the pre-transmembrane region of the HCV E1 envelope glycoprotein on DEPE polymorphism.* Pérez-Berná AJ, González-Álvarez A, Pabst G, Laggner P and Villalaín J. En elaboración
- *Biophysical characterization of the region 274-298 of E1 envelope glycoproteins from HCV: Interaction with model biomembranes.* Pérez-Berná AJ, Guillén J, Pabst G, Laggner P and Villalaín J. En elaboración
- *Searching of HCV inhibition viral-cell fusion* Pérez-Berná AJ, Lavillette D and Villalaín J. En elaboración
- *Identification of the Membrane-Active Regions of the Severe Acute Respiratory Syndrome Coronavirus Spike Membrane Glycoprotein. Using a 16/18-Mer Peptide Scan: Implications for the Viral Fusion Mechanism.* Guillén J, Pérez-Berná AJ, Moreno MR and Villalaín *Journal of Virology*, 1743–1752, 2005
- *Biophysical characterization and membrane interaction of the most membranotropic region of the HIV-1 gp41 endodomain.* Moreno MR, Pérez-Berná AJ, Guillén J, Villalaín. *Biochimica et Biophysica Acta*;1778, 1298-307, 2008
- *A second SARS-COV S2 Glycoprotein internal membrana-active peptide. Biophysical characterization and membrana interaction.* Guillén J; Pérez-Berná AJ.; Moreno MR and Villalaín J. *Biochemistry*, Aceptado Junio 2008.
- *Structure of the C-terminal domain of the pro-apoptotic protein Hrk and its interaction with model membranes.* Bernabeu A, Guillen J, Perez-Berna AJ, Moreno MR and Villalain J. *Biochimica et Biophysica Acta*; 1768, 1659-70, 2007
- *Characterization of the Interaction of Two Peptides from the N Terminus of the NHR Domain of HIV-1 gp41 with Phospholipid Membranes.* Moreno MR, Guillen J, Perez-Berna AJ, Amoros D, Gomez-Sanchez AI, Bernabeu A and Villalain J. *Biochemistry*; 46,10572-84, 2007.
- *Interaction of a peptide from the pre-transmembrane domain of the severe acute respiratory syndrome coronavirus spike protein with phospholipid membranes.* Guillén J, Moreno MR, Pérez-Berna AJ, Bernabeu A and Villalaín J. *The Journal of Physical Chemistry. B*; 111, 13714-25, 2007

- *Membrantropic regions of membrane-fusion proteins. The use of peptide libraries.* Pérez-Berná AJ, Guillén J, Moreno MR and Villalaín J. Libro: Membrane-active peptides: methods and results on structure and function.(Ed. M.R.C. Castanho), IUL La Jolla, California. 2008

COLABORACIÓN EN PROYECTOS DE INVESTIGACIÓN

- “Structure peptides and lipophilic biomolecules of biological relevance in model systems membranes”.

Project DGESIC – PB98-0100 “Spanish Ministry of Education and Science”
Period: 2001-2002 Group leader of the project: Prof. José Villalaín

- “Estructura de péptidos y moléculas lipofílicas de relevancia biológica en sistemas modelo de biomembranas”.

Proyecto: DGESIC – PB98-0100

Periodo: 2001-2002

Investigador Principal: Dr. J. Villalaín

- “Interacción proteína-membrana en sistemas modelo de interés biológico. Caracterización estructural y funcional e interés farmacológico”

Proyecto: MCYT - BMC2002-00158

Periodo: :2003 – 2005

Investigador principal: Dr. J. Villalaín

- “Targeting replication and integration of HIV (TRIoH)” (Thematic call in the area of 'Life sciences, genomics and biotechnology for health'),

Proyecto integrado: FP6- Comisión Europea

Periodo: 2004 – 2006

Investigador principal: J. Villalaín

Coordinator: Prof. M. Witvrouw, Rega Institute for Medical Research, Virology and Chemotherapy, Katholieke Universiteit Leuven

- “Inhibición de la entrada del virus HIV. Búsqueda de nuevos agentes terapéuticos”
Proyecto B07/2004, Consellería de Sanidad, Generalidad Valenciana

Periodo: 2004

Investigador Principal: Dr. J. Villalaín

- “Ayuda Complementaria Al Proyecto Europeo: "Targeting Replication And Integration Of HIV".

Proyecto; SAF2004-0052-E

Periodo: 2005

Investigador Principal: Dr. J. Villalaín

- “Ayuda Complementaria Al Proyecto Europeo: "Targeting Replication And Integration Of HIV".

Proyecto: ACOMP06/017

Periodo: 2006

Investigador principal: Dr. J. Villalaín

- “Caracterización estructural y funcional de la fusión de membrana mediada por virus. Búsqueda de nuevos agentes terapéuticos”

Proyecto: BFU2005-00186/BMC, MEC

Periodo:2006 – 2008

Investigador principal: Dr. J. Villalaín

CONGRESOS

- IV European Biophysics Congress. Alicante (España) Julio 5 -9 2003. Organizadores: Biophysical Societies Association. Comunicación: “*Interaction of the trans-membrane fragment of Bik with model membranes*”. Bernabeu A., Pérez-Berná A.J., Guillén J., y Villalaín J.
- I Conferencias internacionales “Biology after the Genome: A Physical View”. En Zaragoza (España) Febrero 11 -13 2004. Comunicación: “ *Interaction of viscotoxin A3 on model biomembrane systems by NMR*” .Pérez-Berná A.J., Guidici M.A y Villalaín J.
- XXVII Congreso de la Sociedad Española de Bioquímica. Lleida. Septiembre 12– 15 . 2004. Comunicación: “*Interacción con membranas modelo de péptidos provenientes de las proteínas E1 y E2 del virus de la Hepatitis C*” Pérez-Berná A.J., Moreno Raja M, Guillén J y Villalaín J. Comunicación: “*Estudio estructural por RMN de la molécula Triclosan*” Guillén J, Pérez-Berná A.J, Bernabeu A, Villalaín
- Targeting Replication and Integration of HIV TRIoH General Assembly. En el Instituto Georg-Speyer-Haus, Frankfurt, 21 -22 de marzo 2005. Comunicación: “*GP41 and membrana fusion. Looking for targets and inhibitors of HIV fusion*”. Miguel R. Moreno, Jaime Guillén, Pérez-Berná AJ and José Villalaín
- VI European Symposium of the Protein Society. 30 de abril- 4 de Mayo 2005. Barcelona Comunicación: “*Identificación of the membrane active regions of the HCV E1 and E2 proteins*” Pérez-Berná AJ, Miguel Moreno, Jaime Guillén and José Villalaín
- 13th International Meeting on Hepatitis C Virus & Related Viruses. Comunicación: “*Identification of the membrane-active regions of HCV E1 and E2 envelope glycoproteins. Interaction with model membranes*” Pérez Berná AJ, Jaime Guillén, Miguel Moreno, J. Villalain. University of Queensland Cairns Convention Centre, Cairns, Australia. 27- 31 Agosto 2006
- 6th Ibero-American and 4th Portuguese-Spanish Biophysics Congress in Madrid (Spain) Comunicación: “*Biophysical characterization of a peptide derived from the HCV E2 envelope glycoprotein*” Pérez-Berná AJ, Jaime Guillén, Miguel Moreno, Angela Bernabeu, Diego Amorós J. Villalain. Comunicación: “*Putative post-TM region in the long cytoplasmic tail. Interaction of a peptide derived from the LLP2-LLP3 region of gp41 Env endodomain with biomembrane model systems*” Pérez Berná AJ, Jaime Guillén, Miguel Moreno, Angela Bernabeu, Diego Amorós J. Villalain. Sociedad española de biofísica. Madrid. 24 -27 Septiembre 2006
- XXIX Congreso e la Sociedad Española de Bioquímica y Biología Molecular Comunicación: “*Interacción de un peptide derivado del dominio de fusion de la proteína E1 de HCV con sistemas modelo de membrana*”, Pérez Berná AJ, Jaime Guillén, Angela Bernabeu, Miguel Moreno y J. Villalain. Comunicación: “*Interacción de peptidos derivados de la region Post-FP del ectodominio de GP41 con sistemas modelo de membrana*” Moreno M. R., Gomez-Sanchez A. I., Pérez-Berná AJ, J. Guillen , A. Bernabeu y J. Villalain. Comunicación presentations:

“Interacción el dominio Pre-transmembrana de SARS-COV. Implicaciones para el mecanismo de fusión viral.”, J. Guillen, Pérez-Berná AJ, Moreno M. R., A. Berabeu y J. Villalain.

Universidad Miguel Hernández de Elche. 7th -10th de septiembre 2006

- Lipids-Protein Interactions. COST Action D-22. Comunicación: *“Biophysical characterization of a peptide derived from the pretransmembrane domain of HCV E1 glycoprotein”*, Pérez Berná AJ, Jaime Guillén, Miguel Moreno, J. Villalain. Comunicación: *“Interaction of the PreTransmembrane domain of SARS-CoV with phospholipid model membranes”* Jaime Guillén, Miguel Moreno, Pérez-Berná AJ and José Villalain. Comunicación: *“Interaction of a peptide derive from the post-fusion region of GP41 Env ectodomain ith biomembrane model systems”* Moreno M. R., J. Guillen, Pérez-Berná AJ , O’Shea and J. Villalain. Universidad de Murcia 28 -29 abril 2006
- III Biental del Grupo de Resonancia Magnética Nuclear de la RSEQ. Ana Joaquina Pérez Berná fui miembro del comité organizador del congreso. San Juan, Alicante. 15-18 Octubre 2006.
- 2^a Workshop on biophysics of membrane-active peptides. Comunicación: *“Biophysical characterization of the fusogenic regions of E1 and E2 envelope glycoproteins from HCV: Interaction with model membranes”*. Pérez-Berná AJ, Miguel Moreno, Jaime Guillén, Angela Bernabeu, Ana I. Gómez, Diego Amorós J. Villalain. Comunicación: *“Characterization of the putative fusion peptide in the S2 SARS-CoV virus protein”*. Jaime Guillén, Pérez-Berná AJ, Miguel Moreno, Angela Bernabeu, Ana I. Gómez, Diego Amorós, Rodrigo Almeida, Manuel Prieto y J. Villalain. Comunicación: *“Biophysical study of two peptides pertaining to the first part of the NHRsegment of gp41 Env ectodomain of HIV-1 with biomembrane model systems”* Miguel Moreno, Ana I. Gómez Jaime Guillén, Pérez-Berná AJ, Angela Bernabeu, Diego Amorós y J. Villalain. Presentación Oral: *“Membrane-active peptides from membrane fusion proteins”*. José Villalain, Miguel R. Moreno, Jaime Guillén and Pérez-Berná AJ. Lisbon, Science Museum Abril 1 -4 , 2007.
- Targeting Replication and Integration of HIV Fourth General Assembly and Open Symposium in collaboration with the Belgian Society of Biochemistry and Molecular Biology. Comunicación y Presentación Oral: *“Inhibition of gp41-mediated membrane fusion”* José Villalain, Miguel R. Moreno, Ana I. Gómez, Jaime Guillén, and Pérez-Berná AJ Junio 11 -12 , 2007-Convent van Chièvres – Leuven
- XXIX Congreso e la Sociedad Española de Bioquímica y Biología Molecular. Comunicación and oral presentation: *“Glicoproteina Sdel coronavirus del SARS. Zonas implicadas en la fusion de membranas”*. Jaime Guillén-Casas, Pérez-Berná AJ, Miguel. R. Moreno-Raja, Diego Amorós, Ana. I. Gomez Sanchez, Jose Villalain. Malaga, España, Septiembre, 12-15 2007
- 16th International Biophysics Congress (IUPAB) and Biophysical Society 52nd Annual Meeting (USA). Comunicación: *“Characterization Of The Putative Fusion Peptide Of The SARS Coronavirus S2 Glycoprotein”*. Jaime Guillén, Pérez-Berná

AJ, Ana I Gomez-Sanchez, Miguel Moreno and Jose Villalain. Comunicación: “*The Membrane-Active Regions of the Hepatitis C Virus E1 and E2 Envelope. Glycoproteins. Structural and Biophysical Characterization of the Fusogenic Region.*” Pérez-Berná AJ, Jaime Guillen, Miguel Moreno, Ana Isabel Gómez Sánchez, Alejandro González-Álvarez, Georg Pabst, Peter Laggner and José Villalaín. Febrero 2-6, 2008 Long Beach, California, USA

- XI Encuentro Peptídico Ibérico. Presentación Oral: “*The Membrane-Active Regions Of HCV p7 Protein. Biophysical Characterization of the Loop Region*”. Pérez-Berná AJ, Angela Bernabeu, Jaime Guillén, Miguel R. Moreno, Ana Isabel Gómez Sánchez, Alejandro González-Álvarez, Georg Pabst, Peter Laggner and José Villalaín Santiago de Compostela, 6-7 Marzo 2008

CURSOS

- “Stem Cells and clonation”. En Alicante 2002.
- “Paramagnetic and Diamagnetic RMN. Molecular interactions”. En Barcelona. Abril 20 -24 . 2004
- “Enfermedades inflamatorias crónicas”. Universidad Internacional Menéndez Pelayo. Santander 12- 16 Julio 2004.
- “Magnetic nanoparticles”. Madrid. Agosto 2-6. 2004.
- “NMR in drug discovery”. Barcelona 21-22 de Octubre. 2004
- X School of Pure and Applied Biophysics. Time resolved spectroscopic methods in biophysics Organised “Società Italiana di biofisica pura e applicata. Istituto Veneto di scienze lettere ed arti” Venice,– Campo Santo Stefano. Enero 16- 20, 2006

OTROS DATOS DE INTERÉS

- Socio de la Sociedad Española de Bioquímica y Biología Molecular desde 2005.
- Socio de la Sociedad Española de Biofísica desde 2007.

IDIOMAS

- Inglés: Nivel Alto escrito, hablado y leído.

Titulación: Diploma de grado elemental de la escuela de idiomas y cursando 4º curso.

- Alemán: Nivel medio escrito, leído y hablado.

Titulación: Diploma de estudios Básicos de la Escuela Oficial de Idiomas.

- Valenciano: Nivel Alto escrito, hablado y leído.

Titulación: Grado Elemental

INFORMÁTICA

- Nivel alto en ofimática entorno Windows, procesador de textos Word, hojas de cálculo Excel, bases de datos Access, presentaciones Power Point, procesadores de referencias ReferentManager, EndNote...
- Conocimiento de MS-DOS y programas de uso en análisis de datos científicos. Spectracalc, Sigmaplot, Origin, Global Analyse Program, OPUS, VMD, Topspin, felix, anthepro, PyMOL, Mestre, Jasco...
- Tratamiento de imágenes y maquetado de poster PhotoDraw, PowerPoint, Canvas, Publisher....
- Nivel alto en el entorno de Internet tanto para asuntos científicos, búsquedas bibliográficas (Pubmed), proteómica y análisis de secuencias on line.

EQUIPOS QUE UTILIZA O HA UTILIZADO

- Espectrofotómetro, Fecha: 2003-2008, Usuario asiduo.
- Espectrofluorímetro, Fecha: 2003-2008, Usuario asiduo.
- Espectrómetro de Infrarrojo, Fecha: 2003-2008, Usuario asiduo.
- Calorímetros de barrido, Fecha: 2003-2008, Usuario asiduo.
- Espectropolarímetro- Dicrografo, Fecha: 2003-2008, Usuario ocasional.
- Espectrómetro de resonancia magnética nuclear (en disolución BBO, TXI y en estado sólido, HR-MAS, CP-MAS) , Fecha: 2003-2008, Usuario ocasional.
- Difractómetro de rayos X para SAXS y WAXS, Fecha: 2007, Usuario ocasional.